Optimal Design of Integrated Batch Processes

by

Matheos Stylianou Charalambides

November 1996

A thesis submitted for the degree of Doctor of
Philosophy of the University of London and for the
Diploma of Membership of the Imperial College

Department of Chemical Engineering and Chemical Technology
Imperial College of Science, Technology and Medicine
London SW7 2BY, UK.

Στούς γονείς μου Στέλιο καί Αγνή

Σὲ σᾶς ποὺ δκιαφεντεύκετε τὴν προκοπὴν, τὰ γράμματα,

Σὲ τζ'είνους ποὺ τὴν ορφανιὰν τζιαὶ τὴν σ'ηρκὰν πονοῦσιν,

Σ' ὅπκοιους ταβροῦν πομούσουρα τοῦ τόπου, λῆτες, κλάματα,

Σ' όσους τὴν φτώσ'ειαν, τὴν τιμὴν στιμιάζουν τζι' ἀγαποῦσιν

Τὰ φτωσ'ικὰ τραούδκια μου, τὴν ἀρκοντιάν μου δκιῶ τους,

Μὲς στὸ πισσούριν ἔν τοῦ φοῦ τὸ χάραμαν, χαρῶ τους.

Δ.Θ. ΛΙΠΕΡΤΗΣ

Abstract

This thesis considers the optimal design of integrated batch processes, where plant design and scheduling as well as the detailed operating procedure of the individual processing steps are considered simultaneously.

The State-Task Network (STN) representation of process recipes is augmented to facilitate a detailed characterisation of both the materials handled in a process and the transient behaviour of batch processes.

Based on this STN characterisation, a mathematical formulation for the design of batch processes is presented. This results in a multistage optimal control problem with continuous variables corresponding to both the control variables in individual processing steps and the scheduling decisions. The optimisation objective is the maximisation of the net profit of the process, comprising material, utility and annualised capital cost.

A decomposition approach is proposed for solving this problem. The approach is illustrated through a number of examples of significant complexity in the process recipe as well as the process model describing each unit operation.

The above methodology is also extented to address the problem of designing processes that have to operate under limited resource availability. It also deals with the determination of the equipment requirements for the design or retrofit of batch plants.

Contents

List of Figures

List of Tables

Chapter 1

Introduction

Over the last two decades, the chemical industry has shown an increasing interest in batch processes for the production of high value-added chemicals (Parakrama, 1985; Hasebe and Hashimoto, 1992). The batch and semi-batch modes of operation are particularly appropriate for low volume, multiple product processes where the operational flexibility offered by such plants (*e.g.* the possible use of the same set of equipment and other resources for producing a number of different products) can be exploited.

This thesis is concerned with the optimal design of batch processes. This introductory chapter starts with some basic definitions, followed by an examination of the main aspects of the batch process design problem. It then discusses the motivation and basis of the work described in this thesis. An outline of the latter is also given.

1.1. Batch Processes and Processing Steps

In the context of this thesis, a *process* is a set of physical, chemical and biological transformations (processing steps) that transform a set of raw materials to the final products, usually via one or more intermediate materials.

The above definition is valid for all processes, be they batch or continuous. In a *batch* process, each processing step usually involves a single batch unit operation. In the strict batch mode, all

the inputs to such a processing step are charged to an appropriate vessel before the start of the corresponding transformation, and are discharged from the vessel after its end. However, we also consider *semi-batch* operations in which at least part of the input material(s) is added to the vessel during processing, either as a continuous stream or in one or more discrete doses; similarly, part of the product(s) may be removed from the vessel also during processing. In all cases, the conditions within the processing equipment generally vary with time between the start and the end of the operation. Taking proper account of the transient nature of batch operations is one of the main concerns of the work to be presented in this thesis.

An interesting question is what precisely constitutes a distinct processing step. For instance, the entire process may be considered to form a single, albeit extremely complex, processing step. At the other extreme, a single tray in a batch distillation column may be thought of as a processing step since it involves a well-defined transformation of two input materials into two output ones. As far as this thesis is concerned, *a process shall be divided into the maximum number of distinct processing steps so that no exchange of material and/or energy takes place between different processing steps during their operation.*

The above condition implies that if material is added to a processing vessel during the operation, then this material must originate from a storage tank and not from an upstream processing step. Similarly, if material is to be removed from the vessel during the operation, then this material must be accumulated in an isolated storage vessel and not be used by other processing steps before this accumulation is completed [1].

In cases where exchange of material and/or energy between two or more processing operations *does* take place during processing, then we consider all operations interacting in this manner as a *single* processing step even if they are performed in quite distinct equipment items. At a trivial and rather obvious level, this implies that it is an entire batch distillation operation that constitutes a distinct processing step rather than the operations taking place on the individual trays, reboiler, and condenser. More interestingly, two heat-integrated but otherwise quite separate batch unit operations must be considered as a single processing step for the purposes of process design (see Papageorgiou *et al.* (1994)). In the extreme case, a traditional continuous plant will indeed be viewed as a single "batch" processing step as far as our methodology is concerned. Of course, in this case, the periods between plant start-up and shut-down are usually so long compared to the

[1] This often, but not always, coincides with the end of the step that is producing this material.

process time constants that the transient behaviour of the process is often ignored and the process design is based on purely steady-state considerations.

1.2. The Batch Process Design Problem

The design of a batch process has many interacting facets. We consider the most important of these, and the interactions between them in this section.

The precise manner in which each processing step in a batch process is operated is termed its *operating policy*. Consider, for example, a batch distillation operation separating a binary mixture to produce a top distillate product and an undesirable bottom product. Determining an appropriate operating policy for this step includes the following decisions:

- the initial amount of material to be charged to the column (the "batchsize");
- the duration of the distillation operation (the "processing time");
- the variation of the reflux ratio and reboiler heat duty during the operation.

The properties of the raw materials to be used by a batch process being designed are usually known *a priori*. The final products may be similarly defined or simply be subject to design specifications; for instance, in the example above, the final purity of the distillate may have to meet or exceed a certain target. On the other hand, the various intermediates in the process may be much less well defined. In general, the determination of the precise nature of all materials in the process forms another important part of the batch process design problem.

The various batch processing steps in a process are performed in physical plant equipment such as reactor vessels, distillation columns *etc.* Obviously, the characteristics of this equipment have a major effect on the operating policy for the corresponding processing step. For instance, the batchsize for a batch distillation operation is restricted by the capacity of the reboiler still in the distillation column. Similarly, the maximum possible rate of heat provision to this reboiler is determined by the area and heat transfer characteristics of the heating coil inside the still.

The commercial lifetime of many of the high-value products typically manufactured by batch processes is often quite short. In many cases, this implies that a new process has to be implemented

in an existing plant. Fortunately, one important characteristic of most batch plant equipment is that it tends to be fairly generic in nature. For instance, the same reactor vessel may be used in a satisfactory manner to carry out a wide variety of batch reactions[2]. In such cases, the characteristics of the processing equipment are given but one still has to determine the precise operating policy for each processing step and the nature of all the materials in the process.

On the other hand, in some situations a new plant may have to be constructed in order to implement a new batch process. In this case, the characteristics of the processing equipment need to be determined in addition to the other decisions already mentioned. Moreover, in view of the strong interactions between these decisions, process and plant design need to be considered simultaneously.

Processing equipment is only one of the resources that are necessary for implementing a batch process. Auxiliary plant hardware also includes storage capacity, piping and material movement devices such as pumps, conveyor belts *etc.* Furthermore, most processes require the use of utilities such as steam and cooling water, and manpower. We refer to all of these collectively as the *production resources.*

In addition to determining the operating policies for the individual processing steps in a batch process, the nature of all materials in it, and the available production resources, one has to consider the problem of *scheduling* the plant operation over a given time horizon. This involves the determination of the number and timing of the batches of material undergoing each processing step so as to achieve the required production targets, and more generally maximise the economic benefit arising from the production. This is a complex problem because of the interactions between successive processing steps in terms of both overall material balance and detailed timing considerations (*i.e.*, a downstream step cannot be initiated before its input materials are produced by one or more upstream steps). Furthermore, batches overlapping in time may place competing demands on shared resources such as multipurpose equipment, input materials and utilities.

The interactions between the production scheduling and the plant design problems are already well known (see, for instance, the reviews by Reklaitis (1989; 1992)). Essentially, plant design aims to determine the required level of plant resource provision, but this obviously depends on how effectively these resources are being used, *i.e.*, on the quality of the plant schedule. This fact

[2]This contrasts to the situation with continuous reactors, the design of which is usually quite specific to the set of reactions to be performed in them.

is recognised explicitly by recent batch plant design methodologies that take account of detailed scheduling considerations (Shah, 1992; Barbosa-Póvoa, 1994). However, all of this work is based on fixed process recipes.

There are also strong interactions between production scheduling and the operating policy of individual processing steps. Consider, for instance, a simple process involving a batch reaction converting a raw material A to a product B, followed by a batch distillation step that separates B from any unreacted A and recycles the latter. The process is carried out in a plant comprising a batch reactor and a batch distillation column of equal capacity. Optimisation of the individual steps might aim to maximize their respective throughputs. However, there is little sense in increasing the heat load in the column reboiler in order to minimise the distillation time if it is already shorter than the reaction time. On the other hand, it may be profitable to reduce the latter, for instance, by terminating the reaction at a lower conversion at the expense of having to recover and recycle more unreacted A. Overall, as noted by Rippin (1983), incorporating the operating policy in the overall design problem exploits the trade-offs that exist between processing time and intensity of processing, and the effect of the quality of the intermediate materials on the operation of upstream processing steps.

1.3. Motivation and Basis of This Work

As was explained in the previous section, the batch process design problem involves a large number of strongly interacting decisions. Furthermore, acceptable process designs must typically satisfy a wide variety of technical, safety, environmental and commercial constraints. It is, therefore, clear that a systematic methodology is required if this task is to be carried out successfully.

Arguably, one of the major advances in process engineering over the past few years has been the increasing availability of increasingly accurate dynamic models of unit operations – both continuous and batch. While it is true that for some process operations, especially those involving complex biological transformations and materials (*e.g.*, foods), accurate models are still largely unavailable, for many other operations this is no longer the case. In particular, models are now available that can accurately predict the influence of the major operating decisions and equipment characteristics on:

- the detailed time trajectories of the key variables (*e.g.* temperatures, pressures and compo-

sitions) affecting the performance and safety of operation,

- the amounts and quality of the products,
- the economics of the processing cost in terms of both operating and capital costs,

for many of the processing steps involved in important industrial processes.

Another major advance in recent years has been in the area of algorithms for the optimisation of complex time-dependent systems. In particular, we can now deal effectively with a wide variety of different constraint types (*e.g.*, end-point and inequality path constraints) that occur frequently in process engineering applications (see, for instance, Vassiliadis *et al.* (1994a; 1994b)).

Finally, we have recently witnessed a massive expansion in the power and availability of computing hardware, which allows us to contemplate the solution of large problems that were until recently considered intractable.

The work presented in this thesis represents an attempt to develop a systematic framework for the optimal design of batch operations by exploiting the three major developments described above. In particular, the main characteristics of our approach are the following:

- *The use of detailed dynamic models for individual processing steps.*
  This is especially important for ensuring that any design produced truly satisfies all the relevant constraints on product quality and process safety, operability and environmental impact.

- *The mathematical formulation of the batch process design as a formal optimisation problem.*
  The large number of interacting design decisions involved render any non-automatic search[3] for a feasible solution highly problematic. Furthermore, given the high value of the raw materials and final products involved in many batch processes, there may be considerable economic incentive in determining an optimal solution rather than merely a good one. The importance of these factors cannot be overemphasised. For instance, according to Parakrama's survey (1985), the material costs were 50% of the production cost in more than 60% of the companies surveyed, with product quality being cited as one of the most important issues.

[3]For instance, one based on repeated process simulations or experimentation.

Of course, the computational cost of actually solving the integrated batch process design problem once it has been formulated mathematically is likely to be substantial. Despite the significant advances in computer hardware, a number of simplifying assumptions may have to be made to render its solution tractable.

1.4. Outline of This Thesis

The rest of this thesis is structured as follows:

- Chapter 2 provides a critical review of the existing literature on the design of integrated batch processes.
- Chapter 3 introduces a mathematical characterisation of process recipes based on the State-Task Network (STN) process representation. This permits a formal description of both the various materials in the process and the individual processing steps, as well as the interactions between these two.
- Chapter 4 uses the mathematical process characterisation of chapter 3 to formulate the problem of batch process design as an optimisation problem. Some simplifying assumptions are introduced regarding the usage of processing equipment and the availability of intermediate storage capacity.
- Chapter 5 is concerned with methods for the solution of the infinite dimensional multistage dynamic optimisation problem resulting from the formulation presented in Chapter 4.
- Chapters 6 and 7 present two classes of application of our design methodology. The former chapter is concerned with the determination of optimal operating policies for multicomponent batch distillation operations (including those that involve recycles of off-cut material). Chapter 7 studies the optimal design of batch processes comprising multiple reaction and distillation steps and multiple recycles of material.
- Chapters 8 and 9 present extensions to the basic formulation of Chapter 4. In particular, the former considers the design of batch processes when the limited availability of utilities is an important consideration, while the latter relaxes some of the restrictions on the utilisation of processing equipment.

- Finally, chapter 10 presents the main conclusions derived for this work and indicates some promising areas of future research.

Chapter 2

Review of Literature on Batch Process Design

This Chapter presents a review of the earlier work in the area of designing integrated batch processes involving multiple processing steps. Some general conclusions are drawn at the end.

2.1. Introduction

There is already a very substantial body of literature on the optimisation of various aspects of batch process design and operation. Most of this work deals with the problem of planning and scheduling the operation of a given plant, or with the design of a plant to implement a given process recipe. Extensive reviews of both of these areas have been provided by Reklaitis (1989; 1992). More recent reviews have been given by Barbosa-Póvoa (1994) and Papageorgiou (1994).

An area of interest to this thesis that has so far evolved quite separately to the work on plant scheduling and design is that of the optimisation of the operation and design of individual batch unit operations. The application of dynamic optimisation ("optimal control") techniques in this context is now well-established. Particular attention has been paid to the optimisation of batch reactors (see, for instance, the paper by Vassiliadis *et al.* (1993)) and batch distillation (see the review presented at the start of Chapter 6 of this thesis).

In contrast to the above research areas, relatively little has been published on the main subject of interest to this thesis, namely the design of integrated batch processes involving multiple processing steps. The rest of this chapter is devoted to a review of this work.

2.2. The Work of Iribarren and Co-workers

The large number of decisions involved in designing a batch process and plant prompted Iribarren (1985) to adopt a hierarchical solution approach for the design of processes to be implemented in multiproduct batch plants. The nature of each processing stage (*i.e.* whether it is continuous or batch), the provision of intermediate storage, the duplication of equipment items and the merging of stages are among the design decisions tackled. The operation of each stage is expressed in terms of simple algebraic design equations that relate the conversion achieved to the size factor and cycle time for this stage. Also, cost equations are generated to capture the effect of the most important process design variables. At the final step of the design procedure, dynamic simulation is used to compare the most promising alternatives.

The first step in the proposed hierarchical approach involves the determination of the nature of each processing step and the possibility of merging conformable stages. The various alternatives are compared on the basis of the total annualised capital cost criterion assuming one equipment item per stage and unlimited intermediate storage with no capital cost contribution. A systematic way of generating the various alternatives is proposed (Iribarren *et al.*, 1994), with heuristic rules adopted during the search procedure. The heuristic rules favour the merging of consecutive stages, stages with similar size factors and merging of stages that yield a cycle time that is smaller than the limiting one. Switching from the continuous to the batch mode of operation or vice-versa is recommended only if it results in a reduction in capital cost.

The economic incentive for introducing parallel units and intermediate storage in the most promising alternatives is inferred by comparing the lower bound cost (unlimited intermediate storage) and base case cost (no intermediate storage). For a maximum of N parallel equipment items per stage (J), there are N^J structural alternatives. However, this number is reduced to N by employing rounding procedures about the unconstrained optimum. The generation of a number of suboptimal designs is thus traded-off against a reduction in the search space. A similar approach is adopted for allocating intermediate storage.

Salomone *et al.* (1992) considered the effect of process variables on the design of single product batch plants with fixed structural decisions. The multiproduct case was considered by Montagna *et al.* (1994). The basis of the approach are the commonly used equations (Yeh and Reklaitis, 1987):

$$V_j = S_j B \qquad j = 1, \cdots, j \tag{2.1}$$

$$T_j = T_j^0 + T_j^1 B^{a_j} \qquad j = 1, \cdots, j \tag{2.2}$$

relating the required capacity V_j of the equipment at stage j and the corresponding processing time T_j to the batchsize B. The relationships between the "constants" S_j, T_j^0, T_j^1 and a_j appearing in these design equations and the variables describing the process operating conditions are extracted from process models written in a posynomial form, using algebraic manipulation to transform the posynomial models to the required format. For the purposes of the optimisation, unlimited intermediate storage is assumed, thus decoupling the processing steps. The applicability of the posynomial models to represent simple processing steps is illustrated using a citric acid manufacturing process. The values of the coefficients a_j obtained for a batch/continuous filter, batch reactor/CSTR and batch/continuous heater/cooler are comparable to the experimental values provided by Lázaro *et al.* (1989).

The posynomial model was later generalised by Salomone *et al.* (1994) to take into account batch intensive, semi-continuous and batch extensive processing steps. The distinction between these three types of processing step is based on the effect of intensive properties (*e.g.* temperature, pressure) and inlet batchsize on processing time and equipment volume. The approach is also extended to the case of posynomial models derived through experiment or simulation. In the course of the optimisation, "base case" simulations are utilised to update the posynomial constants, assuming that the results of the simulation are equipment size-independent, with the product specifications being the termination conditions of the simulation.

Salomone *et al.* (1994) argue that posynomial models provide a process description of a level of complexity that is appropriate for the purposes of batch process synthesis. The detail offered by considering more rigorous models is considered to be undesirable at this stage due to the increased problem size, computational requirements and the present status of process optimisation techniques. They suggest that the process of optimisation should and can be applied only to the refinement of the design of individual units.

2.3. The Work of Barrera and Co-workers

Barrera (1990) investigated possible solution strategies for the design and operation of multiproduct batch plants. The problem is formulated as a mixed integer non-linear programming problem (MINLP) with the objective function including both manufacturing and allocated fixed costs. Detailed dynamic process models for each product are utilised to calculate size factors relating the processing times, operating variables, batchsizes and output performance measures to the amount of final product. The combinatorial nature and dimensionality of the mathematical formulation and the existence of discrete variables in nonlinear constraints force the utilisation of a decomposition solution strategy. The continuous variables are considered in the "performance" subproblem whereas the discrete ones are considered in the "structure" subproblem.

In the "performance" subproblem, the process operating variables and processing times are considered as the decision variables. Interstage performance attributes (conversion) are treated as individual processing step operating constraints. Fixing the interstage attributes introduces the processing intensity versus the cycle-time trade-off whereas variable interstage attributes introduce the distribution of the performance load trade-offs. The equations describing the operation of each process for each product are solved to determine the effect of the operating variables and processing times on the overall performance of each process by calculating the required residuals and gradients of the objective function and inequality constraints. The existence of material recycles is modelled using external storage units assuming that the material properties are known. An approximate solution strategy is proposed for the solution of the resulting non-linear programming (NLP) problem, as the large number of optimisation parameters slows down the convergence of the sequential quadratic programming (SQP) routine employed and the simulation time increases with the number of products.

The proposed "performance" subproblem for multiproduct plants consists of three major steps: bounds generation, approximate optimisation problem and single product performance subproblems. The upper and lower bounds of the campaign time for each product are calculated by minimising the operating cost and production time of each product respectively. The solution of the approximate quadratic optimisation problem provides the new product campaign times and the solution of each single product performance subproblem provides the overall objective of the plant and checks for the stopping criteria. If the stopping criteria are not satisfied, the procedure is repeated by fitting new quadratic cost approximations.

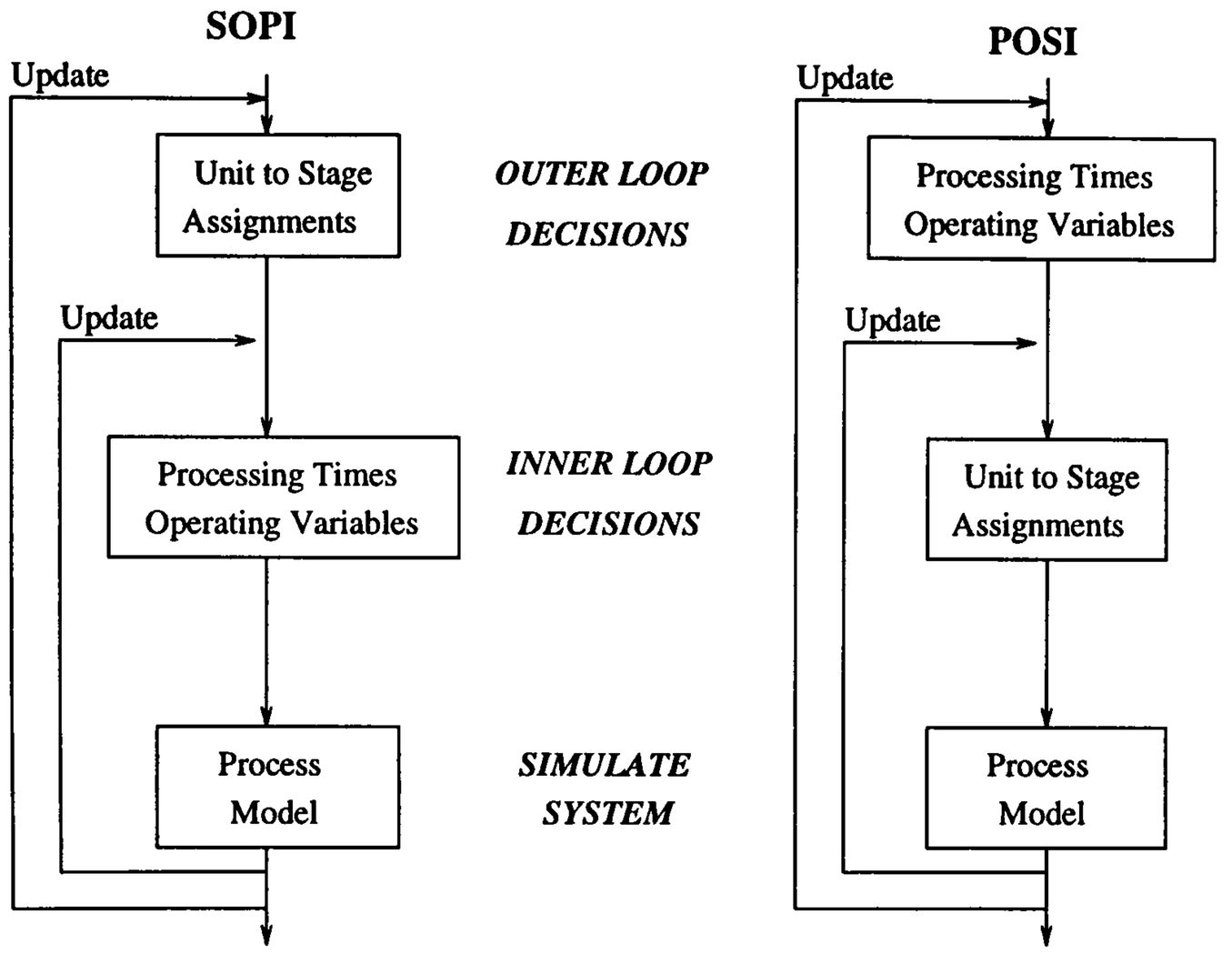

Figure 2.1: POSI and SOPI Nesting Strategies (Barrera, 1990)

The "structure" subproblem considers the sizing of process units and the possibility of utilising a number of units in parallel at each stage, assuming discrete equipment sizes. The solution method used by Barrera involved an approximate method based on local search techniques providing near optimal solutions at low computational expense.

A decomposition approach is adopted for the solution of the combined "performance" and "structure" problem, examining two possible nesting strategies: SOPI (Structure Outside, Performance Inside) and POSI (Performance Outside, Structure Inside) as shown in figure 2.1. Even though the SOPI approach is easier to implement than the POSI one, as standard optimisation techniques can be used, a heavy computational penalty is incurred by solving a "performance" subproblem for every structural alternative.

The work presented by Barrera (1990) has formed the basis for the work of Algor *et al.* (1994) on batch process development. This involves the development of a base case design and the subsequent systematic improvement/optimisation of the base case.

The development of the base case design is performed in six steps:

- Determine the State-Task Network (Kondili *et al.*, 1993) representing the process recipe.
- Develop the individual task models.
- Determine the individual task operating policies and cycle time.
- Determine a feasible schedule for the process.
- If the design is infeasible, assess other process alternatives.
- Synthesise detailed operating procedures.

The hierarchical approach presented above tackles the main issues of process design, suggesting an iterative approach for determining a feasible design. However, iteratively improving a process involving many decision variables may be a formidable, if not impossible, task. Also, not taking account of the interaction between task operating policies, process schedule and plant design may easily lead to suboptimal solutions.

2.4. The Work of Tricoire and Malone

Tricoire (1992) considered the planning, design and synthesis of multiproduct batch processes. Examples of the production of multiple grades of polystyrene and poly(styrene co-acrylonitrile) were utilised to illustrate the approach. Tricoire and Malone (1992) argued that to consider all possible operating variables in the already challenging and computationally demanding plant design problem would be unrealistic, especially for polymer processes where the time-varying profiles and variable initiator feed are a source of virtually infinite operating variables. Global process variables affecting the whole plant design rather than the individual unit operation are selected as decision variables. For example, the reactor temperature profiles are considered as local variables whereas the conversion is a global variable. The operating policy is introduced in the overall design problem through correlations that express the effects of operating variables on processing times, scale factors and batch size. The rest of the unit conditions are fixed by considering each unit operation individually.

The problem is solved using a simulated annealing technique aiming at improving (rather than optimising globally) the design of polymer plants with respect to a performance measure comprising inventory, changeover, operating, recycle, labour, and capital costs and penalties for

early and late production. The solution obtained was compared with a fixed operating condition design and an iterative approach for the optimisation of the design and operating conditions. In the former case, the operating conditions were fixed at the optimal values derived from a single product optimisation whereas in the latter case the operating policies and flowsheet were optimised iteratively. In both cases the overall profit of the process was worse than the simulated annealing approach.

2.5. The Work of Sundaram and Evans

The problem of determining the structure of the recipe for separations by batch distillation was considered by Sundaram and Evans (1993b). The solution of the particular problem addressed provides the separation step sequence, the allocation of equipment items to processing steps, and the operating policy of each processing step (reflux ratio policy, cut location), given the feed and product composition and equipment item inventory.

A general representation scheme was proposed, as shown in figure 2.2, which has embedded in it all possible alternatives of conducting the desired separation. The representation is characterised by levels of processing and separation steps. The number of processing levels denotes the number of separation steps that a product or waste stream has undergone. A separation step represents batch distillation where only one product and waste stream are accounted for. For example, the production of two product streams from the same column is represented by two separation steps. One of the major advantages of the representation is that it does not distinguish between product and waste streams but rather considers the end result where all streams are mixed to yield the desired products. Of course, this advantage is lost if pure component products are mixed together to produce a final product of a given composition.

The synthesis problem is formulated as a non-linear programming problem (NLP) with integer decisions for the existence of any separation step modelled using the cut location, defined as the fraction of feed which ends up as top product. In this way, the separation step is deemed to exist if a top product is produced. The Fenske-Underwood-Gilliland shortcut method (Sundaram and Evans, 1993b) is utilised to describe the operation of the distillation columns. This allows the fast enumeration of the various structural alternatives, which is an important consideration as even the simplest separation can yield a large number of alternatives. In the case of n components to be

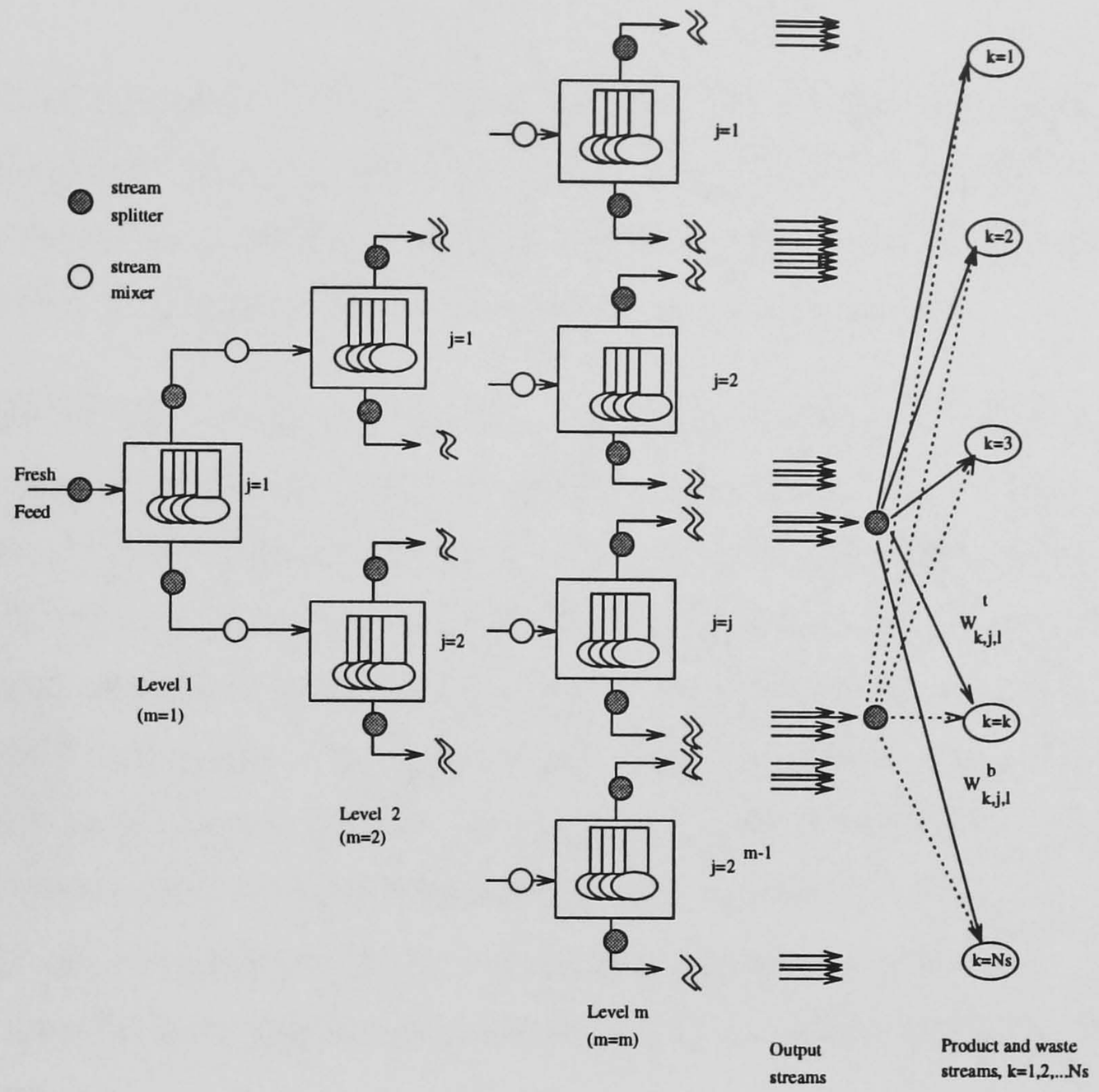

Figure 2.2: Superstructure Representation for Separations by Batch Distillation (Sundaram and Evans, 1994)

separated into n products, with M distillation columns available, the total number of alternatives is given by:

$$N_{structure} = \frac{1}{2n-1}\frac{(4n-4)!}{((2n-2)!)^2}M^{2n-2} \tag{2.3}$$

2.6. The work of Bhatia and Biegler

Recently, Bhatia and Biegler (1996) considered the design and scheduling of batch plants taking account of the transient nature of batch processing. They consider the special case of serial multiproduct processes (without recycle streams), operating under either the zero-wait or unlimited intermediate storage mode of operation. They take account of scheduling through closed form expressions of the cycle time, based on those developed for such processes by Birewar and Grossmann

(1989).

The decisions to be optimised include the operating policy of each processing step, the equipment sizes and the details of the production sequence. The dynamic optimisation problem derived from the use of diffrerential and algebraic models to describe the transient nature of the processing steps is transformed to a NLP using collocation over finite time elements.

The applicability of the mathematical formulation is examined through a couple of small examples; these use material balances only to characterise the reaction tasks and a shortcut model, based on the Underwood and Gilliland correlations, for the distillation task. Although the examples do illustrate the use of dynamic models directly in the optimisation of batch process design, they do not necessarily represent a realistic picture of the size of the problems that need to be tackled when modelling batch process operations. The applicability of such a formulation will therefore depend on its ability to handle large process models, especially for separations with batch distillation. The ability to implement directly the recipes obtained through the optimisation may also be limited by the fact that detailed control profiles are not computed. Finally, it is not clear how the approach may be extended to handle more general process recipes (*e.g.* those involving recycles of material or splitting of batches).

2.7. Conclusions

The utilisation of algebraic models to determine the operating policies for the processing steps and the optimisation of only the most important operating variables is a common feature of the work reviewed in this Chapter. Dynamic process models are utilised either to determine a feasible design or to validate and compare several solution alternatives.

However, for complex process models, generating a simplified algebraic process model is likely to be a formidable, if not impossible, task. Consider, for example, the very common batch operation of distilling a multicomponent mixture to produce multiple useful products and off-cuts. This is an intrinsically complex operation, especially when highly non-ideal mixtures are concerned. Furthermore, the designer has several degrees of freedom at his/her disposal, including the variation of reflux ratio and reboiler heat load with time, as well as the timing of switching from one cut to the next. The generation of a "simple" algebraic model of the operation of the column would involve fitting an algebraic function of all degrees of freedom to each and every variable relating to

the process performance index (*e.g.* utility consumption) and the important operating constraints (*e.g.* product purity). The probability of a simple multivariable algebraic expression being able to fit accurately such a complex dynamic behaviour over a wide range of conditions is indeed minimal!

Generally, algebraic models are often a crude approximation to these intrinsically dynamic processes. This implies that designs obtained through using these models would result in processes that either violate important constraints, or are suboptimal. The implications of constraint violation are particularly severe nowadays within the prevailing climate of environmental and safety awareness. For these reasons, we are led to consider batch process design methodologies that make direct use of detailed dynamic models of batch unit operations. Even though the work of Bhatia and Biegler (1996) goes some way towards addressing this problem, much remains to be done in order to be able to handle realistic levels of complexity in both the overall process recipes and the mathematical models for the processing steps. In particular, it is important to address problems with material recycles which are essential for recovering valuable materials and improve the economics of a process.

Chapter 3

Mathematical Characterisation of Batch Process Recipes

In this chapter, we extend the State-Task Network representation of chemical processes to cover the detailed mathematical characterisation of process recipes. Intensive properties are utilised to characterise the states as described in section 3.2. Section 3.3 focusses on the rigorous representation of the complex time dependent nature of the operations of individual tasks. Section 3.4 describes the equations required to couple the states and tasks. An illustrative example is presented in section 3.5.

3.1. Introduction

The preconception of a chemical industry predominantly comprising continuous processes has faded in recent years, with much attention instead being focussed on batch processes. However, despite the differences between batch and continuous processes, flowsheets or process flow diagrams (PFD) have remained the major tool for representing chemical processes.

Kondili *et al.* (1993) have shown that the PFD representation may lead to ambiguous representations when applied to complex batch process recipes. As an alternative, they proposed the general State-Task Network (STN) process representation. This digraph representation distinguishes two types of node, namely tasks and states, to represent the different processing operations and the different types of material respectively. Each task transforms one or more input states into one or more output states.

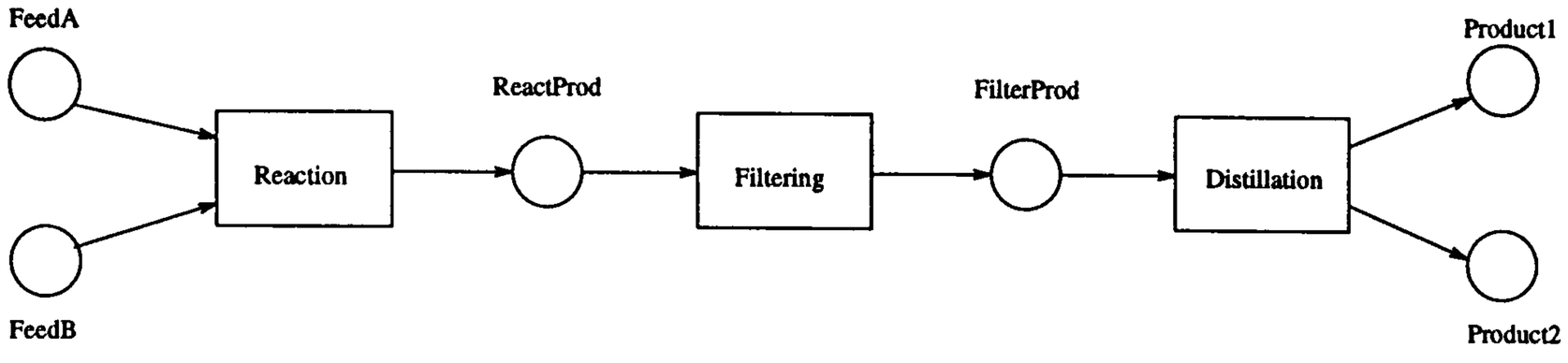

Figure 3.1: State-Task Network (STN) Process Representation

For instance, figure 3.1 shows the STN for a simple process producing two products, $Product1$ and $Product2$, from two raw materials $FeedA$ and $FeedB$. This involves three transformation steps ("tasks"). First a reaction step (*Reaction*) transforms the two raw materials to an intermediate material (state $ReactProd$) which is fed to a filtration step (*Filtering*). The output of the latter step (state $FilterProd$) is further processed in a distillation task (*Distillation*) to produce the two desired products.

Kondili *et al.* (1993) were primarily concerned with scheduling the operation of a given plant implementing a fixed recipe. They therefore adopted a simple mathematical description of the transformations taking place. This is given in terms of:

- The processing time of the task.
- The total resource amounts required for carrying out a single batch of the task. Such resources include utilities (*e.g.* cooling water, steam, electricity) and raw material proportions in the feed. The required amounts are expressed as simple linear functions of the batchsize.
- The proportion of the batchsize transformed to each output state and the relative time of its production with respect to the start of the task. For example, in the case of multicomponent batch distillation, a number of distillate cuts are produced at different times.

We will also employ the State-Task Network representation in the context of the mathematical characterisation of process recipes. We assume that the structure (*i.e.* the set of nodes and arcs) of the STN representing the process under consideration is given. This assumption is not as restrictive as it may appear at first sight, since superstructures incorporating process alternatives can easily be embedded in the STN. For instance, figure 3.2 shows a hypothetical STN segment representing

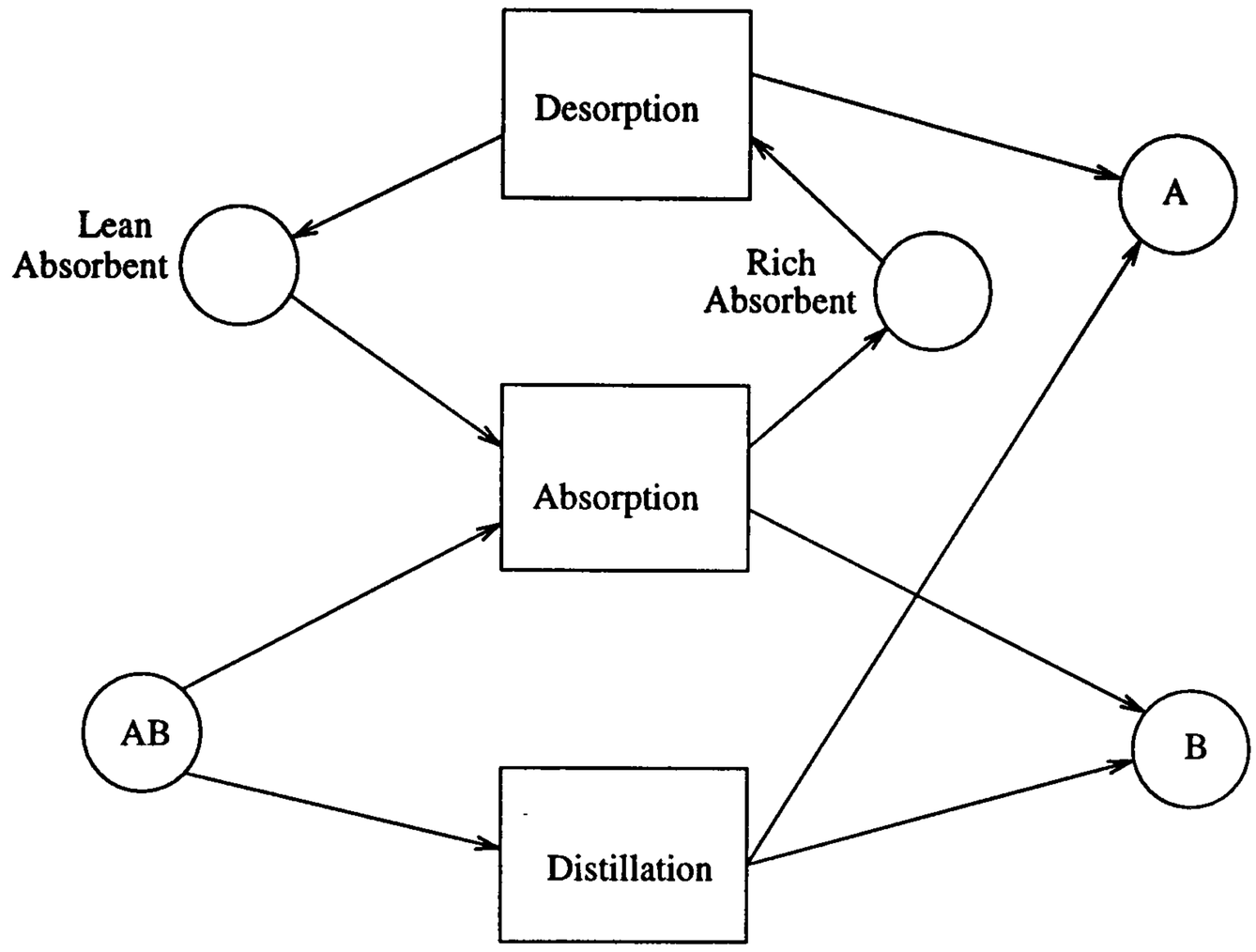

Figure 3.2: State-Task Network Superstructure Representation

the separation of a binary mixture AB into its two components A and B using either distillation or a combination of absorption and desorption operations.

The structure of the State-Task Network would typically be determined by chemists and engineers involved in process development. Computer-based tools to assist in this activity have recently been described in the literature (Linninger *et al.*, 1995; Linninger *et al.*, 1996; Modi *et al.*, 1996).

In contrast to the simple characterisation of tasks and states adopted by Kondili *et al.* (1993), we will need to consider much more detailed models since neither the processing times, nor the detailed operating policy of each task is fixed at the process design stage. The actual quality and other properties of each state of material in the process are generally also unknown. The mathematical characterisation of tasks, states and the interaction between them are the subject of the rest of this chapter.

3.2. State Characterisation

Each state s in the STN is characterised by vector of intensive properties z_s. Typically, z_s will comprise the composition, temperature and pressure of state s. However, for more complex processes (*e.g.* polymerisation or crystallisation), z_s may include properties such as polymer chain length or crystal size distributions, or various moments thereof.

Commercial (*e.g.* quality of final product) or safety (*e.g.* stability of intermediates) considerations may dictate that the properties z_s lie within given bounds:

$$z_s^{min} \leq z_s \leq z_s^{max} \qquad \forall s \tag{3.1}$$

It is also possible to impose restrictions on derived properties of a state (*e.g.* its pH, colour or melt index) that depend on the variables z_s. These usually lead to more general constraints of the form:

$$C_s^I(z_s) \leq 0 \qquad \forall s \tag{3.2}$$

3.3. Task Characterisation

The operation of most types of task involved in typical batch processes (*e.g.* reaction, distillation, filtration) is described by mixed systems of differential-algebraic equations (DAEs). For a task i, this set of equations is of the form:

$$f_i(x_i(t), \dot{x}_i(t), y_i(t), u_i(t), \nu_i) = 0 \qquad \forall i, t \in [0, \tau_i] \tag{3.3}$$

where τ_i is the task duration, and $x_i(t)$ and $y_i(t)$ denote the differential and algebraic variables respectively. The variables $u_i(t)$ represent the possible control manipulations (*e.g.* the reflux flowrate for a batch distillation operation), while ν_i are time-invariant parameters, the values of which are to be determined (*e.g.* the capacity and other characteristics of a new item of equipment in which the task is to be carried out).

Some batch/semi-continuous unit operations involve variations of properties with respect to spatial position as well as time. Typical examples of such distributed operations include packed distillation columns and chromatographic separations. In general, the models of these operations include partial differential and algebraic (PDAE) equations but these can always be reduced to

DAE systems of the form (3.3) by discretisation of spatial dimension(s) (see, for instance Oh and Pantelides (1994)).

In addition to the task description, safety and operability considerations may result in inequality constraints which must be enforced at all times during the operation of the task. These are of the general form:

$$h_i(x_i(t), \dot{x}_i(t), y_i(t), u_i(t), \nu_i) \leq 0 \qquad \forall i, t \in [0, \tau_i] \tag{3.4}$$

For instance, the temperature of the contents of a reactor vessel may have to be maintained below a given upper limit at all times during a batch reaction to avoid the risk of thermal runaway.

Other considerations typically give rise to point equality and inequality constraints which are to be enforced only at a finite set of times $\{t_{i\kappa}\}$. These are of the form:

$$g^E_{i\kappa}(x_i(t_{i\kappa}), \dot{x}_i(t_{i\kappa}), y_i(t_{i\kappa}), u_i(t_{i\kappa}), \nu_i) = 0 \qquad \forall i, t_{i\kappa} \in [0, \tau_i], \kappa = 1, 2, \cdots \tag{3.5}$$

$$g^I_{i\kappa}(x_i(t_{i\kappa}), \dot{x}_i(t_{i\kappa}), y_i(t_{i\kappa}), u_i(t_{i\kappa}), \nu_i) \leq 0 \qquad \forall i, t_{i\kappa} \in [0, \tau_i], \kappa = 1, 2, \cdots \tag{3.6}$$

In practice, one of the times $t_{i\kappa}$ will usually coincide with the task duration τ_i, with (3.5) and (3.6) expressing constraints relating to the final condition of the task ("end-point" constraints). For instance, the final conversion or selectivity in a batch reactor may be required not to exceed a certain upper limit in order to avoid undesirable side-reactions. In fact, the task duration τ_i may be implicitly defined by these constraints.

The time invariant parameters are normally restricted to lie within given limits:

$$\nu_i^{min} \leq \nu_i \leq \nu_i^{max} \qquad \forall i \tag{3.7}$$

For example, the initial charge to a reaction task is bounded from above by the reactor vessel capacity and from below by the minimum amount required for the reactor stirrer to operate satisfactorily.

Similar bounds exist on the control variables, and they may themselves depend on the time-invariant parameters ν_i. For instance, the maximum possible steam supply to the reboiler of a distillation column may well depend on the size of the reboiler and the associated heat transfer equipment:

$$u_i^{min}(\nu_i) \leq u_i(t) \leq u_i^{max}(\nu_i) \qquad \forall i, t \in [0, \tau_i] \tag{3.8}$$

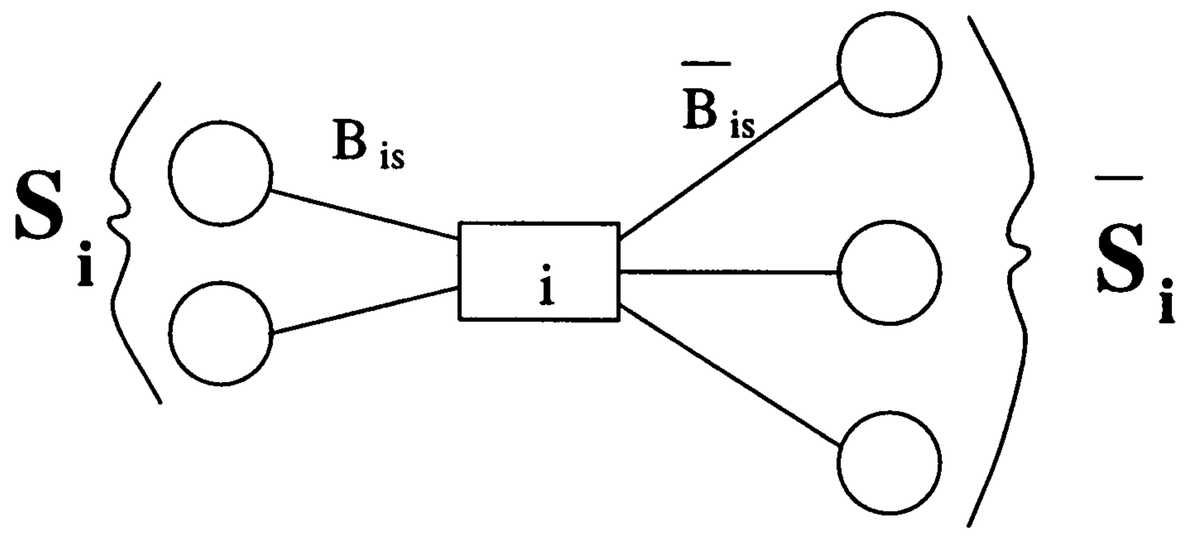

Figure 3.3: Task Connection to Input and Output States

The above discussion assumes a transient model for unit operations. However, in some cases, it may be preferable to model a unit operation in terms of a set of purely algebraic equations of the form:

$$f_i(y_i, \nu_i) = 0 \qquad \forall i \tag{3.9}$$

For instance, modelling the detailed transient behaviour of a mixing task would require a complex fluid dynamical computation. This level of detail may be unnecessary, and it may be more convenient to describe the mixing operation in terms of simple "steady-state" mass and energy balances coupled with an overall processing time τ_i. The latter may be constant or variable. In the latter case, τ_i could depend on the time invariant parameters ν_i (*e.g.* the total amount of material being mixed).

3.4. State-Task Coupling

Having considered the description of the tasks and states individually, we need to establish the relationships that determine the coupling of these two types of entity as defined by the STN.

3.4.1. Interactions Between a Task and Its Input States

Consider a task i that consumes a set of states S_i and produces another set of states $\bar{S}_i$ as shown in Figure 3.3.

The total amount of state $s \in S_i$ consumed by i during its operation is denoted by B_{is}. We

assume that, in general, the task receives a discrete amount B_{is}^d at the start of its operation and a further amount B_{is}^c added continuously (but not necessarily at a constant flowrate) during the operation. However, we do not allow discrete additions of feedstocks during the task operation.[1] We therefore have:

$$B_{is} = B_{is}^d + B_{is}^c \qquad \forall i, s \in S_i \tag{3.10}$$

The initial conditions for processing each batch will depend on the amounts B_{is}^d and the intensive properties z_s of the states $s \in S_i$. In general, they may be written as:

$$I_i(x_i(0), \dot{x}_i(0), y_i(0), u_i(0), \nu_i, \{z_s, B_{is}^d, s \in S_i\}) = 0 \qquad \forall i \tag{3.11}$$

We assume that (3.11) is a complete and non-redundant set of initial conditions that allow, together with the model equations (3.3), the determination of the initial values $\{x_i(0), \dot{x}_i(0), y_i(0)\}$ if all other quantities occurring in them are specified.

The amount B_{is}^c of a state $s \in S_i$ that is added in a continuous fashion can generally be related to the final values of the other task variables through an end-point constraint of the form:

$$B_{is}^c = B_{is}^c(x_i(\tau_i), \dot{x}_i(\tau_i), y_i(\tau_i), u_i(\tau_i), \nu_i) \tag{3.12}$$

For instance, if the rate of addition of a feed state s to task i is treated as a control variable $u(t)$ for this task, we can introduce a variable $X(t)$ representing the total amount added up to time $t \in [0, \tau]$ defined via:

$$\dot{X} = u \quad ; \quad X(0) = 0 \tag{3.13}$$

In this case, equation (3.12) will be simply:

$$B_{is}^c = X(\tau) \tag{3.14}$$

3.4.2. Interactions Between a Task and Its Output States

The output(s) from a task can be produced at the end of its operation and/or in a continuous fashion during it. In any case, the total amount $\bar{B}_{is}$ and quality z_s of the material produced in a state $s \in \bar{S}_i$ can normally be related to the final values of the task variables through general algebraic equations of the form:

$$\bar{B}_{is} = \bar{F}_{is}(x_i(\tau_i), \dot{x}_i(\tau_i), y_i(\tau_i), u_i(\tau_i), \nu_i) \qquad \forall i, s \in \bar{S}_i \tag{3.15}$$

[1] This restriction is introduced primarily for notational simplicity. In fact, discrete charges may be accommodated within our formulation and solution procedure in the manner described by Vassiliadis *et al.* (1993).

and

$$z_s = F_{is}(x_i(\tau_i), \dot{x}_i(\tau_i), y_i(\tau_i), u_i(\tau_i), \nu_i) \qquad \forall i, s \in \bar{S}_i \tag{3.16}$$

For instance, let $D(t)$, $t \in [0, \tau_i]$ denote the flowrate of the distillate stream from the top of a batch distillation task i, and $w_j(t)$, $t \in [0, \tau_i]$ denote the mole fraction of component $j = 1, .., c$ in this stream. Then the amount of component j, $M_j(t)$, collected in the distillate tank up to a time t is given by:

$$\frac{dM_j}{dt} = Dw_j, \quad M_j(0) = 0, \quad j = 1, .., c \tag{3.17}$$

These equations may be considered to be part of the model of the distillation task. The total amount of distillate state s produced by task i is then given by:

$$\bar{B}_{is} = \sum_{j=1}^{c} M_j(\tau_i) \tag{3.18}$$

and the intensive properties (*e.g.* component mole fractions) of this state by:

$$(z_s)_j = \frac{M_j(\tau_i)}{\sum_{k=1}^{c} M_k(\tau_i)}, \quad j = 1, .., c \tag{3.19}$$

3.4.3. Other Constraints

In addition to the constraints (3.10)-(3.12) and (3.15)-(3.16), the quality and quantity of the various states consumed and produced by task i may be related to each other and/or to the time-invariant parameters ν_i characterising the task. For instance, the ratio of the amounts of two different feed states may be fixed or be constrained to lie within given bounds; a minimum recovery of a key component may be specified; and the total batchsize cannot exceed the capacity of the equipment used. We, therefore, have additional constraints of the general form:

$$G_i\left(\nu_i, \{z_s, B_{is}, s \in S_i\}, \{z_s, \bar{B}_{is}, s \in \bar{S}_i\}\right) \leq 0 \qquad \forall i \tag{3.20}$$

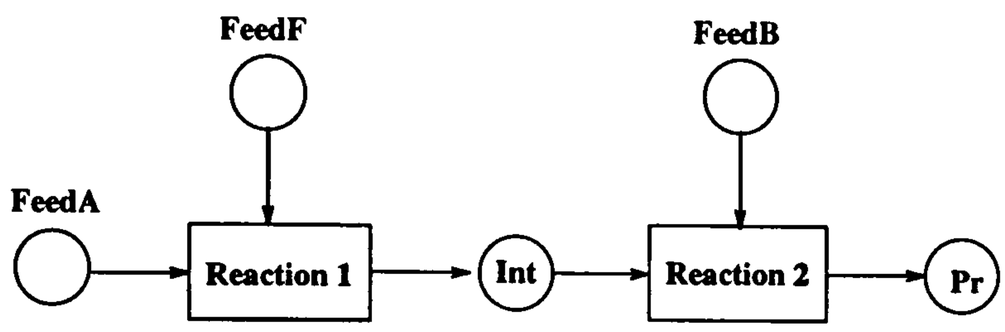

Figure 3.4: Illustrative Example: State Task Network

3.5. An Illustrative Example

A two-stage reaction process is utilised to illustrate the proposed mathematical characterisation of process recipes. Two feedstocks $FeedA$ and $FeedB$ are transformed to the desired product Pr as shown in the State-Task Network in figure 3.4.

The exothermic reaction scheme $\mathcal{A}+\mathcal{F} \rightarrow \mathcal{C}+\mathcal{F}$ takes place in the first reaction stage (Reaction 1), in the presence of catalyst $\mathcal{F}$. The reaction consumes reactant $\mathcal{A}$ (state $FeedA$) which can be added as a discrete charge at the start of the processing or continuously throughout the reaction. The reaction is externally cooled, restricting the reaction temperature to below 500 K in order to avoid activating any side reactions.

The output of Reaction 1 (state Int) is combined with an aqueous solution of component $\mathcal{B}$ (state $FeedB$) in Reaction 2 to yield the desired product state (Pr). Both inputs are added as discrete charges at the start of processing. In Reaction 2, two endothermic reactions take place in parallel transforming component $\mathcal{C}$ to components $\mathcal{D}$ and $\mathcal{E}$ according to the following reaction scheme:

$$\begin{aligned} \mathcal{C}+\mathcal{B} &\rightarrow \mathcal{D} \\ \mathcal{C}+\mathcal{D} &\rightarrow \mathcal{E} \end{aligned}$$

The reaction temperature of this task should never exceed 500 K. Also, the final temperature of Reaction 2 must be less than 300 K so that the reaction is quenched before attempting to discharge the reactor contents.

Quality specifications on the product state Pr require that it contains 48.0% to 50.0 % component $\mathcal{D}$ and less than 10 % component $\mathcal{A}$.

3.5.1. State Characterisation

We use the vector of mole fractions X_s of components $\mathcal{A}$ to $\mathcal{F}$ and the specific enthalpy h_s as the set of intensive variables characterising the various states s of material in this process.

The required quality specifications on the final product can be then imposed directly via the appropriate bounds (*cf.* constraint 3.1) on the intensive properies characterising product state Pr:

$$0.48 \leq \quad X_{\mathcal{D},Pr} \leq 0.50 \tag{3.21}$$

$$X_{\mathcal{A},Pr} \leq 0.10 \tag{3.22}$$

3.5.2. Task Characterisation

The operation of both reaction tasks in this example is modelled using standard material and energy balances.

The mathematical model describing the chemical transformation taking place in Reaction 1 ($i = 1$) is given by equations (3.23) to (3.32). For the sake of completeness, these take account of all components although some of these do not actually occur in this task. In deriving this model, we have assumed well-stirred tank operation and ideal liquid mixture; kinetic and potential energy and mechanical work have been omitted from the energy balance, and the distinction between enthalpy and internal energy has been ignored.

Material Balance

$$V_1 \frac{dN_{\mathcal{A}1}}{dt} = -k_1 C_{\mathcal{A}1} C_{\mathcal{F}1} V_1 + F_{\mathcal{A}} \tag{3.23}$$

$$V_1 \frac{dN_{\mathcal{C}1}}{dt} = k_1 C_{\mathcal{C}1} V_1 \tag{3.24}$$

$$\frac{dN_{j1}}{dt} = 0.0, \quad j = \mathcal{B}, \mathcal{D}, \mathcal{E}, \mathcal{F} \tag{3.25}$$

Rate Constant

$$k_1 = A_1 e^{\left(\frac{-E_{a1}}{RT_1}\right)} \tag{3.26}$$

Total Molar Hold-up

$$N_1 = \sum_{j=\mathcal{A}}^{\mathcal{F}} N_{j1} \tag{3.27}$$

Concentrations

$$C_{j1} = \frac{N_{j1}}{V_1}, \quad j = \mathcal{A}, .., \mathcal{F} \tag{3.28}$$

Total Volume

$$V_1 = \sum_{j=\mathcal{A}}^{\mathcal{F}} \frac{N_{j1}}{\rho_j^o} \tag{3.29}$$

Mole Fractions

$$X_{j1} = \frac{N_{j1}}{N_1}, \quad j = \mathcal{A}, .., \mathcal{F} \tag{3.30}$$

Energy Balance

$$\frac{dH_1}{dt} = F_{FeedA} h_{FeedA} + V_1 k_1 C_{\mathcal{A}1} C_{\mathcal{F}1} (-\Delta H_{R1}) - Q_{cw} \tag{3.31}$$

$$H_1 = \sum_{j=\mathcal{A}}^{\mathcal{F}} N_{j1} h_j^o(T_1) \tag{3.32}$$

where $N_{ki}^{\dagger}$ denotes the molar hold-up of component k in task i, N_1 the total molar hold-up, C_{ki} the concentration of component k in task i, F_{FeedA} and h_{FeedA} the molar feed addition rate and specific enthalpy of $FeedA$, and V_1 the total volume of the reaction mixture. k_1, A_1, E_{a1} and ΔH_{R1} denote respectively the reaction constant, frequency factor and activation energy and enthalpy of reaction for the reaction scheme taking place. The density and specific enthalpy of pure component j are denoted by ρ_j^o and $h_j^o(T)$ respectively.

Equations (3.23)-(3.32) are a typical example of a DAE model (3.3). Here the differential variables are $x_1 \equiv \{N_j, j = \mathcal{A}, .., \mathcal{F}; H_1\}$ while the algebraic ones are $y_1 \equiv \{V_1, T_1, (C_{j1}, X_{j1}, j = \mathcal{A}, .., \mathcal{F})\}$.

The external cooling load (Q_{cw}) and molar feed addition rate ($F_{\mathcal{A}}$) of reactant $\mathcal{A}$ are adopted as the control variables u_1. Both of these are subject to upper bounds:

$$0 \leq Q_{cw}(t) \leq Q_{cw}^{max}, \quad \forall t \in [0, \tau_1] \tag{3.33}$$

---

† Subscript j represents the vector of compounds $\mathcal{A}$, $\mathcal{B}$, $\mathcal{C}$, $\mathcal{D}$, $\mathcal{E}$, and $\mathcal{F}$. Subscript i takes the value of 1 for Reaction 1 and 2 for Reaction 2

$$0 \leq F_{\mathcal{A}}(t) \leq F_{\mathcal{A}}^{max}, \quad \forall t \in [0, \tau_1] \tag{3.34}$$

where Q_{cw}^{max} denotes the maximum external cooling load. $F_{\mathcal{A}}^{max}$ denotes the maximum molar addition rate of reactant $\mathcal{A}$.

The requirement of a reaction temperature less than 500 K at any time during the operation of the reaction task is an example of constraint (3.4), given by:

$$T_1(t) \leq 500 \qquad \forall t \in [0, \tau_1] \tag{3.35}$$

In addition to the above constraint, it is also important that the volume V_1 of the reactor contents never exceeds a maximum allowable utilisation fraction α_{R_1} of the nominal reactor capacity V_{R_1}. This leads to an additional inequality path constraint:

$$V(t) \leq \alpha_{R_1} V_{R_1} \qquad \forall t \in [0, \tau_1] \tag{3.36}$$

In the case of the second reaction stage (task $i = 2$), the chemical transformations taking place are modelled through equations (3.37) to (3.50) employing a similar set of assumptions to those used for modelling task $i = 1$:

Material Balance

$$\frac{dN_{\mathcal{A}2}}{dt} = 0 \tag{3.37}$$

$$V_2 \frac{dN_{\mathcal{B}2}}{dt} = -k_2 C_{\mathcal{B}2} C_{\mathcal{C}2} V_2 \tag{3.38}$$

$$V_2 \frac{dN_{\mathcal{C}2}}{dt} = \left(-k_2 C_{\mathcal{B}2} C_{\mathcal{C}2} - k_3 C_{\mathcal{C}2} C_{\mathcal{D}2}\right) V_2 \tag{3.39}$$

$$V_2 \frac{dN_{\mathcal{D}2}}{dt} = \left(k_2 C_{\mathcal{B}2} C_{\mathcal{C}2} - k_3 C_{\mathcal{C}2} C_{\mathcal{D}2}\right) V_2 \tag{3.40}$$

$$V_2 \frac{dN_{\mathcal{E}2}}{dt} = k_3 C_{\mathcal{C}2} C_{\mathcal{D}2} V_2 \tag{3.41}$$

$$\frac{dN_{\mathcal{F}2}}{dt} = 0 \tag{3.42}$$

Rate Constants

$$k_2 = A_2 e^{(\frac{-E_{a2}}{RT_2})} \tag{3.43}$$

$$k_3 = A_3 e^{(\frac{-E_{a3}}{RT_2})} \tag{3.44}$$

Total Molar Hold-up

$$N_2 = \sum_{j=\mathcal{A}}^{\mathcal{F}} N_{j2} \tag{3.45}$$

Concentrations

$$C_{j2} = \frac{N_{j2}}{V_2}, \quad j = \mathcal{A}, .., \mathcal{F} \tag{3.46}$$

Total Volume

$$V_2 = \sum_{j=\mathcal{A}}^{\mathcal{F}} \frac{N_{j2}}{\rho_j^o} \tag{3.47}$$

Mole Fractions

$$X_{j2} = \frac{N_{j2}}{N_2}, \quad j = \mathcal{A}, .., \mathcal{F} \tag{3.48}$$

Energy Balance

$$\frac{dH_2}{dt} = V_2(k_2 C_{\mathcal{B}2} C_{\mathcal{C}2}(-\Delta H_{R2}) + k_3 C_{\mathcal{C}2} C_{\mathcal{D}2}(-\Delta H_{R3})) + Q_{steam} \tag{3.49}$$

$$H_2 = \sum_{j=\mathcal{A}}^{\mathcal{F}} N_{j2} h_j^o(T_2) \tag{3.50}$$

Again, equations (3.37)-(3.50) form a DAE system with the differential variables $x_2 \equiv \{N_{j2}, j = \mathcal{A}, .., \mathcal{F}; H_2\}$, the algebraic variables $y_2 \equiv \{V_2, T_2, (C_{j2}, X_{j2}, j = \mathcal{A}, .., \mathcal{F})\}$ and the control $u_2 \equiv \{Q_{steam}\}$. The latter is subject to an upper bound Q_{steam}^{max} reflecting the limited availability of steam to this task:

$$0 \leq Q_{steam}(t) \leq Q_{steam}^{max}, \quad \forall t \in [0, \tau_2] \tag{3.51}$$

The requirement of a reaction temperature less than 500 K at any time during the operation of the reaction task is an example of constraint (3.4), given by:

$$T_2(t) \leq 500 \qquad \forall t \in [0, \tau_2] \tag{3.52}$$

For this task, we also have the end-point constraint (*cf.* (3.6)):

$$T_2(\tau_2) \leq 300 \tag{3.53}$$

and, also analogously to constraint (3.36),

$$V_2(t) \leq \alpha_{R_2} V_{R_2} \qquad \forall t \in [0, \tau_2] \tag{3.54}$$

3.5.3. State-Task Coupling

Interactions Between Tasks and their Input States

The total amount of $FeedA$ consumed by task Reaction 1, $B_{1,FeedA}$, comprises a discrete amount $B^d_{1,FeedA}$ and a continuously fed amount $B^c_{1,FeedA}$:

$$B_{1,FeedA} = B^d_{1,FeedA} + B^c_{1,FeedA} \tag{3.55}$$

To calculate the total amount of $FeedA$ fed continuously during the operation, an additional equation is introduced in the set of DAEs characterising the operation of Reaction 1:

$$\frac{dM}{dt} = F_A, \quad M(0) = 0 \tag{3.56}$$

We then have:

$$B^c_{1,FeedA} = M(\tau_1) \tag{3.57}$$

Catalyst $\mathcal{F}$ is added only as a discrete charge at the beginning of processing of Reaction 1. Concequently the total amount of $FeedF$ consumed is simply given by:

$$B_{1,FeedF} = B^d_{1,FeedF} \tag{3.58}$$

The initial conditions (*cf.* equation (3.11)) for the model of Reaction 1 are:

$$N_{j1}(0) = X_{j,FeedA} B^d_{1,FeedA} + X_{j,FeedF} B^d_{1,FeedF}, \quad j = \mathcal{A}, .., \mathcal{F} \tag{3.59}$$

$$H_1(0) = h_{FeedA} B^d_{1,FeedA} + h_{FeedF} B^d_{1,FeedF} \tag{3.60}$$

where X_{js} and h_s denote the mole fraction of component j and the specific enthalpy of state $s(= FeedA, FeedF)$.

Reaction 2 consumes both of its input states, Int and $FeedB$, as discrete charges at the start of its operation. We therefore have simply:

$$B_{2,Int} = B^d_{2,Int} \tag{3.61}$$

$$B_{2,FeedB} = B^d_{2,FeedB} \tag{3.62}$$

The initial conditions for Reaction 2 are:

$$N_{j2}(0) = X_{j,Int}B^d_{2,Int} + X_{j,FeedB}B^d_{2,FeedB}, \quad j = \mathcal{A}, .., \mathcal{F} \tag{3.63}$$

$$H_2(0) = h_{Int}B^d_{2,Int} + h_{FeedB}B^d_{2,FeedB} \tag{3.64}$$

Interactions Between Tasks and their Output States

For the process under consideration, only material states Int and Pr have unknown intensive properties as $FeedA$, $FeedB$ and $FeedF$ are all feedstocks with known properties.

The algebraic equations defining the coupling between Int and $Reaction1$ (*cf.* equations 3.15 and 3.16) are given by equations (3.65)-(3.67):

$$\bar{B}_{1,Int} = B_1(\tau_1) \tag{3.65}$$

$$X_{j,Int} = X_{j1}(\tau_1), \quad j = \mathcal{A}, .., \mathcal{F} \tag{3.66}$$

$$h_{Int} = \sum_{j=\mathcal{A}}^{\mathcal{F}} X_{j1}(\tau_1)h^o_j(T(\tau_1)) \tag{3.67}$$

In the case of state Pr produced by Reaction 2, we have:

$$\bar{B}_{2,Pr} = B_2(\tau_2) \tag{3.68}$$

$$X_{j,Pr} = X_{j2}(\tau_2), \quad j = \mathcal{A}, .., \mathcal{F} \tag{3.69}$$

$$h_{Pr} = \sum_{j=\mathcal{A}}^{\mathcal{F}} X_{j2}(\tau_2) h_j^o(T(\tau_2)) \tag{3.70}$$

3.6. Concluding Remarks

The State-Task Network for process representation has been augmented in the mathematical characterisation of batch process recipes. This allows the abstract representation of process recipes of arbitrary complexity.

The proposed mathematical characterisation of batch process recipes allows the rigorous description of both the states and tasks in a process recipe. The states are described by a vector of intensive properties, with restrictions being placed on derived properties through general constraints. This introduces more detail in the state-task coupling, with the quantity as well as the quality of the various materials in a process being taken into account.

The chemical, physical or biological transformations taking place in a task are represented as a general set of differential and algebraic equations with a diversity of process constraints for enforcing safety and operability considerations. The restriction of algebraic task models for the task inherent in most of the work on batch process design is removed, with the level of modelling complexity depending mainly on how well one can characterise the various processing steps.

In the next chapter, we consider how this process recipe characterisation may be used to formulate the problem of designing integrated batch processes.

Chapter 4

Mathematical Formulation for the Design of Batch Processes

The mathematical characterisation of batch processes established in the previous chapter is quite general. In this chapter, we consider its application to the design of a new process. Section 4.1 considers the simplifying assumptions utilised for the development of an aggregated design formulation which is presented in 4.2-4.3. An illustrating example is presented in section 4.4.

4.1. Simplifying Assumptions

As we have already explained in Chapter 2, there are strong interactions between process design on one hand, and plant design and scheduling on the other. Here we introduce some simplifying assumptions in this context:

- *Plant Design*: Each task is assumed to take place in a single dedicated item of equipment, the size and other characteristics of which may be either fixed or determined by the optimisation.
- *Plant Operation*: All batches of material undergoing the same task in a particular equipment item are assumed to be identical, being processed in exactly the same way.
- *Plant Scheduling*: We assume that the set of tasks $\mathcal{T}$ in a process STN can be partitioned into N disjoint subsets $\mathcal{P}_n, n = 1, .., N$:

$$\mathcal{T} = \bigcup_{n=1}^{N} \mathcal{P}_n \tag{4.1}$$

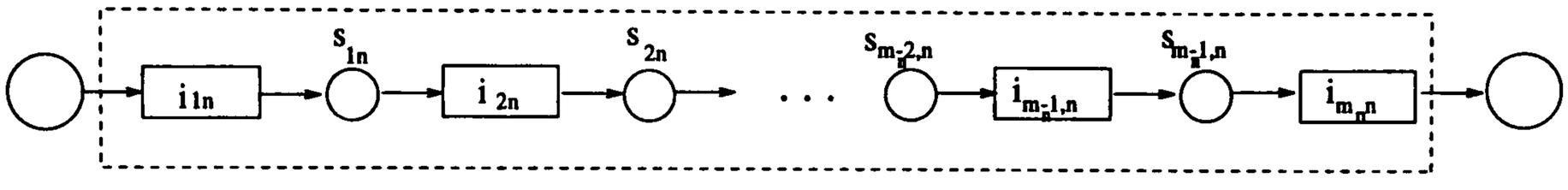

Figure 4.1: Zero-Wait Train

$$\mathcal{P}_n \bigcap \mathcal{P}_{n'} = \emptyset \qquad \forall n, n' \neq n \tag{4.2}$$

such that the tasks within each subset $\mathcal{P}_n$ form a linear processing network, and operate in a zero-wait mode. The m_n tasks in $\mathcal{P}_n$ are denoted as i_{kn}, $k = 1, 2, .., m_n$, and the state that effects the coupling between task i_{kn} and task $i_{k+1,n}$ as s_{kn} (see figure 4.1).

The "zero-wait" operation of a train $\mathcal{P}_n$ implies that a batch of material s_{kn} produced by task $i_{kn}, k = 1, .., m_n - 1$ in the train is immediately taken up by task $i_{k+1,n}$ for further processing. This may be a necessary restriction if this material is unstable and cannot be stored for any significant length of time.

On the other hand, we assume that all materials being consumed and produced by each train $\mathcal{P}_n$ are stable and that they can be stored in unlimited amounts in the plant. We denote the set of these stable states by $\mathcal{SS}$.

On the basis of the above assumptions, the overall process STN will be of the form shown in figure 4.2. We note that nothing prevents a train $\mathcal{P}_n$ from comprising a single task only ($\mid \mathcal{P}_n \mid = 1$); task T8 in figure 4.2 is an example of such a case. We also emphasise that stable states are not exclusively consumed and produced by the first and last task respectively of each "zero-wait" train. For instance, in the process of figure 4.2, the stable state S8 is produced by task T4 occurring in the middle of a "zero-wait" train.

4.2. Material Balance Constraints

We consider first the operation of each "zero-wait" train n. As is well known (Reklaitis, 1992), it is possible to operate the tasks in such a train in an overlapping mode. For instance, figure 4.3 shows an operating schedule for a train comprising three tasks with processing times of 1 hr, 3 hr and 2 hr respectively. This establishes a cycle time τ_n^{cycle} which cannot be less than the processing

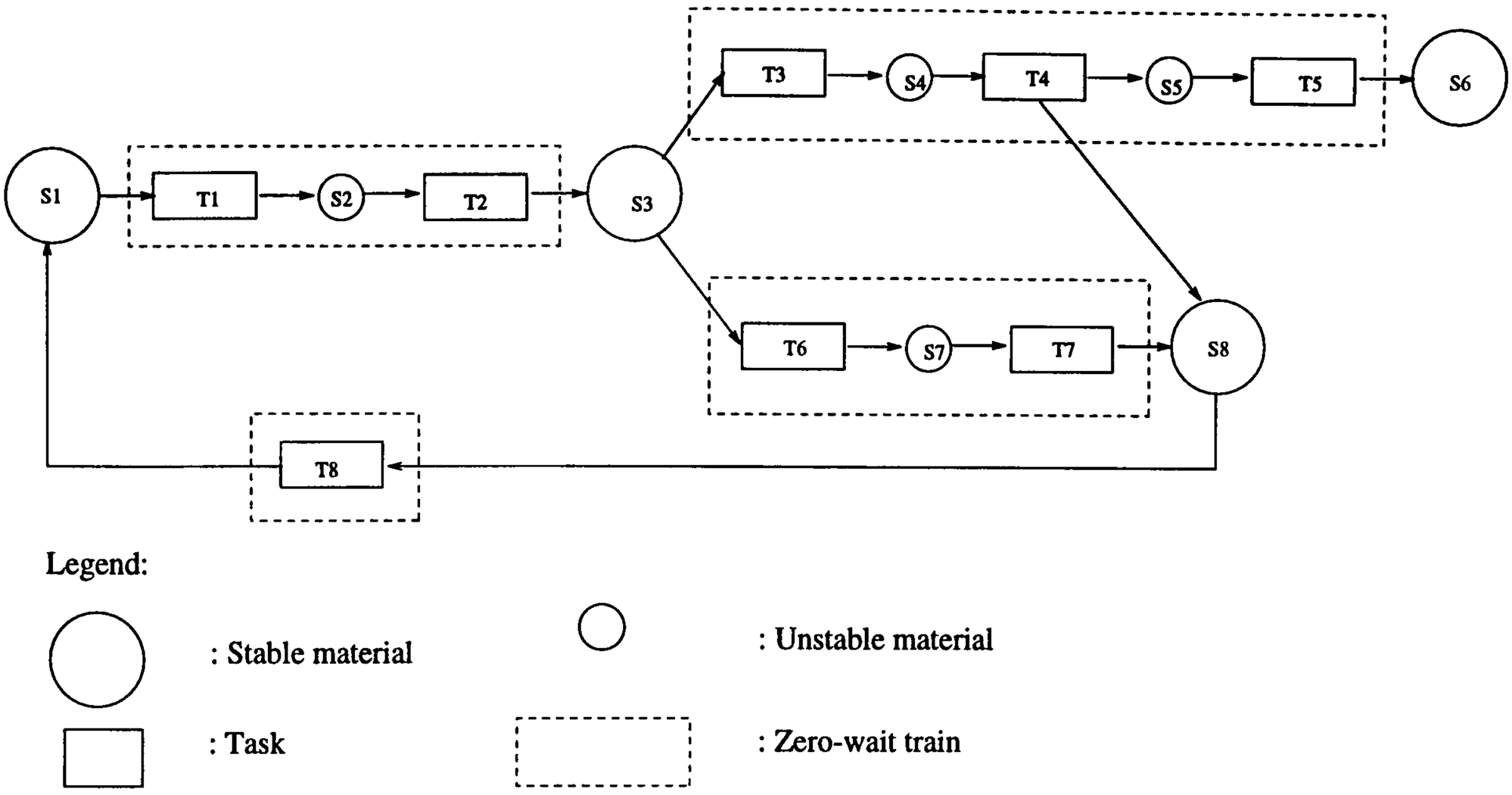

Figure 4.2: Overall Process STN

time of any task in the train:

$$\tau_n^{cycle} \geq \tau_i, \quad \forall n, i \in \mathcal{P}_n \tag{4.3}$$

Thus, the train, the operation of which is illustrated in figure 4.3, produces a new batch of product every 3 hr $(= \max(1hr, 2hr, 3hr))$.

The difference between the processing time τ_i of a task i and the cycle time τ_n^{cycle} of the zero-wait train n to which it belongs, is the *idle time* that task i incurs between processing successive batches:

$$\tau_i^{idle} = \tau_n^{cycle} - \tau_i, \quad \forall n, i \in \mathcal{P}_n \tag{4.4}$$

Given the unstable nature of the material in state s_{kn} between tasks i_{kn} and $i_{k+1,n}$ in a zero-wait train n, the amount of this material produced by task i_{kn} must be equal to the amount consumed by task $i_{k+1,n}$. We therefore have

$$\bar{B}_{i_{kn},s_{kn}} = B_{i_{k+1,n},s_{kn}} \quad \forall n, k = 1, .., m_n - 1] \tag{4.5}$$

where the quantities $\bar{B}_{is}$ and B_{is} are as defined in section 3.4.

We now turn our attention to the stable states. In general, a stable state s will be consumed by

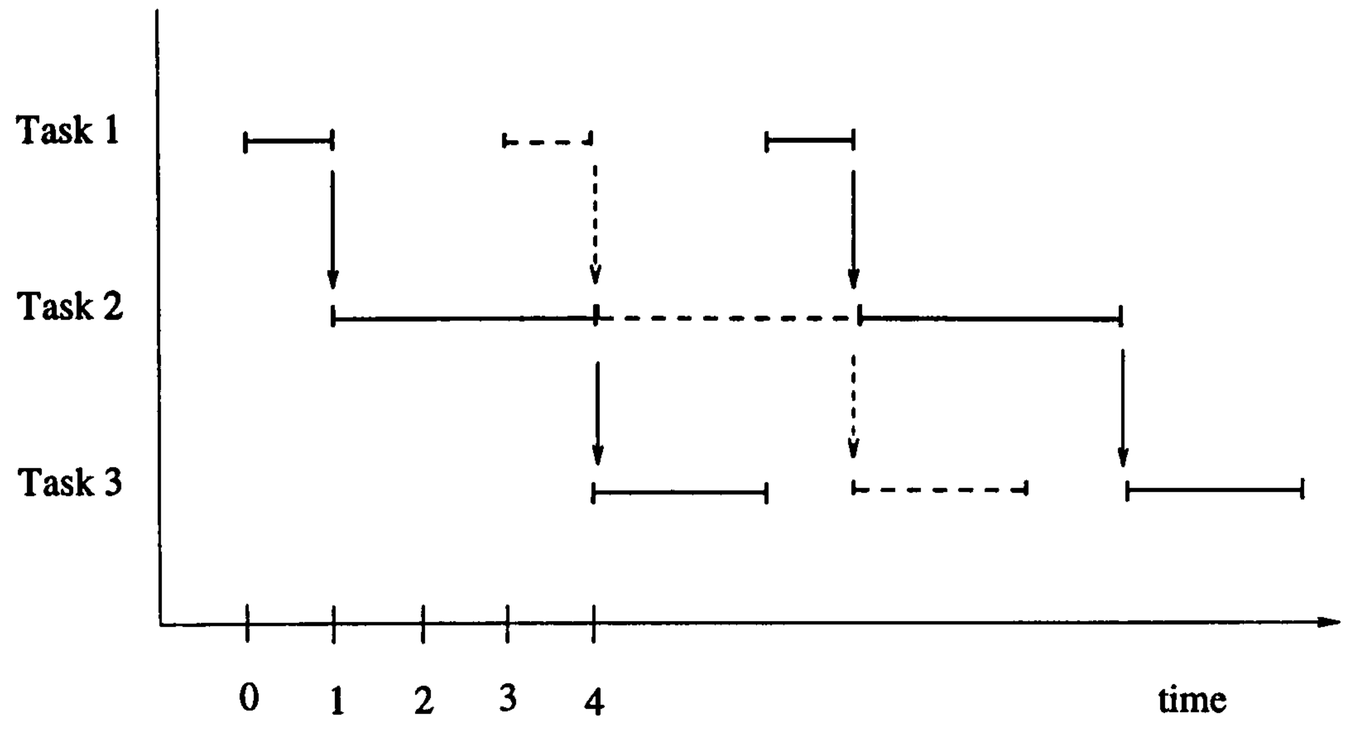

Figure 4.3: Gantt Chart for "Zero-Wait" Train Operation ($\tau_1 = 1hr$; $\tau_2 = 3hr$; $\tau_3 = 2hr$)

a subset $\mathcal{N}_s$ of the zero-wait trains in the STN and produced by another subset $\bar{\mathcal{N}}_s$. Furthermore, such states may also be raw materials or final products of the entire process. We therefore formulate the following material balance constraints:

$$\sum_{n \in \bar{\mathcal{N}}_s} \sum_{i \in \mathcal{P}_n} \frac{\bar{B}_{is}}{\tau_n^{cycle}} = \sum_{n \in \mathcal{N}_s} \sum_{i \in \mathcal{P}_n} \frac{B_{is}}{\tau_n^{cycle}} + R_s \qquad \forall s \in \mathcal{SS} \tag{4.6}$$

We note that, since task i in "zero-wait" train n produces an amount $\bar{B}_{is}$ of material s every τ_n^{cycle} time units, the quantity $\bar{B}_{is}/\tau_n^{cycle}$ is the average rate of such production. This is summed over all tasks[1] i in train n, and all trains n capable of producing s, overall giving rise to the first term on the left hand side of (4.6). A similar consideration leads to the double summation on the right hand side of (4.6) representing the total average consumption rate of s.

The quantity R_s appearing on the right hand side of (4.6) is the net rate at which material state s is produced. Thus, R_s is negative for raw materials and positive for end products. In the case of intermediate materials, R_s can be either zero or a positive number as these may be allowed to accumulate. More generally, R_s will be limited to lie within given minimum and maximum limits:

$$R_s^{min} \leq R_s \leq R_s^{max} \qquad \forall s \tag{4.7}$$

If net accumulation of any intermediate material s is undesirable, setting $R_s^{min} = R_s^{max} = 0$ will ensure that this does not take place.

[1]Of course, in most practical cases, $\bar{B}_{is}$ will be zero for all but one of the tasks i in train n.

4.3. Objective Function

The total net revenue of the process is adopted as the performance criterion for the optimisation. In the most general case, this comprises the capital cost of the equipment, the operating costs including those related to utilities and raw materials, and the revenue from the products.

The sizes and other characteristics of any *new* equipment items that are to be included in the process form part of the time invariant parameters ν_i for the task under consideration. The capital cost is consequently a function of these characteristics and is denoted by $C_i(\nu_i)$. The capital cost of already *existing* items of equipment is taken as zero.

The operation of the various tasks may require the consumption of utilities such as cooling water, steam and electricity. The instantaneous rate $r_{ui}(t)$ of consumption of a utility u by a batch of task i will generally vary over the duration of the task. In principle, it can be expressed in terms of the values of the variables describing the task:

$$r_{ui}(t) = r_{ui}(x_i(t), \dot{x}_i(t), y_i(t), u_i(t), \nu_i) \qquad \forall u, i, t \in [0, \tau_i] \tag{4.8}$$

The *total* amount of utility u consumed during a batch of task i is then given by:

$$U_{ui}(\tau_i) = \int_0^{\tau_i} r_{ui}(x_i(t), \dot{x}_i(t), y_i(t), u_i(t), \nu_i)dt \qquad \forall u, i \tag{4.9}$$

which can be expressed in differential equation form as:

$$\frac{dU_{ui}}{dt} = r_{ui}(x_i(t), \dot{x}_i(t), y_i(t), u_i(t), \nu_i); \qquad U_{ui}(0) = 0 \qquad \forall u, i, t \in [0, \tau_i] \tag{4.10}$$

Thus, $U_{ui}(t)$ can be viewed as an additional element of the vector of differential variables $x_i(t)$ that are used to describe task i.

Combining the above objective function contributions yields the overall objective function for the process as a measure of the net revenue per unit time of operation:

$$max \qquad -\lambda \sum_i C_i(\nu_i) - \sum_u C_u \sum_n \frac{1}{\tau_n^{cycle}} \sum_{i \in \mathcal{P}_n} U_{ui}(\tau_i) + \sum_s C_s R_s \tag{4.11}$$

where λ is the capital cost annualisation factor, C_u the unit cost of utility u, and C_s the unit cost (or value) of material in state s.

Material	$FeedA$	$FeedB$	$FeedF$	Int	Pr
Unit value ($'000£/kmol$)	10	10	20	-1	50

Table 4.1: Illustrative Example: Unit Values for Process Materials

We note that the last term of (4.11) is, in fact, the revenue from final product production (corresponding to states s with $R_s > 0$) minus the cost of raw material supplies (corresponding to states s with $R_s < 0$) . The accumulation of intermediates can be treated as either a cost or a revenue for the process by utilising a negative or positive value for the unit cost (C_s) respectively. For instance, undesirable by-products (*e.g.* wastes) may have a negative C_s reflecting the cost of their disposal.

The minimisation of the above objective is achieved by manipulating the design and operation of each processing step through the control variables $u_i(t)$, the time invariant parameters ν_i, the processing time τ_i and the amounts of each state s consumed by each task B_{is}. The intensive properties of each state and, for stable states, the rate R_s of external supply or delivery are also considered as optimisation parameters.

4.4. Illustrative Example

Consider again the two-stage reaction process described in section 3.5. We aim to design an optimal set of equipment items and determine optimal operating policies for each of the two tasks in this process. According to the assumptions introduced in section 4.1, a single equipment item is to be dedicated to each task. All material states are stable and consequently unlimited intermediate storage is utilised for each state. A possible plant flowsheet is given in figure 4.4. The unit values for the materials handled in the process are given in Table 4.1. It should be noted that the unit value of Int is set to a small negative number, reflecting the undesirability of building up stocks of this material. The cost of the cooling energy consumed in Reaction 1 and heating energy consumed in Reaction 2 are 0.002 $£/GJ$ and 4.0 $£/GJ$ respectively.

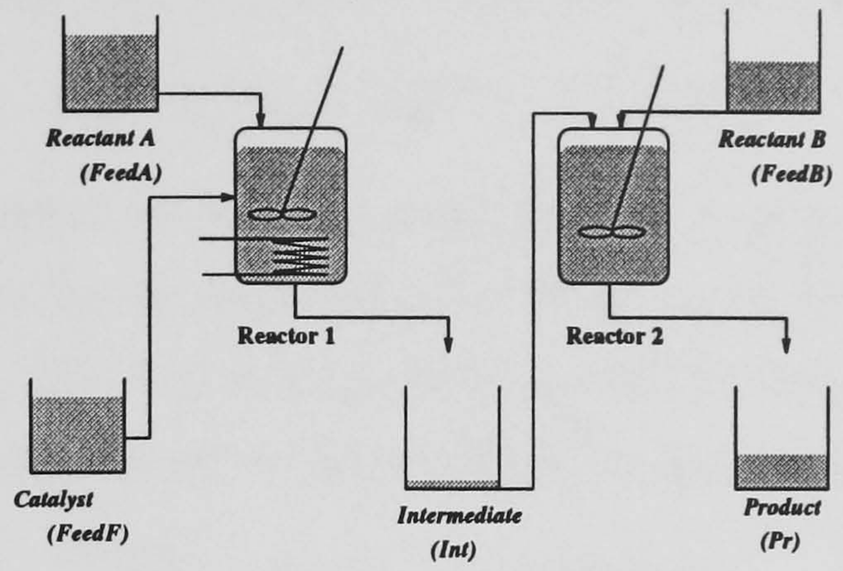

Figure 4.4: Illustrative Example: Plant Flowsheet

4.4.1. Material Balance Constraints

Since all materials handled in the process are stable, there are two zero-wait trains with one task in each. We therefore have:

$$\tau_1^{cycle} \geq \tau_1 \tag{4.12}$$

$$\tau_2^{cycle} \geq \tau_2 \tag{4.13}$$

Applying equation (4.6) to every material state yields:

$$State\ FeedA \qquad R_{FeedA} = \frac{B_{1,FeedA}}{\tau_1^{cycle}} \tag{4.14}$$

$$State\ FeedF \qquad R_{FeedF} = \frac{B_{1,FeedF}}{\tau_1^{cycle}} \tag{4.15}$$

$$State\ FeedB \qquad R_{FeedB} = \frac{B_{2,FeedB}}{\tau_2^{cycle}} \tag{4.16}$$

$$State\ Int \qquad \frac{\bar{B}_{1,Int}}{\tau_1^{cycle}} = \frac{B_{2,Int}}{\tau_2^{cycle}} + R_{Int} \tag{4.17}$$

$$State\ Pr \qquad R_{Pr} = \frac{\bar{B}_{2,Pr}}{\tau_2^{cycle}} \tag{4.18}$$

4.4.2. Objective Function

The objective function of the process is given by equation (4.11), taking into account capital cost, utility consumption and material revenue.

The capital cost of the plant will generally be a function $C(V_R)$ of the reactor sizes V_{R_1} and V_{R_2}. The latter are examples of time invariant parameters ν_i (*cf.* section 3.3). For the purposes of

the optimisation, they will normally be subject to lower and upper limits (*cf.* equation (3.9)):

$$V_{R_i}^{min} \leq V_{R_i} \leq V_{R_i}^{max}, \quad i = 1, 2 \tag{4.19}$$

In this example, the instantaneous rates of consumption of cooling energy in Reaction 1 and heating energy in Reaction 2 can be identified directly with the control variables Q_{cw} and Q_{steam} respectively (*cf.* equation 4.8). The calculation of the total consumption of cooling and heating energy in the two tasks can be expressed in differential form (see section 4.3):

$$\frac{dU_{cw,1}}{dt} = Q_{cw}, \quad U_{cw,1}(0) = 0 \tag{4.20}$$

$$\frac{dU_{steam,2}}{dt} = Q_{steam}, \quad U_{steam,2}(0) = 0 \tag{4.21}$$

Therefore, the net revenue of the process is calculated through:

$$max \quad 50R_{Pr} - R_{Int} + 10R_{FeedA} + 10R_{FeedB} + 20R_{FeedF} - C_{cw}\frac{U_{cw,1}}{\tau_1^{cycle}} - C_{steam}\frac{U_{steam,2}}{\tau_2^{cycle}} - \lambda(C(V_{R_1}) + C(V_{R_2})) \tag{4.22}$$

4.5. Concluding Remarks

A mathematical formulation for the design of batch processes has been proposed in this chapter. The formulation is based on the mathematical characterisation of process recipes presented in Chapter 3.

The formulation assumes that the flowsheet structure is given and aims at determining the precise nature of the materials handled in the process, the operating policies of the various processing stages and the sizes of the equipment items if desired.

An aggregate view of production scheduling is considered, allowing for both stable as well as unstable material states. In the former case, unlimited intermediate storage is provided whereas in the latter case zero-wait task trains are assumed.

The total net revenue of the process is adopted as the performance criterion for the optimisation taking into account the annualised capital cost of the process, the net production revenue from material consumption and production and the utility consumption. The solution method adopted for the resulting infinite dimensional dynamic optimisation problem is considered in the next chapter.

Chapter 5

Mathematical Solution Methods for the Integrated Batch Process Design Problem

The mathematical formulation presented in Chapter 4 is a complex infinite dimensional multistage dynamic optimisation problem. This chapter describes the solution methodology adopted for the solution of this problem in the context of the optimal design of integrated batch processes. We also briefly consider the implementation of a prototype sofware tool for integrated batch process design.

5.1. Summary of Mathematical Formulation

For the sake of ease of reference in the remainder of this chapter, we start by summarising the main components of the mathematical formulation presented in chapters 3 and 4:

$$max \qquad -\lambda \sum_i C_i(\nu_i) - \sum_u C_u \sum_n \frac{1}{\tau_n^{cycle}} \sum_{i \in \mathcal{P}_n} U_{ui} + \sum_s C_s R_s \tag{4.9}$$

subject to:

State constraints: For every state s,

$$z_s^{min} \leq z_s \leq z_s^{max} \qquad \forall s \tag{3.1}$$

$$C_s^I(z_s) \leq 0 \qquad \forall s \tag{3.2}$$

Task constraints: For every task i,

$$f_i(x_i(t), \dot{x}_i(t), y_i(t), u_i(t), \nu_i) = 0 \qquad \forall i, t \in [0, \tau_i] \tag{3.3}$$

$$h_i(x_i(t), \dot{x}_i(t), y_i(t), u_i(t), \nu_i) \leq 0 \qquad \forall i, t \in [0, \tau_i] \tag{3.4}$$

$$g^E_{i\kappa}(x_i(t_{i\kappa}), \dot{x}_i(t_{i\kappa}), y_i(t_{i\kappa}), u_i(t_{i\kappa}), \nu_i) = 0 \qquad \forall i, t_{i\kappa} \in [0, \tau_i], \lambda = 1, 2, \cdots \tag{3.5}$$

$$g^I_{i\kappa}(x_i(t_{i\kappa}), \dot{x}_i(t_{i\kappa}), y_i(t_{i\kappa}), u_i(t_{i\kappa}), \nu_i) \leq 0 \qquad \forall i, t_{i\kappa} \in [0, \tau_i], \lambda = 1, 2, \cdots \tag{3.6}$$

$$\nu_i^{min} \leq \nu_i \leq \nu_i^{max} \qquad \forall i \tag{3.7}$$

$$u_i^{min}(\nu_i) \leq u_i(t) \leq u_i^{max}(\nu_i) \qquad \forall i, t \in [0, \tau_i] \tag{3.8}$$

$$I_i(x_i(0), \dot{x}_i(0), y_i(0), u_i(0), \nu_i, \{z_s, B^d_{is}, s \in S_i\}) = 0 \qquad \forall i \tag{3.11}$$

State-task Coupling: For every task i,

$$B_{is} = B^d_{is} + B^c_{is} \qquad \forall i, s \in S_i \tag{3.10}$$

$$B^c_{is} = B^c_{is}(x_i(\tau_i), \dot{x}_i(\tau_i), y_i(\tau_i), u_i(\tau_i), \nu_i) \qquad \forall s \in S_i \tag{3.12}$$

$$\bar{B}_{is} = \bar{F}_{is}(x_i(\tau_i), \dot{x}_i(\tau_i), y_i(\tau_i), u_i(\tau_i), \nu_i) \qquad \forall i, s \in \bar{S}_i \tag{3.15}$$

$$z_s = F_{is}(x_i(\tau_i), \dot{x}_i(\tau_i), y_i(\tau_i), u_i(\tau_i), \nu_i) \qquad \forall i, s \in \bar{S}_i \tag{3.16}$$

$$G_i\left(\nu_i, \{z_s, B_{is}, s \in S_i\}, \{z_s, \bar{B}_{is}, s \in \bar{S}_i\}\right) \leq 0 \qquad \forall i \tag{3.17}$$

Other Constraints:

$$\tau_n^{cycle} \geq \tau_i, \quad \forall n, i \in \mathcal{P}_n \tag{4.3}$$

$$\bar{B}_{i_{kn}, s_{kn}} = B_{i_{k+1,n}, s_{kn}} \quad \forall n, k \in [1, m_n - 1] \tag{4.5}$$

$$\sum_{n \in \bar{\mathcal{N}}_s} \sum_{i \in \mathcal{P}_n} \frac{\bar{B}_{is}}{\tau_n^{cycle}} = \sum_{n \in \mathcal{N}_s} \sum_{i \in \mathcal{P}_n} \frac{B_{is}}{\tau_n^{cycle}} + R_s \qquad \forall s \in \mathcal{SS} \tag{4.5}$$

$$R_s^{min} \leq R_s \leq R_s^{max} \qquad \forall s \tag{4.6}$$

$$\frac{dU_{ui}}{dt} = r_{ui}(x_i(t), \dot{x}_i(t), y_i(t), u_i(t), \nu_i); \qquad U_{ui}(0) = 0 \qquad \forall u, i, t \in [0, \tau_i] \tag{4.10}$$

This is a constrained optimisation problem in the following variables:

For each task i	: τ_i, ν_i, $\{x_i(t), y_i(t), u_i(t), t \in [0, \tau_i]\}$,
For each state s	: z_s, R_s (stable states only),
For each task-input state pair $(i; s \in S_i)$	: B_{is}, B^d_{is}, B^c_{is},
For each task-output state pair $(i; s \in \bar{S}_i)$	: $\bar{B}_{is}$.

Note that, in the above, we have included the utility consumption variables U_{ui} for task i within the vector of differential variables x_i.

5.2. Handling the Infinite Dimensional Nature of the Optimisation Problem

A major difficulty with the problem described in section 5.1 is its infinite dimensional nature. This arises from the fact that a subset of the variables describing each task i, namely $x_i(t)$, $y_i(t)$ and $u_i(t)$, are, in fact, functions of time t over the finite domain $[0, \tau_i]$.

Similarly, certain of the constraints, notably the task model (3.3) and the inequality path constraints (3.4) must hold all *all* times $t \in [0, \tau_i]$ rather than just at a finite number of distinct points.

Two major methodologies for dealing with infinite dimensional dynamic optimisation problems have emerged over the past couple of decades. Both aim to reduce the problem to a finite dimensional one.

5.2.1. The Complete Parameterisation Approach

This approach (Cuthrell and Biegler, 1987; Renfro *et al.*, 1987) approximates all the time-varying variables in the model ($x_i(t)$, $y_i(t)$, $u_i(t)$) in terms of finite sets of parameters:

$$\left.\begin{aligned} x_i(t) &= \chi_i(t, \alpha_i) \\ y_i(t) &= \psi_i(t, \beta_i) \\ u_i(t) &= \phi_i(t, \gamma_i) \end{aligned}\right\} \quad t \in [0, \tau_i] \tag{5.1}$$

where $\chi_i(\cdot,\cdot)$, $\psi_i(\cdot,\cdot)$ and $\phi_i(\cdot,\cdot)$ are functions of a *given*, relatively simple mathematical form (*e.g.* piecewise polynomials defined over a finite element partition of the domain $t \in [0, \tau_i]$). On the other hand, α_i, β_i, γ_i are *finite* sets of parameters to be determined by the optimisation.

Once the variables have been discretised in the above manner, the infinite dimensional constraints (3.3) and (3.4) can also be replaced by finite approximations. For instance, this can be achieved by enforcing these constraints at a finite number of collocation points in each finite element.

Overall, then, the infinite dimensional problem described in section 5.1 becomes a large nonlinear programming (NLP) problem involving the maximisation of the nonlinear objective function (4.11) subject to a large set of nonlinear equality and inequality constraints, with respect to the finite dimensional vector of the following variables:

$$\begin{gathered} \tau_i, \nu_i, \alpha_i, \beta_i, \gamma_i, \qquad \forall i \\ z_s, \quad \forall s; \quad R_s \quad \forall s \in \mathcal{SS} \\ B_{is}, B_{is}^d, B_{is}^c \quad \forall ij, s \in S_i \\ \bar{B}_{is} \quad \forall i, j, s \in \bar{S}_i \end{gathered} \tag{5.2}$$

5.2.2. The Control Vector Parameterisation Approach

One potential problem with the complete parameterisation approach is the size of the NLP that it generates. In particular, the models describing some tasks of interest to this thesis (*e.g.* batch distillation) may comprise several hundreds or even thousands of equations (3.3) and variables $x_i(t)$ and $y_i(t)$. Furthermore, process design problems of industrial relevance could comprise several such tasks (see, for instance, the example presented and solved in section 7.2). The parameterisation of these problems along the lines discussed in section 5.2.1 could therefore result in NLPs involving tens of thousands of constraints and variables.

An alternative to complete parameterisation is the control vector parameterisation approach (Sargent and Sullivan, 1977; Morison and Sargent, 1986; Vassiliadis *et al.*, 1994b; Vassiliadis *et al.*, 1994a). Here we apply parameterisation to the control variables $u_i(t)$ only:

$$u_i(t) = \phi_i(t, \gamma_i), \qquad \forall i \tag{5.3}$$

which allows the controls u_i to be expressed in terms of a finite vector of parameters γ_i for each task i.

We note that, for task i, once we specify the values of:

- the control parameters, γ_i;
- the time invariant parameters, ν_i;
- the intensive properties z_s for each input state $s \in S_i$;
- the amounts B^d_{is}, $s \in S_i$ that form the initial charge to this task;

we can solve the initial conditions (3.11) which can now be written as:

$$I_i(x_i(0), \dot{x}_i(0), y_i(0), \phi_i(0, \gamma_i), \nu_i, \{z_s, B^d_{is}, s \in S_i\}) = 0 \qquad \forall i \tag{5.4}$$

together with the model equations at time $t = 0$:

$$f_i(x_i(0), \dot{x}_i(0), y_i(0), \phi_i(0, \gamma_i), \nu_i) = 0 \tag{5.5}$$

to determine the initial values:

$$\{x_i(0), \dot{x}_i(0), y_i(0)\} \tag{5.6}$$

of the variables in task i.

Once this initialisation is complete, and given the task processing time τ_i, we can integrate the DAE system (3.3) written as:

$$f_i(x_i, \dot{x}_i, y_i, \phi_i(t, \gamma_i), \nu_i) = 0 \qquad \forall i, t \in [0, \tau_i] \tag{5.7}$$

to determine $x_i(t)$, $\dot{x}_i(t)$, $y_i(t)$, $t \in [0, \tau_i]$. From this solution, we can also evaluate the residuals of path constraints (3.4) and point constraints (3.5)-(3.6):

$$h_i(x_i(t), \dot{x}_i(\tau_i), y_i(\tau_i), \phi_i(\tau_i, \gamma_i), \nu_i), \qquad \forall i \tag{5.8}$$

$$g^E_{i\kappa}(x_i(t_{i\kappa}), \dot{x}_i(t_{i\kappa}), y_i(t_{i\kappa}), \phi_i(t_{i\kappa}, \gamma_i), \nu_i), \qquad \forall i, \kappa = 1, 2, .. \tag{5.9}$$

$$g^I_{i\kappa}(x_i(t_{i\kappa}), \dot{x}_i(t_{i\kappa}), y_i(t_{i\kappa}), \phi_i(t_{i\kappa}, \gamma_i), \nu_i), \qquad \forall i, \kappa = 1, 2, .. \tag{5.10}$$

We can also calculate the amounts B^c_{is} of input states $s \in S_i$ fed to task i in a continuous manner *during* its operation (*cf.* equation 3.12):

$$B^c_{is} = B^c_{is}(x_i(\tau_i), \dot{x}_i(\tau_i), y_i(\tau_i), \phi_i(\tau_i, \gamma_i), \nu_i) \tag{5.11}$$

and the amounts $\bar{B}_{is}$ and composition z_s of all output states $s \in \bar{S}_i$ of task i (*cf.* equations 3.15-3.16):

$$\bar{B}_{is} = \bar{F}_{is}(x_i(\tau_i), \dot{x}_i(\tau_i), y_i(\tau_i), \phi_i(\tau_i, \gamma_i), \nu_i) \qquad \forall i, s \in \bar{S}_i \tag{5.12}$$

$$z_s = F_{is}(x_i(\tau_i), \dot{x}_i(\tau_i), y_i(\tau_i), \phi_i(\tau_i, \gamma_i), \nu_i) \qquad \forall i, s \in \bar{S}_i \tag{5.13}$$

Finally, we can obtain the contribution of the task operating cost to the objective function (4.8) by evaluating the utility consumption (*cf.* equation 4.9):

$$U_{ui}(\tau_i) = \int_0^{\tau_i} r_{ui}(x_i(t), \dot{x}_i(t), y_i(t), \phi_i(\tau_i, \gamma_i), \nu_i)dt \qquad \forall u, i \tag{5.14}$$

The above computation scheme is summarised in figure 5.1. We note that its overall effect is that, given values of the finite set of parameters:

$$\Theta_i \equiv \left\{\gamma_i, \nu_i, \tau_i, \{t_{i\kappa}, \forall \kappa\}, \{z_s, B^d_{is}, s \in \bar{S}_i\}\right\}, \qquad \forall i \tag{5.15}$$

the task variables $x_i(t)$, $y_i(t)$, $t \in [0, \tau_i]$ are completely eliminated via the solution of the task model (5.7) and the initial conditions (5.4). The elimination allows us to evaluate all other path and point constraints associated with the task, as well as its contribution to the objective function. Consequently, the optimisation problem is expressed in terms of the relatively small set of task parameters:

$$\Theta \equiv \bigcup_i \Theta_i \tag{5.16}$$

We note that the sets Θ_i for different tasks i are not necessarily disjoint since two or more tasks may share the same input state (and consequently, the same z_s). Moreover, the optimisation will also involve certain parameters, such as R_s (*cf.* section 4.2) not directly associated with tasks. We will return to consider the form of the overall optimisation problem and its solution in more detail in section 5.4.

5.3. Implementational Issues for Control Vector Parameterisation

Our implementation of control vector parameterisation is largely based on the ideas recently described by Vassiliadis *et al.* (1994b). In this section, we outline our treatment of some important implementational issues.

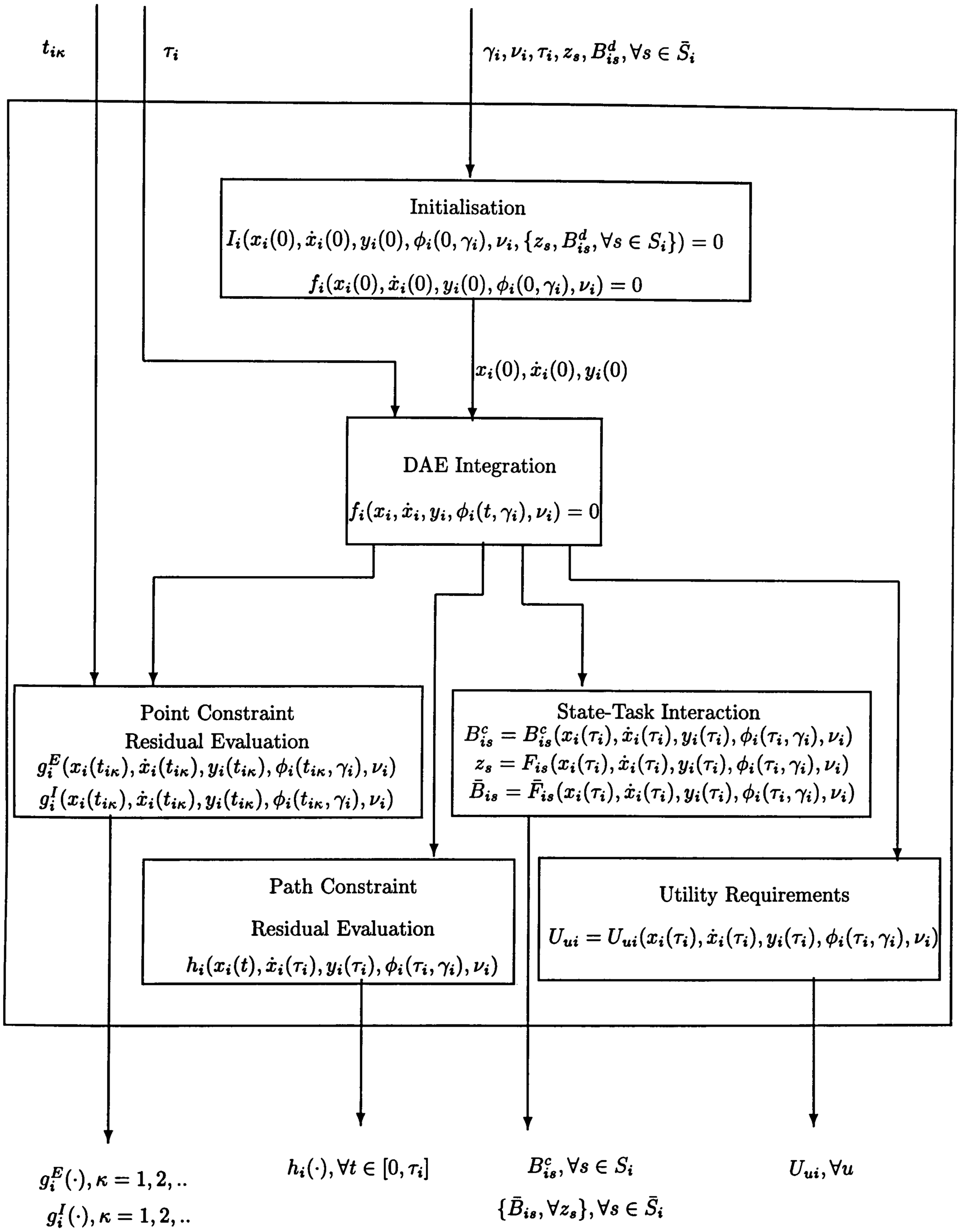

Figure 5.1: Computational Sequence for Task i in Control Vector Parameterisation Approach

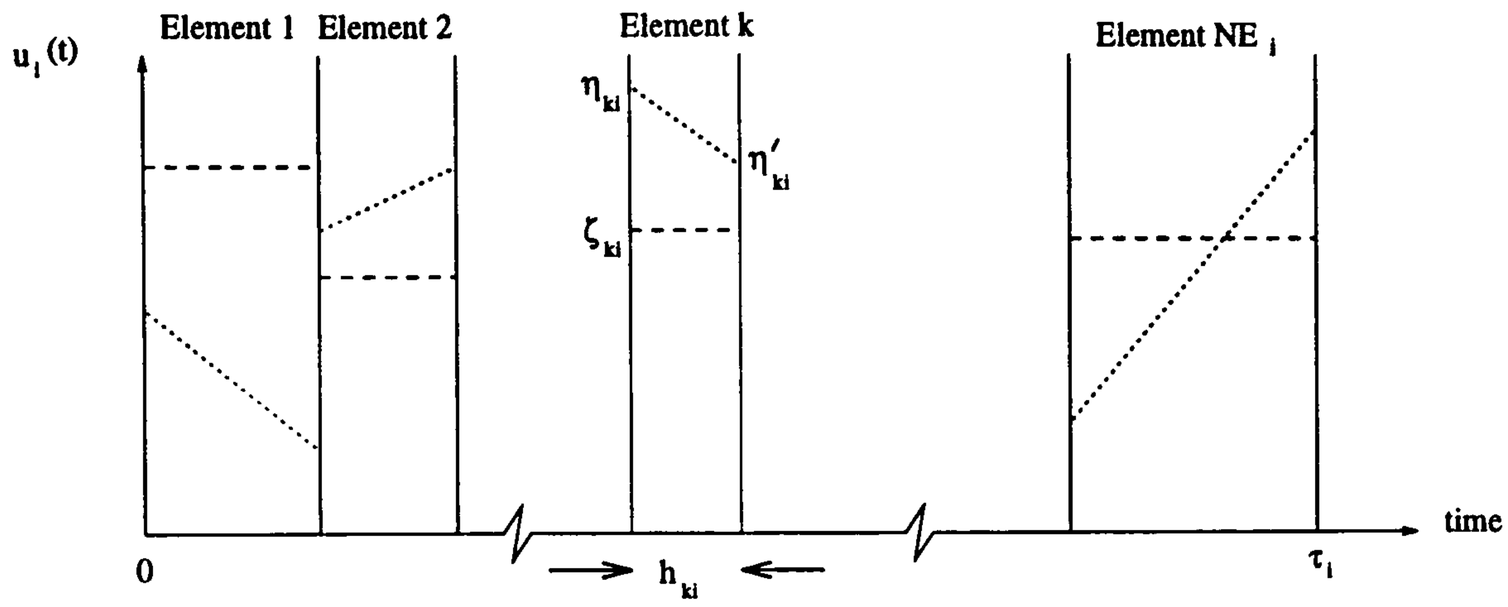

Figure 5.2: Control Variable Parameterisation

5.3.1. Choice of Control Variable Parameterisation

We partition the domain $[0, \tau_i]$ into a number of finite elements and allow control variables to be expressed as piecewise polynomials on this partition. In particular, we allow the following forms of control variables:

- piecewise constant;
- piecewise linear.

These are illustrated in figure 5.2. We note that piecewise constant controls can be described by a single parameter ζ_{ki} per finite element, while two parameters (η_{ki}, η'_{ki}) are necessary for piecewise linear controls. The length of each finite element h_{ki} is also treated as a parameter. Thus for the piecewise constant case, we have the set of control parameters (*cf.* equation 5.3):

$$\gamma_i \equiv \{\zeta_{ki}, h_{ki}, k = 1, .., NE_i\} \tag{5.17}$$

while for the piecewise linear one,

$$\gamma_i \equiv \left\{\eta_{ki}, \eta'_{ki}, h_{ki}, k = 1, .., NE_i\right\} \tag{5.18}$$

One very desirable property of these simple control variable parameterisations is the fact that the variable bound constraints (3.8) can be expressed directly in terms of the corresponding

parameters. Thus, for the piecewise constant case, the infinite dimensional constraint (3.8) can be written as:

$$u_i^{min}(\nu_i) \leq \zeta_{ki} \leq u_i^{max}(\nu_i) \qquad \forall i, k = 1, .., NE_i \tag{5.19}$$

and for the piecewise linear case, as:

$$\left.\begin{array}{l} u_i^{min}(\nu_i) \leq \eta_{ki} \leq u_i^{max}(\nu_i) \\ u_i^{min}(\nu_i) \leq \eta'_{ki} \leq u_i^{max}(\nu_i) \end{array}\right\} \forall i, k = 1, .., NE_i \tag{5.20}$$

In both cases, we have the constraint:

$$\sum_{k=1}^{NE_i} h_{ki} = \tau_i \quad \forall i \tag{5.21}$$

In the interest of avoiding numerical problems caused by one or more elements vanishing, we also impose a lower bound on the element lengths:

$$h_{ki} \geq \epsilon \quad \forall i, k = 1, .., NE_i \tag{5.22}$$

where ϵ is a small positive quantity.

Although the above choice of only two forms of control parameterisation may appear to be rather restrictive, it does cover the forms of control action used in most practical batch applications. Moreover, other forms of control may be derived directly from them. For instance, a piecewise linear control $u_i(t)$ with continuity at finite element boundaries can be handled by treating u_i as a differential variable (*i.e.* part of the x_i vector) defined via the equation:

$$\dot{u}_i = \hat{u}_i; \qquad u_i(0) = \hat{\nu}_i \tag{5.23}$$

where the newly introduced variable $\hat{u}_i(t)$ is treated as a piecewise *constant* control and $\hat{\nu}_i$ as a time invariant parameter. This idea is illustrated schematically in figure 5.3.

5.3.2. Handling of Inequality Path Constraints

Inequality path constraints such as (5.8) pose special problems because of their infinite dimensional nature *i.e.* the fact that they are required to hold at *all* times $t \in [0, \tau_i]$. The efficient treatment of

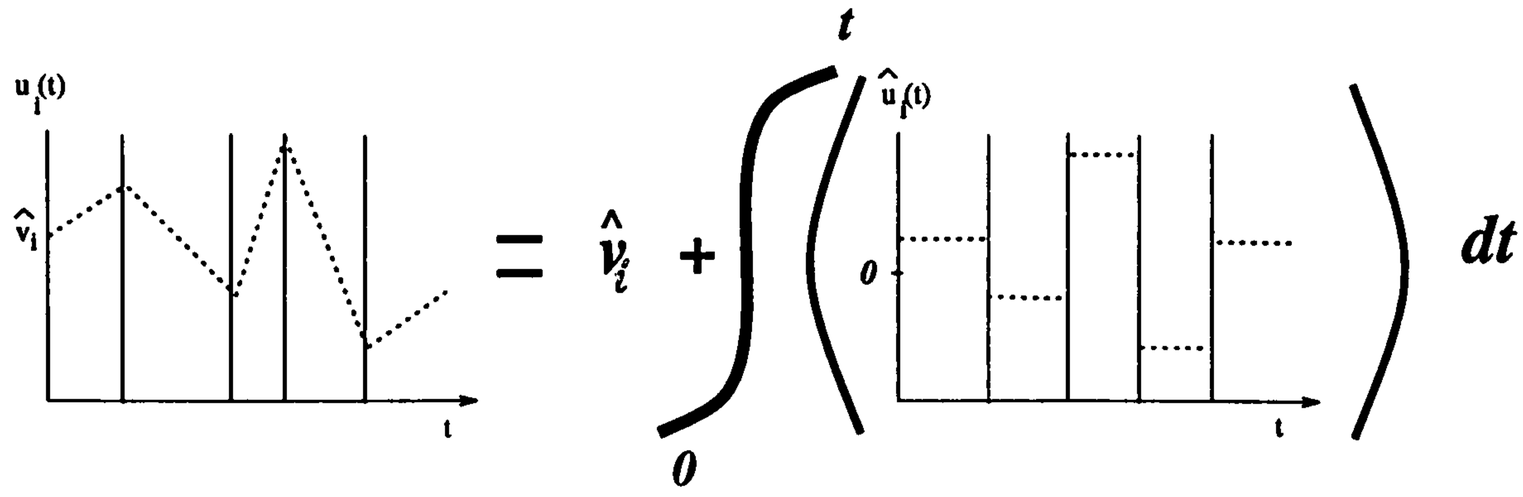

Figure 5.3: Piecewise Linear Control with Continuity at Finite Element Boundaries

such constraints has been a major issue in research on dynamic optimisation algorithms for more than two decades. A review has recently been given by Vassiliadis *et al.* (1994a; 1994b).

In our implementation, we adopt the approach proposed by Vassiliadis *et al.* (1994b). This converts the infinite dimensional constraint (5.8) to:

- A single end-point inequality constraint:

$$X_i(\tau_i) \leq \epsilon \tag{5.24}$$

where ϵ is a small positive tolerance and X_i is a new differential variable defined by the differential equation:

$$\dot{X}_i = \left[\max\left(0, h_i(x_i(t), \dot{x}_i(t), y_i(t), \phi_i(\tau_i, \gamma_i), \nu_i)\right)\right]^2 \tag{5.25}$$

subject to the initial condition: $X_i = (0)$.

- A set of interior point inequality constraints:

$$h_i(x_i(t_{ik}), \dot{x}_i(t_{ik}), y_i(t_{ik}), \phi_i(t_{ik}, \gamma_i), \nu_i) \leq 0, \quad k = 0, .., NE_i + 1 \tag{5.26}$$

where t_{ik} are selected to be the boundaries of the finite elements used for the control parameterisation (see section 5.3.1), *i.e.*:

$$t_{i0} = 0 \tag{5.27}$$

$$t_{ik} = \sum_{k'=1}^{k} h_{k'}, \qquad k = 1, .., NE_i \tag{5.28}$$

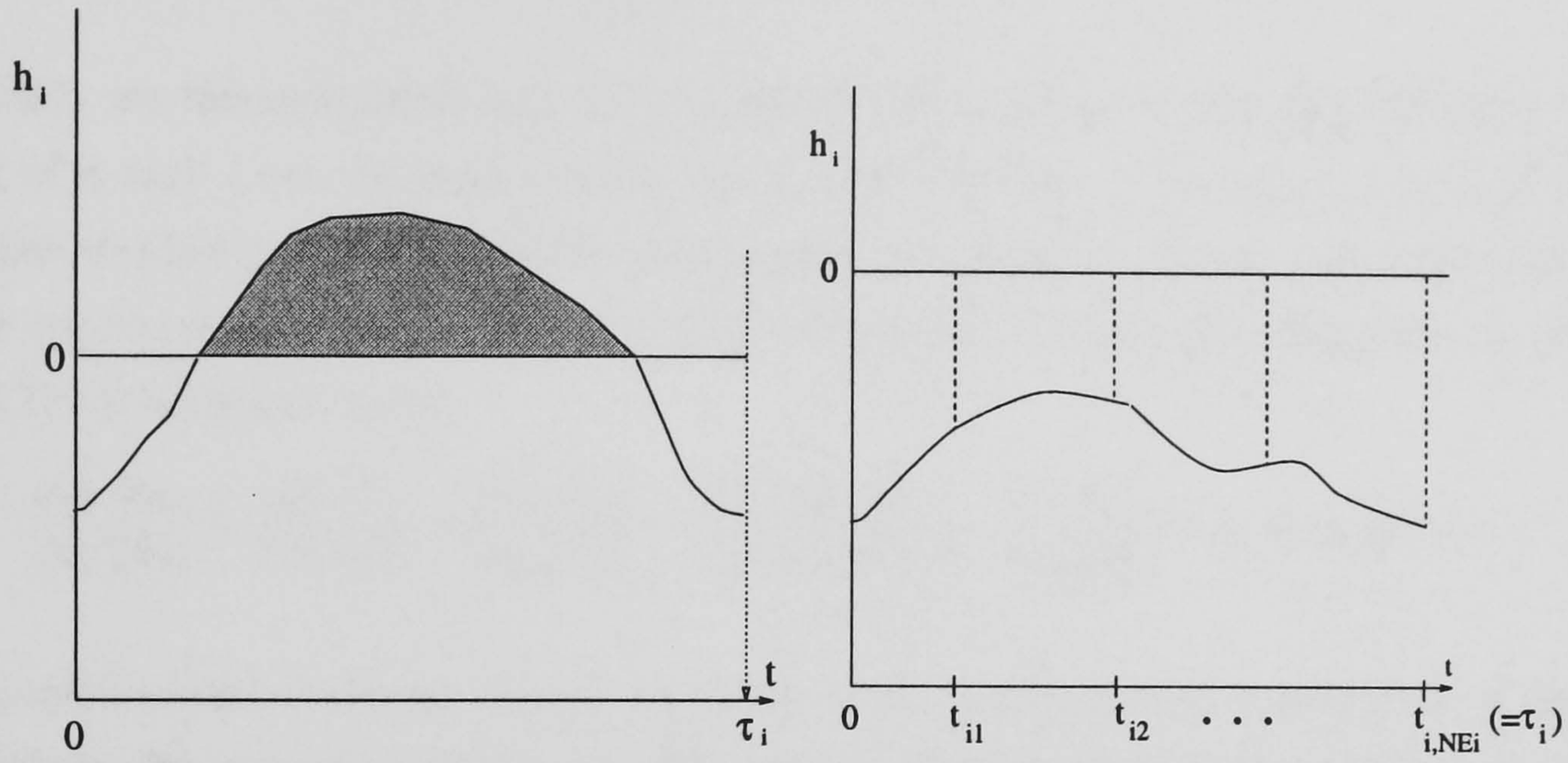

(a) Role of End-point Constraint (b) Role of Interior Point Constraints

Figure 5.4: Handling of Inequality Path Constraints

We note that (5.25) defines $X_i(\tau_i)$ to be the integral of the square of the constraint violation corresponding to the shaded area in figure 5.4(a). Thus constraint (5.24) is, in principle, sufficient to ensure that the original inequality path constraint (5.8) is satisfied everywhere within the given tolerance ϵ. However, as argued by Vassiliadis *et al.* (1994a), this constraint often causes erratic behaviour in the NLP solver. This is principally because, when $X_i(\tau_i) = 0$, no information is provided to the solver as to the relative position of the constraint $h_i(\cdot)$ with respect to its upper bound 0. This deficiency may be remedied by including the constraint (5.10) at a number of distinct points interspersed over the time domain $t \in [0, \tau_i]$. Thus, even if the path constraint is not violated at some iteration during the optimisation, its position at the element boundaries is still made known to the optimiser (see figure 5.4(b)).

In conclusion, it should be noted that strictly speaking the computational procedure summarised in figure 5.1 produces the residuals of the *finite* representations (5.24) and (5.26) of the path inequality constraints (5.8). Our experience with the approach is that it overall leads to satisfactory numerical behaviour in most practical applications.

5.3.3. Evaluation of Constraint and Objective Function Gradients

In section 5.3.1, we demonstrated how the values of the constraints and the objective function contribution of a task i can be expressed in terms of the vector of parameters Θ_i (*cf.* equation 5.15). However, sophisticated NLP solvers also require gradients for these quantities with respect to Θ_i. These can be obtained from the *sensitivity* equations obtained by differentiating the model equations (5.7) with respect to Θ_i:

$$\frac{\partial f_i}{\partial x_i}\frac{\partial x_i}{\partial \Theta_i} + \frac{\partial f_i}{\partial \dot{x}_i}\frac{\partial \dot{x}_i}{\partial \Theta_i} + \frac{\partial f_i}{\partial y_i}\frac{\partial y_i}{\partial \Theta_i} + \frac{\partial f_i}{\partial u_i}\frac{\partial \phi_i}{\partial \gamma_i}\frac{\partial \gamma_i}{\partial \Theta_i} + \frac{\partial f_i}{\partial \nu_i}\frac{\partial \nu_i}{\partial \Theta_i} = 0, \forall t \in [0, \tau_i] \tag{5.29}$$

where all partial derivatives shown should be understood to correspond to matrices of the appropriate dimensions. We note that the matrix $\frac{\partial \gamma_i}{\partial \Theta_i}$ is generally zero, with element (l, m) exceptionally being 1 if the m*th* element of vector Θ_i corresponds to the l*th* parameter γ_i. Matrix $\frac{\partial \nu_i}{\partial \Theta_i}$ has an analogous structure.

The "sensitivities"of the DAE system 5.7 are the gradients of the task variables x_i, y_i with respect to the parameters Θ_i:

$$\frac{\partial x_i}{\partial \Theta_i}(t), \frac{\partial y_i}{\partial \Theta_i}(t), \quad \forall t \in [0, \tau_i] \tag{5.30}$$

They can be obtained by integrating equation (5.29) subject to the initial conditions:

$$\frac{\partial I_i}{\partial x_i}\frac{\partial x_i}{\partial \Theta_i}(0) + \frac{\partial I_i}{\partial \dot{x}_i}\frac{\partial \dot{x}_i}{\partial \Theta_i}(0) + \frac{\partial I_i}{\partial y_i}\frac{\partial y_i}{\partial \Theta_i}(0) + \frac{\partial I_i}{\partial u_i}\frac{\partial \phi_i}{\partial \gamma_i}\frac{\partial \gamma_i}{\partial \Theta_i} + \frac{\partial I_i}{\partial \nu_i}\frac{\partial \nu_i}{\partial \Theta_i} = 0, \quad \forall t \in [0, \tau_i] \tag{5.31}$$

obtained by differentiating (5.4) with respect to Θ_i. Here all partial derivatives of I_i are understood to be evaluated at the initial values of the model variables; similarly $\frac{\partial \phi_i}{\partial \gamma_i}$ is evaluated at $t = 0$.

The integration of the sensitivity equations (5.29) can be carried out simultaneously with the original equations (5.7). Some efficiency gains can be achieved by exploiting the similarity in structure of the two systems (Dunker, 1984; Caracotsios and Stewart, 1985).

Once $\frac{\partial x_i}{\partial \Theta_i}(t)$, $\frac{\partial y_i}{\partial \Theta_i}(t)$, $t \in [0, \tau_i]$ have been evaluated, the gradients of the various constraints and the other quantities relating to task i can easily be calculated by the chain rule of differentiation. For instance, differentiating equation (5.12) with respect to Θ_i yields the gradients of the amount $\bar{B}_{is}$ of each output state $s \in \bar{S}_i$ produced by task i:

$$\frac{\partial \bar{B}_{is}}{\partial \Theta_i} = \frac{\partial \bar{F}_{is}}{\partial x_i}\frac{\partial x_i}{\partial \Theta_i}(\tau_i) + \frac{\partial \bar{B}_{is}}{\partial \dot{x}_i}\frac{\partial \dot{x}_i}{\partial \Theta_i}(\tau_i) + \frac{\partial \bar{B}_{is}}{\partial y_i}\frac{\partial y_i}{\partial \Theta_i}(\tau_i) + \frac{\partial \bar{B}_{is}}{\partial u_i}\frac{\partial \phi_i}{\partial \gamma_i}\frac{\partial \gamma_i}{\partial \Theta_i} + \frac{\partial \bar{B}_{is}}{\partial \nu_i}\frac{\partial \nu_i}{\partial \Theta_i} \tag{5.32}$$

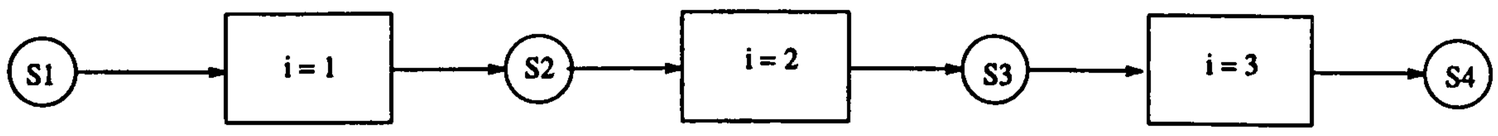

Figure 5.5: Three Task Process

5.4. Solution Algorithms for Multistage Systems

In section 5.2.2, we showed how the behaviour of a task i is completely determined in terms of a finite vector of parameters Θ_i. These include the intensive properties z_s for all input states $s \in S_i$ to the task (*cf.* equation 5.15).

An important part of the task behaviour concerns the determination of the intensive properties z_s of its *output* states $s \in \bar{S}_i$ (*cf.* equation 5.13). Of course, in many cases, these states will themselves affect downstream tasks i' forming part of *their* sets of parameters Θ'_i.

The above coupling between the tasks in the process establishes a *multistage* optimisation problem, with each task corresponding to a different stage. It also raises certain questions regarding the most appropriate way of solving this problem within the control vector parameterisation framework.

5.4.1. Algorithms Based on Exploitation of Task Coupling

Consider, for instance, a process comprising a sequence of three tasks $i = 1, 2, 3$ producing a final product $S4$ from a raw material $S1$ via intermediates $S2$ and $S3$ (see figure 5.5).

We note that the intensive properties z_{S2} of $S2$ are fully determined by the set of parameters Θ_1 describing task 1. They do not, therefore, need to be treated as independent optimisation parameters. Consequently, we define a *reduced* set of parameters $\bar{\Theta}_2$ for task $i = 2$ which does *not* include z_{S2}:

$$\bar{\Theta}_2 \equiv \left\{\gamma_2, \nu_2, \tau_2, \{t_{2\kappa}, \forall\kappa\}, B^d_{2,S2}\right\} = \Theta_2 - \{z_{S2}\} \tag{5.33}$$

where the *full* parameter set Θ_2 is as defined in (5.15).

Now, the behaviour of task $i = 2$ is fully determined by $\bar{\Theta}_2$ *plus* Θ_1 (since z_{S2} is a function of the latter). Consequently, these parameters fully determine the intensive properties z_{S3} of state $S3$

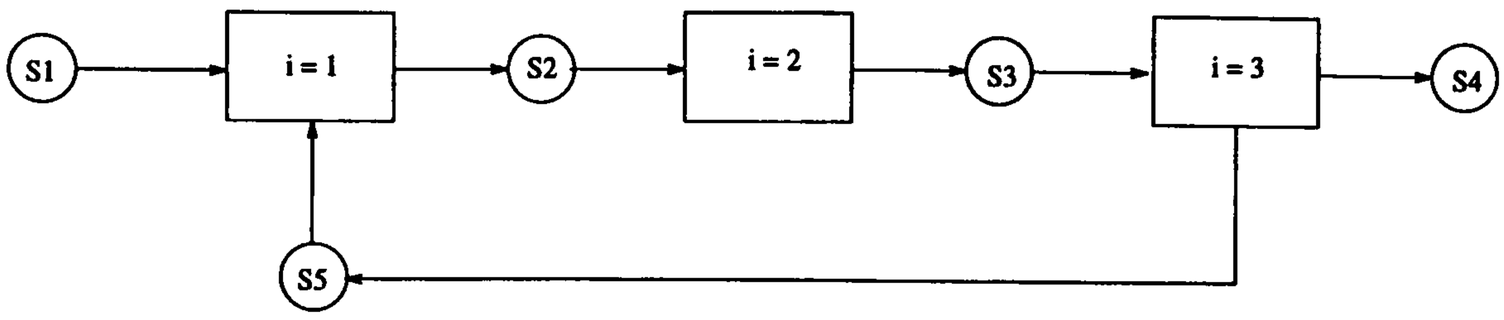

Figure 5.6: Three Task Process with Recycle

which are not, therefore, independent optimisation decisions. We can, therefore, define a reduced parameter set $\bar{\Theta}_3$ for task $i = 3$ which does not include z_{S3}:

$$\bar{\Theta}_3 \equiv \left\{\gamma_3, \nu_3, \tau_3, \{t_{3\kappa}, \forall\kappa\}, B^d_{3,S3}\right\} = \Theta_3 - \{z_{S3}\} \tag{5.34}$$

Thus, the behaviour of task $i = 3$ (and, hence, the overall performance of the process) is fully determined by the set of parameters:

$$\bar{\Theta} = \Theta_1 \bigcup \bar{\Theta}_2 \bigcup \bar{\Theta}_3 = \Theta - \{z_{S2}, z_{S3}\} \tag{5.35}$$

where $\Theta \equiv \bigcup_{i=1}^{3} \Theta_i$ (*cf.* equation 5.16). We note that, by exploiting the coupling between the tasks, we have been able to define the optimisation problem in terms of a reduced set of parameters $\bar{\Theta}$ which is potentially much smaller that the original set Θ.

The above treatment is, in fact, consistent with the algorithm proposed by Vassiliadis *et al.* (1994b) for the optimisation of multistage systems comprising a linear sequence of stages. Each stage is described by a DAE system, with its initial condition being determined from the final condition of the previous stage via so-called "junction" conditions.

5.4.2. Difficulties with Exploitation of Task Coupling

One difficulty with the approach described in section 5.4.1 arises with processing structures that are not purely sequential. For instance, suppose the process of figure 5.5 is modified to include a recycle stream of material $S5$ as shown in figure 5.6.

In this case, the reduced set of optimisation parameters $\bar{\Theta}$ must include, in addition to z_{S1}, the intensive properties of at least one of the three states on the loop (*i.e.* z_{S2}, or z_{S3}, or z_{S5}) even

though these are determined by the behaviour of a task in the process. This is necessary in order to permit the computation to be carried out – for instance, if $\bar{\Theta}$ includes both z_{S1} and z_{S5}, we can compute the sequence of tasks $i = 1, 2, 3$ just as before.

Of course, once we determine the behaviour of task $i = 3$, this will also determine new values z'_{S5} for the intensive properties of $S5$. In general, these will not be the same as those assumed initially. This, therefore, effectively establishes a set of equality constraints of the form (*cf.* equation 5.13):

$$z_{S5} - F_{3,S5}(x_3(\tau_3), \dot{x}_3(\tau_3), y_i(\tau_3), \phi_3(\tau_3, \gamma_3), \nu_3) = 0 \tag{5.36}$$

that must be enforced by the optimisation.

A different, and potentially more serious, difficulty with the multistage approach is of a numerical nature. Consider, again, the simple process illustrated in figure 5.5 and suppose that our objective is to maximise the production of product $S4$ subject to some quality constraints expressed in terms of intensive properties z_{S4}. This is to be achieved by manipulating the control variables $u_1(t)$, $u_2(t)$, $u_3(t)$ pertaining to the three tasks under consideration or , equivalently, the corresponding parameters γ_1, γ_2, γ_3. The potential difficulty with this is that, due to the long sequence of operations involved and the many intervening decision parameters, the optimisation algorithm will receive little information on the effects of the upstream decisions γ_1 on the amount and quality of the final product state $S4$. This phenomenon may exhibit itself as an ill-conditioned NLP problem, its effects becoming increasingly severe as the size of the process being optimised increases.

5.4.3. An Algorithm with Implicit Task Coupling

For the reasons explained in section 5.4.2, our algorithm for the solution of the multistage dynamic optimisation problem does *not* attempt to exploit the task coupling in order to reduce the size of the optimisation problem being solved. Instead, it operates on the entire parameter set Θ defined by equations (5.15) and (5.16). The task coupling is handled implicitly by enforcing the state intensive property constraints (5.13) and the mass balance constraints (5.12) as equality constraints in the optimisation.

A further justification for our decision not to insist on minimising the number of optimisation

parameters at the expense of having a less well-conditioned optimisation problem is based on a computational cost analysis. In particular, the cost per iteration of the sequential quadratic programming (SQP) that we use (see section 5.5.1) comprises two main components:

(a) the cost of integrating the DAE system (5.7) and the associated sensitivity equations (5.29); and

(b) the cost of forming and solving the quadratic programming subproblem that determines the next step in the optimisation decision variables.

We note that (a) does not actually depend on whether the optimisation is carried out in the full parameter space, Θ, or the reduced one, $\bar{\Theta}$. This is because, even if some parameters are not included in $\bar{\Theta}$, we still need the gradients of the corresponding task variables with respect to them. For instance, in the example illustrated in figure 5.5, the parameters z_{S2} have been eliminated from $\bar{\Theta}$ since they are fully determined by the parameters Θ_1 associated with the first task $i = 1$ (*cf.* section 5.4.1). Thus, the variables $x_2(t)$, $y_2(t)$ are now functions of Θ_1. However, in order to calculate the corresponding gradients, we still need the sensitivities $\frac{\partial x_2}{\partial z_{S2}}$, $\frac{\partial y_2}{\partial z_{S2}}$ which will then be combined with $\frac{\partial z_{S2}}{\partial \Theta_1}$ to yield:

$$\frac{\partial x_2}{\partial \Theta_1} = \frac{\partial x_2}{\partial z_{S2}} \frac{\partial z_{S2}}{\partial \Theta_1} \tag{5.37}$$

$$\frac{\partial y_2}{\partial \Theta_1} = \frac{\partial y_2}{\partial z_{S2}} \frac{\partial z_{S2}}{\partial \Theta_1} \tag{5.38}$$

according to the chain rule of differentiation.

On the other hand, component (b) of the computational cost *does* depend on the number of decision variables and constraints in the optimisation. This would seem to be an argument in favour of operating in the reduced space $\bar{\Theta}$ rather than in the full space Θ. However, in most problems of any practical significance,

$$Cost(a) >> Cost(b) \tag{5.39}$$

Therefore, any reduction on the cost of (b) would result in very small reductions in the cost per iteration of the optimisation algorithm. This would be more than offset by even the smallest increase in the number of iterations caused by any deterioration of the conditioning of the optimisation problem.

As already mentioned at the end of section 5.2.2, in addition to Θ, the optimisation decision parameters generally include the state production rates R_s. The complete optimisation problem as seen by the NLP solver is summarised below:

$$\max_{\Theta,\{R_s,\forall s\}} \quad -\lambda \sum_i C_i(\nu_i) - \sum_u C_u \sum_n \frac{1}{\tau_n^{cycle}} \sum_{i \in \mathcal{P}_n} U_{ui}(\Theta_i) + \sum_s C_s R_s$$

subject to:

$$\left.\begin{array}{c} z_s^{min} \le z_s \le z_s^{max} \\ C_s^I(z_s) \le 0 \end{array}\right\} \forall s$$

$$\left.\begin{array}{l} h_i(\Theta_i) \le 0 \\ \left.\begin{array}{c} g_{i\kappa}^E(\Theta_i) = 0 \\ g_{i\kappa}^I(\Theta_i) \le 0 \end{array}\right\} \kappa = 1,2,.. \\ \left.\begin{array}{l} u_i^{min}(\nu_i) \le \zeta_{ki} \le u_i^{max}(\nu_i) \\ or: \quad u_i^{min}(\nu_i) \le \eta_{ki} \le u_i^{max}(\nu_i) \\ u_i^{min}(\nu_i) \le \eta'_{ki} \le u_i^{max}(\nu_i) \\ h_{ki} \ge \epsilon \end{array}\right\} \forall k = 1,..,NE_i \\ \sum_{k=1}^{NE_i} h_{ki} = \tau_i \\ B_{is} = B_{is}^d + B_{is}^c(\Theta_i), \forall s \in S_i \\ \left.\begin{array}{c} \bar{B}_{is} = \bar{F}_{is}(\Theta_i) \\ z_s = F_{is}(\Theta_i) \end{array}\right\} \forall s \in \bar{S}_i \\ G_i(\Theta_i) \le 0 \\ \nu_i^{min} \le \nu_i \le \nu_i^{max} \end{array}\right\} \forall i$$

$$\tau_n^{cycle} \ge \tau_i, \quad \forall n, i \in \mathcal{P}_n$$

$$\bar{B}_{i_{kn},s_{kn}} = B_{i_{k+1,n},s_{kn}} \quad \forall n, k \in [1, m_n - 1]$$

$$\sum_{n \in \bar{\mathcal{N}}_s} \sum_{i \in \mathcal{P}_n} \frac{\bar{B}_{is}}{\tau_n^{cycle}} = \sum_{n \in \mathcal{N}_s} \sum_{i \in \mathcal{P}_n} \frac{B_{is}}{\tau_n^{cycle}} + R_s \qquad \forall s \in \mathcal{SS}$$

$$R_s^{min} \le R_s \le R_s^{max}, \forall s$$

It is to be understood that the finite representation of inequality path constraints $h_i(\cdot) \le 0$ in terms of constraints (5.24) and (5.26) is used in the above formulation (*cf.* section 5.3.2).

5.5. A Prototype Integrated Batch Process Design Tool

By this point in the thesis, it will be quite apparent to the reader that both the mathematical formulation presented in chapters 3 and 4, and the solution approach described in this chapter are rather complex. The complexity arises both from the amount of data that need to be provided in order to arrive at a well-defined problem, and from the subsequent mathematical manipulations.

As part of the work described in this thesis, we have attempted to develop a prototype software tool that facilitates the definition and reliable solution of batch process design problems of practical significance. In the rest of this section, we consider the various issues associated with the design and implementation of this prototype.

5.5.1. Defining Models for Batch Unit Operations

Much of the complexity of specifying a batch process design problem lies in the definition of the mathematical models of the transient behaviour of the individual unit operations (*cf.* equations 3.3). As already mentioned, each of these models often comprises hundreds of differential and algebraic equations (DAEs) and variables. Furthermore, in some cases, the need to take account of spatial variation within the unit operation may result in sets of partial differential and algebraic equations (PDAEs) distributed over one or more space dimensions. As mentioned in section 3.3, by discretising the spatial variations in an appropriate manner, these PDAE systems can always be reduced to sets of ordinary differential and algebraic equations involving temporal variations only. However, the actual implementation of such discretisations is often far from straightforward.

Fortunately, much work has already been carried out in recent years on software tools for the modelling of complex time-dependent operations (see, for instance, Pantelides and Britt (1994)). The *gPROMS* (*g*eneral *PRO*cess *M*odelling *S*ystem) package (Barton and Pantelides, 1994) is one such tool. *gPROMS* offers a high level symbolic language for the definition of transient process models. Complex models (*e.g.* those of distillation columns) can be formed by the hierarchical combination of simpler models (*e.g.* column trays), and this decomposition can be repeated recursively to an arbitrary number of levels. Discontinuities in process models can also be defined.

One other important feature of *gPROMS* is its support for the definition of models of spatially or otherwise distributed unit operations in terms of systems of integral, partial differential and

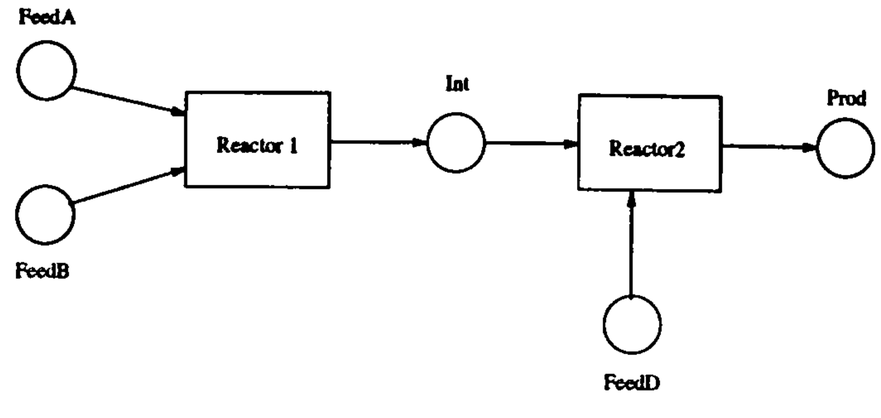

Figure 5.7: STN for Simple Two Reaction Process

algebraic equations (IPDAEs) (Oh and Pantelides, 1994). These are automatically discretised by the package to sets of DAEs in time.

For all the above reasons, we have based our prototype batch process design tool on models of individual unit operations defined within the *gPROMS* language. To illustrate the use of our tool, we consider a simple process involving two reaction tasks in sequence (see figure 5.7):

The first task carries out the reactions:

$$2A \xrightarrow{k_1} B$$
$$B \xrightarrow{k_2} C$$

while the second task involves a further set of reactions:

$$D + B \xrightarrow{k_3} E$$
$$D + C \xrightarrow{k_4} F$$

The *gPROMS* input files for the modelling and simulation of these tasks shown in figures 5.8 and 5.9 respectively. Note that the energy dynamics have been ignored in these models. For more information on the *gPROMS* language, the interested reader is referred the PhD theses by Barton (1992) and Oh (1995).

5.5.2. Defining Additional Optimisation Information

The task model equations (3.3) certainly form a very significant fraction of the total amount of data that need to be defined for the batch process design problem. However, many other items of

```
MODEL Reactor1

VARIABLE
  C                          AS  ARRAY(6) OF  Concentration
  V_in                       AS  Volume
  K1,K2                      AS  Rate_Constant
  TR                         AS  Temperature
  OPER_COST, CAP_COST        AS  Objective_Function

EQUATION
  #..Component mass balance equations
  $C(1) = -2*K1*C(1)^2           ;
  $C(2) =  K1*C(1)^2 - K2*C(2)   ;
  $C(3) =  K2*C(2)               ;
  $C(4) =  0.0                   ;
  $C(5) =  0.0                   ;
  $C(6) =  0.0                   ;

  #..Reaction rates
  K1 = 0.0444 * exp( -2500.0 / TR ) ;
  K2 = 6889.0 * exp( -5000.0 / TR ) ;

  #..No capital or utility costs
  OPER_COST = 0.0 ;
  CAP_COST  = 0.0 ;

END # Model Reactor1

#-----------------------------------------------------

PROCESS Reaction_1

UNIT
  R1 AS   Reactor1

ASSIGN
  WITHIN R1 DO
    TR     :=  350.0 ;
    #..Input to reaction task
    V_in   :=    100 ;
  END

INITIAL
  WITHIN R1 DO
    C(1)   := 2000.0 ;
    C(2:6) :=    0.0 ;
  END
END
```

Figure 5.8: *gPROMS* input file for reaction task R1

```
MODEL Reactor2

VARIABLE
  C                          AS  ARRAY(6) OF  Concentration
  V_in                       AS  Volume
  K3,K4                      AS  Rate_Constant
  TR                         AS  Temperature
  OPER_COST, CAP_COST        AS  Objective_Function

EQUATION
  #..Component mass balance equations
  $C(1) =  0                                ;
  $C(2) = -K3*C(2)*C(4)                     ;
  $C(3) = -K4*C(3) *C(4)                    ;
  $C(4) = -K3*C(2)*C(4)-K4*C(3)*C(4)        ;
  $C(5) =  K3*C(2)*C(4)                     ;
  $C(6) =  K4*C(3)*C(4)                     ;

  #..Reaction rates
  K3 = 20.0444 * exp( -3400.0 / TR ) ;
  K4 = 0.003 * exp( -100.0 / TR ) ;

  #..No capital or utility costs
  OPER_COST = 0.0 ;
  CAP_COST  = 0.0 ;

END # Model Reactor
#-------------------------------------------------

PROCESS Reaction_2

UNIT
  R2 AS   Reactor2

ASSIGN
  WITHIN R2 DO
    TR     :=  350.0 ;
    #..Input to reaction task
    V_in   :=    100 ;
  END

INITIAL
  WITHIN R2 DO
    C(1)   := 201.0 ;
    C(2)   := 672.0 ;
    C(3)   :=   5.0 ;
    C(4)   := 200.0 ;
    C(5:6) :    0.0 ;
  END
END
```

Figure 5.9: *gPROMS* input file for reaction task R2

information also need to be provided. Since these are not part of the normal *gPROMS* input, they are supplied in a separate input file.

The additional information that needs to be specified primarily concerns the structure of the State-Task Network describing the process, and its association with the detailed DAE task models defined in the *gPROMS* language.

The overall structure of the optimisation input file is as follows[1]:

```
STN <State-Task Network Name>
    <State Entity Information>
    <Task Entity Information>
END
```

State Entity Information

This provides the following information for each state s in the process STN:

- A unique name by which this state will be identified.
- The name, initial estimate, and lower and upper bound for each intensive property z_s of this state.
- An initial estimate and a lower and upper bound for the net production rate R_s of this state.
- The unit value C_s for this state.

The syntax of the input language to characterise a state is:

[1]In the syntax specifications shown in this section, entries in CAPITAL typewriter font denote language keywords while entries in *italics* surrounded by angle brackets denote information to be provided by the user

STATE <*statename*>

VARIABLE

<intensiveproperty> = <guess> : <lowerbound> : <upperbound> ;

END

PRODUCTION = <*guess*> : <*lowerbound*> : < *upperbound*> ;

VALUE = <*value* > ;

If the lower and upper bounds of any quantities are omitted, then this quantity is assumed to be fixed at the specified value for the purposes of the optimisation.

As an example, the following is the specification of the state *Int* in the simple example being considered in this section:

STATE *Int*

VARIABLE

CA = 301.0 : 0.0 : 4000.0 ;

CB = 792.0 : 0.0 : 4000.0 ;

CC = 56.0 : 0.0 : 4000.0 ;

CD = 0.0 : 0.0 : 4000.0 ;

CE = 0.0 : 0.0 : 4000.0 ;

CF = 0.0 : 0.0 : 4000.0 ;

END

PRODUCTION = 0.00 : 0.00 : 50.00 ;

VALUE = -1.00 ;

We note that in this case, the state is characterised in terms of the molar concentrations of the six components occuring in it. The initial estimates (guesses) listed above were obtained by performing a dynamic simulation of Reaction 1.

Task Entity Information

This provides the following information for each task i in the process STN:

- A unique name by which this task will be identified.
- The name of a *gPROMS* PROCESS (see section 5.5.1 and figure 5.7) which describes the dynamic behaviour of this task.
- Information on this task's input states: for each such state $s \in S_i$, we :
  - specify its unique name;
  - specify an initial estimate of the initial discrete charge amount ("Batchsize") B_{is}^d, and a lower and upper bound for this quantity; we also identify this with a variable in the *gPROMS* model of the task.
  - identify each intensive state property with a *gPROMS* model variable.
- Information on this task's output states; for each such state $s \in \bar{S}_i$, we identify:
  - the amount $\bar{B}_{is}$ produced by the task;
  - the intensive variables in this state, with corresponding variables in the *gPROMS* model of the task.
- An initial estimate and lower and upper bounds for the task duration.
- An initial estimate and lower and upper bounds for the task idle time (optional).
- The number of finite elements ("intervals") for the discretisation of the control variables in this task, and also an initial estimate and a lower and upper bound on the duration of each such interval.
- The optimisation decision variables (comprising both control variables and time-invariant parameters) for this task. These are identified in terms of their *gPROMS* model name and are classified as `PIECEWISE CONSTANT` or `PIECEWISE LINEAR` for control variables, and `CONSTANT` for time invariant parameters. An initial estimate and lower and upper bounds of the values of these design variables in each interval are also provided.
- The operating and annualised capital cost of the task identified in terms of *gPROMS* model variables.
- End-point equality and inequality constraints specified in terms of one or more *gPROMS* model variables and their final values or allowable ranges.

- Interior point constraints. These are enforced at interval boundaries. The name(s) of the corresponding *gPROMS* model variable(s), the interval at the end of which these are to be constrained and the allowable range of values at this point must also be specified.

A summary of the syntax for specifying task information is shown in figure 5.10, and an example of its use (corresponding to task Reaction 1 of figure 5.7), is presented in figure 5.11.

5.5.3. Implementation of the prototype tool

As we have seen in section 5.5.1, the model of each task i in the process is defined in a separate *gPROMS* input file. The *gPROMS* code command is then used to create automatically FORTRAN subroutines[2] for the residuals and partial derivatives (Jacobian matrix) of the model equations (3.3) with respect to all variables occurring in them (including x_i, y_i, $\dot{x}_i$, u_i, and v_i).

The code generation step for each task also creates a file with information on the task model. This includes various size parameters for the model, such as the number of equations, variables, and non-zero elements in its sparse Jacobian matrix. The name, initial guess, and lower and upper bounds of each variable are also included, as is its classification into differential, algebraic or input variables. The latter category includes both control variables and time invariant parameters. A file containing the sparsity pattern of the model (*i.e.*, which equation contains which variable) is also generated automatically at this stage.

Once this "export" of information from the *gPROMS* models is completed, a separate program reads and validates the optimisation input file (see section 5.5.2). In addition to purely lexical and syntactical checks, the validation involves two types of consistency check:

- Self-consistency checks within the optimisation input file.

  For instance, if a task refers to a certain state as an input, the system will check that indeed such a state has been already been declared.

- Cross-checking with information residing in the various files created from the *gPROMS* input files at the previous step.

[2]Note that such FORTRAN code generation is *not* part of the normal *gPROMS* operation.

TASK < *STN task name* >AS <*gPROMS task name*>

INSTATE < *STN state name*>

BATCHSIZE = < *guess* > : < *lower bound*> : <*upper bound* > IS < *gPROMS variable name* > ;

< *State intensive property name*> IS < *gPROMS variable name*>

.....

.....

OUTSTATE < *STN state name* >

BATCHSIZE IS < *gPROMS variable name*>

< *State intensive property name*> IS < *gPROMS variable name* >

.....

.....

DURATION = <*guess*> : <*lower bound*> : <*upper bound*> ;

IDLE_TIME = <*guess*> : <*lower bound*> : <*upper bound*> ;

INTERVALS <*number, NE*>

INTERVAL<*1*> = <*guess*> : <*lower bound*> :<*upper bound*> ;

.....

INTERVAL<*NE*> = <*guess*> : <*lower bound*> :<*upper bound*> ;

DECISION_VARIABLES

< *gPROMS variable name*> AS CONSTANT

[<*guess*> : <*lower bound*> : <*upper bound*>]

<*gPROMS variable name* > AS PIECEWISE CONSTANT

INTERVAL<*1*> : [<*guess*> : <*lower bound*> : <*upper bound*>]

.....

INTERVAL <*NE*> : [<*guess*> : <*lower bound*> : <*upper bound*>]

<*identifier*> AS PIECEWISE LINEAR

INTERVAL<*1*> : [<*guess*> : <*lower bound*> : <*upper bound*>]

.....

INTERVAL <*NE*> : [<*guess*> : <*lower bound*> : <*upper bound*>]

OBJECTIVE

<*gPROMS variable name*> AS OBJECTIVE_FUNCTION

<*gPROMS variable name* > AS CAPITAL_COST

CONSTRAINTS

<*gPROMS variable name*> IN [<*lower bound*> : <*upper bound*>];

<*gPROMS variable name*> INTERVAL <number> IN [<lower bound> : <upper bound>] ;

<*gPROMS variable name*> = [<*value*>];

Figure 5.10: Syntax for specifying task entity information

```
TASK Reaction1 AS  R1
  INSTATE FeedA
    BATCHSIZE  = 100 : 100 : 100 IS  TASK1.V_IN ;
    C(1)    IS   TASK1.Cin(1)
    C(2)    IS   TASK1.Cin(2)
    C(3)    IS   TASK1.Cin(3)
    C(4)    IS   TASK1.Cin(4)
    C(5)    IS   TASK1.Cin(5)
    C(6)    IS   TASK1.Cin(6)

  OUTSTATE Int1
    BATCHSIZE  IS   TASK1.V_IN
    C(1)    IS   TASK1.C(1)
    C(2)    IS   TASK1.C(2)
    C(3)    IS   TASK1.C(3)
    C(4)    IS   TASK1.C(4)
    C(5)    IS   TASK1.C(5)
    C(6)    IS   TASK1.C(6)

  DURATION  = 78.0 : 45 : 120.0 ;
  IDLE_TIME = 0.0 : 0.0 : 50.0 ;

  INTERVALS 5
  INTERVAL 1 = 38.0 : 5.0 : 100.0 ;
  INTERVAL 2 = 10.0 : 5.0 : 100.0 ;
  INTERVAL 3 = 10.0 : 5.0 : 100.0 ;
  INTERVAL 4 = 10.0 : 5.0 : 100.0 ;
  INTERVAL 5 = 10.0 : 5.0 : 100.0 ;

DECISION_VARIABLES
  TASK1.TR AS PIECEWISE CONSTANT
    INTERVAL 1  : [ 326.27440  : 298.0 : 398.0 ]
    INTERVAL 2  : [ 320.18582  : 298.0 : 398.0 ]
    INTERVAL 3  : [ 309.86101  : 298.0 : 398.0 ]
    INTERVAL 4  : [ 310.80069  : 298.0 : 398.0 ]
    INTERVAL 5  : [ 311.29742  : 298.0 : 398.0 ]

 OBJECTIVE
   TASK1.OPER_COST AS OBJECTIVE_FUNCTION
   TASK1.CAP_COST  AS CAPITAL_COST
```

Figure 5.11: Example of syntax language applied to Reaction 1

For instance, if a variable is identified as a control variable for a given task, the system will check whether indeed the *gPROMS* model for that unit operation contains such a variable, and that the latter is classified as an input.

Once the interpretation and the validation of the optimisation input file is complete, the system creates automatically a main FORTRAN program to drive the entire computation. This is compiled and linked with the FORTRAN subroutines describing the individual task models, as well as the necessary numerical routines.

The numerical task to be carried out is illustrated in figure 5.12. At the highest level, this is essentially the solution of the nonlinear programming (NLP) problem summarised at the end of section 5.4.3. The current implementation of the design tool uses the SRQPD code (Chen and Macchietto, 1989) for this purpose. SRQPD is a dense-matrix implementation of the sequential quadratic programming algorithm proposed by Chen (1988). From the software architecture point of view, an interesting characteristic of this code is the fact that it operates in "reverse communication" mode (Gonnet, 1974). This means that, instead of the normal practice of the NLP code calling various subroutines for the evaluation of the values and/or gradients of the objective function and the constraints, SRQPD returns to the calling program every time it requires any such information. It is then the responsibility of the calling program to obtain the requested information and call the SRQPD code again. In the context of our batch process design tool, this is a particularly important feature given the complexity of the computation of this information (see figure 5.1).

The evaluation of the objective function and the constraints in the NLP summarised in section 5.4.3 involves the integration of the model equations (5.7) and the corresponding sensitivity equations (5.9) subject to the initial conditions (5.4) and (5.31) respectively, for each task i given values of the parameters Θ_i (*cf.* figure 5.1). In our current implementation, this is done using the DASOLV code (Jarvis and Pantelides, 1992). This is an efficient implementation of the Backward Differentiation Formulae (BDF) integration methods (Gear, 1971) for large sparse DAE systems.

Once the solution of the mathematical problem is successfully completed, our prototype system generates two result files. The first such file is called PPP.out (where PPP is the name of the State-Task Network) and contains a summary report on the optimisation run, including:

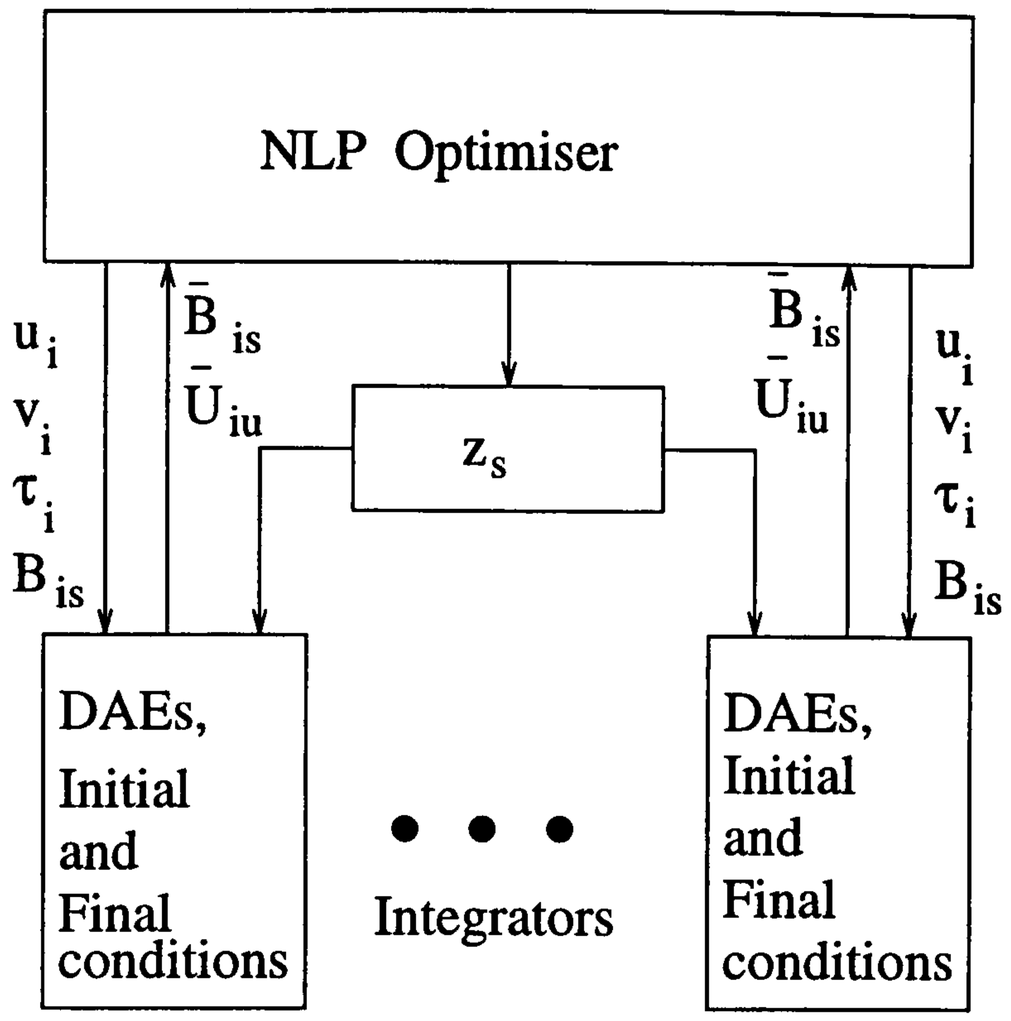

Figure 5.12: Proposed Solution Methodology

- The values of the optimisation parameters.
- The final value of the objective function.
- Analysis of the computational performance of the solution method.

The second of the two types of files generated is called PPP_SSS.gPLOT (where SSS is the task name). It should be noted that separate PPP_SSS.gPLOT file is generated for each task declared in the optimisation input file. Each file contains the optimal time profiles of all the variables, including x_i, y_i, u_i and ν_i, for the corresponding task. Graphical output for presentation purposes can then be produced from this file.

5.6. Concluding Remarks

This chapter has considered numerical methods for the solution of the mathematical formulation of the integrated batch process design problem. In particular, it has shown how control vector parameterisation can be used to deal with the infinite dimensionality of this problem, converting

it to a finite dimensional NLP. Alternative ways of handling the multistage nature of the problem in this context were also examined.

Some attention was also focussed on the design and implementation of a software tool aiming at facilitating the definition of the large amount of data associated with a batch process design problem.

At this stage, it is worth emphasising that despite our careful analysis of the mathematical nature of the problem and the potential solution algorithms, the problem of designing an integrated batch process inherently remains a highly complex one, and the corresponding computational cost for any but the simplest examples is likely to be significant. Moreover, the software tool presented in section 5.5 is still very much in a prototype state.

Notwithstanding these limitations, however, the mathematical and software developments described in this chapter render the solution of many significant batch process design problems feasible, both in principle and in practice. This will be demonstrated with the examples presented in the next two chapters.

Chapter 6

Batch Process Design Applications: I. Multicomponent Batch Distillation

The optimisation of individual batch unit operations can be viewed as a special case of the design of integrated batch processes in which a single task interacts with a number of states of material. In this chapter, we focus on the optimal operation of multicomponent batch distillation. This is an interesting application of our methodology because of both the size and complexity of the underlying model, and the complex interactions between the task and the different materials it produces. The latter interactions arise from the possibility of recycling some of the "off-cut" material produced by the distillation. Section 6.2 considers the separation of a ternary mixture without off-cut recycle. The effect of off-cut recycling on the net revenue of this process is examined in sections 6.3-6.4.

6.1. Introduction

Batch distillation operations are frequently encountered in processes producing high value-added products. The major advantage of such a separation technique is the flexibility offered by its multipurpose nature, with the ability to produce multiple distillate products from a single distillation column. In addition to this, it can handle a wide range of compositions and components in the feed charge.

The inherently transient behaviour of batch distillation operations is usually described by a set of differential material and energy balances, with algebraic equations used to express the

thermodynamic relations such as phase equilibrium. The dimensionality and stiffness of the underlying set of DAEs renders even the simulation of such processes a difficult task. As a result, the development of alternative models to reduce computational time without affecting the accuracy of the results has been attempted. Sundaram and Evans (1993a), and Diwekar and Madhavan (1991) proposed short-cut models based on the Fenske-Underwood-Gilliland equations (FUG) of continuous distillation design. Also, Diwekar (1994) considered both simplified column dynamics and augmented short-cut models. The effect of the various modelling assumptions for both rigorous and short cut methods has recently been examined by Bosley and Edgar (1994). Reactive and azeotropic batch distillation are becoming increasingly important industrial processes, especially in fine and specialty chemicals manufacture. The rigorous modelling and simulation of reactive batch distillation has been considered by Albet *et al.* (1991), and more recently, work has appeared in the literature on modelling and analysis of azeotropic batch distillation systems (see, for instance, Ahmad and Barton (1995); Watson *et al.* (1995)).

Apart from the modelling aspects of batch distillation, a number of authors have addressed the problem of determining an optimal reflux ratio policy.

... The work presented in the literature can be classified according to the objective function used:

1. *Maximum Distillate*: Maximise the amount of product subject to purity constraints (Logsdon and Biegler, 1993; Mujtaba, 1989).

2. *Minimum Time*: Minimise the processing time subject to product quantity and quality constraints (Diwekar, 1992; Mujtaba, 1989).

3. *Maximum Profit*: Maximise a profit function subject to quantity and quality constraints (Diwekar *et al.*, 1989; Mujtaba and Macchietto, 1993; Logsdon *et al.*, 1989).

6.2. Ternary Batch Distillation without Recycles

As an example of batch distillation, we consider the separation of 2.93 *kmol/batch* of a ternary mixture consisting of 40.7% cyclohexane, 39.4% n-heptane and 19.9% toluene. This problem was initially studied by Nad and Spiegel (1987). The distillation operation was simulated for a column

with 20 theoretical trays, with the pressure varying from 0.962 *bar* at the top to 1.013 *bar* at the bottom. The vapour liquid equilibrium calculations were based on the UNIQUAC model, and enthalpy effects were neglected.

Mujtaba and Macchietto (1994) considered both the design and the operation of the column used for this ternary separation, treating the number of trays, processing time, cut location and reflux policy as decision variables. The number of trays was considered as a continuous optimisation variable with the required gradients calculated by finite differences using function and constraint values at the rounded off value of N and at its closest higher integer value. The DAE model utilised takes into account both material and energy balances, with constant condenser vapour flow. The vapour-liquid equilibrium calculations were based on the Soave-Redlich-Kwong (SRK) equation of state. The objective used was the maximisation of the annual profit taking into account net revenues (products and raw materials), operating costs and annualised capital costs. The annualised capital (ACC) and operating (OC) costs, as considered by Mujtaba and Macchietto (1994), in $\$/yr$, are given by:

$$ACC = 1500V^{0.5}N^{0.8} + 9500V^{0.65} \tag{6.1}$$

$$OC = 180V \tag{6.2}$$

where V is the condenser vapour load ($kmol/hr$). Here, we assume that N is fixed at the optimal value ($N = 17$) determined by Mujtaba and Macchietto (1994) and aim to derive an optimal operating policy for this column.

6.2.1. Process Description

The distillation setup is shown in figure 6.1(a). The products of the process include the first and second main cuts (collected in drums D_1 and D_2 respectively) and the residue remaining in the reboiler at the end of the operation. The remaining cuts (collected in R_1 and R_2) have no economic value.

The corresponding State-Task Network is shown in figure 6.1(b). Purity requirements of 89.5% cycloxehane, 86.3% n-heptane and 99.0% toluene are imposed on states D_1, D_2 and B_f respectively. Also at least 95% of the cyclohexane loaded into the column must be recovered by the end of the first "off-cut". All materials are assumed to be stable.

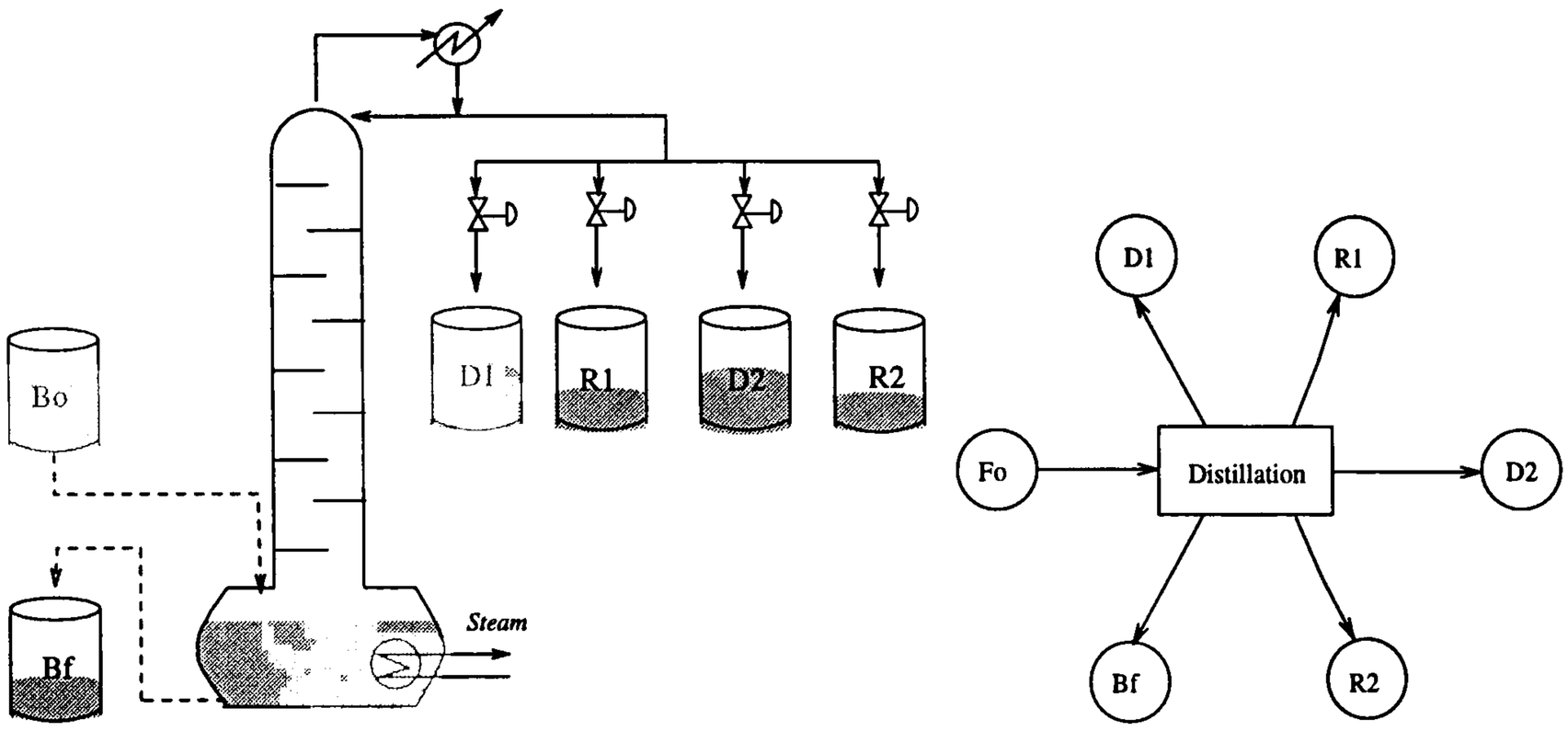

(a) Distillation Column Setup

(b) State Task Network

Figure 6.1: Ternary Batch Distillation: Distillation Column Setup and State-task Network

The distillation column comprises 17 theoretical trays and is operated at atmospheric pressure. The vapour flowrate to the condenser is kept constant at 2.75 $kmol/hr$. The normalised reflux ratio[1] is allowed to vary between 0.75 and 0.99.

6.2.2. Economic Data

Since the number of trays and the vapour flow to the condenser are both fixed, only the net production revenue and the operating cost affect the total revenue of the process. For the purposes of the optimisation, we adopt the unit values given by Mujtaba and Macchietto (1994) for the various materials in the process, as shown in Table 6.1. It should be noted that the unit values of off-cuts R_1 and R_2 are set to small negative numbers, reflecting the undesirability of building up stocks of these materials.

[1]Defined as the ratio of the flowrate of the reflux stream to that of the vapour stream entering the condenser.

Material	Unit value ($/kmol)
F_O	2.0
D_1	30.0
R_1	-1.0
D_2	26.0
R_2	-1.0
B_f	24.0

Table 6.1: Ternary Batch Distillation: Unit Values for Process Materials

6.2.3. Modelling Considerations

The operation of the distillation column is modelled assuming constant liquid hold-ups on the trays and the condenser, negligible vapour hold-up, and fast energy dynamics. The initial charge to the column fills the reboiler, trays and total condenser with liquid at the charge composition. Molar hold-ups of 3.28 and 31.52 *moles* are assumed for each of the column trays and total condenser respectively. Non-ideal Soave-Redlich-Kwong (SRK) vapour-liquid equilibrium models (Reid *et al.*, 1987) are used with the pure component critical parameters given by Daubert and Danner (1985). A detailed description of the SRK model used is given in Appendix A. The process model and data utilised are given in Appendices A and B respectively.

For the purposes of the optimisation, the operating time of the distillation process is divided into 6 intervals of variable duration, with the first, second, third and fourth cuts being produced at the ends of intervals 2, 3, 5 and 6 respectively. The reflux ratio is treated as a piecewise constant control variable (*cf.* equation 5.3). The purity and recovery requirements are implemented as end-point inequality constraints (*cf.* constraints 5.10).

6.2.4. Results and Discussion

The overall optimisation problem involves 19 optimisation parameters consisting of the mean rate of material accumulation in each of the 6 states of materials, the values of the control variables over the 6 control intervals and the durations of the latter, and the total processing time. Four inequality constraints are utilised to enforce the product quality requirements and seven equality

constraints for the material balance on each state (*cf.* equation 4.6) and summation of the control intervals (*cf.* equation 5.21). The DAE model for the distillation column comprises 862 equations, 779 of which are algebraic.

The solution of the problem using the SRQPD sequential quadratic programming code (Chen and Macchietto, 1989) required 27 quadratic programming (QP) subproblems and 39 line-search evaluations of the objective function and constraints[2]. The overall computation time was approximately 16 *hr* on a SUN SPARC 10/41 workstation.

Over a horizon of one year[3], the process consumes 3861.24 *kmol* of fresh feed producing 1488.95, 615.69 and 478.18 *kmol* of products D_1, D_2 and B_f respectively, and 1085.50 and 192.91 *kmol* of off-cuts R_1 and R_2 respectively. The optimal revenue of the process is 20336.78 $\$/yr$. A detailed economic breakdown is given in Table 6.2[4].

The optimal processing time is approximately 6 *hr* with the details of the process recipe given in the form of an *annotated STN* in figure 6.2(a). As such diagrams are used to describe optimal process recipes throughout the rest of this thesis, it is important to understand clearly the significance of the various items of information presented in them:

---

[2]The optimisation and integration tolerances were set to 10^{-3} and 10^{-6} respectively.

[3]We assume 8000 working hours per year.

[4]It should be noted that, in the economic breakdown tables presented in this chapter, the total annualised operating and capital costs are quoted for the sake of completeness only. Since the number of trays N and the vapour flow to the condenser are both fixed, these two costs are also fixed and do not affect the optimisation.

As is the usual STN convention, each rectangle corresponds to a task. The information below the name of task i is its processing time τ_i (usually in hours). If the task incurs some idle time (*cf.* section 4.2), this is also shown on the diagram under the task rectangle (see figure 7.5 for an example).

Circles represent states of material, again according to the standard STN convention. The information presented in a rounded dashed box next to each state s is the vector of intensive properties, z_s. The actual length and composition of this vector will, of course, vary from one example to the next.

The arrow from a state node s to a task node i in the diagram is annotated with B_{is}, the amount of material of state s that is fed to task i per batch.

The arrow from a task node i to a state node s is annotated with $\bar{B}_{is}$, the amount of material of state s that is produced by task i per batch.

It can be seen that the purity specifications on D_1, D_2 and B_f are all active at the optimal solution. The variation of normalised reflux ratio with time and the composition trajectories in the reboiler pot are shown in figure 6.2(b). The composition trajectories in the accumulator tanks are shown in figures 6.3(a) and 6.3(b) respectively.

The optimal revenue for the process as reported by Mujtaba and Macchietto (1994) is 15168.00 $\$/yr$ with a processing time of 7.68 hr. We have verified this value of the objective by running a simulation using our model with the reflux ratio profile presented by Mujtaba and Macchietto (1994). The difference between the two results can be attributed to the relaxation of the cyclohexane recovery specification. In particular, our optimisation calculations allow the cyclohexane recovery in the first off-cut to exceed 95% if this improves the economics of the process while Mujtaba and Macchietto (1994) fix this recovery at precisely 95%. This results in a larger amount of off-cut product rich in n-heptane. Also discarding n-heptane in the off-cut reduces the time required for the second main-cut. Consequently, our solution results in a shorter processing time, with a significant improvement in the total revenue of the process.

Total Annualised Capital Cost	**42320.00 $/yr**
Total Operating Cost	**495.00 $/yr**

Material	Amount $kmol/yr$	Revenue $/yr
F_O	-3861.24	-7722.48
D_1	1488.95	44668.56
R_1	1085.50	-1085.50
D_2	615.69	16007.89
R_2	192.91	-192.91
B_F	478.18	11476.22
Total Production Revenue		**63151.78**
TOTAL NET REVENUE		**20336.78 $/yr**

Table 6.2: Ternary Batch Distillation: Economic Breakdown of Optimal Solution

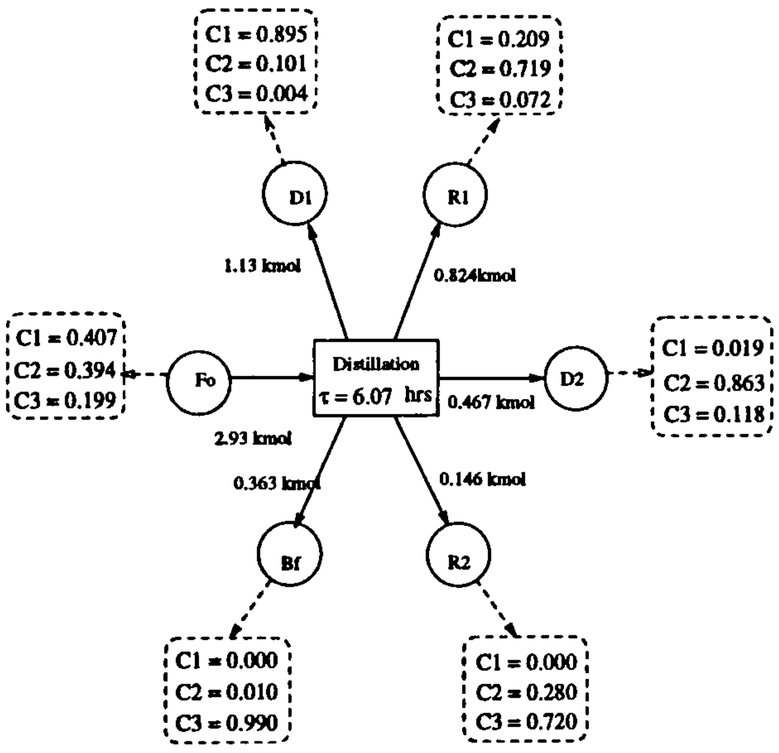

(a) Optimal process recipe (C1 = Cyclohexane mole fraction, C2 = n-Heptane mole fraction, C3 = Toluene mole fraction.)

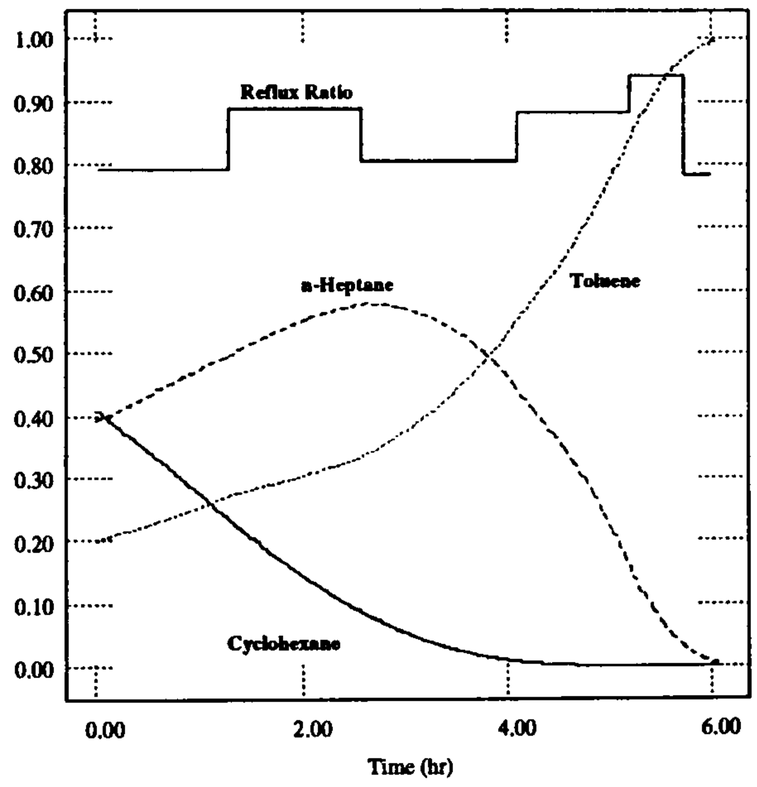

(b) Reflux Ratio and Reboiler Composition

Figure 6.2: Ternary Batch Distillation: Optimal Process Recipe, Reflux Ratio Variation and Reboiler Composition Trajectories

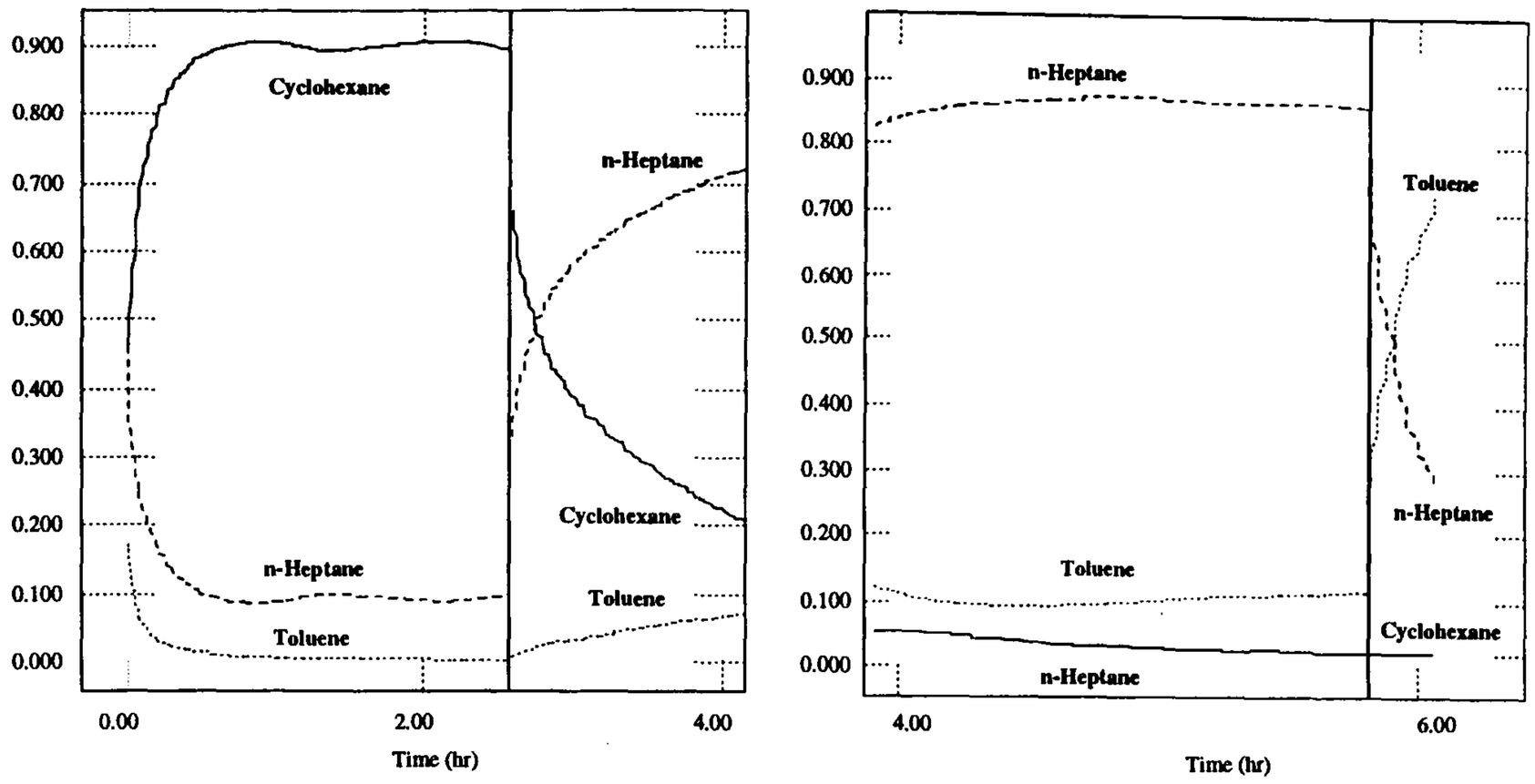

(a) First Main-Cut and Off-Cut (b) Second Main-Cut and Off-Cut

Figure 6.3: Ternary Batch Distillation: Accumulator Composition Profiles

6.3. Ternary Batch Distillation with Combined Off-cut Recycle

The separation of the ternary mixture considered in section 6.2 produces two off-cuts, R_1 and R_2, that contain high quantities of valuable n-heptane and toluene; this can clearly be seen from the composition of these states in the annotated process recipe shown in figure 6.2(a). Therefore, instead of treating these materials as waste, it may be more profitable to mix them with fresh feed and reprocess them. This will effectively reduce both the waste disposal cost incurred in the process and the overall fresh feed consumption.

A possible recycle policy would involve the recovery of a single off-cut instead of the two off-cuts R_1 and R_2. This can simply be done by directing the flow of the distillate liquid to the same accumulator tank during both off-cut generation phases of the column operation. The combined off-cut can then be recycled. This recycle policy would be particularly attractive if the cost of the accumulator tanks is significant.

The distillation setup is shown in figure 6.4(a), with the corresponding State-Task Network shown in 6.4(b). In the rest of this section, we consider this recycle policy for a constant *total*

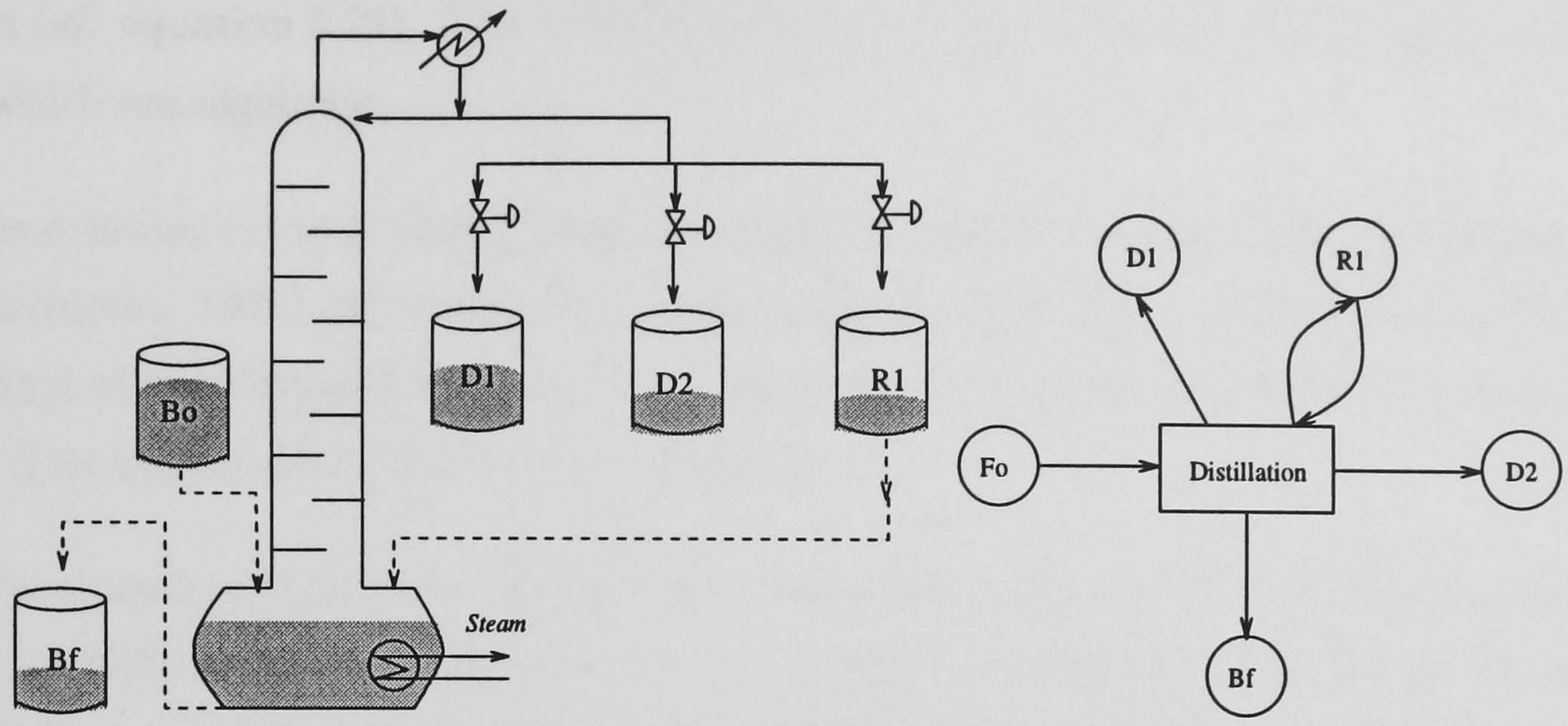

(a) Distillation Column Setup (b) State Task Network

Figure 6.4: Ternary Batch Distillation (Combined Off-cut Recycle): Distillation Column Setup and State Task Network

(*i.e.* fresh feed plus recycled off-cut) initial charge, with up to 1.0 $kmol/batch$ of R_1 being recycled and added to the initial charge. The product purity and specifications remain the same as for the problem of section 6.2.

For the purposes of the optimisation, the operating time of the distillation process is divided into 6 intervals of variable duration. The two main-cuts $D1$ and $D2$ are produced at the ends of intervals 2 and 5 respectively. The off-cut R_1 is collected during control intervals 3 and 5. The reflux ratio is treated as a piecewise constant control variable (*cf.* equation 5.3).

6.3.1. Results and Discussion

The overall optimisation problem involves 23 optimisation parameters consisting of the mean rate of material accumulation in each state, the values of the control over the control intervals and the durations of the latter, the total processing time, and the intensive properties of state R_1. Six inequality constraints are utilised to enforce the product quality requirements and fixed total initial charge (*cf.* equation 5.10), and 9 equality constraints for the material balance on each state (*cf.*

equation 4.6), the state-task coupling for R_1 (*cf.* equation 5.13) and the summation of the control intervals (*cf.* equation 5.28). The DAE model for the distillation column comprises 854 equations, 771 of which are algebraic.

The solution of the problem using the SRQPD sequential quadratic programming code (Chen and Macchietto, 1989) required 20 quadratic programming (QP) subproblems and 31 line-search evaluations of the objective function and constraints[5]. The overall computation time was approximately 3 *hr* on a SUN SPARC 10/51 workstation.

Over a horizon of one year, the process consumes 2565.85 *kmol* of fresh feed producing 1144.55, 1033.02 and 388.28 *kmol* of products D_1, D_2 and B_f respectively. The off-cut R_1 is completely recycled. The optimal revenue of the process is 22567.04 $\$/yr$, as detailed in Table 6.3. The optimal processing time is approximately 7.04 *hr*, and a detailed description of the process recipe is given in figure 6.5. The variation of normalised reflux ratio with time and the composition trajectories in the reboiler pot are given in figure 6.6(a), and the composition trajectories in the accumulator tanks in figure 6.6(b).

Compared to the distillation column setup presented in section 6.2, there is an increase in the total revenue of the process of 2230.26 $\$/yr$. By recycling the combined off-cut, the cost associated with feedstock consumption and off-cut accumulation is reduced by 3433.33 $\$/yr$; this can be seen by comparing tables 6.2 and 6.3. This improvement is somewhat decreased by the reduction in the product revenue of 1638.93 $\$/yr$: although the combined value of products D_1, D_2 and B_f produced *per batch* is higher with the recycle than without it (\$62.05 *vs* \$54.75 respectively), the increase in the processing time (7.04 *hr* *vs* 6.00 *hr* respectively) causes an overall decrease in the product revenue per unit time.

Another interesting feature of the solution is that, even though there is a substantial reduction in the production of D_1 from 1488.95 to 1144.55 $kmol/yr$ and of B_f from 478.18 to 388.28 $kmol/yr$, there is an equivalent increase in the amount of D_2 produced. This shift in the relative magnitude of the amounts of product produced is achieved by reducing the amount of n-heptane in the off-cut (see figures 6.2(a) and 6.5) by operating at a higher reflux ratio and for longer during the control interval dedicated to the production of R_1 (see figures 6.2(b) and 6.6(a)).

[5]The optimisation and integration tolerances were set to 10^{-3} and 10^{-6} respectively.

Total Annualised Capital Cost		**42320.00 \$/yr**
Total Operating Cost		**495.00 \$/yr**
Material	Amount ($kmol/yr$)	Revenue (\$/yr)
F_O	-2565.85	-5131.70
D_1	1144.55	34336.50
R_1	0.0	0.00
D_2	1033.02	26858.52
B_F	388.28	9318.72
Total Production Revenue		**65382.04**
TOTAL NET REVENUE		**22567.04 \$/yr**

Table 6.3: Ternary Batch Distillation (Combined Off-cut Recycle): Economic Breakdown of Optimal Solution

Luyben (1988) considered the effect of both design and operational parameters on the capacity factor of a batch distillation column with off-cut recycle. His simulation, employing a fixed reflux ratio policy but variable cycle time, demonstrated a decrease in the capacity factor of batch distillation (defined as the total amount of product(s) produced per unit cycle time) when all the off-cuts are recycled back to the next batch. This can be attributed to the fixed reflux ratio policy utilised in those calculations and highlights the need for rigorous methodologies for separations with batch distillation.

6.4. Ternary Batch Distillation with Multiple Off-cut Recycles

A separate accumulation tank is used for each off-cut (*cf.* figure 6.1(a)), the quantity of each off-cut, if any, to be recycled and mixed with fresh feed can be determined separately. We now return to the process introduced in section 6.2, but this time we allow the separate recycle of R_1 and R_2. The distillation setup and the corresponding State-Task Network are shown in figures 6.7(a) and 6.7(b) respectively.

As we consider a fixed reboiler capacity, the total initial charge (including both fresh feedstock and the amount of off-cut recycled) must be 2.93 $kmol/batch$. Therefore, if off-cut material is to be recycled, the total amount of fresh feed consumed must be reduced.

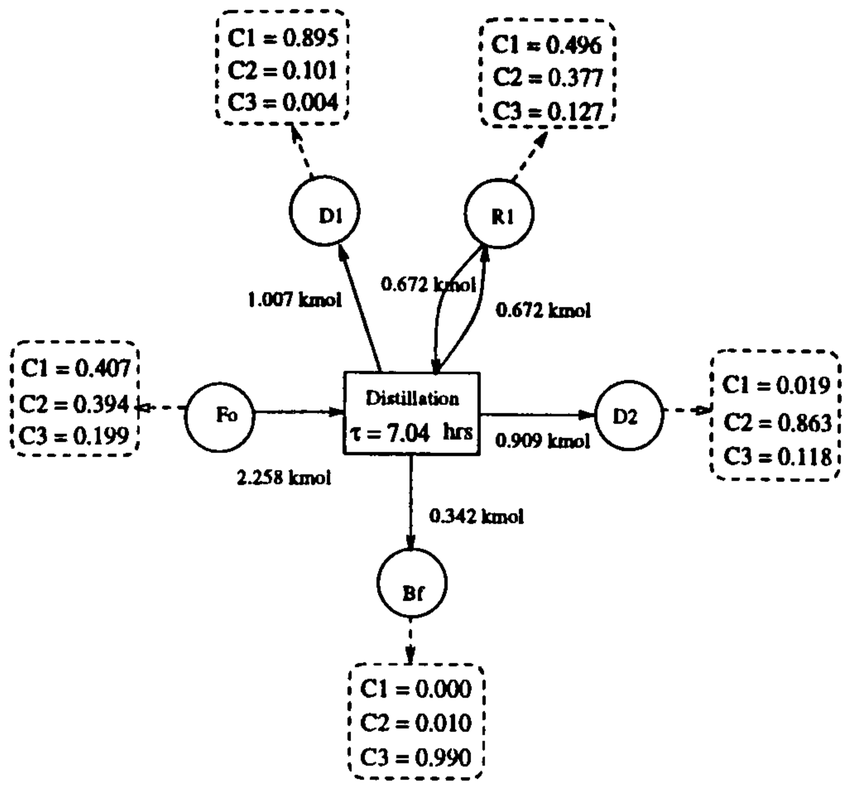

Figure 6.5: Ternary Batch Distillation (Combined Off-cut Recycle): Optimal Process Recipe (C1 = Cyclohexane mole fraction, C2 = n-Heptane mole fraction, C3 = Toluene mole fraction.)

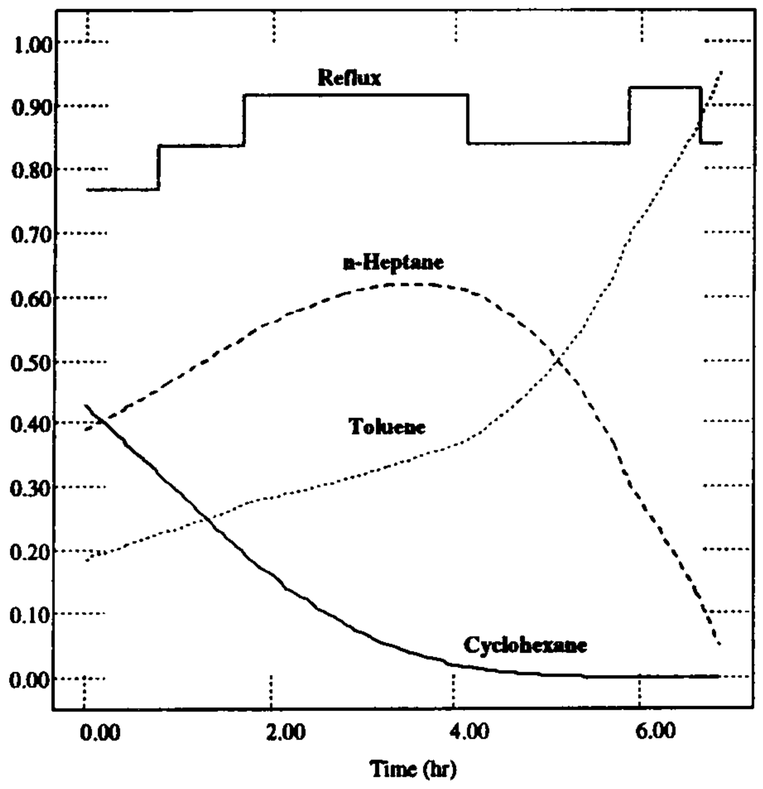

(a) Reflux Ratio and Reboiler Composition

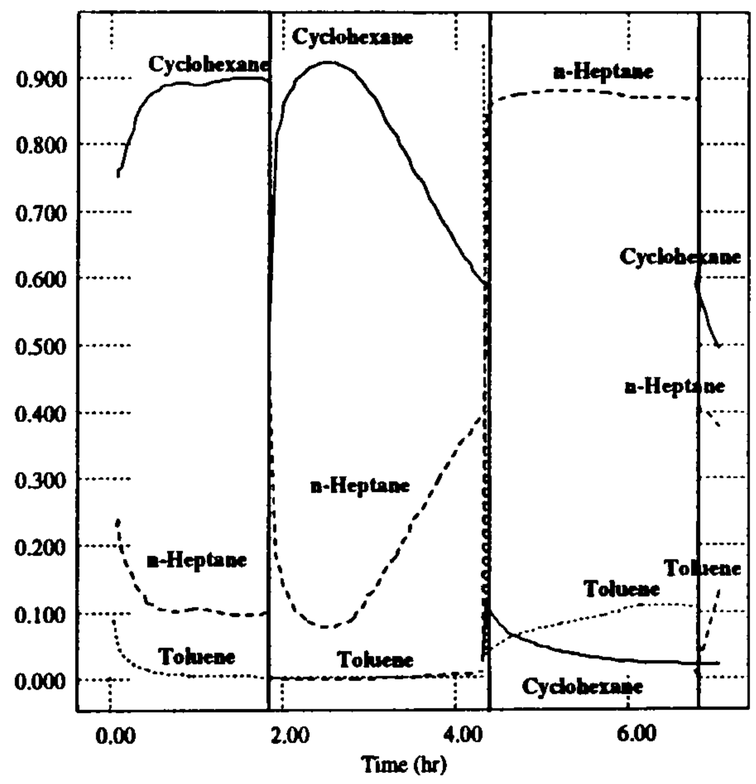

(b) Distillate Tanks Composition

Figure 6.6: Ternary Batch Distillation (Combined Off-cut Recycle): Reflux Ratio Variation and Reboiler and Optimal Distillate Tanks Composition Trajectories

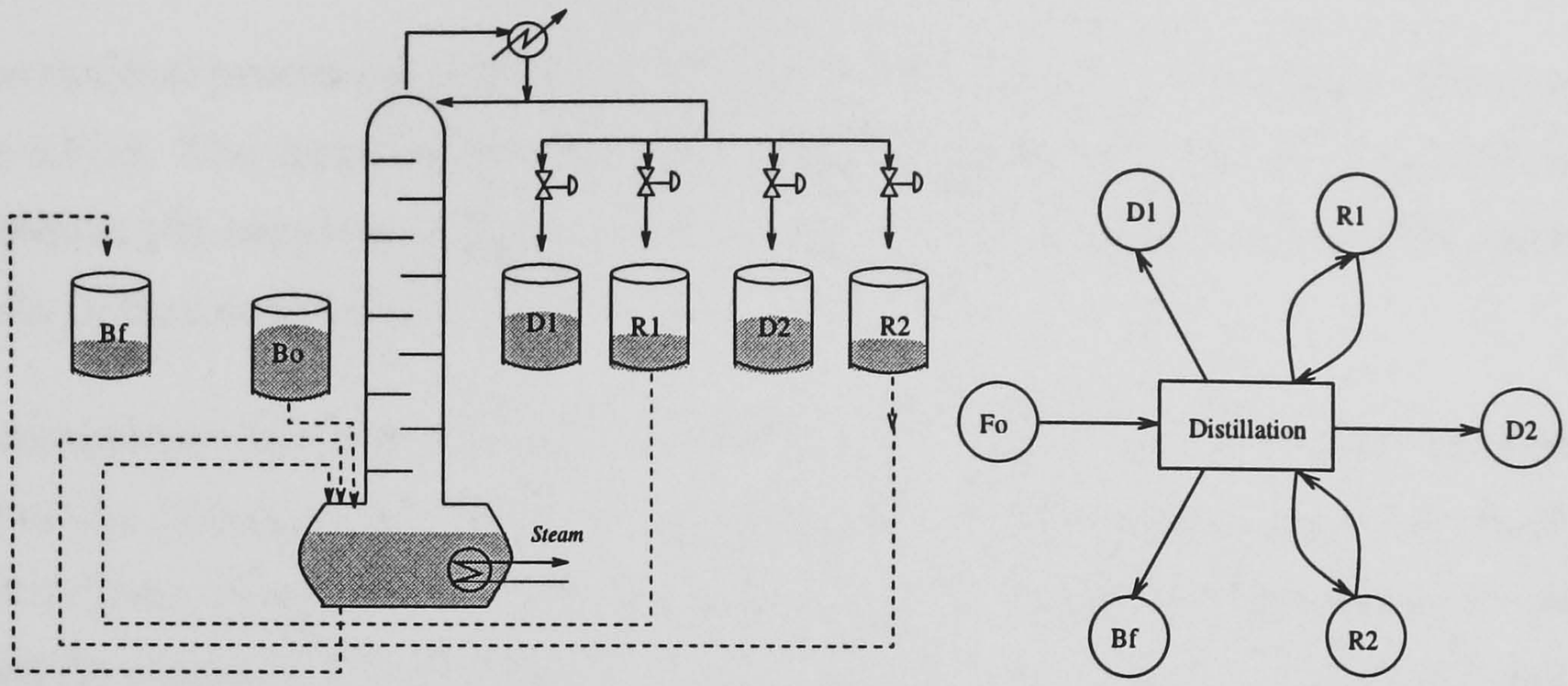

(a) Distillation Column Setup (b) State Task Network

Figure 6.7: Ternary Batch Distillation (Multiple Off-cut Recycles): Distillation Column Setup and State-Task Network

6.4.1. Results and Discussion

The set of DAEs required to describe the operation of the distillation column is the same as that for the example of section 6.2. As both off-cuts can be recycled, their compositions have to be treated as additional optimisation parameters, yielding a total of 23 optimisation decision variables. Also, the additional six equality constraints (*cf.* constraint 5.13) for the state-task coupling of the two recycle states and inequality constraints for the fixed initial charge result in a total of six inequality and twelve equality constraints.

The solution of this problem using the SRQPD code required 66 quadratic programming (QP) subproblems and 134 line-search evaluations of the objective function and constraints[6]. The overall computational processing time was approximately 16 *hr* on a SUN SPARC 10/41 workstation.

Over a horizon of one year, the process consumes 2773.11 *kmol* of fresh feed producing 1235.98, 1068.45 and 311.98 *kmol* of products D_1, D_2 and B_f respectively. No R_2 is recycled, and this results in an accumulation of 156.69 $kmol/yr$ of this material. On the other hand, the off-cut R_1 is completely recycled, for reasons similar to those described in the context of the example considered

[6]The optimisation and integration tolerances were set to 10^{-3} and 10^{-6} respectively.

in section 6.3. The optimal revenue of the process is 23828.71 $\$/yr$ as detailed in Table 6.4.

The optimal processing time is 6.77 hr, and a detailed description of the process recipe is given in figure 6.8(a). The variation of normalised reflux ratio with time and the composition trajectories in the reboiler pot are given in figure 6.8(b). The composition trajectories in the accumulator tanks are shown in figures 6.9(a) and 6.9(b).

A comparison of tables 6.3 and 6.4 indicates that, in this case, there is an increase in the total revenue of the process of 1697.63 $\$/yr$ as compared to the distillation column setup presented in section 6.3. Even though there is a decrease in the production of B_f, the increase in the production of D_1 and D_2 results in this increase in the net revenue of the process. This is achieved by recycling only R_1 which is rich in cyclohexane and n-heptane as the cost incurred by discarding all of R_2 is only 156.69 $\$/yr$.

To understand why the second off-cut is not also recycled, we note that the first off-cut contains 62.0% cyclohexane and the second one 73.4% toluene. This provides some justification for the recycle policy determined by the optimisation as remixing of already separated products is not a thermodynamically sound policy. This result is in agreement with the optimal policy reported by Mujtaba (1989) of recycling the off-cuts sequentially rather than simultaneously. In this case, the first off-cut is recycled at the start of the distillation whereas the second off-cut is introduced just before the start of the second main cut.

6.5. Concluding Remarks

The optimal operation of a multicomponent batch distillation operation has been considered for the separation of a ternary component mixture. Two distillation column set-ups have been considered, with and without off-cut recycles.

Table 6.5 provides a summary of the net revenue of the process for each of the recycle policies examined. It is clear that off-cut recycle improves the economics of the process under consideration. As expected, the best net revenue is achieved for the last scenario, which has a larger initial charge and consequently a larger production rate. Of course, more generally, the desirability of off-cut recycling will depend on the relative values of the feedstock, off-cuts and products. For example,

Total Annualised Capital Cost	**42320.00 $/yr**
Total Operating Cost	**495.00 $/yr**

Material	Amount ($kmol/yr$)	Revenue ($/yr$)
F_O	-2773.11	-5546.22
D_1	1235.98	37079.40
R_1	0.0	0.00
D_2	1068.45	27779.70
R_2	156.69	-156.69
B_F	311.98	7487.52
Total Production Revenue		**66643.71**
TOTAL NET REVENUE		**23828.71 $/yr**

Table 6.4: Ternary Batch Distillation (Multiple Off-cut Recycles): Economic Breakdown of Optimal Solution

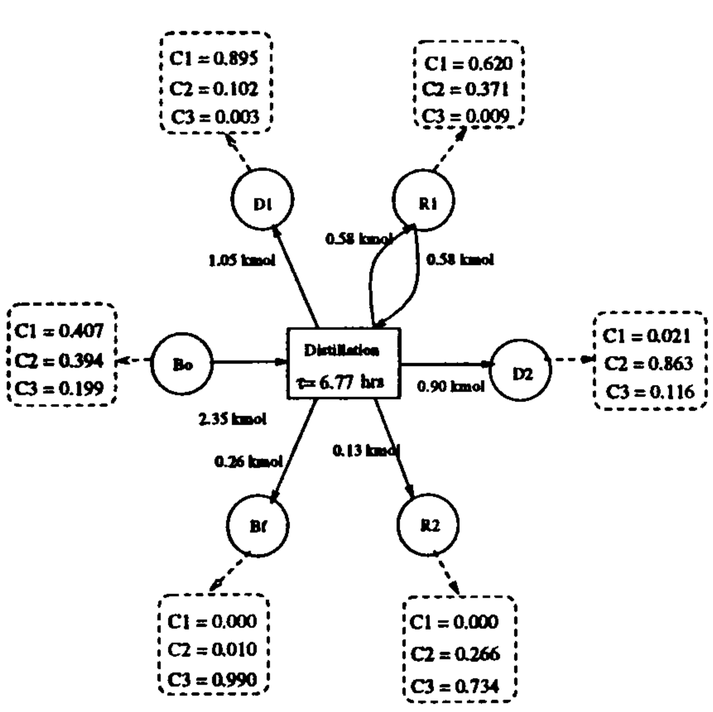

(a) Optimal process recipe (C1 = Cyclohexane mole fraction, C2 = n-Heptane mole fraction, C3 = Toluene mole fraction.)

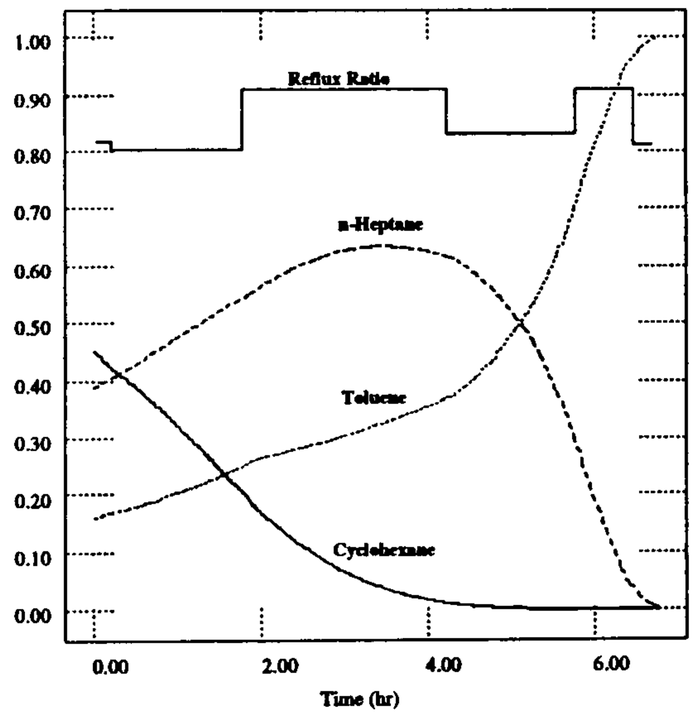

(b) Reflux Ratio and Reboiler Composition Trajectories

Figure 6.8: Ternary Batch Distillation (Multiple Off-cut Recycles): Optimal Process Recipe, Reflux Ratio Variation and Reboiler Composition Trajectories

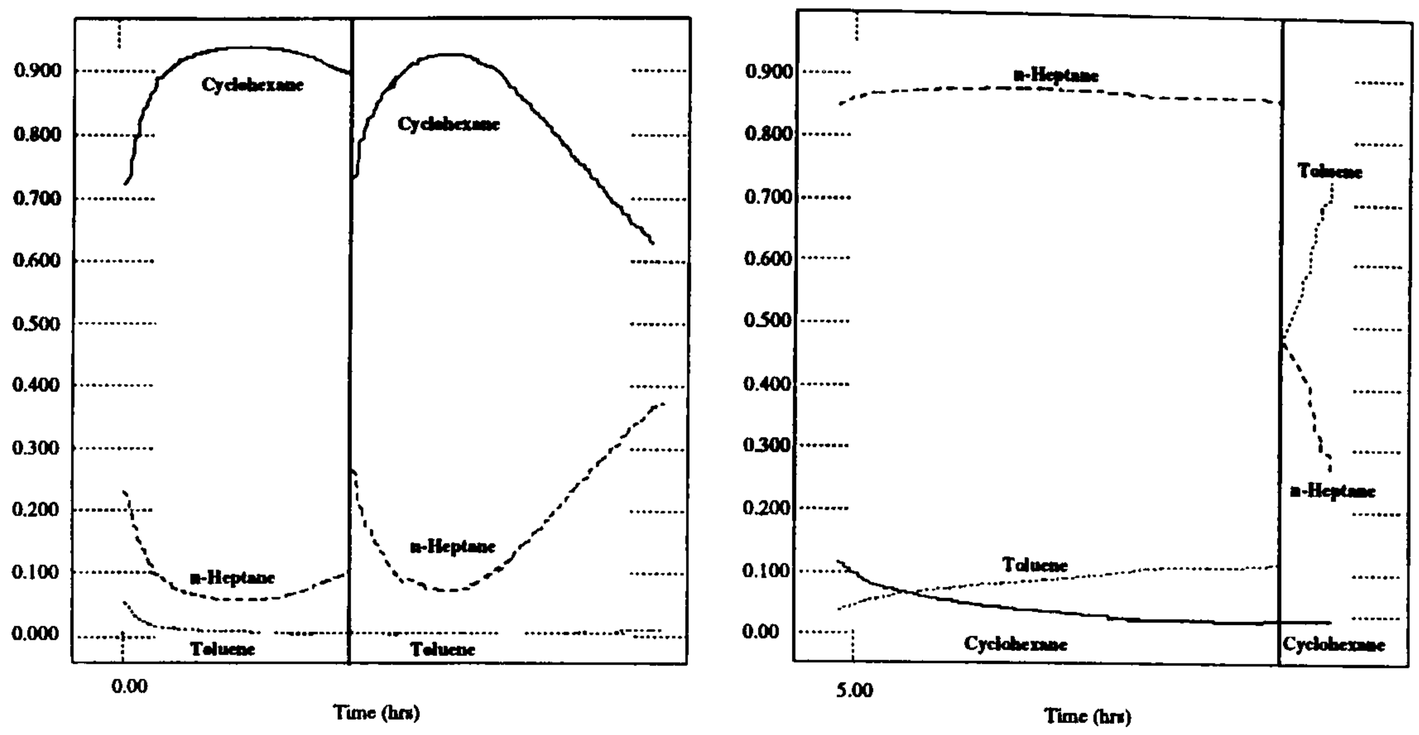

(a) First Main-Cut and Off-Cut (b) Second Main-Cut and Off-Cut

Figure 6.9: Ternary Batch Distillation (Multiple Off-cut Recycles): Accumulator Composition Profiles

in the case of negligible feedstock off-cut costs, recycling of off-cuts will reduce the net revenue of the process.

As far as our batch process design methodology is concerned, the examples presented in this chapter have provided some evidence of its generality and applicability. In particular, they have shown how recycles of material can easily be handled in a general manner without the need for deriving special purpose solution algorithms as was necessary in the past (see, for instance, Mujtaba and Macchietto (1993)).

Scenario	Total Revenue $/yr	Description
1	20336.78	No off-cut recycling and 2.93 *kmol* total initial charge.
2	22567.04	Combined off-cut recycling and 2.93 *kmol* total initial charge.
3	23828.71	Off-cut recycling and 2.93 *kmol* total initial charge.

Table 6.5: Ternary Batch Distillation: Summary of Net Revenue for the Various Distillation Scenarios

Chapter 7

Batch Process Design Applications: II. Reaction/Separation Processes

Most batch processes comprise multiple processing steps transforming a set of raw materials to a number of desired products. In many cases, recycle streams are utilised to recover unconverted materials and improve the process economics. In this chapter, we consider three examples to illustrate the applicability of the proposed design formulation to such processes. The first example involves a three stage process with multiple recycle streams. In Example 2, a six stage process with two possible recycle streams is considered, allowing us to examine the effect of recycling unreacted feedstocks on the total revenue of the process. Finally, the case of zero-wait task trains is considered for a process with a number of unstable material states.

7.1. Example 1: Reaction-Distillation Process I

The process under consideration is described by the STN of figure 7.1 and is to be implemented in a batch plant of the form shown in figure 7.2. Three tasks are utilised to transform pure feedstocks, A and B to the final product, Pr. Three additional materials are produced. One of them, Res, is too heavy to be of any practical use within the process and must be discarded. However, the other two, $Rec1$ and $Rec2$, can be recycled.

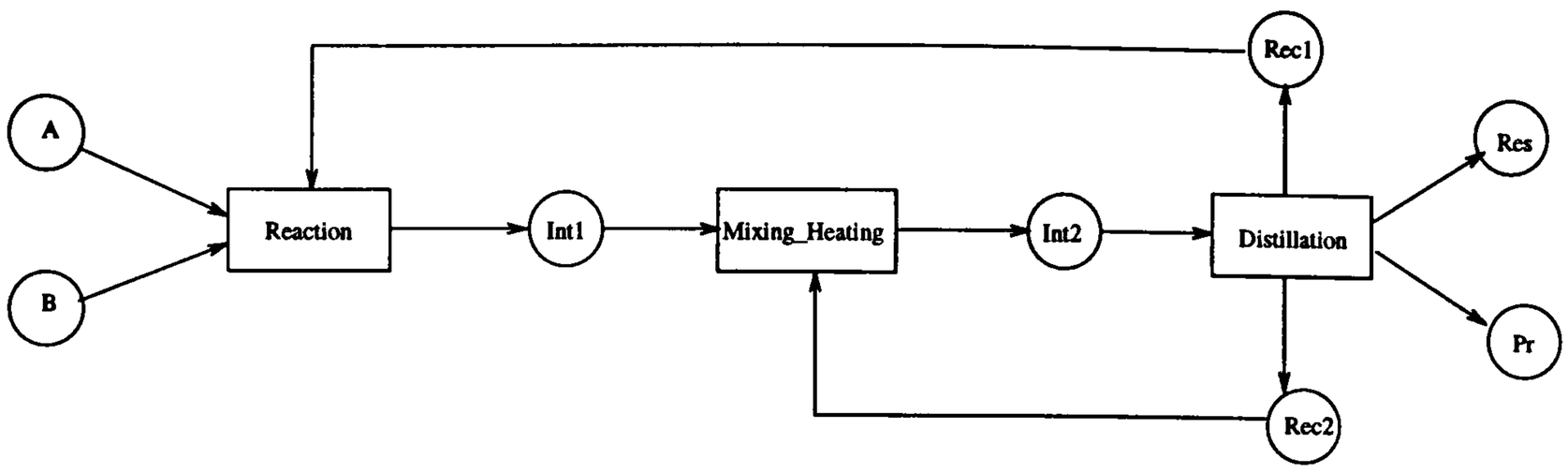

Figure 7.1: Example 1: State-Task Network

7.1.1. Process Description

The main reaction $A + B \rightarrow C$ and the side reaction $B + C \rightarrow D$ take place in the liquid phase in the reactor. The side reaction is favoured at higher temperatures and consumes the desired product C. The reactor contents must be kept below a maximum temperature of $350K$ at all times in order to avoid vapourisation of the reacting mixture; the temperature may be controlled by manipulating the flowrate of the cooling water in a cooling jacket. The maximum cooling water flowrate is 3.6 *tonnes/hr*.

The mixing-heating task pre-heats the reactor product *Int*1 to $360K$, a temperature close to the bubble point of the material fed to the distillation column. At the same time, it mixes it with any recycled amount of *Rec*2. The heating medium used is saturated steam at a pressure of 4 *bar*. The steam flowrate is assumed to be constant throughout the heating operation, up to a maximum of 1 *tonne/hr*.

The distillation column produces three distillate cuts. Saturated steam at 4 *bar* is used in the reboiler. It is assumed that the volatility of the four components in the process decreases in the order $A > B > C > D$. Consequently, the first cut *Rec*1 recovers the unreacted reactants A and B; clearly, these can be recycled back to the reaction. The second cut *Rec*2 comprises a mixture of the reactants with the desired product C; this may be mixed with fresh reactor product to undergo distillation. The desired product C is recovered in the third cut with a specified minimum purity of 95 %. All three distillate cuts are cooled down to $300K$ using cooling water at $288K$ before entering their respective distillation tanks (see figure 7.2). The residue *Res* remaining in the column reboiler, trays and condenser at the end of the distillation is primarily component D and

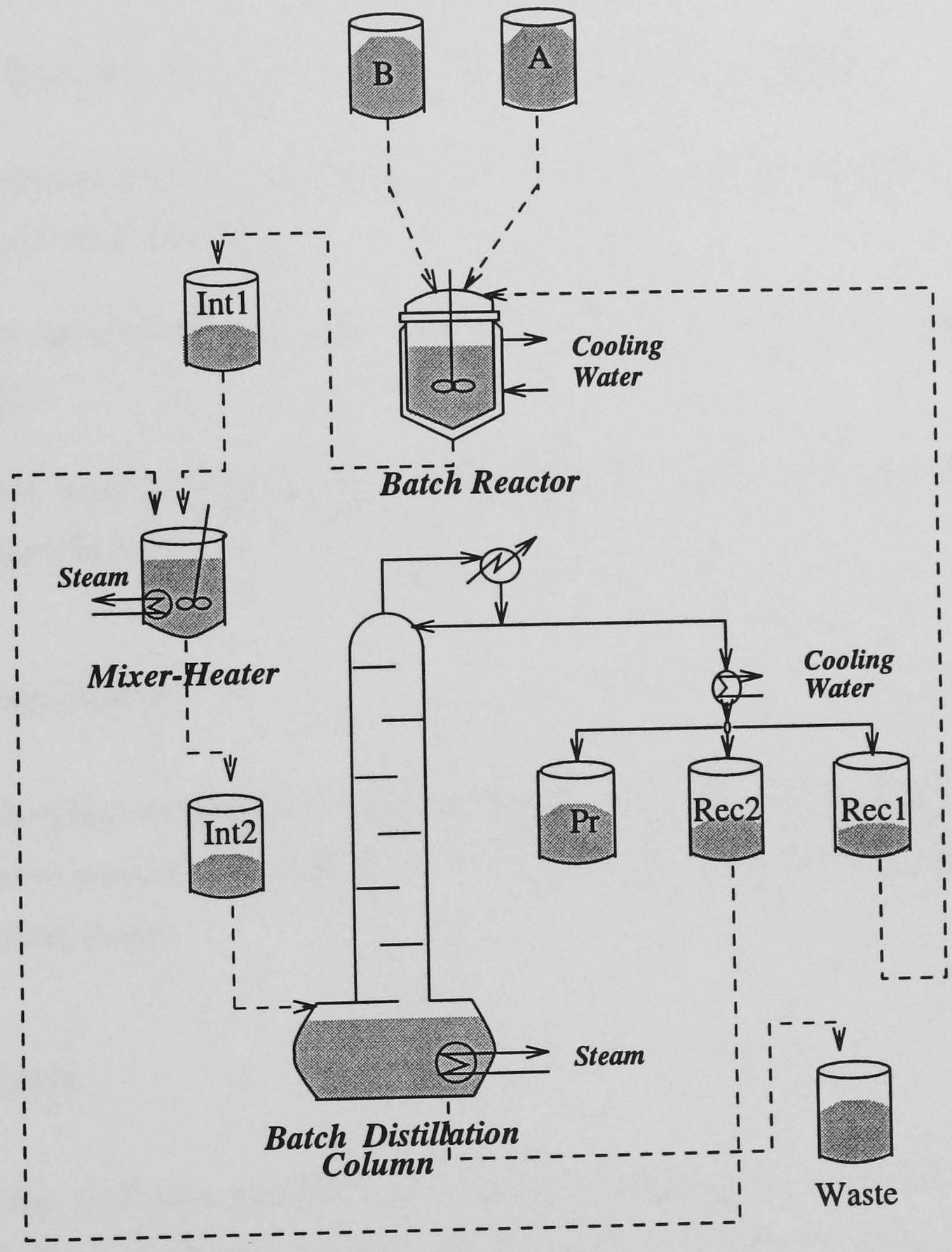

Figure 7.2: Example 1: Plant Flowsheet

Equipment Item	Minimum Capacity ($kmol$)	Maximum Capacity ($kmol$)	Cost Coefficient ($rcu/kmol^{0.8}.hr$)
Reactor	15.0	50.0	0.086
Mixer-Heater	15.0	50.0	0.033
Distillation Column	15.0	40.0	0.185

Table 7.1: Example 1: Plant Equipment Characteristics.

is discarded. The normalised reflux ratio is allowed to vary between 0.5 and 0.99 and the reboiler load between 550.0 and 1250 MJ/hr.

All materials are assumed to be stable. Thus each task can be viewed as a separate zero-wait train (*cf.* section 4.1).

The detailed task models and physical property and the kinetic data used are given in Appendices A and B respectively.

7.1.2. Available Equipment

It is assumed that the plant will comprise one equipment item dedicated to each task. The equipment capacities are constrained to lie within the limits shown in Table 7.1. The distillation column comprises 12 theoretical trays.

7.1.3. Economic Data

The unit values of the various materials in the process are shown in Table 7.2[1]. Note that the values of $Int1$, $Int2$, $Rec1$, $Rec2$ and Res are negative, reflecting the undesirability of building up stocks of these materials.

The unit costs for the cooling water and steam utilities are 0.2 and 10.0 $rcu/tonne$ respectively.

Finally, we assume that the annualised capital cost of equipment item i is given by $\alpha_i Batchsize^{0.8}$. The values of the coefficients α_i are given in the last column of Table 7.1.

[1] rcu = Relative Cost Unit.

Material	Unit value ($rcu/kmol$)
A	3.0
B	3.0
$Int1$	-0.1
$Int2$	-0.1
$Rec1$	-0.1
$Rec2$	-0.1
Res	-0.1
Pr	30.0

Table 7.2: Example 1: Unit Values for Process Material

7.1.4. Modelling Considerations

The reactor operation is modelled in terms of a set of standard dynamic material and energy balances. The cooling driving force is taken as the difference between the outlet cooling water temperature and the temperature of the reactor contents which are assumed to be well-mixed. The cooling water flowrate can be varied in a piecewise constant fashion over the duration of the reaction. For the purposes of the optimisation, we assume that this is done over 5 time intervals of variable length. The duration of each interval is allowed to vary between $0.02hr$ and $3.00hr$.

The operation of the mixer-heater unit is modelled in terms of standard dynamic material and energy balances. For the purposes of the optimisation, the steam flowrate is treated as a time invariant parameter. This is equivalent to allowing a single time interval for the required temperature change to take place. The duration of the interval is allowed to vary between $1.00hr$ and $5.00hr$.

The operation of the distillation column is modelled assuming constant liquid hold-ups on the trays and the condenser, negligible vapour hold-up, and fast energy dynamics. The initial charge to the column fills the reboiler, trays and total condenser with liquid at the charge composition. A molar hold-up of 50.0 *moles* is assumed for both the column trays and total condenser. An ideal mixture model is adopted for the prediction of the vapour-liquid equilibrium. Both reflux ratio and reboiler load are utilised as piecewise constant control variables. For the purposes of the optimisation, the operating time of the distillation step is divided into 6 intervals of variable

duration, with the first and second cuts being produced at the ends of intervals 2 and 4 respectively. The duration of each interval is allowed to vary between $0.02hr$ and $2.00hr$.

The detailed form of the models is presented in Appendix A while the data used in them are listed in Appendix B.2.

7.1.5. Results and Discussion

The overall model of the process involves a total of 420 differential and algebraic equations describing the task operation. The number of decision variables manipulated by the optimisation is 76. The solution using the SRQPD sequential quadratic programming code (Chen and Macchietto, 1989) required 126 quadratic programming (QP) subproblems and 112 line-search evaluations of the objective function and constraints[2]. The overall computational processing time was approximately 22 *hr* on a SUN SPARC 10/41 workstation.

The total net revenue of the process is 98.3 rcu/hr producing 5.151 $kmol/hr$ of *Prod*. To achieve this, 5.313 and 7.285 $kmol/hr$ of A and B respectively are consumed. A detailed economic breakdown of the solution obtained is provided in Table 7.3 showing the equipment cost with the various equipment sizes, the production revenue and operating costs. It can be seen that the intermediates *Int*1, *Int*2, *Rec*1 and *Rec*2 are not allowed to accumulate, but some accumulation of the waste *Res* is unavoidable.

The Reaction task consumes 12.27 and 16.81 $kmol/batch$ of A and B respectively, with a processing time of 1.98 *hr*. The profile of the cooling water flowrate in the reactor and the resulting temperature profile are shown in figures 7.3(a) and 7.3(b) respectively. It can be seen that the solution satisfies the constraint on the maximum temperature, never allowing the latter to exceed 350 K.

The Mixing-Heating task consumes 35.30 and 0.41 $kmol/batch$ of *Int*1 and *Rec*2 respectively, with a processing time set to the lower bound of 1.0 *hr*. For this particular processing task, an idle time of 2.0 *hr* is utilised to match the production rates of the reaction and distillation task. The fact that the lower bound on the processing time is active does not affect the revenue of the process as the total steam consumption required to heat up the initial charge to the required temperature is

[2]The optimisation and integration tolerances were set to 10^{-3} and 10^{-6} respectively.

Equipment Item	Capacity ($kmol$)	Annualised Cost (rcu/hr)
Reactor	39.08	1.61
Mixer-Heater	35.71	0.58
Distillation Column	32.29	2.98
Total Annualised Equipment Cost		**5.17**
Material	Net Production Rate ($kmol/hr$)	Revenue (rcu/hr)
A	-5.313	-15.94
B	-7.285	-21.86
$Int1$	0.000	0.00
$Int2$	0.000	0.00
$Rec1$	0.000	0.00
$Rec2$	0.000	0.00
Res	2.284	-0.23
Pr	5.151	154.53
Total Production Revenue		**116.50**
Utility	Mean Consumption Rate ($tonne/hr$)	Cost (rcu/hr)
Cooling water	34.72	6.94
Steam	0.609	6.09
Total Utility Cost		**13.03**
TOTAL NET REVENUE		**98.30**

Table 7.3: Example 1: Economic Breakdown of Optimal Solution

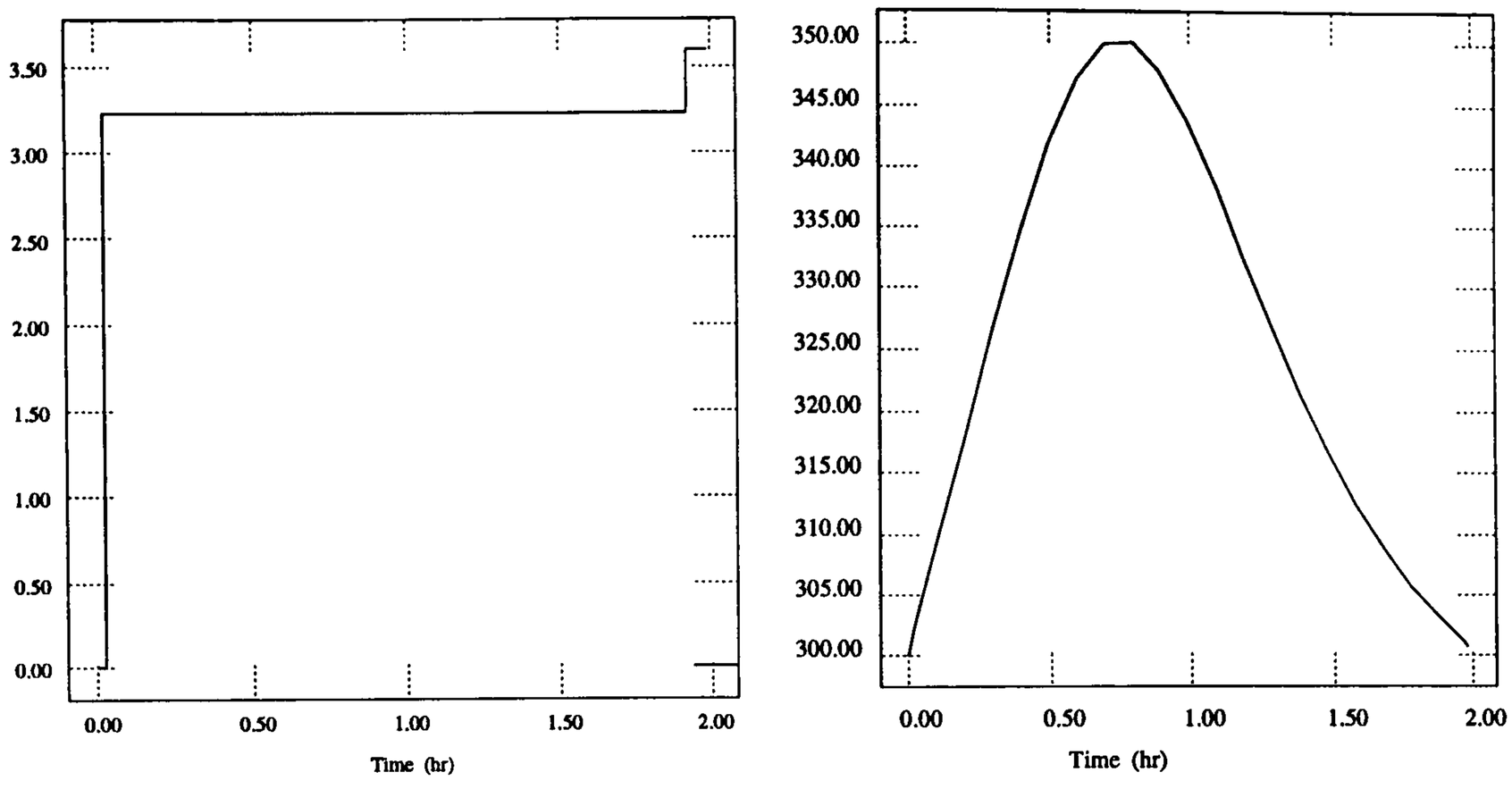

(a) Cooling Water Flowrate Variation $(tonne/hr)$

(b) Temperature (K)

Figure 7.3: Example 1: Reaction Optimal Profiles

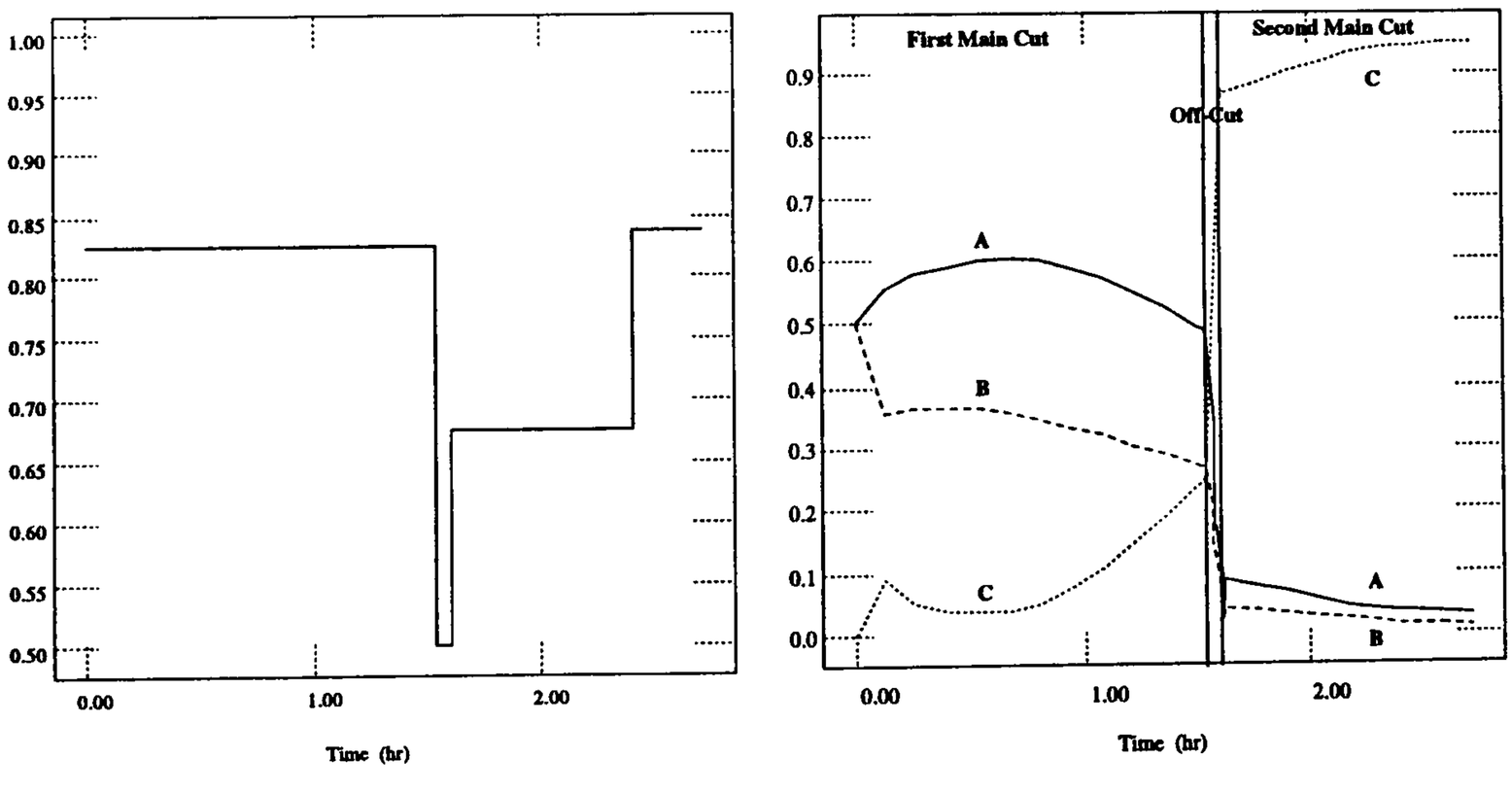

(a) Reflux Ratio Variation

(b) Accumulator Composition Trajectories

Figure 7.4: Example 1: Distillation Optimal Profiles

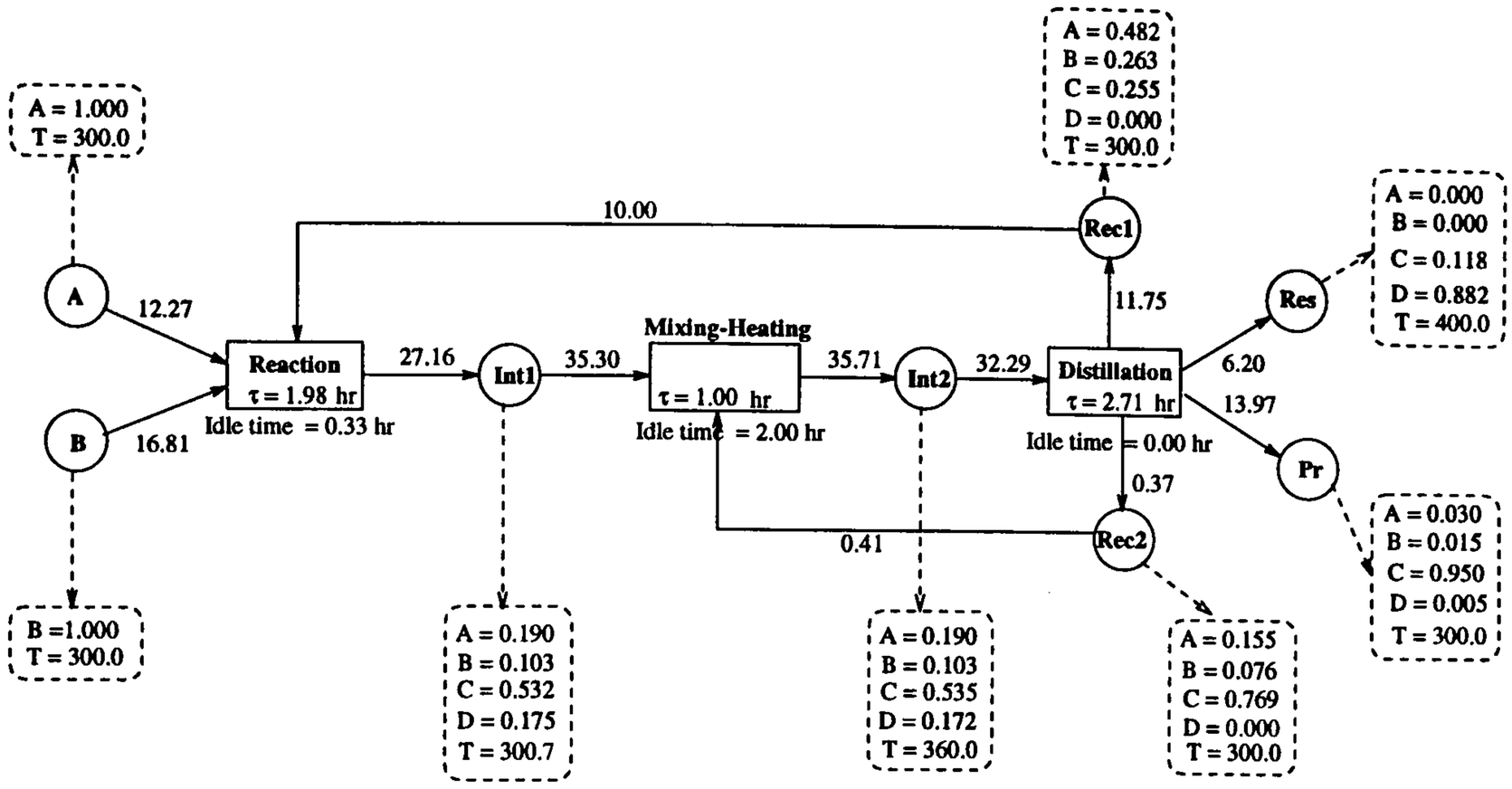

Figure 7.5: Example 1: Optimal Process Recipe

only a function of composition and batchsize. This implies that, if a smaller time where to be used, a higher steam flowrate and idle time would be used to compensate for the decrease in processing time, retaining the total steam consumption and production rate at the same level. It should be noted that the 360 K temperature requirement for $Int2$ is achieved by a steam consumption rate of approximately 0.06 $tonnes/hr$.

The Distillation task consumes 32.29 $kmol/batch$ of $Int2$ with a processing time of 2.71 hr. The optimal variation of the normalised reflux ratio in the distillation column is shown in figure 7.4(a). At the optimal solution, the reboiler heat load is held at its maximum value of 1250 MJ/hr throughout the entire distillation. The resulting composition trajectories of the various distillate cuts collected in the accumulator are shown in figure 7.4(b). It is interesting to note that the amount of off-cut produced and recycled to the mixer/heater is very small (about 1% of the distillation batchsize): it is more profitable for more material to be included in the first main cut which is recycled to the reactor.

The characteristics of the recipe are summarised in the annotated State-Task Network of figure 7.5 [3].

[3]See section 6.2 on how to interpret the annotated STN.

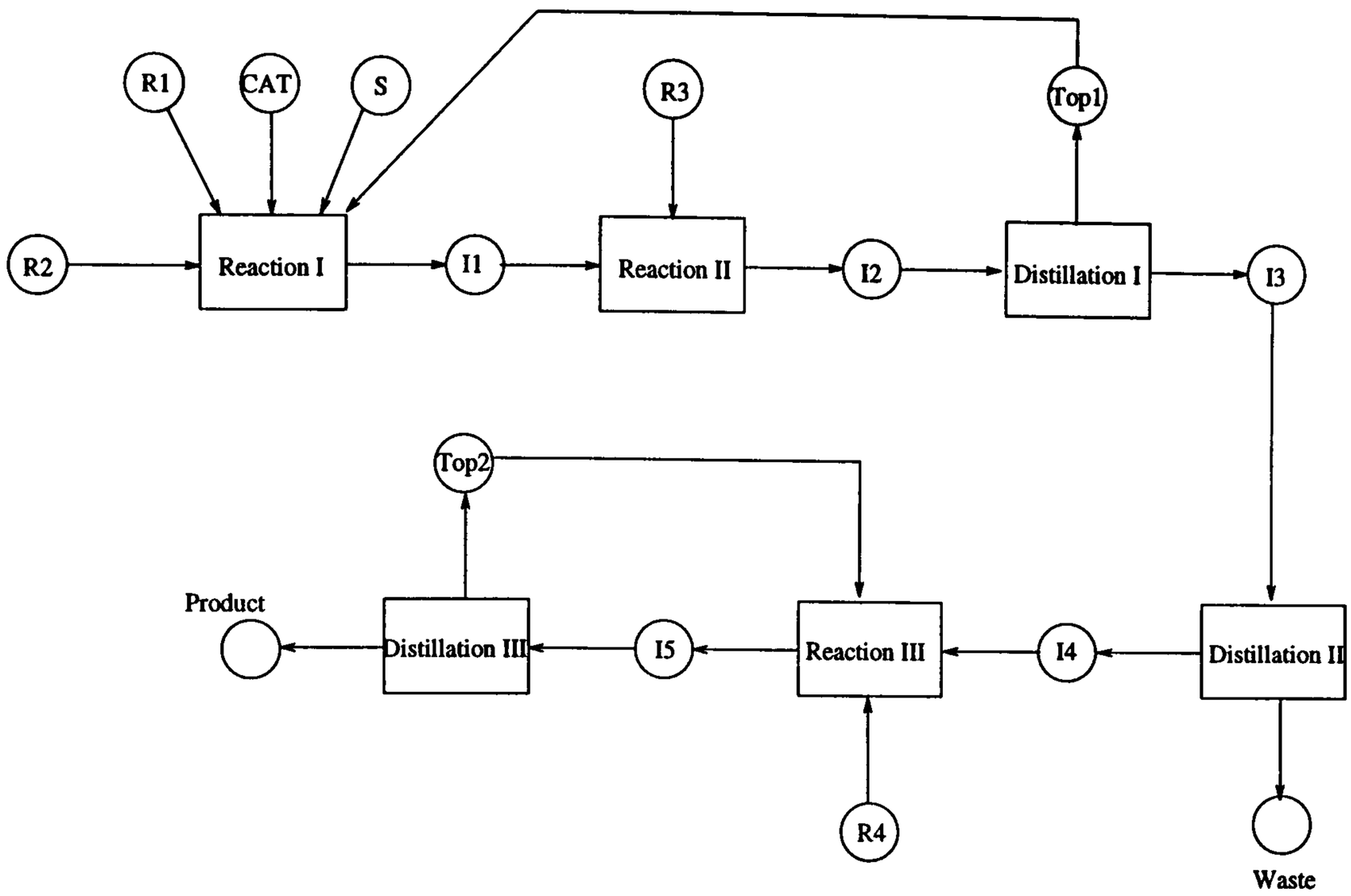

Figure 7.6: Example 2: State Task Network

7.2. Example 2: Reaction-Distillation Process II

The structure of this process is similar to that of the "Lucretex" process originally described by Barrera (1990). The process recipe is described by the STN of figure 7.6 and is to be implemented in the batch plant shown in figure 7.7. A main *Product* is produced from pure feedstocks R_1, R_2, R_3 and R_4 in three reaction and three distillation tasks. Three side products are also produced: Top_1 and Top_2 are mixtures of feedstock components while $Waste$ contains mainly active and deactivated catalyst particles and heavy byproducts. All the materials in this process are assumed to be stable and can therefore be stored in unlimited amounts.

7.2.1. Process Description

Reaction I transforms feedstocks R_1 and R_2 to intermediate I_1 via the exothermic liquid phase reaction scheme:

$$R_1 + R_2 \rightarrow I_1$$

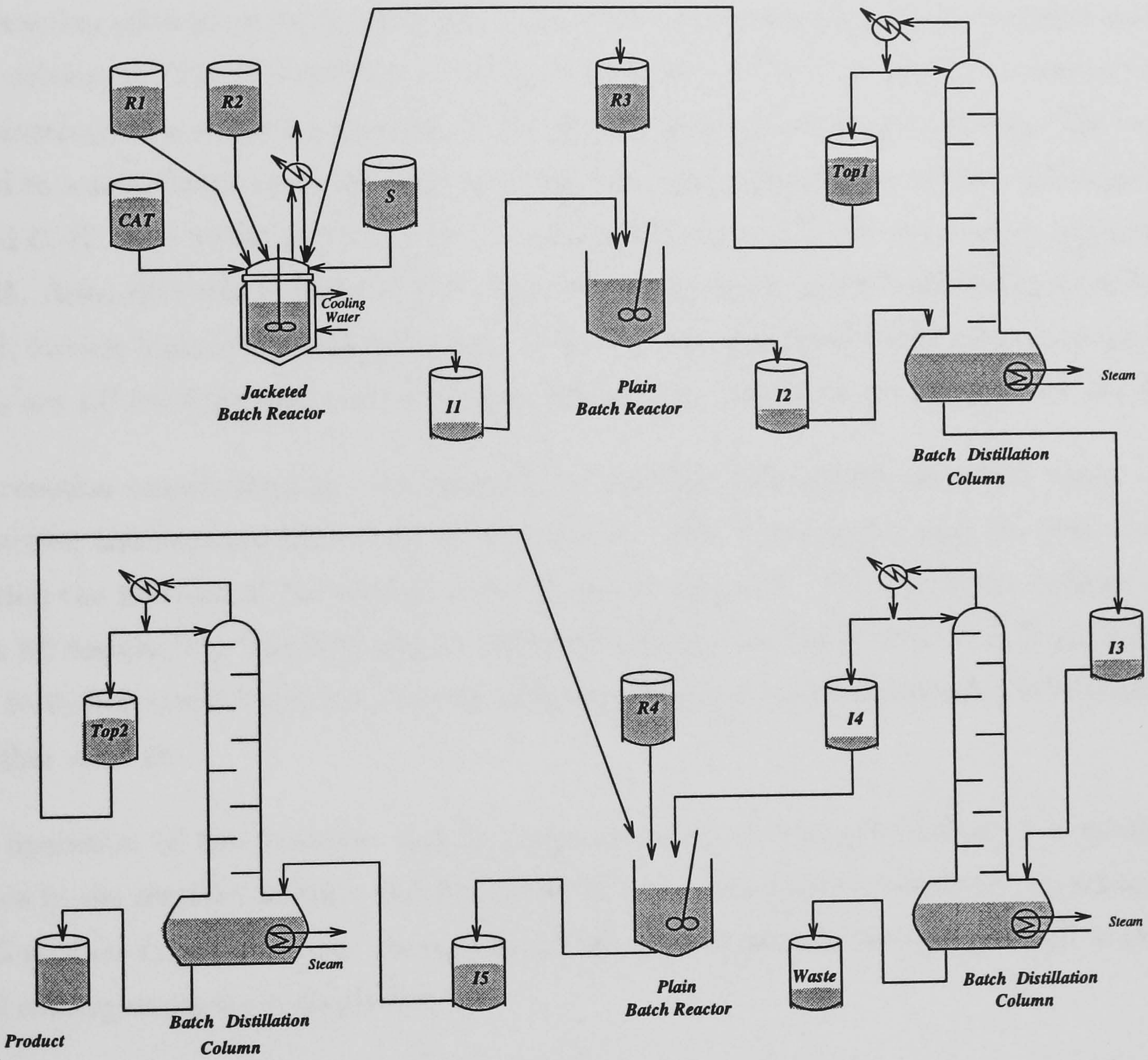

Figure 7.7: Example 2: Plant Flowsheet

$$
\begin{aligned}
R_1 + I_1 &\rightarrow A \\
I_1 &\rightarrow C + G \\
I_1 + C &\rightleftharpoons I_2 \\
CAT &\rightarrow CAT^*
\end{aligned}
$$

The reaction takes place in the presence of activated catalyst particles CAT, supplied in slurry form, and solvent S. The deactivation of catalyst particles to CAT^* is also taken into account, with the deactivation rate being a function of the concentration of active catalyst only. The reactor is operated in a semi-batch mode allowing both discrete initial charges and continuous supplies of R_1, R_2 and CAT. The molar ratio of S to R_2 in the total amount fed to the reactor must always exceed 1.35. Also, the ratio of litres of S to kilograms of R_2 at the end of processing must be less than 0.016, forcing high conversions with respect to R_2. The maximum supply flowrates for both R_1 and R_2 are 1.0 $kmol/hr$ and for the catalyst 500 dm^3/hr. All feeds are available at 338 K.

The reaction temperature is constrained to lie between 333 and 380 K at all times. Also, a final reaction temperature below 353 K is required. The temperature may be controlled by manipulating the flowrate of the cooling water in a cooling jacket. The maximum cooling water flowrate is 8.0 $tonnes/hr$. The final reactor selectivity, defined as the ratio of A to C produced, is restricted to lie between 0.9 and 2.6, thereby excluding the possibility of producing a final product pure in either A or D.

The operation of this reaction task is complicated by the high volatility of a number of components in the reaction mixture and the production of a gaseous byproduct G. To ensure that only gas G escapes from the reactor during the operation, a partial condenser is utilised to provide additional cooling as shown in figure 7.7.

Reaction II transforms I_1 and pure feedstock R_3 to intermediate I_2 via the reaction:

$$C + 2R_3 \rightarrow E$$

The reactor operates isothermally at 348 K with the relative proportions of each input state and processing time being the only decision variables.

The unreacted raw material and more volatile intermediates in I_2 are removed as Top_1 in **Distillation I** with the heavy materials remaining in the reboiler as bottom product, I_3. **Distillation**

II purifies I_3 to I_4 by removing undesirable heavy components as $Waste$.

Reaction III transforms pure reactant R_4 and intermediate I_4 to final product D via the reaction:

$$R_4 + 2E \rightarrow D + 2R_3$$

The reactor is operated isothermally with the reaction temperature as a design parameter bounded between 310 and 368 K. For the above reaction scheme to be valid, the initial amount of R_4 should be at least 25 times larger than the initial amount of reactant E.

Distillation I is operated at constant atmospheric pressure. **Distillation II** and **Distillation III** are operated at 0.036 and 0.039 *bar* respectively, as they are used to separate heavier mixtures. This, in effect, reduces the operating temperature of the column and thus the condenser heat load. The normalised reflux ratio is allowed to vary between 0.70 and 0.99 for **Distillation I** and **Distillation II**, and between 0.60 and 0.99 for **Distillation III**.

To enforce the removal of the volatile components in Distillation I, the percentage of volatile components in the bottom product is constrained not to exceed 1%. The distillate product of Distillation I is allowed to be recycled back to Reaction I. Finally, the final product (*Product*) should contain at least 99% (by mass) A and D, with the ratio A/D lying between 1.5 and 6.5. The distillate from Distillation III may be recycled back to Reaction III.

The time for charging and discharging each processing task is taken into account as an idle time of 30 *mins* added to the processing time.

7.2.2. Available Equipment

It is assumed that the equipment items dedicated to the various tasks are available in continuous ranges as shown in Table 7.4.

All three distillation columns in the process are assumed to have 8 theoretical trays each, with a constant vapour flow to the condenser of 15 $kmol/hr$.

Equipment Item	Task	Equipment Size		Cost Coefficient a_r
		Minimum (dm^3)	Maximum (dm^3)	($/($dm^3$)$^{0.6}$hr)
Jacketed Reactor	Reaction I	1895.50	3785.00	0.95
Plain Reactor	Reaction II	1895.50	3785.00	0.54
Plain Reactor	Reaction III	1895.50	3785.00	0.54
Distillation Column	Distillation I	2838.75	7570.00	1.48
Distillation Column	Distillation II	2838.75	7570.00	1.48
Distillation Column	Distillation III	2838.75	7570.00	1.48

Table 7.4: Example 2: Plant Equipment Characteristics

7.2.3. Economic Data

The unit values of the various materials are given in Table 7.5. The negative unit values for the intermediates indicate that it is not desirable to have any net accumulation of these states. States Top_1 and Top_2 are mainly unreacted feedstock with a disposal cost.

Capital Costs

The *annualised capital cost* (C_c) of the process is calculated on an hourly basis. For the reactors, the capital cost depends only on the size of the equipment and is calculated through the following correlation:

$$C_c = \alpha_r V_R^{0.6} \tag{7.1}$$

where V_R is the reactor volume and α_r a cost coefficient, given in Table 7.4. It should be noted that the first reactor item has the highest α_r since it has a cooling jacket and a partial condenser.

In the case of the distillation columns, the capital cost (C_c) is of the form

$$C_c = \alpha_r V_D^{0.6} + 0.00033(760 - P)^2 \tag{7.2}$$

comprising both size-dependent and pressure-dependent terms. P is the operating pressure of the column in $mmHg$ and V_D the reboiler volume in dm^3. The last term in equation (7.2) accounts for the extra capital cost incurred when operating the column at sub-atmospheric pressures. Apart

Feedstocks		Intermediates		Product/Waste	
Material	Unit value ($/kmol$)	Material	Unit value ($/kmol$)	Material	Unit value ($/tonne$)
R_1	238.7088	I_1	-100.0	$Product$	50000.0
R_2	1186.608	I_2	-100.0	$Waste$	-13600.0
R_3	39.41166	I_3	-100.0		
R_4	0.180155	I_4	-100.0		
CAT	35(per dm^3)	I_5	-100.0		
S	134.89442	Top_1	-100.0		
		Top_2	-100.0		

Table 7.5: Example 2: Unit Values for Process Materials

from the allowable reboiler volume variations, all three columns are identical and this is reflected in them having the same unit cost coefficient α_r.

Operating Costs

The total *operating cost* (C_{o1}, \$) per batch for Reaction I is due only to the cooling jacket load (Q_c, $kcal/hr$) and is of the form:

$$C_{o1} = 0.004585 \int_0^{\tau_1} Q_c(t)dt \tag{7.3}$$

where τ_1 is the processing time. Tasks Reaction II and Reaction III are operated isothermally with no significant operating cost.

The operating cost per batch for each distillation task (C_o, \$) takes into account the reboiler load, expressed in terms of the vapour flowrate to the condenser (V, mol/hr), the operating pressure (P) and the condenser cooling load (Q_s, $kcal/hr$):

$$C_o = \int_0^{\tau} \left(0.0177V + 0.0011(760 - P)^2 + 0.00065Q_s(t)\right) dt \tag{7.4}$$

where τ is the processing time.

Since V and P are assumed to be constant throughout the duration of the distillation task,

the above simplifies to:

$$C_o = \left[0.0177V + 0.0011(760 - P)^2\right]\tau + 0.00065 \int_0^\tau Q_s(t)dt \tag{7.5}$$

7.2.4. Modelling Considerations

Both material and energy balances are utilised to model the reactors. Of special interest is the first reactor which is modelled as a two phase system assuming ideal vapour-liquid equilibrium. Temperature control is carried out by manipulating the flowrate of the cooling water in the cooling jacket. The cooling driving force is taken as the difference between the outlet cooling water temperature and the temperature of the reactor contents which are assumed to be well-stirred. The flowrates of the various reactants and the cooling water are varied in a piecewise fashion. For the purposes of the optimisation, it is assumed that this is done over 6 time intervals of variable duration. The latter is allowed to vary between 0.6 *hr* and 2.0 *hr*.

The operation of the distillation columns is modelled with both material and energy balances assuming constant liquid hold-ups on the trays and in the condenser, negligible vapour hold-up, fast energy dynamics, and ideal vapour-liquid equilibrium. The initial charge to the column fills the reboiler, trays and total condenser with liquid at the charge composition. A molar hold-up of 100.0 *moles* is assumed for both the column trays and total condenser. For all three distillation tasks, the reflux ratio is a piecewise constant control variable. For the purposes of the optimisation, the operating time of each distillation step is divided into two intervals of variable duration. The latter is allowed to vary between 1.0 *hr* and 8.0 *hr*.

The full spectrum of components is utilised only for Reaction I and Reaction II. For the rest of the tasks, "R_1" represents the combined components R_1, R_2, I_1 and C, whereas I_2 groups together I_2, CAT and CAT^*.

The detailed mathematical models and physical data utilised in this example are provided in Appendices A and B.3 respectively.

7.2.5. Results and Discussion

In addition to the main product, the process under consideration produces three material states, namely $Top1$, $Top2$ and $Waste$. The first two material states, $Top1$ and $Top2$, can be recycled back to $ReactionI$ and $ReactionIII$ respectively, consequently reducing the incurred waste treatment costs. Three possible recycle policies have been considered:

- Policy 1: No recycle streams,
- Policy 2: Recycle $Top1$ to Reaction I,
- Policy 3: Recycle $Top1$ to Reaction I and $Top2$ to Reaction III

The overall model of the process involves a total of 1219 differential and algebraic equations describing the tasks. The number of decision variables manipulated by the optimisation is 120, with 94 constraints of which 56 are equalities. The solution of the optimisation problem using the SRQPD code (Chen and Macchietto, 1989) required 73 quadratic programming (QP) sub-problems and 116 line-search evaluations of the objective function and constraints[4]. The overall computational time was approximately 6 hr on a SUN SPARC 10/41 workstation.

The net revenue achieved with policy 1 is 10879.00 $\$/hr$. Of more interest is policy 2 which achieves an 8% higher net revenue of 11778.13 $\$/hr$. Policy 2 produces 338 kg/hr of $Product$ by consuming 2.71, 1.71, 0.22, 5.48 and 0.53 $kmol/hr$ of R_1, R_2, R_3, R_4 and S respectively. Reaction I also consumes 0.55 dm^3/hr of CAT. None of the intermediate materials $I_1 - I_5$ is allowed to accumulate. A detailed economic breakdown of the solution obtained is provided in Table 7.6 showing the equipment cost with the various equipment sizes, the production revenue and operating costs.

The characteristics of the recipe are summarised in the annotated STN of figure 7.8, with material quantities expressed in $kmol$ (unless otherwise specified), temperatures in K and time in hours. Each state of material is characterised by the mole fraction of the components present. For Reaction II, Distillation I and Distillation II, the optimisation introduces some idle time over and above the 30 $mins$ of charging and discharging, to ensure that the mean processing rates of all tasks balance correctly.

[4]The optimisation and integration tolerances were set to 10^{-2} and 10^{-5} respectively.

Equipment Item	Capacity (dm^3)	Annualised Cost ($/hr)
Reactor (Reaction I)	3785.00	1.33
Reactor (Reaction II)	1892.50	0.50
Reactor (Reaction III)	3785.00	0.76
Distillation Column (Distillation I)	2985.00	1.80
Distillation Column (Distillation II)	6812.81	4.76
Distillation Column (Distillation III)	7570.00	4.90
Total Annualised Equipment Cost		**14.05**
Material	Net Production Rate ($kmol/hr$)	Revenue ($/hr)
R_1	-2.71	-646.90
R_2	-1.71	-2029.10
R_3	-0.22	-8.67
R_4	-5.48	-0.99
S	-0.53	-71.49
CAT	-0.55(dm^3/hr)	-19.25
I_1	0.00	0.00
I_2	0.00	0.00
I_3	0.00	0.00
I_4	0.00	0.00
I_5	0.00	0.00
Top_1	0.00	0.00
Top_2	5.49	-549.00
$Waste$	0.02 (tonnes/hr)	-272.00
$Product$	0.338 (tonnes/hr)	16900.00
Total Production Revenue		**13302.60**
Task		Operating Cost ($/hr)
Reaction I		171.64
Distillation I		215.77
Distillation II		294.77
Distillation III		828.42
Total Operating Cost		**1510.42**
TOTAL NET REVENUE		**11778.13**

Table 7.6: Example 2: Economic Breakdown of Optimal Solution (Policy 2)

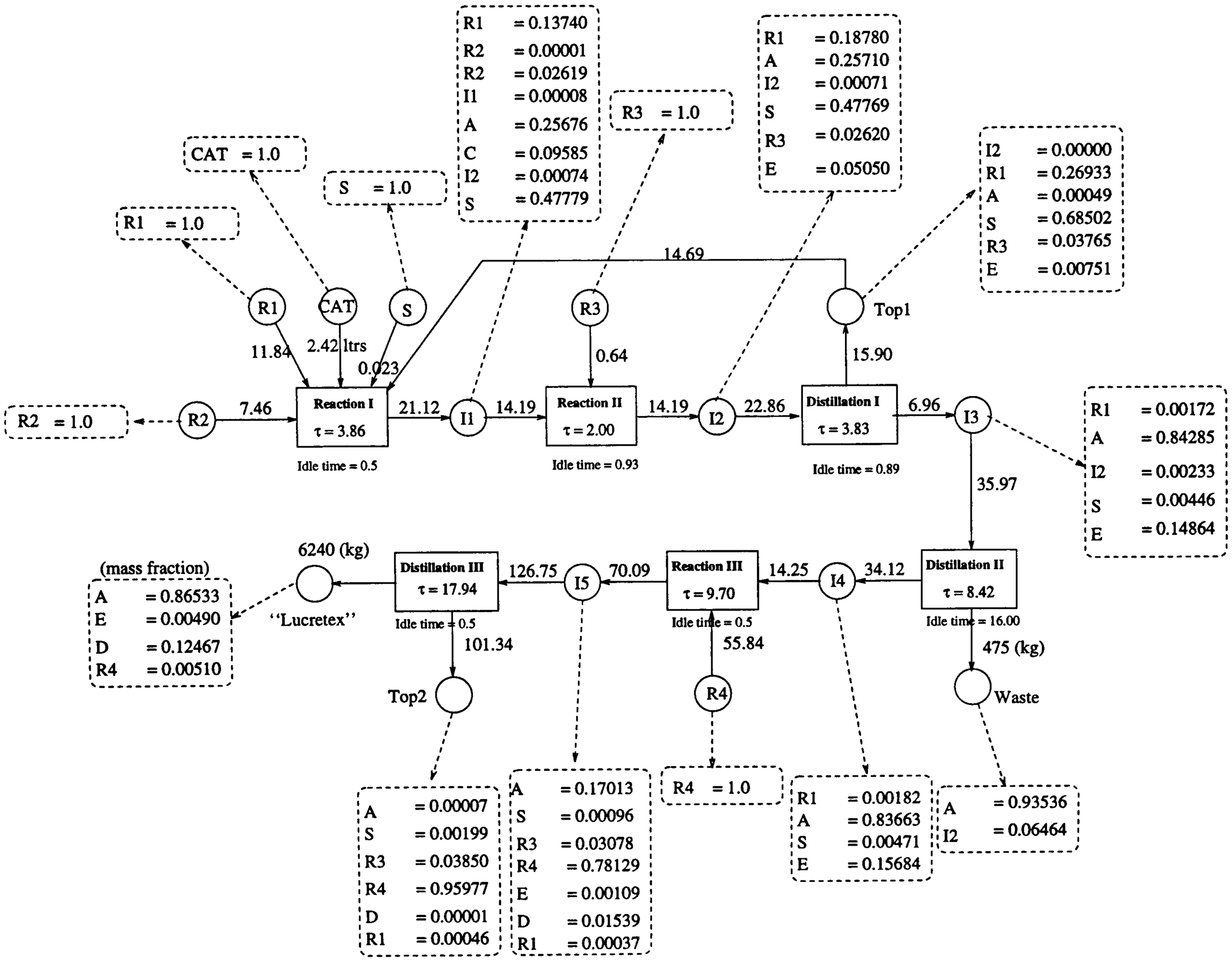

Figure 7.8: Example 2: Optimal Process Recipe (Policy 2)

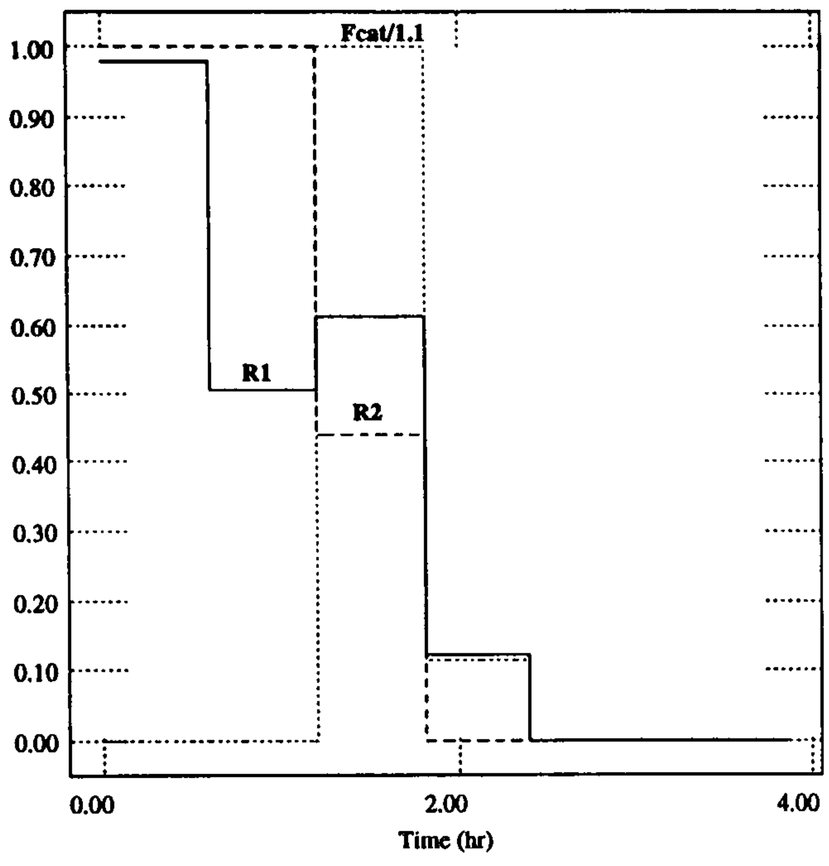

(a) Feed Addition Rates (R1 and R2 in $kmol/hr$, Cat in dm^3/hr)

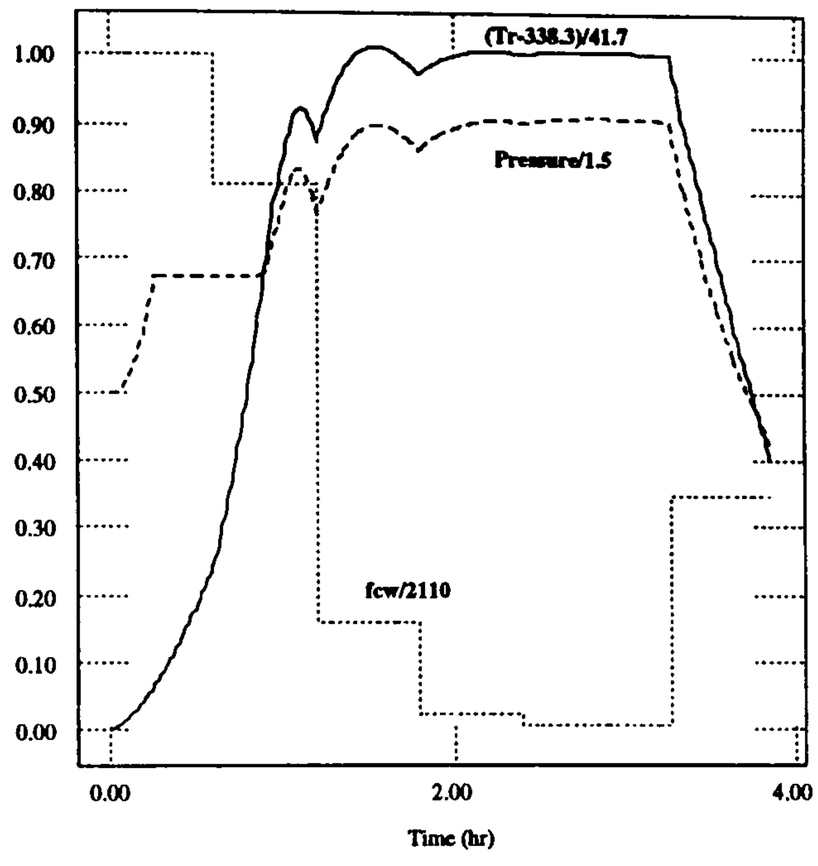

(b) Temperature (K), Pressure (bar) and Cooling Water Flowrate ($tonnes/hr$)

Figure 7.9: Example 2: Temperature, Pressure and Flowrate Profiles in Reaction I (Policy 2)

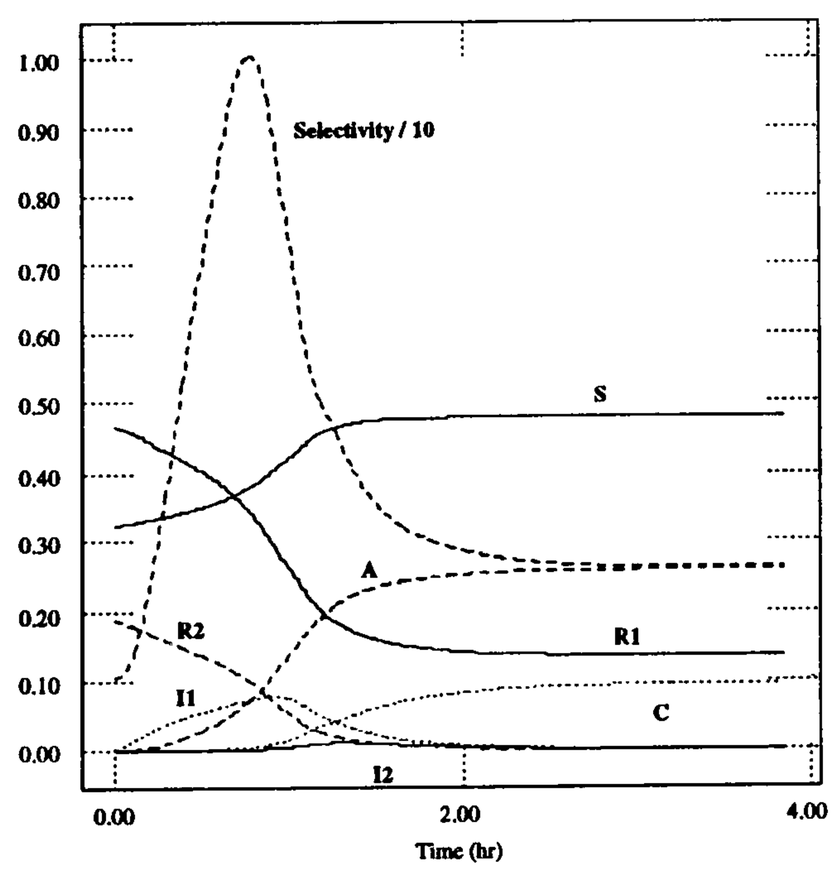

(a) Liquid Phase Composition and A/C Selectivity

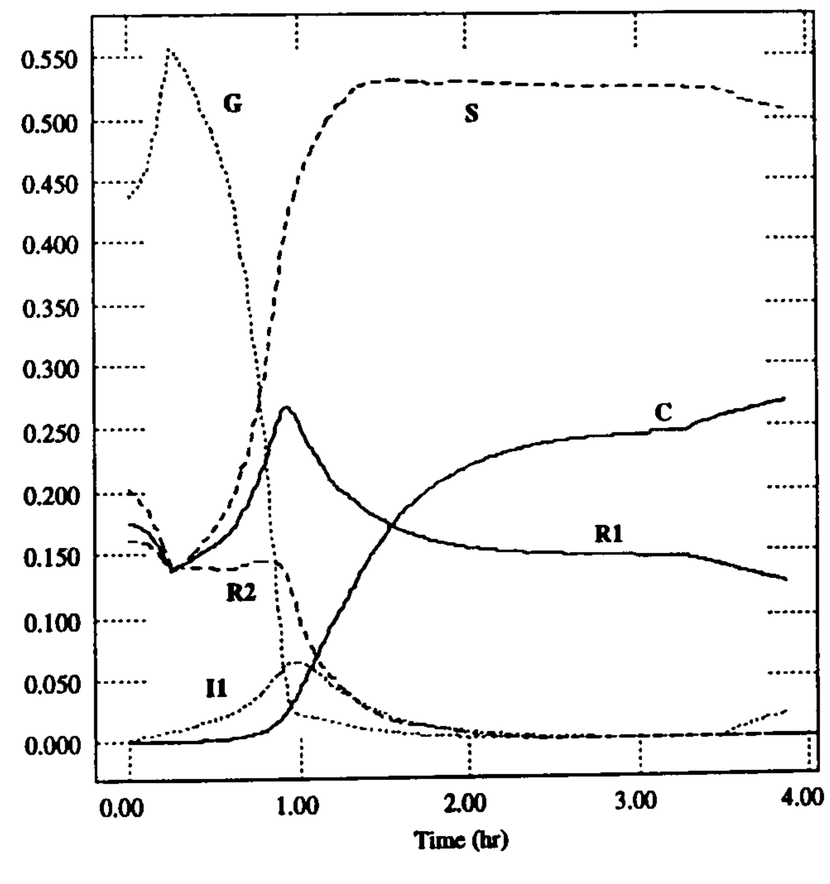

(b) Vapour Phase

Figure 7.10: Example 2: Vapour and Liquid Phase Composition Profiles in Reaction I (Policy 2)

Each batch of Reaction I consumes 11.83, 7.47 and 12.31 $kmol$ of R_1, R_2 and S respectively, and 2.40 dm^3 of CAT, with a processing time of 3.86 hr. The initial charge to the reactor contains 10.50, 6.00, 0.023 kmol R_1, R_2 and S, and 1.68 dm^3 CAT. Additional amounts of catalyst, R_1 and R_2 are added continuously in the first half of the operation as shown in figure 7.9(a). The selectivity of component A with respect to component C is 2.6, with the selectivity trajectory shown in figure 7.10(a). For the reactor to reach approximately 100% conversion of R_2, R_1 is maintained at relatively high concentrations throughout the operation of this task (see figure 7.10(a)). Since traces of R_2 are left at the end of the task, the second constraint on the ratio of S to R_2 is satisfied. Also, the molar ratio of S to R_2 in the total amount fed to the reactor is 1.35.

It is interesting to note that the operating policy ensures that the final reaction mixture contains only negligible amounts of intermediates I_1 and I_2, and that the mole fractions of these two components go through a peak in the first half of the processing, as shown in figure 7.10(a). At the start of the reaction, the concentrations of R_1 and R_2 are high, favouring the generation of I_1. However as the concentration of I_1 increases, reaction $R_1 + I_1 \rightarrow A$ as well as the forward reaction generating I_2 (favoured at high temperature) set in, thereby depleting I_1. On the other hand as I_1 is depleted and the concentrations of I_2 are high, the reverse reaction consuming I_2 is favoured. Overall, little I_1 and I_2 are left in the final mixture. It should also be noted that the operating policy takes into account the fact that the solvent reduces the reaction rates and concequently the production rate of this processing task. Therefore, the amount of solvent S added is such that it ensures the satisfaction of the constraint on the molar ratio of S to R_2.

The variation in the reaction temperature of Reaction I with the corresponding cooling water flowrate are given in figure 7.9(b). A high cooling water flowrate is adopted at the beginning of the processing in order to reduce the initial rate of temperature rise, and at the end to cool down the mixture to the required temperature of 355 K quickly. The pressure, the variation of which is also shown in figure 7.9(b), stays at or above atmospheric levels almost throughout the operation. The steep pressure decrease near the end of the processing is due to the rapid reduction in temperature. The vapour phase composition is shown in figure 7.10(b), consisting mainly of R_1, R_2, S, C and the non-condensible gas G.

Reaction II consumes 14.18 and 0.64 $kmol/batch$ of I_1 and R_3 respectively and operates for 2.00 hr. Reaction III is operated at the maximum allowable temperature of 368 K for 9.70 hr and consumes 14.25 and 55.84 $kmol/batch$ of I_4 and R_4 respectively.

Distillation I separates 22.86 *kmol/batch* of I_2 producing 15.90 *kmol/batch* of top product, comprising mainly S and R_1. A 6.96 *kmol* residue comprising mainly A and E remains in the reboiler at the end of this operation. The reflux ratio is 0.7065 for the first 1.0 *hr* and 0.700 for the last 2.83 *hr*.

Distillation II separates 35.97 *kmol/batch* of I_3 and produces 34.11 *kmol* of top product, comprising mainly A and E, with a processing time of 8.42 *hr*. At the end of the processing, 0.46 *tonnes*, comprising mainly A and CAT, remain in the reboiler. The negligible quantities of I_2 generated in Reaction I combined with the fact that it is not possible to evaporate all the material from the reboiler pot, explain the high mole-fraction of A in the accumulator tank. The reflux ratio is maintained at its lower bound of 0.7 throughout the operation of the task.

Finally, in Distillation III, 126.75 *kmol/batch* of I_5 are separated producing 6.24 *tonnes* of the desired product as a bottom product and 101.34 *kmol/batch* of top product containing mainly $R4$. The processing time of this task is 17.94 *hr*. The distillation column is operated at a constant normalised reflux ratio of 0.6. The ratio of A to D in the final product is 6.5.

From the process recipe shown in figure 7.8, it can be seen that $Top2$ primarily contains R_4, with a mole fraction of 0.96. This seems to suggest that there may be some benefit in allowing $Top2$ to be recycled back to Reaction II in accordance with recycle Policy 3. However, this is not the case and any attempt to optimise the process with two recycles (as shown in figure 7.6) simply results in the $Top2$ recycle being set to zero or a very small value. Physically, this behaviour can be explained as follows: the liquid molar volume of this mixture is 0.0206 $m^3/kmol$ whereas the liquid molar volume of R_4 is 0.0196 $m^3/kmol$. As there is a constraint on the molar ratio of E to R_4 fed to Reaction III, the amount of material processed per batch must be reduced if $Top2$ is to replace R_4. Of course, it is possible to counterbalance this reduction in the amount of product per batch by reducing the conversion in Reaction III, and consequently its processing time, to keep the throughput of the process at the same level. Any reduction in conversion, however, will reduce the amount of D produced per batch. Also, Distillation III is a bottleneck on the process (*i.e.* it has no idle time beyond the 0.5 hr allowed for charging and discharging), which implies that if the rest of the units are operated at higher throughput, I_5 will accumulate. However, R_4 is the cheapest material handled in the process and therefore it is preferable not to recover it but rather to use only fresh feedstock R_4 in Reaction III.

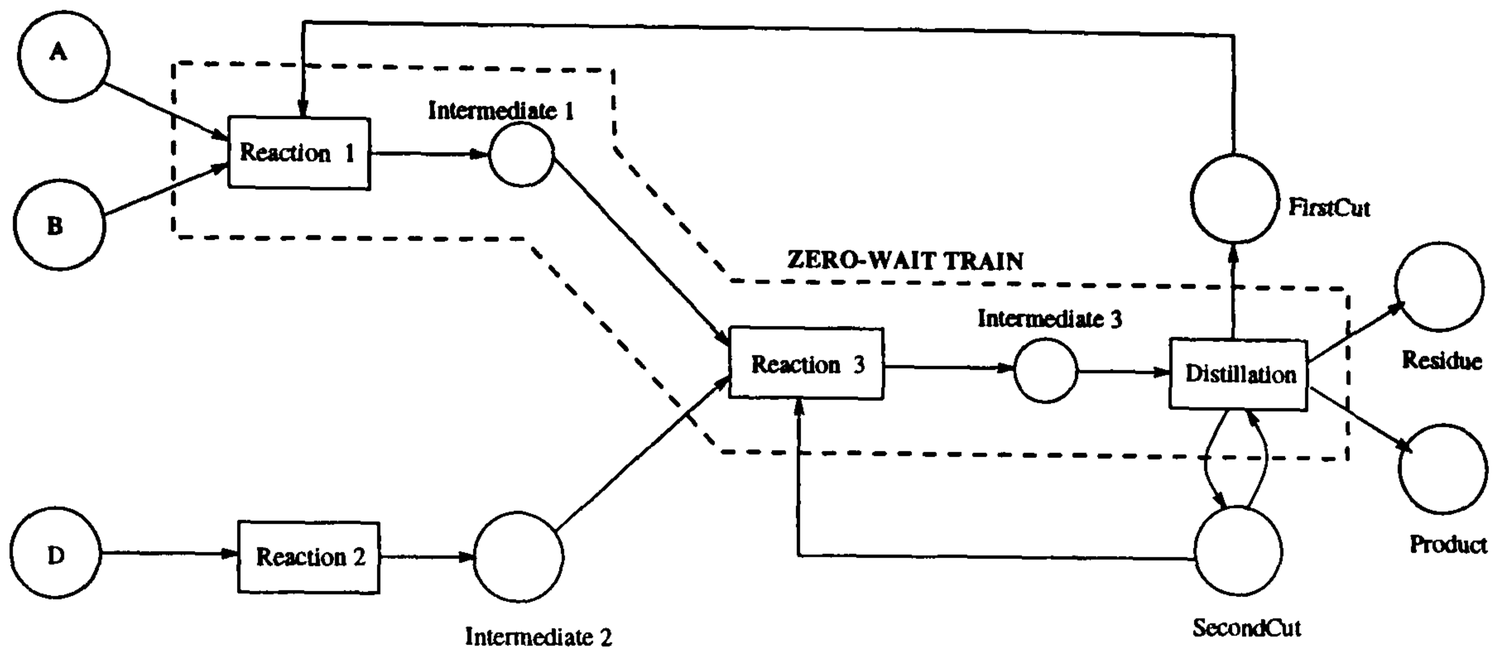

Figure 7.11: Example 3: State Task Network

7.3. Example 3: A Process with Zero-Wait Trains

The STN and equipment configuration for this example are shown in figures 7.11 and 7.12 respectively. Three feedstocks A, B and D are transformed to the final product *Product*. States *Intermediate*1 and *Intermediate*3 are unstable, forcing tasks Reaction 1, Reaction 3 and Distillation to operate in a zero-wait mode, forming a zero-wait train. Unlimited intermediate storage is assumed for all other states.

7.3.1. Process Description

The main reaction $A + B \rightarrow 2C$ and the side reaction $B + C \rightarrow W_1$ take place in the liquid phase in the first reaction step. Due to the highly exothermic nature of these reactions, the amount of reactant A in the initial charge must be at least twice the amount of reactant B. To avoid high concentrations of B (which would favour the side reaction), it is also possible to feed B in a semi-continuous fashion *during* the reaction rather than as an initial charge. The maximum possible feed rate is 10.0 $kmol/hr$. The reactor contents must be kept below a maximum temperature of 350 K in order to avoid vapourisation of the reacting mixture, with the final reaction temperature being constrained between 305 and 310 K. The temperature may be controlled by manipulating the flowrate of the cooling water in a cooling jacket. The maximum cooling water flowrate is 7.2 $tonnes/hr$, but the actual flowrate can be varied over the duration of the reaction. The cooling water supply temperature is 293.3 K.

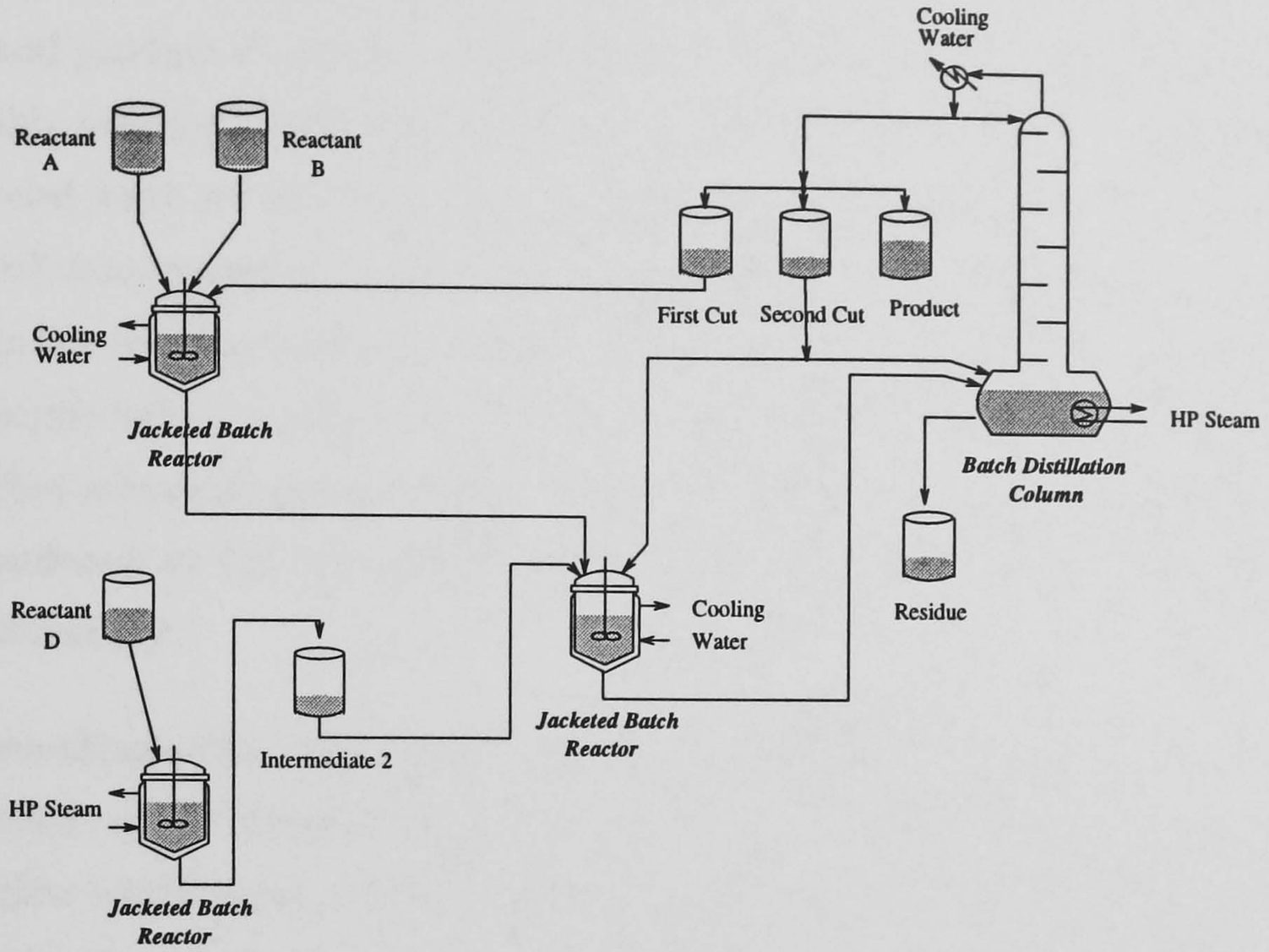

Figure 7.12: Example 3: Plant Flowsheet

The liquid phase endothermic reaction sequence $D \rightarrow E \rightarrow F$ takes place in the second reaction step. Saturated steam at 40.8 *bar* is utilised to heat the reaction mixture. The maximum steam flowrate is 4.0 $tonnes/hr$, but the actual flowrate can be varied. The reaction temperature must be kept below 400 K, with a final value between 298.3 and 310 K.

The outputs of the first two reactors are combined in the third reactor, with the main reaction $E + C \rightarrow 2P$ producing the desired compound P, and the side reactions $D + P \rightarrow W_2$ and $B + P \rightarrow W_3$ producing heavy compounds W_2 and W_3. The reaction scheme is highly exothermic and takes place in the liquid phase. Limitations on reaction temperature and cooling water flowrate identical to those for the first reactor are imposed.

The distillation task produces three distillate cuts. Saturated steam at 40.8 *bar* is used in the reboiler, and cooling water at 293.3 K in the reflux condenser. The volatility of the ten components in the process decreases in the order $C > A > B > D > E > P > F > W_1 > W_2 > W_3$. Consequently, the first cut recovers unreacted C, A and B which can be recycled back to the first reaction. The composition of the second cut depends on the extent of the reaction in the second

and third reactors. Preliminary simulation studies have shown that the second cut contains mainly reactant A and product P, as both the second and third reactors are operated at high conversions. Therefore, this may be mixed with fresh reactor product to undergo distillation; alternatively, it can be recycled back to the third reactor to undergo further reaction. The STN of figure 7.11 allows both of these recycling possibilities. Recycling the second cut back to the first reactor is not considered as the reaction between reactant B with product P would generate undesired compound W_3 and consume valuable product. The desired product P is recovered in the third distillate cut with a specified minimum purity of 99%. The residue (*Residue*) remaining in the column, reboiler, trays and condenser at the end of the distillation consists primarily of components F, W_1, W_2 and W_3, and is discarded.

The normalised reflux ratio and vapour flow to the condenser are used as the control variables for the operation of the distillation. The reflux ratio is allowed to vary between 0.5 and 0.99 and the vapour flow to the condenser between 6 and 12 $kmol/hr$. The inlet and outlet temperatures of the cooling water to the condenser are fixed at 293.3 and 333.3 K respectively.

The detailed task models and physical property and the kinetic data used are given in Appendices A and B.4 respectively.

7.3.2. Equipment Items

For the design of this process, we assume that a single equipment item is dedicated to each task and that each item is available in continuous sizes ranging from 1.25 to 3.00 m^3 for reactor 1 and 3, 2.25 to 3.00 m^3 for reactor 2, and 1.90 to 2.50 m^3 for the distillation column reboiler. The number of (theoretical) trays in the distillation column is fixed at 8.

7.3.3. Economic Data

The unit values of the various materials in the process are shown in Table 7.7. Note that these values are negative for *Intermediate*1, *Intermediate*2, *Intermediate*3, *FirstCut*, *SecondCut* and *Residue*, reflecting the undesirability of building up stocks of these materials.

The unit costs for the cooling water and steam utilities are 0.005 and 6.230 £/*tonne* respec-

Material	Unit value ($£/kmol$)
A	1.5
B	2.0
D	2.0
$Intermediate1$	-1.0
$Intermediate2$	-1.0
$Intermediate3$	-1.0
$FirstCut$	-1.0
$SecondCut$	-1.0
$Residue$	-1.0
$Product$	40.0

Table 7.7: Example 3: Unit Values for Process Materials

tively. The capital cost for each reactor (C_R) is expressed as a function of the reactor volume only, assuming that the height of the reactor is 1.7 times the radius of the vessel (Douglas, 1988):

$$C_R(£) = \left(\frac{M\&S}{280}\right) 3402.1 V_E^{0.63} \tag{7.6}$$

where V_E is the volume of the equipment item in m^3 and $M\&S$ denotes the Marshall and Swift index. A value of 1037.7 (648.56 for costs expressed in £) is adopted for the latter[5].

The distillation column installation cost (C_D) takes into account a variable reboiler size and fixed number of trays. Assuming that the height of the reboiler is twice its radius, this yields an expression for the installation cost as a function of reboiler volume only (Douglas, 1988):

$$C_D(£) = \left(\frac{M\&S}{280}\right) (3235.1 V_E^{0.43} + 16.1) \tag{7.7}$$

The objective function to be maximised is the net revenue per unit time of operation. It comprises the value of the products, the cost of the raw materials and utilities, and the annualised capital cost of the equipment items.

[5]As quoted in the "Chemical Engineering" magazine, July 1995 issue.

7.3.4. Modelling Considerations

The operation of all three reactors is modelled in terms of a set of standard material and energy balances. The cooling water flowrate in the first and second reactions, and steam flowrate in the second reaction, are manipulated in a piecewise constant fashion. For the purposes of the optimisation, we assume that this is done over 5 control intervals of variable length. The latter is allowed to vary between 0.2 and 3.0 hr. The inlet and outlet cooling water temperatures are taken as constant at 293.3 and 303.3 K respectively. The feed flowrate of B in the first reactor is also allowed to vary in a piecewise fashion.

The operation of the distillation column is modelled assuming constant liquid hold-ups on the trays and the condenser, negligible vapour hold-up, and fast energy dynamics. The initial charge to the column fills the reboiler, trays and total condenser with liquid at the charge composition. A molar hold-up of 50.0 *moles* is assumed for both the column trays and total condenser. Both reflux ratio and reboiler steam flowrate are treated as piecewise constant control variables. For the purposes of the optimisation, the operating time is divided into 4 intervals of variable duration. The latter is allowed to vary between 0.2 and 2.0 hr. The first and second cuts are produced at the ends of intervals 1 and 2 respectively. A constant temperature driving force is assumed for the total condenser.

7.3.5. Results and Discussion

The overall model of the process involves a total of 815 differential and algebraic equations describing the operation of the tasks. The number of decision variables manipulated by the optimisation is 121, with 99 constraints. The solution using the SRQPD sequential quadratic programming code (Chen and Macchietto, 1989) required 74 quadratic programming (QP) subproblems and 113 line-search evaluations of the objective function and constraints[6]. The overall computation time was approximately 11 hr on a SUN SPARC 5 workstation.

The total net revenue of the process is approximately 49 $£/hr$ producing 1812 mol/hr of the desired product. This is achieved by consuming 913, 1416 and 2765 mol/hr of feedstocks A, B and D respectively. None of the stable intermediates $Intermediate2$, $FirstCut$ and $SecondCut$,

[6]The optimisation and integration tolerances were set to 10^{-2} and 10^{-5} respectively.

is allowed to accumulate.

A detailed economic breakdown of the solution obtained is provided in Table 7.8 and the recipe is summarised in the annotated State-Task Network of figure 7.13. The cycle time of the zero-wait train is 5.47 hr. It is interesting to note that the optimal processing times for all three tasks in the train are the same and equal to the train cycle time. Reaction 2 has the highest production rate, so some idle time is introduced between successive batches of Reaction 2 in order to ensure that the processing rates of all tasks balance correctly.

Reaction 1 consumes 5.00, 7.76 and 7.64 $kmol/batch$ of A, B and $FirstCut$ respectively. In the case of B, only 0.02 $kmol$ are added in the initial charge, while the rest of the amount is added continuously in the first half of the operation as shown in figure 7.14(a). This ensures that the concentration of reactant B is kept low, thus suppressing the side-reaction that generates by-product W_1. The variation in reaction temperature and the cooling water profile enforcing it are shown in figure 7.14(a). The rapid rise in temperature at the start of processing is due to the high concentration of reactants A and B, and a large flowrate of cooling water is required so as to avoid exceeding the 350 K limit on the reaction temperature. However, the depletion of reactant B half-way through the task operation results in a smaller cooling water flowrate being required for temperature control. The last hour of operation is mainly used for reducing the temperature in order to satisfy the final temperature constraint of 305-310 K. One could argue that more cooling water could be used at this stage, thereby decreasing the processing time and probably the total cooling water consumption. However, as this task is not the bottleneck of the zero-wait task train, a reduction in processing time would merely result in the introduction of more idle time for this particular task. Also, as the reaction rates are negligible by this stage of the operation, the total utility consumed is not really a function of time but rather a function of temperature, composition and batchsize. These arguments provide another illustration of the type and complexity of decisions that have to be made in the context of an integrated batch process design.

Reaction 2 consumes 30.00 $kmol/batch$ of D and operates for 10.85 hr. The steam flowrate and the resulting temperature profile for this processing step are given in figure 7.14(b). The high steam flowrate at the start of the task raises the temperature close to the maximum of 400 K. The subsequent reduction in temperature is due to the endothermic nature of the reaction taking place. The small steam flowrate throughout the rest of the operation serves to sustain the reaction rate and finally to enforce the final temperature constraint.

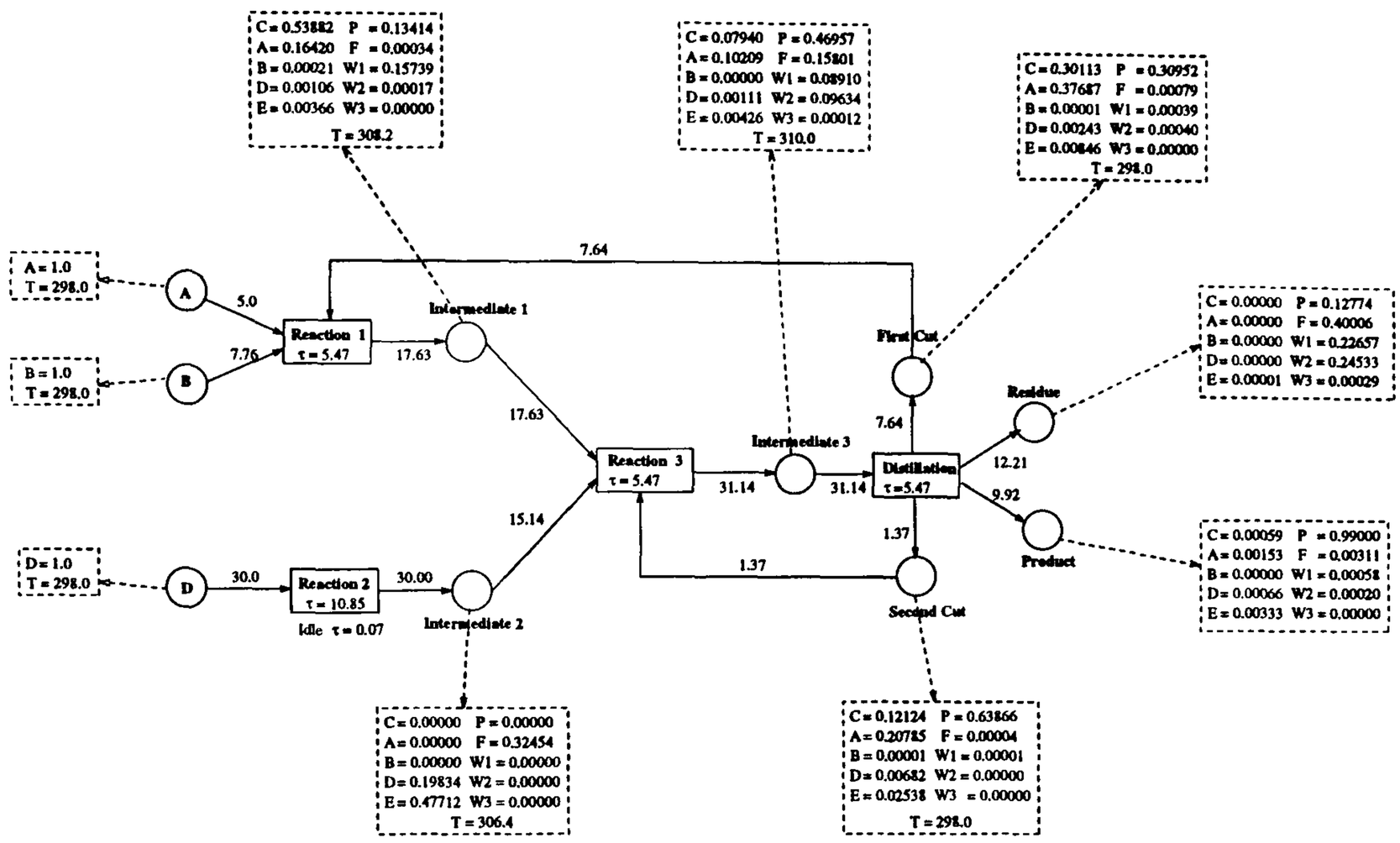

Figure 7.13: Example 3: Optimal Process Recipe

Reaction 3 consumes 17.63, 15.14 and 1.37 *kmol/batch* of *Intermediate*1, *Intermediate*2 and *SecondCut* respectively. The flowrate of cooling water and the resulting reaction temperature profile are shown in figure 7.14(c). At the start of the reaction, a large flow of cooling water is required to maintain the reaction temperature below the 350 K limit whereas at the end of the task all the available cooling water is utilised to satisfy the final temperature constraint and keep the processing time as small as possible.

Finally, the Distillation task consumes 31.14 *kmol/batch* of *Intermediate*3. The optimal variation of the normalised reflux ratio in the distillation column is shown in figure 7.15(a) with the resulting distillate composition for the three cuts given in figure 7.15(b). The vapour flowrate to the condenser of the distillation column is kept at its maximum of 12 *kmol/hr* throughout the operation. It should be noted that, despite the relatively large mole fraction of P in the second cut, the latter is not recycled back to the distillation; rather, it all goes back to Reaction 2 to make the most of the unreacted C and E in it.

Equipment Item	Size (m^3)	Cost $(£/hr)$
Reactor 1	1.48	1.87
Reactor 2	3.00	2.77
Reactor 3	3.00	2.77
Distillation Column	2.38	1.92
Total Equipment Cost		**9.33**
Material	Net Production Rate $(kmol/hr)$	Revenue $(£/hr)$
A	-0.913	-1.37
B	-1.416	-2.83
D	-2.765	-5.53
*Intermediate*1	0.000	0.00
*Intermediate*2	0.000	0.00
*Intermediate*3	0.000	0.00
FirstCut	0.000	0.00
SecondCut	0.000	0.00
Residue	2.229	-2.23
Product	1.812	72.48
Total Production Revenue		**60.52**
Utility	Mean Consumption Rate $(tonne/hr)$	Cost $(£/hr)$
Cooling water	9.024	0.045
Steam	0.400	2.492
Total Utility Cost		**2.54**
TOTAL NET REVENUE		**48.65**

Table 7.8: Example 3: Economic Breakdown of Optimal Solution

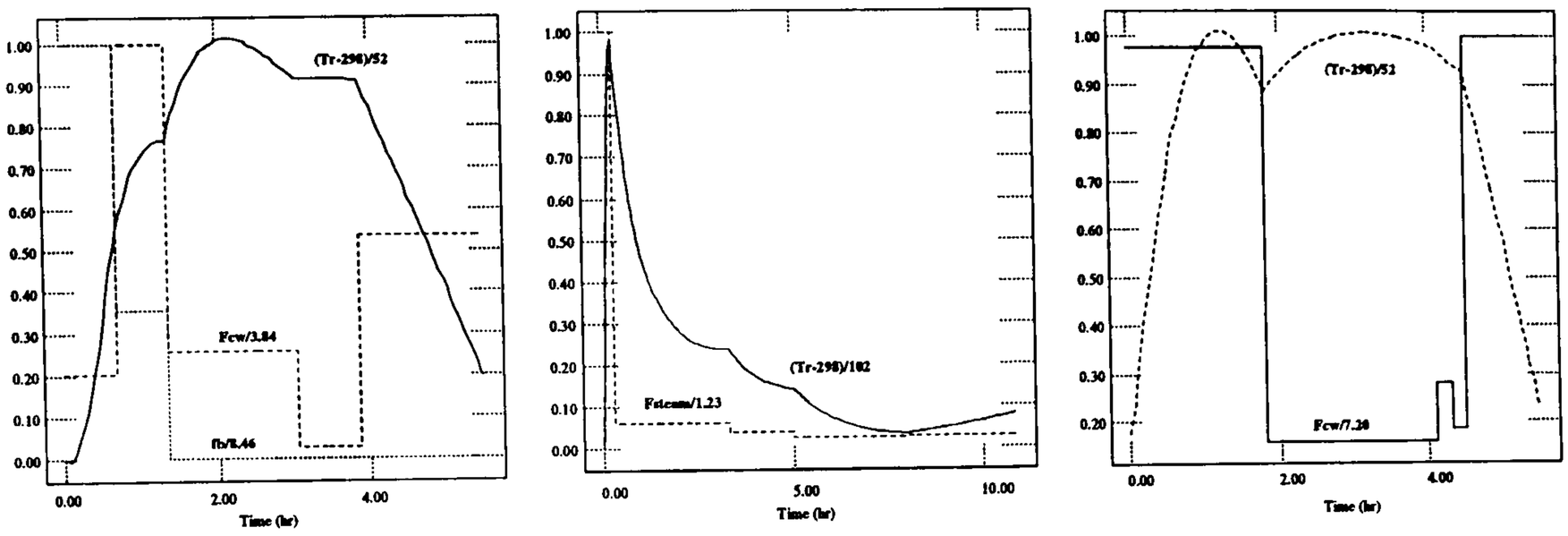

(a) Reaction 1 Operating Policy

(b) Reaction 2 Operating Policy

(c) Reaction 3 Operating Policy

Figure 7.14: Example 3: Reaction Tasks Operating Profiles

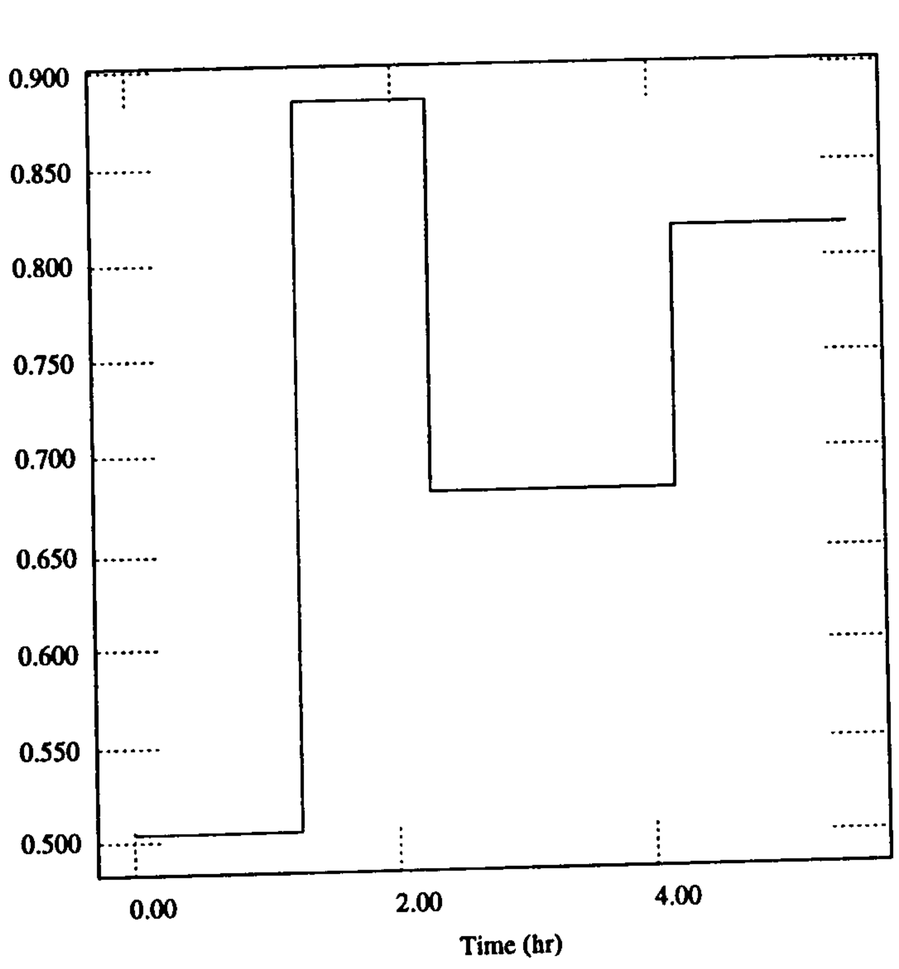

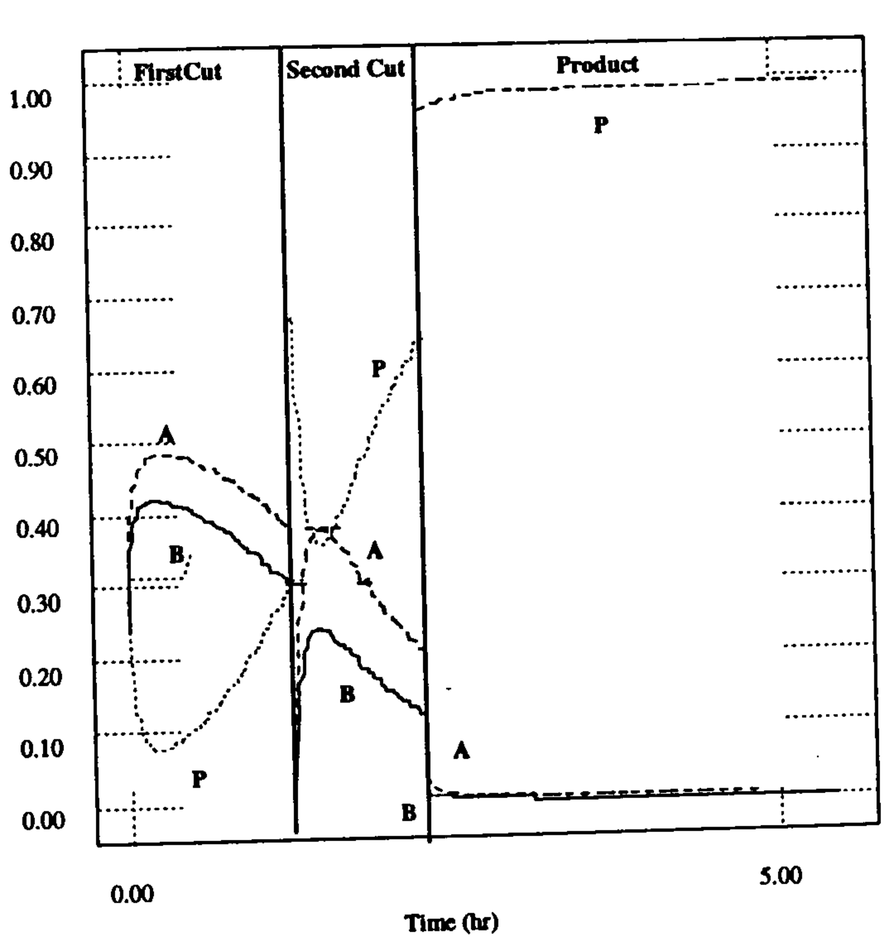

(a) Reflux Ratio

(b) Accumulator Tank Composition

Figure 7.15: Example 3: Distillation Optimal Operating Profiles

7.4. Concluding Remarks

The various features of the proposed design methodology have been demonstrated through a number of examples of diverse complexity in terms of process models, recipe and plant structure.

The recovery of unreacted raw materials to be recycled for further processing is widely used in batch operations to improve the process economics. The concept of a "state" employed by our formulation allows us to tackle processes with arbitary numbers of such recycle streams in a natural fashion. It should be noted that the optimisation has the freedom to set the value of any recycle under consideration to zero, should this prove profitable. In this sense, the STN that is initially postulated serves as a "superstructure" incorporating several process structure alternatives.

In addition to the complexity of the process recipe, large numbers of differential and algebraic equations were required for the description of the process models in these examples (notably Example 2). This provides further evidence that that the use of detailed dynamic models to describe processing steps is indeed feasible using currently available computer hardware.

Of course, the computational cost associated with these calculations is often quite substantial, involving several hours of CPU time. We shall return to this issue in Chapter 10. Here, it suffices to say that computational cost is not an overriding consideration in the context of process design compared to the potential benefits of obtaining an optimal solution, or even just a better one than would be possible using less rigorous approaches.

Chapter 8

Integrated Batch Process Design Subject to Limited Utility Availability

This chapter considers the design of integrated batch processes when there are restrictions on the maximum availability of utilities such as steam, cooling water and electricity. This is often an important consideration when designing a new process to operate within an existing plant. A conservative utility availability constraint is formulated and an example of its use is presented.

8.1. Introduction

The operation of a batch process may require the consumption of resources such as cooling water, steam and raw materials for the production of product in the required quantity and quality. It is often the case that the availability of one or more resources is limited. Therefore, the operation of the various processing steps may have to be designed so that the overall plant resource requirements do not exceed the maximum resource availability at any time. Such a case may arise if a new product is to be introduced at an existing site with various production routes sharing the available resources. Therefore the entire process, including the new route, should be designed and operated within the available resources if plant retrofit is not desired. The obvious option of upgrading the resource provision may not be economically sensible or even feasible due to the high capital cost of the resource generation and distribution facilities, or limitations on space availability and plant layout.

For shared raw materials, the utilisation of the State-Task Network allows the representation of process recipes with tasks sharing the same input states, and the material balance over each state determines the consumption and production of each state. Consequently, in the case of limited availability of a particular state s, the bounds on the net consumption rate R_s (see equation (4.7)) could be adjusted accordingly to reflect the maximum total supply rate of raw material available for consumption.

The consumption rates of utilities at the level both of the individual unit operations and of the entire plant exhibit a transient behaviour. In the former case, this is due to the transient nature of batch unit operations. In the latter case, an additional reason is that the schedule of operations is usually a complex sequence of various processing steps, with the utility demand at any time instant depending on the combination of tasks that are currently in operation. Therefore, it is reasonable to assume that while optimising the operation of a batch process subject to limited utility availability, one may also need to optimise the schedule of operations as well as the operation of individual units.

Traditionally, the problem of limited utility availability has been tackled at the scheduling level. The processing steps are sequenced in order to satisfy the required product demands, consuming only the available utilities, with the variation of utility consumption rate over the operation of each task usually treated as a constant or a simple function of batchsize (see, for instance Kondili *et al.* (1993)).

8.2. A Conservative Utility Constraint

Our methodology for the design of batch processes takes an aggregated view of plant scheduling. We, therefore, seek to ensure that the utility availability constraints will never be violated irrespective of the detailed schedule of operation of the process. Conservatively, this can be achieved by requiring that, even if the instances of maximum utility consumption rates of all tasks in the process were to coincide with each other at some time during the plant operation, no violation of the maximum utility available will ensue.

We denote the maximum consumption rate of utility u by task i by F_{ui}^{max} and the maximum plant availability of utility u as F_u^{max}. We can then express the above conservative utility constraint

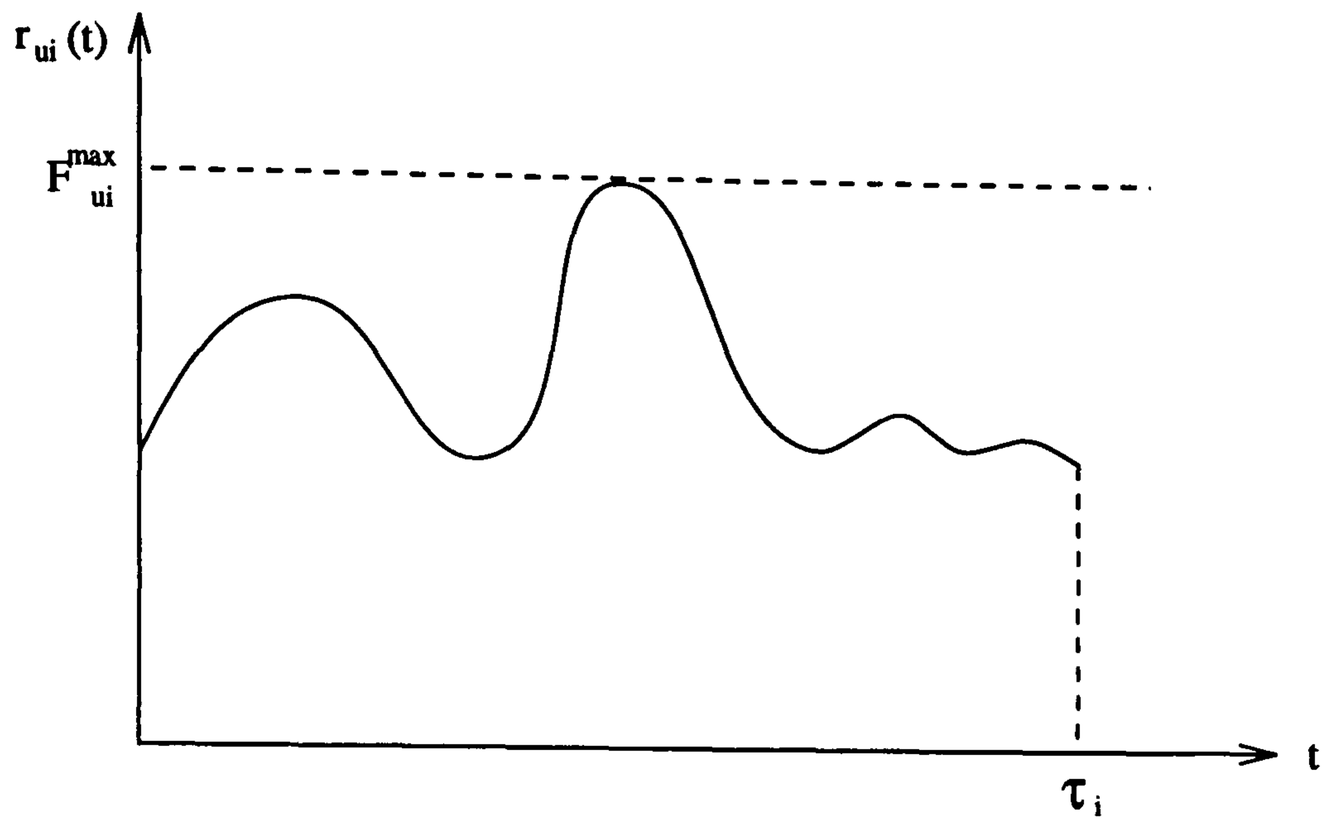

Figure 8.1: Instantaneous and Maximum Rate of Consumption of Utility u by Task i

in the form[1]:

$$\sum_{n=1}^{N} \sum_{i \in \mathcal{P}_n} F_{ui}^{max} \leq F_u^{max} \qquad \forall \quad u \tag{8.1}$$

where the double summation on the left hand side is taken over all tasks i in all zero-wait trains n in the process.

The maximum consumption of utility u for task i, F_{ui}^{max}, must be related to the rate of instantaneous consumption of utility u by task i. Typically, this instantaneous rate $r_{ui}(t)$ will be one of the variables $x_i(t)$, $y_i(t)$ or (most probably) $u_i(t)$ characterising the task, or be related to them directly via an algebraic expression (*cf.* equation 4.8). In any case, we have:

$$F_{ui}^{max} \equiv \max_{0 \leq t \leq \tau_i} (r_{ui}(t)) \tag{8.2}$$

as shown in figure 8.1. In practice, this can be enforced by incorporating the inequality path constraint:

$$F_{ui}^{max} \geq r_{ui}(t), \qquad \forall i, u, t \in [0, \tau_i] \tag{8.3}$$

within the model of the task. For the purposes of the optimisation, the quantity F_{ui}^{max} will then be treated as one of the time invariant parameters ν_i associated with task i.

In the context of the solution algorithm discussed in chapter 5, constraint (8.3) can generally be treated as one of the inequality path constraints 3.4 (*cf.* section 5.3.2). However, if $r_{ui}(t)$

[1]See section 4.1 for notation used.

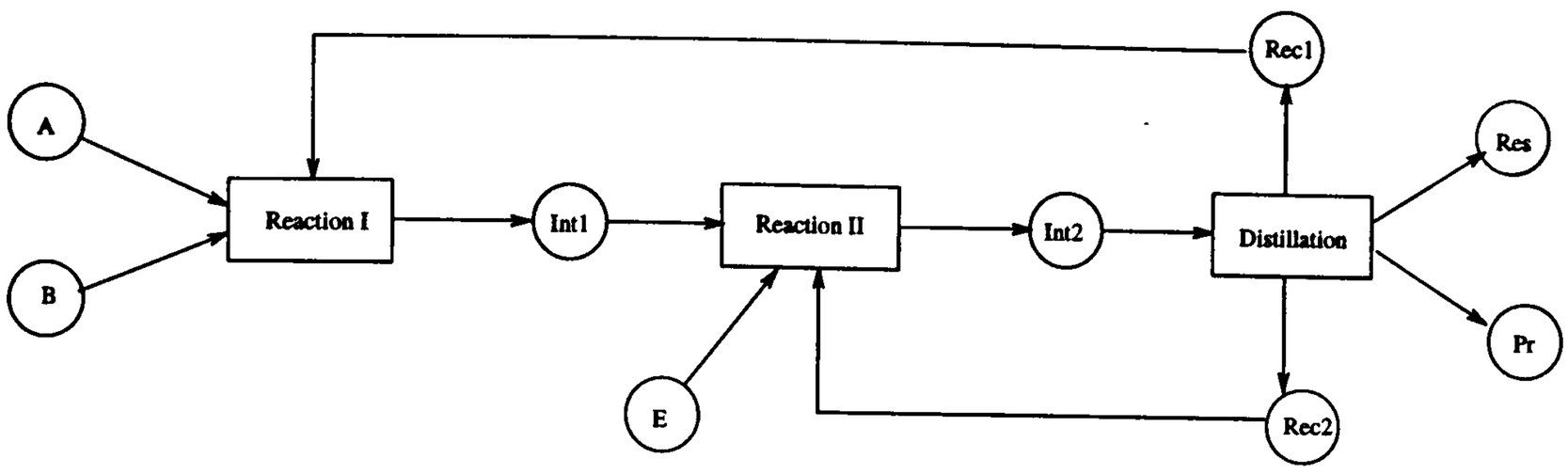

Figure 8.2: State-Task Network for Example Problem

corresponds to a control variable $u_i(t)$ (*e.g.* cooling water flowrate) in task i, (8.3) can be expressed directly in terms of the parameterisation of this control. For example, for a piecewise constant control (*cf.* section 5.3.1), we simply have:

$$\zeta_{ki} \leq F_{ui}^{max} \qquad \forall, k = 1, .., NE_i \tag{8.4}$$

while for a piecewise linear one:

$$\left.\begin{array}{l} \eta_{ki} \leq F_{ui}^{max} \\ \eta_{ki}^{'} \leq F_{ui}^{max} \end{array}\right\} \forall k = 1, .., NE_i \tag{8.5}$$

8.3. An Example of Batch Process Design Under Limited Utility Availability

To illustrate the effects of limited utility availability on the design of optimal process recipes, we consider the problem of implementing the recipe described by the STN of figure 8.2 in an existing plant. The new process transforms pure feedstocks, A, B and E to the final product, Pr. Three additional materials are produced. One of them, Res, is too heavy to be of any practical use within the process, but the other two, $Rec1$ and $Rec2$, can be recycled. The overall operation of the process is limited by a maximum overall cooling water flowrate of 5.0 $tonne/hr$.

8.3.1. Process Description

The main reaction $A + B \rightarrow 2C$ and the side reaction $C \rightarrow D$ take place in the liquid phase in the reactor. The total amount of reactant A added must exceed the total amount of reactant

B by at least 50%. B may be added during the reaction in a semi-continuous manner, the rate of its addition being a control variable. The reactor contents must be kept below a maximum temperature of 350 K in order to avoid vapourisation of the reacting mixture; the temperature may be controlled by manipulating the flowrate of the cooling water in a cooling jacket. The maximum cooling water flowrate is 5.0 $tonne/hr$.

The output from the first reaction task is mixed with E in Reaction II, with the reaction $C + E \rightarrow 2F$ yielding the desired product F. To avoid undesirable side reactions, the total amount of reactant E added cannot exceed 50% of the total amount of component C, and the temperature must be kept below 330 K. The reaction takes place in the liquid phase under isothermal conditions, the enthalpy of reaction being negligible.

The distillation task produces three distillate cuts. Saturated steam at 4 bar is used in the reboiler. The volatility of the six components in the process decreases in the order $A > B > C > E > F > D$. Consequently, the first cut $Rec1$ recovers the unreacted reactants A and B; clearly these can be recycled back to Reaction I. The second cut $Rec2$ comprises a mixture of the reactants with the intermediate C; this may be mixed with fresh Reaction I product to undergo distillation. The desired product F is recovered in the third cut with a specified minimum purity of 95 %. The residue Res remaining in the column, reboiler, trays and condenser at the end of the distillation is primarily component D and is discarded. The normalised reflux ratio is allowed to vary between 0.70 and 0.99, and the reboiler load between 550.0 and 900 MJ/hr. The maximum cooling water flowrate to the total condenser is 5.0 $tonne/hr$.

All the process materials are stable and can be stored in unlimited amounts.

8.3.2. Available Equipment

For the design of this process, we assume that a single equipment item is dedicated to each task, as shown in figure 8.3. The capacity of the equipment items utilised for Reaction I, Reaction II and Distillation are 3.0, 1.2 and 6.0 m^3 respectively. The distillation column has 12 theoretical trays.

A minimum utilisation factor of 75% is imposed on all equipment items. In the case of the distillation column, this restriction implies that the initial charge should occupy at least 75% of the reboiler still.

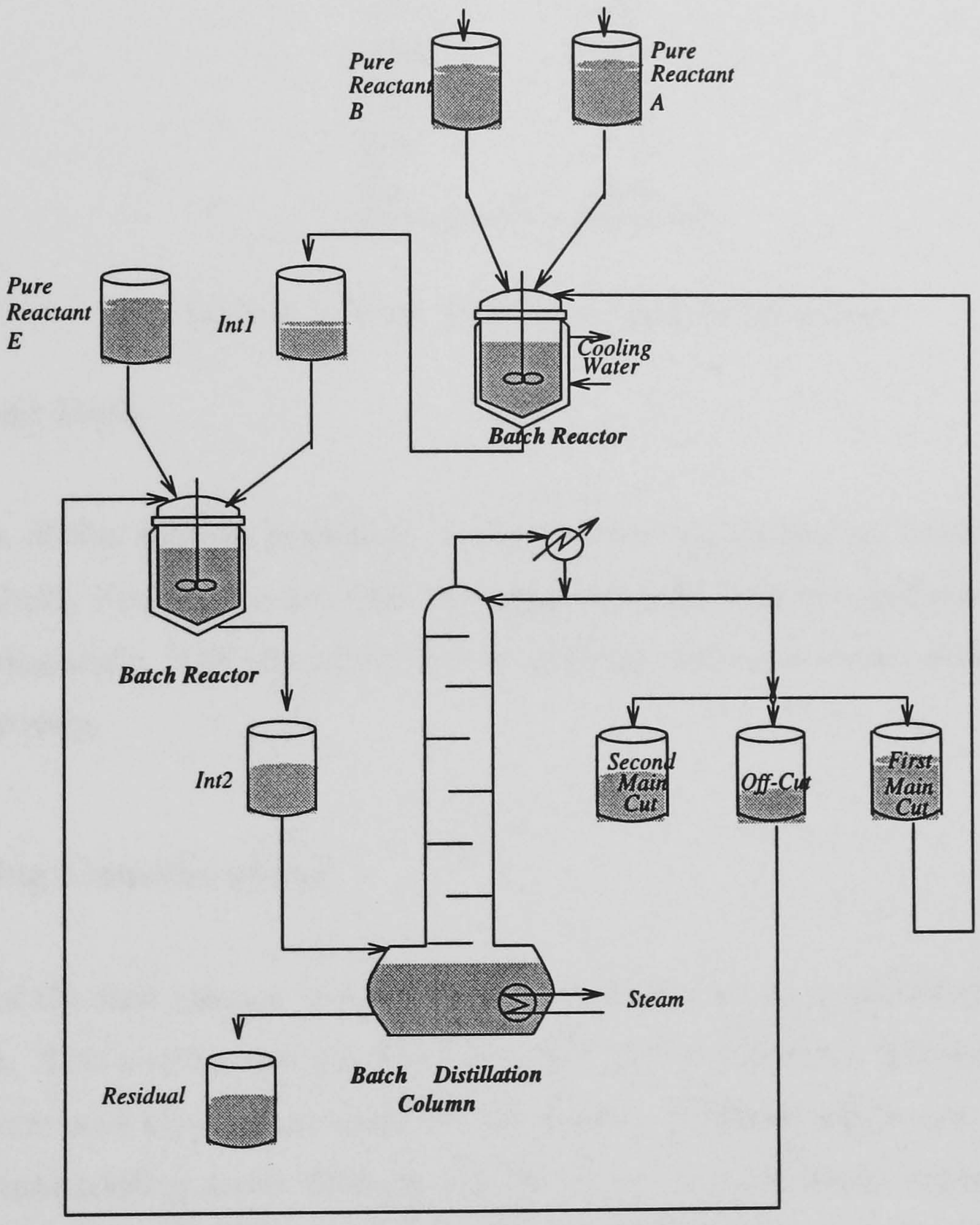

Figure 8.3: Plant Flowsheet for Example Problem

Material	Unit value ($rcu/kmol$)
A	3.0
B	3.0
E	1.0
$Int1$	-0.1
$Int2$	-0.1
$Rec1$	-0.1
$Rec2$	-0.1
Res	-0.1
Pr	40.0

Table 8.1: Unit Values for Process Materials

8.3.3. Economic Data

The unit values of the various materials in the process are shown in Table 8.1. Note that the values of $Int1$, $Int2$, $Rec1$, $Rec2$ and Res are negative, reflecting the undesirability of building up stocks of these materials. The unit costs for the cooling water and steam utilities are 0.2 and 10.0 rcu/ton[2] respectively.

8.3.4. Modelling Considerations

The operation of the first reactor is modelled in terms of a set of standard dynamic material and energy balances. The cooling driving force is taken as the difference between the outlet cooling water temperature and the temperature of the reactor contents which are assumed to be well-stirred. The actual cooling water flowrate can be varied in a piecewise constant fashion over the duration of the reaction. For the purposes of the optimisation, we assume that this is done over 5 time intervals of variable length. The interval durations are allowed to vary between 0.1 hr and 4.0 hr.

The isothermal reaction scheme taking place in the second reactor is modelled in terms of standard material balances. For the purposes of the optimisation, the reaction temperature is treated as a time invariant parameter, allowing us to use only one time interval.

[2] relative cost units.

The operation of the distillation column is modelled assuming constant liquid hold-ups on the trays and the condenser, negligible vapour hold-up, and fast energy dynamics. The initial charge to the column fills the reboiler, trays and total condenser with liquid at the charge composition. A molar hold-up of 50.0 *moles* is assumed for both the column trays and total condenser. Both the normalised reflux ratio and the reboiler steam load are treated as piecewise constant control variables. For the purposes of the optimisation, the operating time of distillation is divided into 6 intervals of variable duration, with the first and second cuts being produced at the ends of intervals 2 and 4 respectively. The interval durations are allowed to vary between 0.1 hr and 4.0 hr.

The detailed unit operation models and the data used in them are presented in Appendices A and B.5 respectively.

8.3.5. Case I: Solution without Plant Utility Constraints

First, we consider the optimisation of the process described earlier in this section assuming unlimited availability of steam and cooling water. Of course, the rates of consumption of these utilities by the individual unit operations are still limited by other technical constraints (*e.g.* piping restrictions) as described in section 8.3.1.

The overall model of the process involves a total of 588 differential and algebraic equations describing the task operation. The number of decision variables manipulated by the optimisation is 76, with 50 constraints of which 36 are equalities. The solution of the problem using the SRQPD sequential quadratic programming code (Chen and Macchietto, 1989) required 51 quadratic programming (QP) subproblems and 65 line-search evaluations of the objective function and constraints[3]. The overall computational processing time was approximately 2 hr on a SUN SPARC 10/51 workstation.

The total net revenue of the process is 108.25 rcu/hr realised by producing 3.09 $kmol/hr$ of Pr. To achieve this, 1.061, 1.062 and 1.561 $kmol/hr$ of A, B and E respectively are consumed. It can be seen that the intermediates $Int1$, $Int2$, $Rec1$ and $Rec2$ are not allowed to accumulate, but some accumulation of the waste Res is unavoidable. A detailed economic breakdown of the solution obtained, including both the production revenue and operating costs, is provided in Table

[3]The optimisation and integration tolerances were set to 10^{-2} and 10^{-5} respectively.

Material	Net Production Rate ($kmol/hr$)	Revenue (rcu/hr)
A	-1.061	-3.83
B	-1.062	-3.83
E	-1.561	-1.56
$Int1$	0.000	0.00
$Int2$	0.000	0.00
$Rec1$	0.000	0.00
$Rec2$	0.000	0.00
Res	0.593	-0.06
Pr	3.090	123.60
Total Production Revenue		**114.32**
Utility	Mean Consumption Rate ($tonne/hr$)	Cost (rcu/hr)
Cooling Water	5.090	1.02
Steam	0.505	5.05
Total Utility Cost		**6.07**
TOTAL NET REVENUE		**108.25**

Table 8.2: Economic Breakdown of Optimal Solution without Utility Constraints

8.2.

The characteristics of the optimal recipe are summarised in the annotated State-Task Network of figure 8.4.

Reaction 1 consumes 7.53, 7.53 and 18.03 $kmol/batch$ of A, B and $Rec1$ respectively, and operates for 4.82 hr. Only 6.63 $kmol$ of B are added in the initial charge to the reactor. The feed addition policy for the rest of reactant B and the composition trajectories are given in figure 8.5(b). We note that the constraint on the ratio of components A and B in the initial charge is not active. More specifically, the mole fractions of A and B in $Rec1$ are 0.27927 and 0.04703 respectively (*cf.* figure 8.4), and therefore the amounts A and B in the charge are 12.57 and 7.48 respectively. The cooling water flowrate and resulting temperature are given in figure 8.5(a) with the temperature maintained below 350 K throughout the operation of the task. The maximum cooling water requirement is approximately 2.29 $tonne/hr$. Reaction 2 consumes 8.05, 2.69 and 2.45 $kmol/batch$ of $Int1$, E and $Rec2$ respectively and operates for 1.73 hr at the highest possible reaction temperature of 330 K. We note that the constraint on the ratio of components E and C

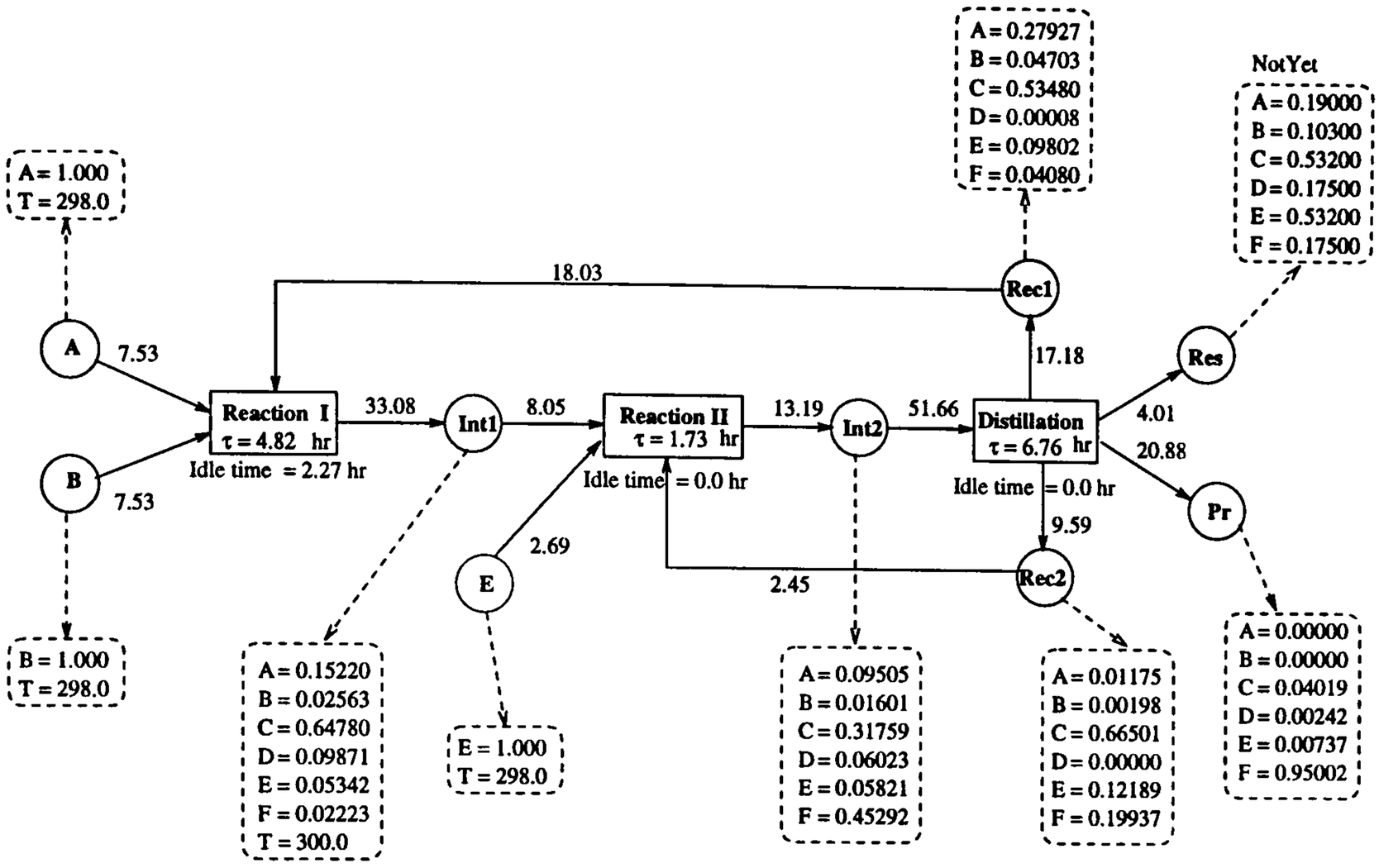

Figure 8.4: Optimal Process Recipe without Utility Constraints

in the initial charge (see section 8.3.1) is not active.

Finally, the Distillation task consumes 51.66 *kmol/batch* of *Int*2. The optimal variation of the normalised reflux ratio in the distillation column and the resulting composition profiles in the three distillate tanks are shown in figure 8.6(a). The heat load to the reboiler is held constant at 861.71 MJ/hr throughout the task operation. The variation of the cooling water flowrate to the condenser is shown in figure 8.6(c) with a maximum cooling water consumption of 5.0 *tonne/hr*.

8.3.6. Case II: Solution with Limited Cooling Water Availability

Since unlimited intermediate storage is available for all material states in the process, both the Reaction 1 and Distillation tasks operate on completely independent cycle times. This implies that the maximum utility consumption of the process will occur when the instances of maximum cooling water consumption of Reaction 1 and Distillation coincide. As can be seen from figures 8.5(a) and 8.6(c), such a coincidence would result in a total cooling water demand of 7.29 *tonne/hr*.

We now consider how the process design needs to be modified if the *total* availability of cooling

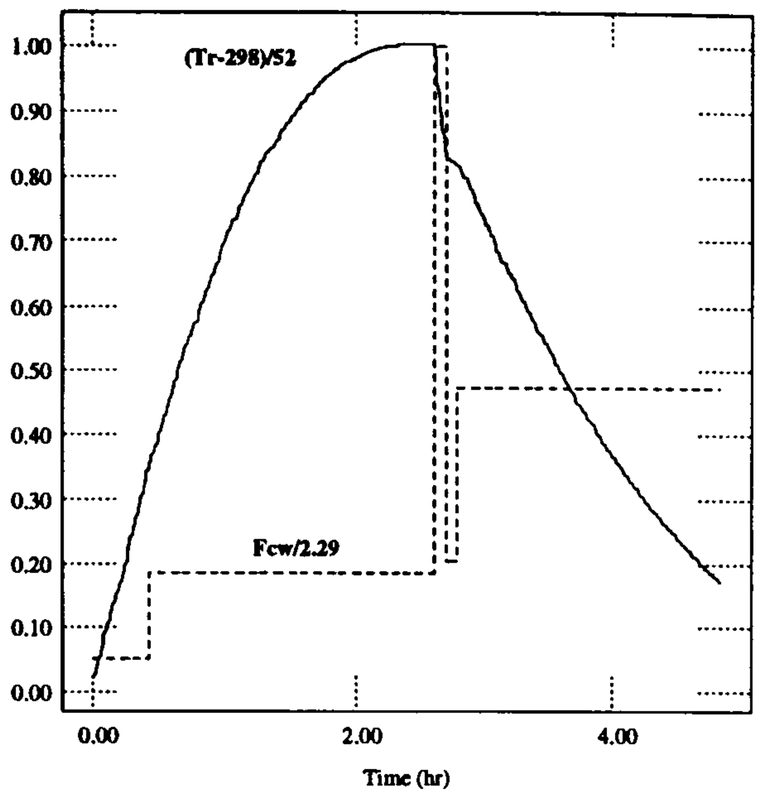

(a) Temperature (K) and Cooling Water Flowrate ($tonne/hr$)

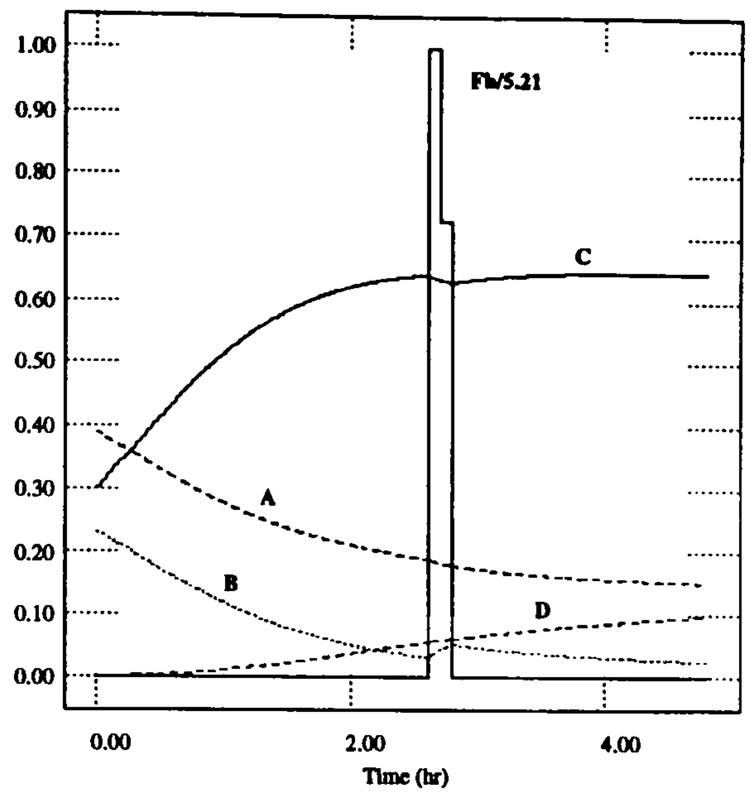

(b) Mole Fraction (A, B, C, D) and Reactant B Addition Flowrate ($kmol/hr$)

Figure 8.5: Reaction 1: Optimal Operating Profiles without Utility Constraints

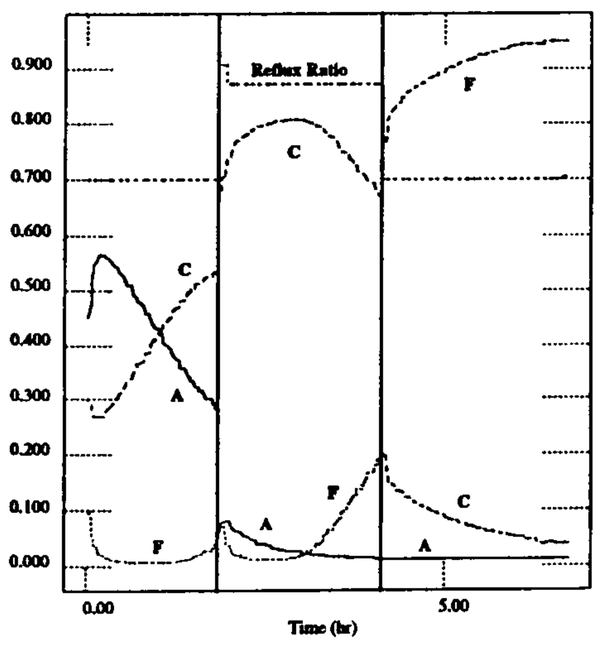

(a) Reflux Ration and Distillate Tank Composition Profiles

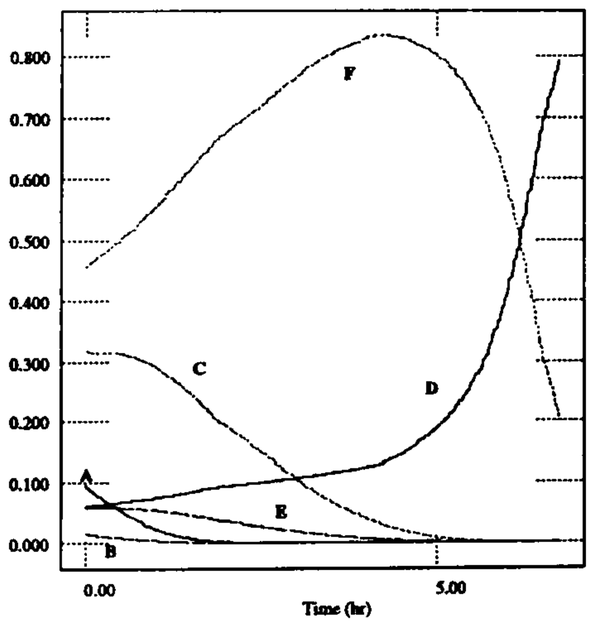

(b) Reboiler Composition

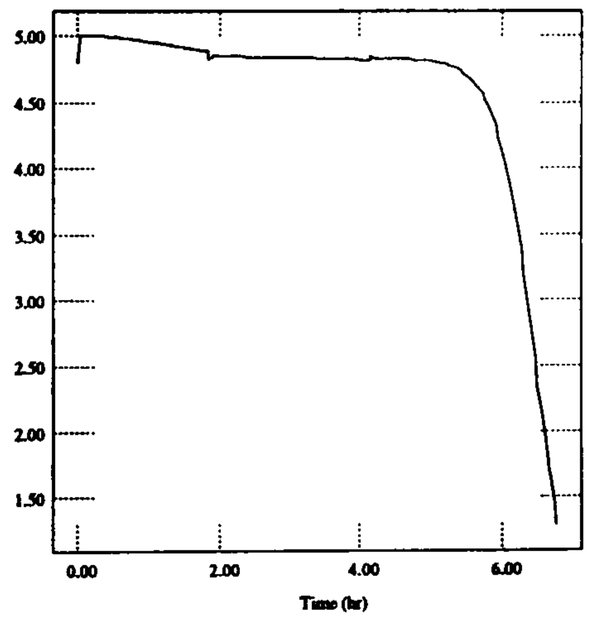

(c) Condenser Cooling Water Flowrate ($tonne/hr$)

Figure 8.6: Distillation: Optimal Operating Profiles without Utility Constraints

water in the plant is limited to 5 *tonne/hr*.

In general, one way of reducing the overall cooling water demand of the process might be to change the production schedule. However, such an approach would not really provide a satisfactory solution in this case as the distillation column condenser consumes approximately 5.0 *tonne/hr* throughout its operation (see figure 8.6(c)), and the distillation task has no idle time (see figure 8.4). This implies that, in order to avoid the demand for cooling water exceeding the availability, the tasks must be operated in a practically non-overlapping mode with the introduction of appropriate idle times. This would substantially decrease the throughput of the process.

We, therefore, consider applying the methodology presented in section 8.2 to this problem. The number of equations required to model the overall process remains the same as before, but we have two additional optimisation decision variables (a total of 78) due to the introduction of the time-invariant parameters F_{ui}^{max} characterising the maximum cooling water consumption rates by the Reaction 1 and Distillation tasks. We also have 6 additional inequality constraints (a total of 56), one for the path constraint[4] introduced for the Distillation (*cf.* equation 8.3) and five for the piecewise constant control utilised for the cooling water profile of Reaction 1 (*cf.* equation 8.4).

The solution of the problem using the SRQPD sequential quadratic programming code (Chen and Macchietto, 1989) required 26 quadratic programming (QP) subproblems and 34 line-search evaluations of the objective function and constraints[5]. The overall computational processing time was approximately 1.2 *hr* on a SUN SPARC 10/51 workstation.

The total net revenue of the process is 101.58 *rcu/hr* realised by producing 2.856 *kmol/hr* of *Pr*. To achieve this, 0.981, 0.981 and 1.427 *kmol/hr* of *A*, *B* and *E* respectively are consumed. A detailed economic breakdown of the solution obtained is provided in Table 8.3 showing the production revenue and operating costs. It can be seen that the intermediates *Int*1, *Int*2, *Rec*1 and *Rec*2 are not allowed to accumulate, but some accumulation of the waste *Res* is unavoidable. Overall, however, it is interesting to note that, despite the apparently severe restrictions in utility availability, the optimisation has managed to limit the reduction in the total net revenue to about 6% only (*cf.* Table 8.2).

---

[4]Note that the cooling water is not a control variable in the distillation task but is determined implicitly by the need to produce a saturated liquid product in the column condenser.

[5]The optimisation and integration tolerances were set to 10^{-2} and 10^{-5} respectively.

Material	Net Production Rate ($kmol/hr$)	Revenue (rcu/hr)
A	-0.981	-2.94
B	-0.981	-2.94
E	-1.427	-1.43
$Int1$	0.000	0.00
$Int2$	0.000	0.00
$Rec1$	0.000	0.00
$Rec2$	0.000	0.00
Res	0.533	-0.05
Pr	2.856	114.24
Total Production Revenue		**106.88**
Utility	Mean Consumption Rate (ton/hr)	Cost (rcu/hr)
Cooling water	4.691	0.94
Steam	0.436	4.36
Total Utility Cost		**5.30**
TOTAL NET REVENUE		**101.58**

Table 8.3: Economic Breakdown of Optimal Solution with Utility Constraints

The characteristics of the recipe are summarised in the annotated State-Task Network of figure 8.7. Reaction 1 consumes 7.76, 7.76 and 16.71 $kmol/batch$ of A, B and $Rec1$ respectively, and operates for 7.92 hr. The cooling water flowrate and the resulting temperature variation are shown in figure 8.8(a). A comparison of figures 8.5(a) and 8.8(a) shows that the utility constraint results in the reactor being operated at a lower temperature (below 324 K) with a constant cooling water flowrate of 0.68 $tonne/hr$ throughout the operation. The lower operating temperature reduces the rate of reaction and, hence, the rate of heat generation to a level that can be removed with the available cooling water supply. This has an impact on the throughput of the task as a longer processing time (7.92 hr *vs.* 4.82 hr) is now required to achieve a reasonable conversion. The feed addition policy of reactant B and composition trajectories for Reaction 1 are given in figure 8.8(b).

The significant impact of the utility constraints on the operation of this task is also vividly demonstrated by the change in the addition policy for reactant B. In the unconstrained case, half of the amount of reactant B was added as a discrete charge at the start of the operation and the rest is fed in at a high flowrate over an interval of approximately 10 minutes, about half-way through the reaction, which practically amounts to a second discrete charge (see figure 8.5(b)). On

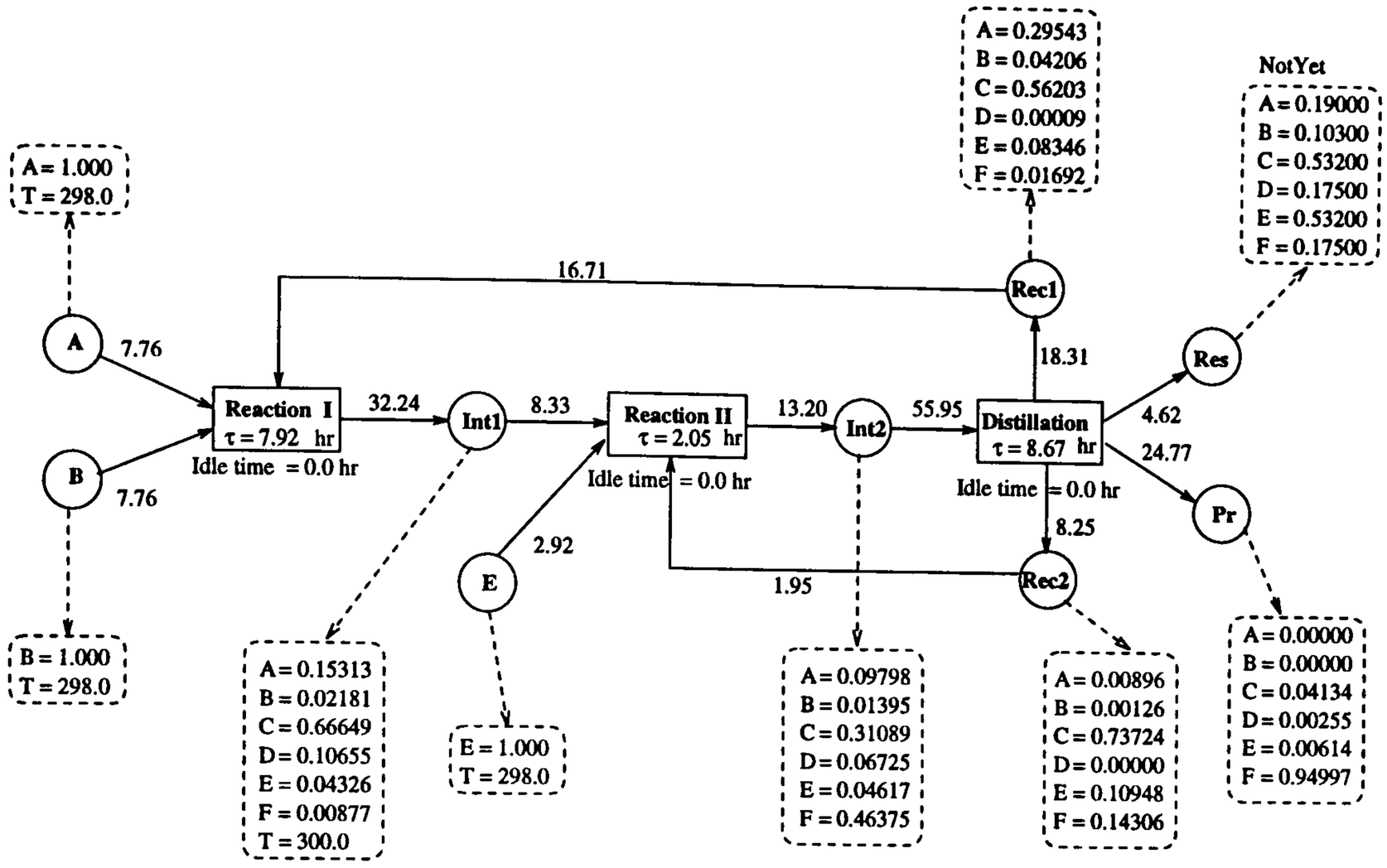

Figure 8.7: Optimal Process Recipe with Utility Constraints

the other hand, in the constrained case, the *entire* amount of reactant B is added continuously during the first half of the operation. The main reason for this is again to reduce the reaction rate and, consequently, the required cooling water flowrate.

Reaction 2 consumes 8.33, 2.92 and 1.95 $kmol/batch$ of $Int1$, E and $Rec2$ respectively and operates for 2.05 hr at the highest possible temperature of 330 K.

Finally, the Distillation task consumes 55.95 $kmol/batch$ of $Int2$. The optimal variation of the normalised reflux ratio in the distillation column and the resulting composition profiles in the three distillate tanks is given in figure 8.9(a). The reduction of the heat load to the reboiler to 743.75 MJ/hr has reduced the maximum cooling water consumption by the condenser to 4.32 $tonne/hr$ as shown in figure 8.9(c).

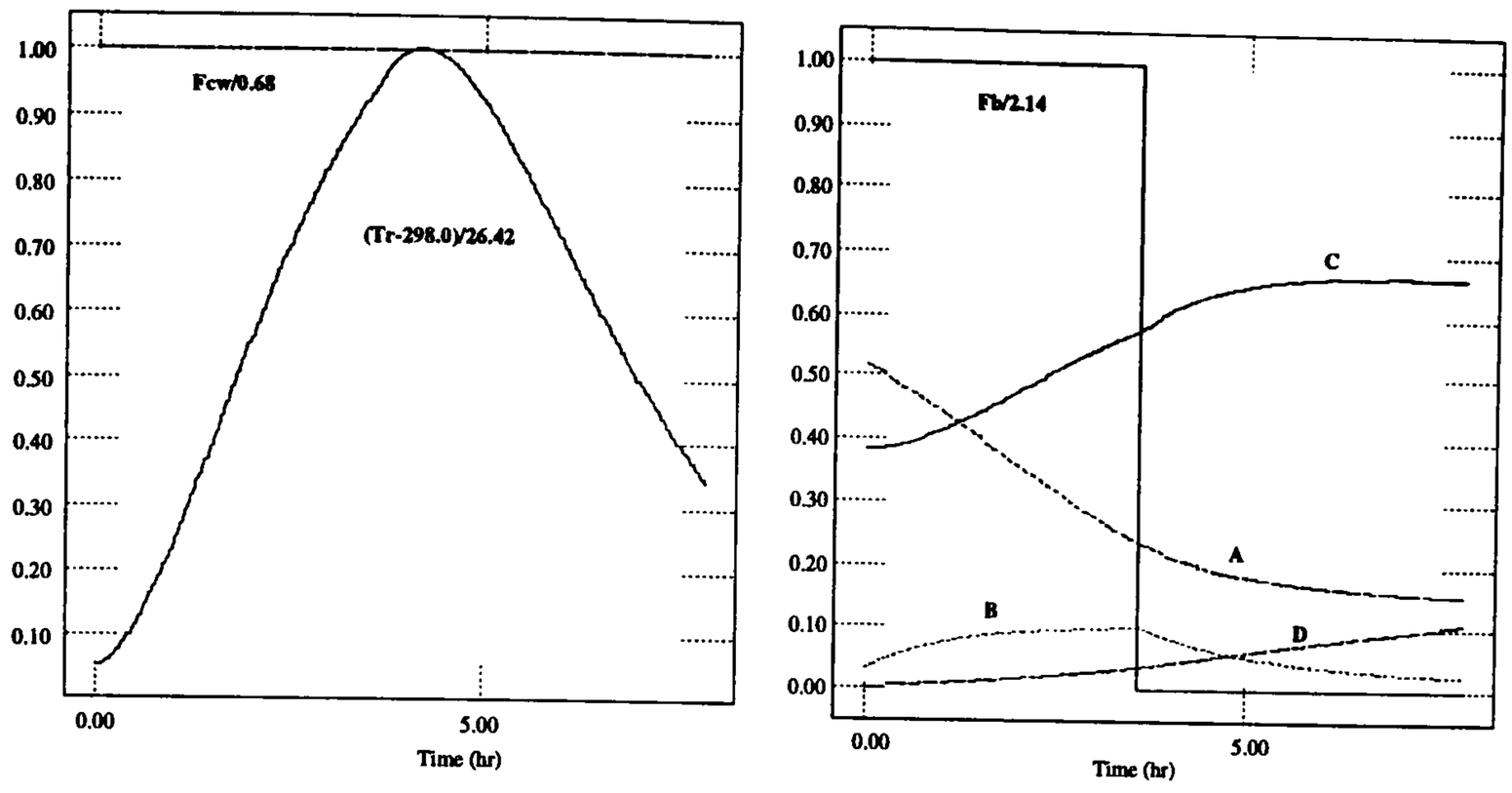

(a) Temperature (K) and Cooling Water Flowrate ($tonne/hr$)

(b) Mole Fraction (A, B, C, D) and Reactant B Addition Flowrate ($kmol/hr$)

Figure 8.8: Reaction 1: Optimal Operating Profiles with Utility Constraints

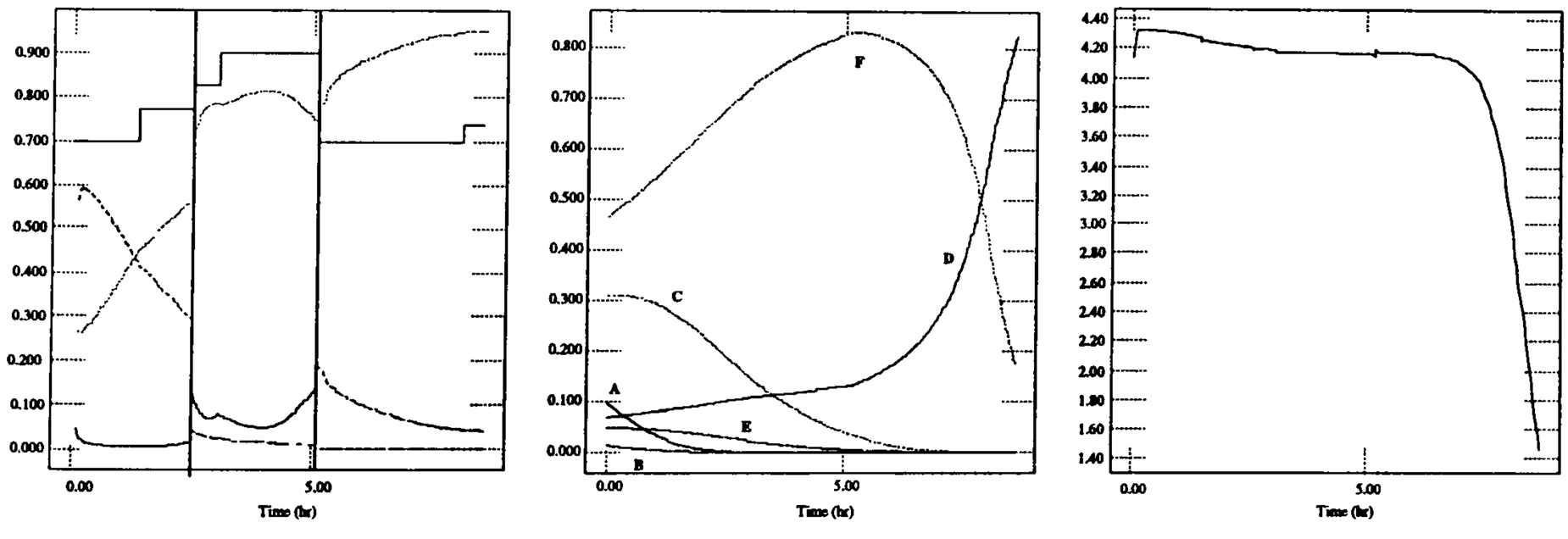

(a) Reflux Ration and Distillate Tank Composition Profiles

(b) Reboiler Composition

(c) Condenser Cooling Water Flowrate ($tonne/hr$)

Figure 8.9: Distillation: Optimal Operating Profiles with Utility Constraints

8.4. Conclusions

This chapter has extended the methodology for the design of integrated batch processes to processes with restrictions on the maximum availability of utilities. We adopt a conservative approach in tackling the limited utility availability problem and seek to ensure that the utility availability constraints are never violated irrespective of the detailed schedule of operation for the process.

The example presented provides a good demonstration of the impact of utility limitations on the operation of a process. It also emphasises once again the need to design batch processes in an integrated fashion.

Chapter 9

Integrated Batch Process Design Using Multipurpose Equipment Items

This chapter considers the design of batch processes with the inventory of available equipment items containing multipurpose equipment item. In particular, we consider the case in which an item of equipment may be used for more than one task as well as the case in which a task may be performed in more than one equipment item. The STN modifications required to tackle this type of design problems is presented through an example.

9.1. Introduction

A basic assumption of the mathematical formulation for the design of integrated batch processes presented in Chapters 3-4 is that a single equipment item is dedicated to each processing step. However, in many cases, the inventory of available equipment items may contain equipment items suitable for more than one task. We therefore need to extend the design formulation to take into account the possibility of multipurpose equipment items.

We retain the assumptions regarding plant operation and plant scheduling introduced in section 4.1. However, the assumption regarding plant design is modified to:

- *Plant Design*: Each task may generally take place in a number of equipment items from an existing equipment item inventory.

As might well be expected, multipurpose equipment items tend to introduce additional complexity to plant scheduling considerations. In particular, the actual times at which a multipurpose equipment item is processing one of its allocated tasks become important when an equipment item can process a number of tasks in the same zero-wait task train. Consequently, and in order to retain the aggregate nature of the plant scheduling constraints, we assume that there are no zero-wait train tasks in the process. This is equivalent to each zero-wait train of tasks ($\mathcal{P}_n$) containing only one task ($m_n = 1$). We also assume that the cleaning of the multipurpose equipment items does not depend on the sequence of tasks that they process.

Finally, we assume that the processing equipment under consideration can be categorised into a number of types j such that all items of the same type have the same capacity and are suitable for the same subset I_j of task trains in the STN. For instance, a plant may have several reactor vessels differing in their capacity and material of construction. Conversely, we allow each task i to be carried out by a set of equipment types K_i. For instance, a non-corrosive reaction task i may be performed in:

$$K_i \equiv \left\{ \begin{array}{c} 10 \textit{ tonne stainless steel reactors}, \\ 15 \textit{ tonne stainless steel reactors}, \\ 10 \textit{ tonne glass lined reactors}. \end{array} \right\} \tag{9.1}$$

9.2. STN Modifications for Handling Multipurpose Equipment Items

Consider the case of a task i that transforms a material S_1 to another material S_2 (see figure 9.1(a)) and which can take place in two different types of equipment items, j and j'. The optimal policy for operating the task will generally be different depending on the type of equipment used. Of course, one can insist that the task produce exactly the same product(s) irrespective of these differences. This is equivalent to the STN modification shown in figure 9.1(b). Here, task i_j and $i_{j'}$ correspond to task i being performed in equipment of type j and j' respectively; however, both tasks are required to produce material(s) with the same intensive properties.

On the other hand, such a restriction may be unnecessary, leading to suboptimal solutions. It may also be infeasible as it may well be impossible to produce *exactly* the same (in terms of composition, temperature *etc.*) material using two equipment items of different types. In such cases, it may be preferable to employ the STN modification shown in figure 9.10(c). Here, tasks

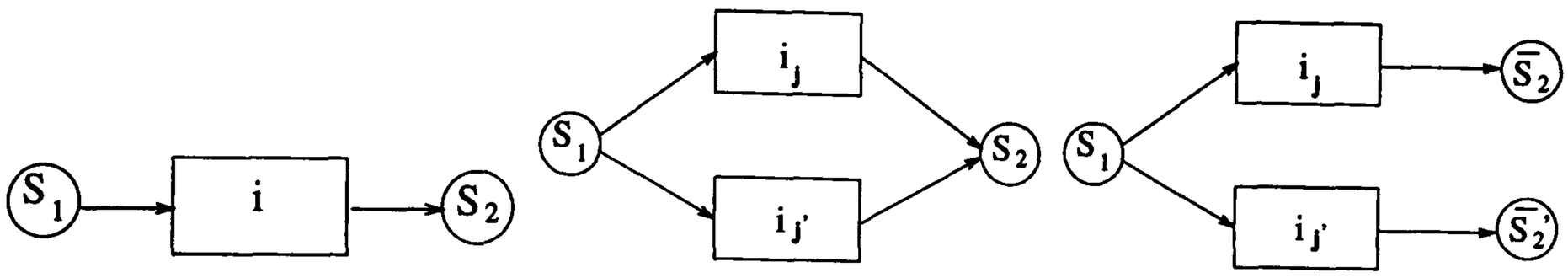

(a) Original STN segment (b) STN modification I (c) STN modification II

Figure 9.1: STN Modifications for Multipurpose Equipment Items

i_j and $i_{j'}$ are allowed to produce two different types of material, $\bar{S}_2$ and $\bar{S}_{2'}$ respectively. Any downstream task consuming S_2 in the original STN will now be allowed to consume a mixture of $\bar{S}_2$ and $\bar{S}_2'$. This type of STN modification will be illustrated by the example presented in section 9.4.

9.3. Mathematical Formulation

During the production horizon H, each equipment item can process a number of batches possibly undergoing a number of different tasks. To ensure that the overall operating time of an equipment item is not greater than the total available time, we have to introduce equipment utilisation constraints. If we denote the number of batches of task i taking place in equipment of type j by M_{ij}, these constraints are of the form:

$$\sum_{i \in I_j} M_{ij}\tau_i \quad \leq \quad Hm_j \qquad \forall \quad j \tag{9.2}$$

where m_j is the number of identical equipment items of type j. M_{ij} is treated as a continuous optimisation variable as, for long production horizons, it will normally be large enough for any rounding-off error to be negligible. If M_{ij} turns out to be zero in the optimal solution, then this implies that task i should *not* actually be carried out in equipment of type j.

If we denote the amounts of state s consumed and produced by task i performed in equipment of type j by B_{ijs} and $\bar{B}_{ijs}$ respectively, a material balance for each state s yields:

$$\sum_i \sum_{j \in K_i} M_{ij}\bar{B}_{ijs} = \sum_i \sum_{j \in K_i} M_{ij}B_{ijs} + R_s H \qquad \forall \quad s \tag{9.3}$$

where, as in the original formulation, R_s is the net rate of production of material s from external sources. This equation replaces (4.6) in the original formulation.

Finally, the original objective function (4.11) is now modified to:

$$\max \quad -\lambda \sum_j C_j m_j - \frac{1}{H} \sum_u C_u \sum_i \sum_{j \in K_i} M_{ij} U_{uij} + \sum_s C_s R_s \tag{9.4}$$

where C_j is the cost of each equipment item of type j, and U_{uij} is the amount of utility u consumed by a batch of task i taking place in an item of type j.

We note that, if a *new* plant is to be constructed to implement the process being designed, the number m_j of equipment items of type j will generally be unknown. This greatly increases the complexity of the mathematical problem as these variables take integer values. On the other hand, if the new process is to be implemented in an existing plant, then m_j are given, the first term of equation (9.4) can be omitted and the formulation is very similar to the one presented in Chapter 4. In this thesis, we limit ourselves to the latter case.

9.4. An Example of Batch Process Design Using Multipurpose Equipment

We consider again Example 3 presented in section 6.2, but now we assume that all material states are stable. The process under consideration is described by the STN of figure 9.2. The inventory of available equipment items comprises:

- Two reactor vessels, $R1$ and $R2$ of different capacities, each equipped with a cooling jacket and being suitable for performing both Reaction 1 and Reaction 3.
- A reactor vessel fitted with a heating coil suitable for Reaction 2.
- A distillation column $B1$ with 8 theoretical trays.

Since $R1$ and $R2$ are of different capacities, we treat them as two different types of equipment. We therefore have four types of equipment in the plant, each comprising a single item (*i.e.* $m_j = 1, j = 1,..,4$). The corresponding capacities are listed in Table 9.1 while the plant flowsheet is shown in figure 9.3.

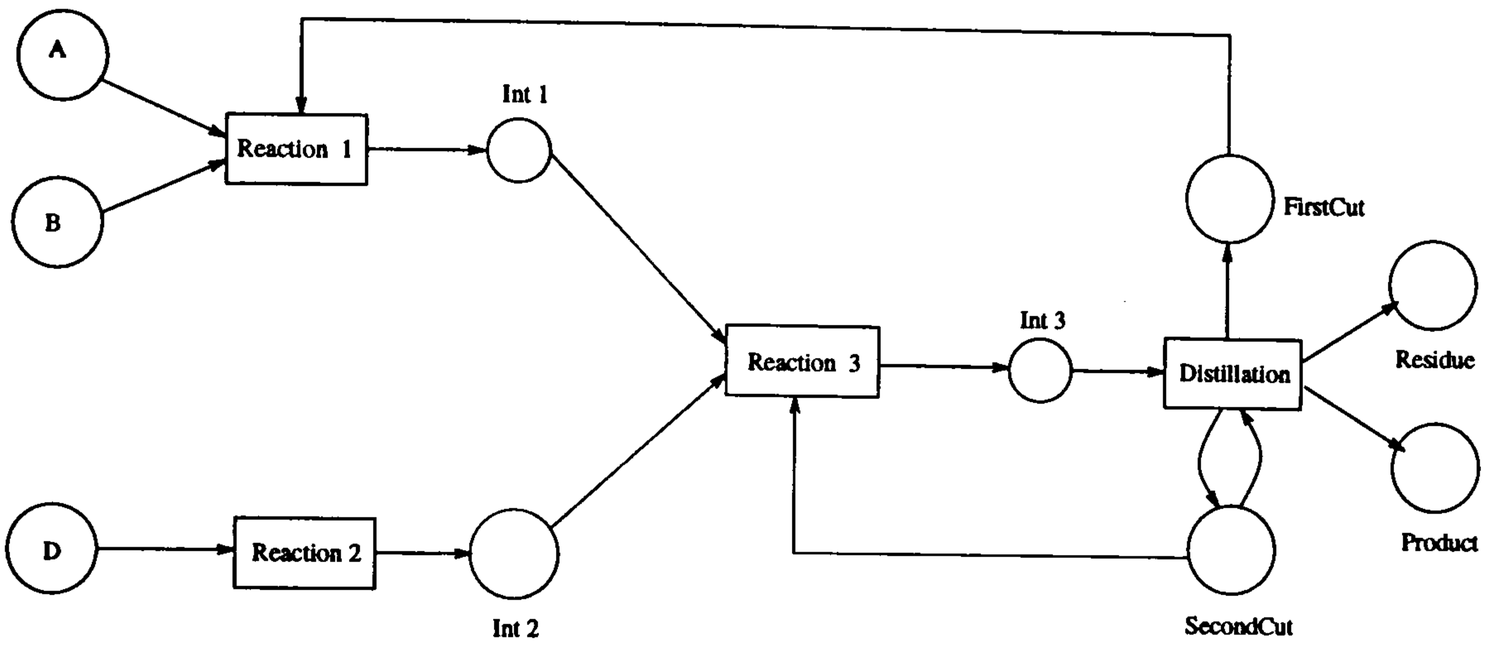

Figure 9.2: Process State-Task Network

Equipment Item	Capacity (m^3)	Suitable Tasks
$R1$	3.00	Reaction 1, Reaction 3
$R2$	2.50	Reaction 1, Reaction 3
$R3$	2.50	Reaction 2
$B1$	1.33	Distillation

Table 9.1: Equipment Inventory

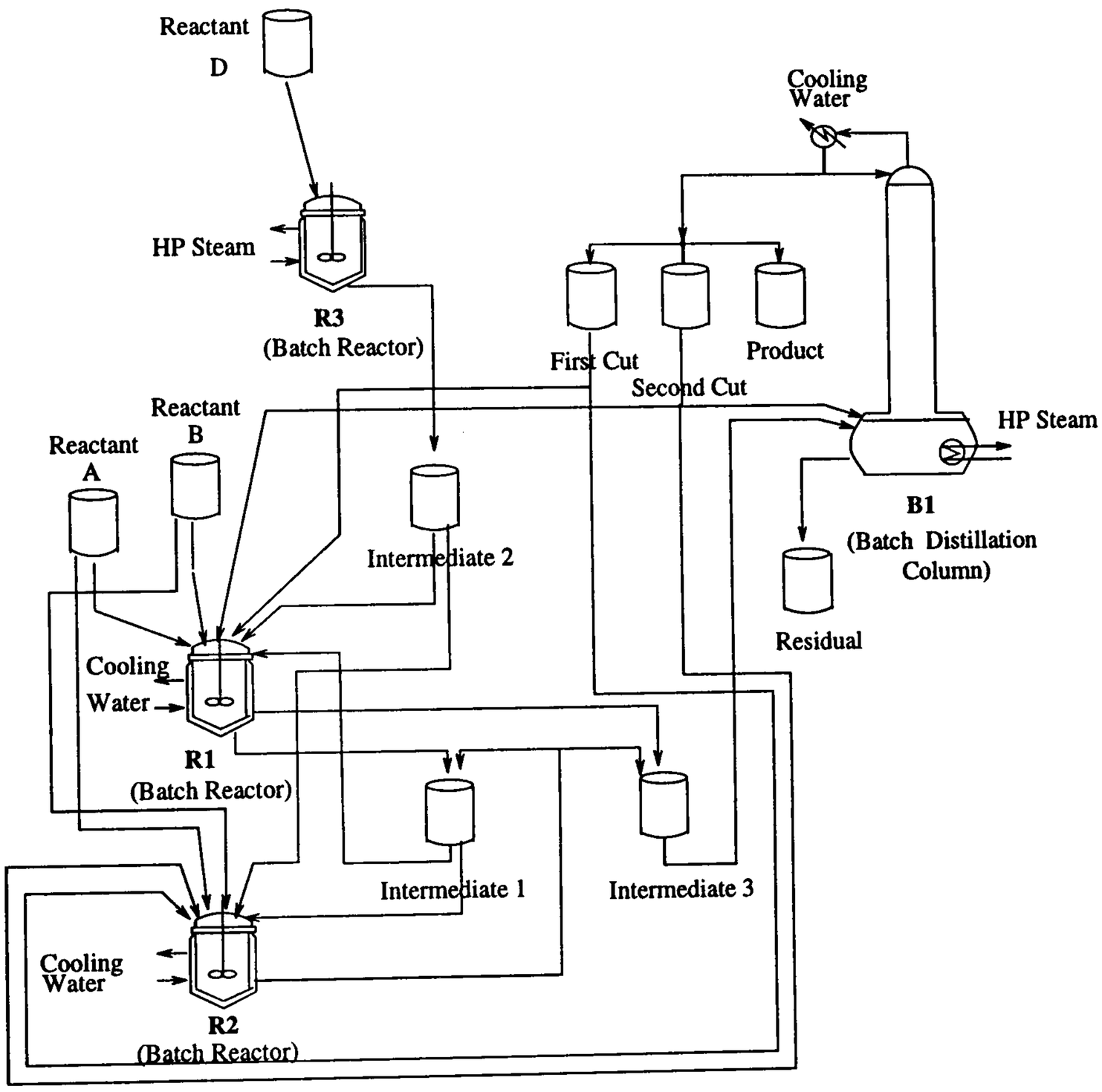

Figure 9.3: Plant Flowsheet

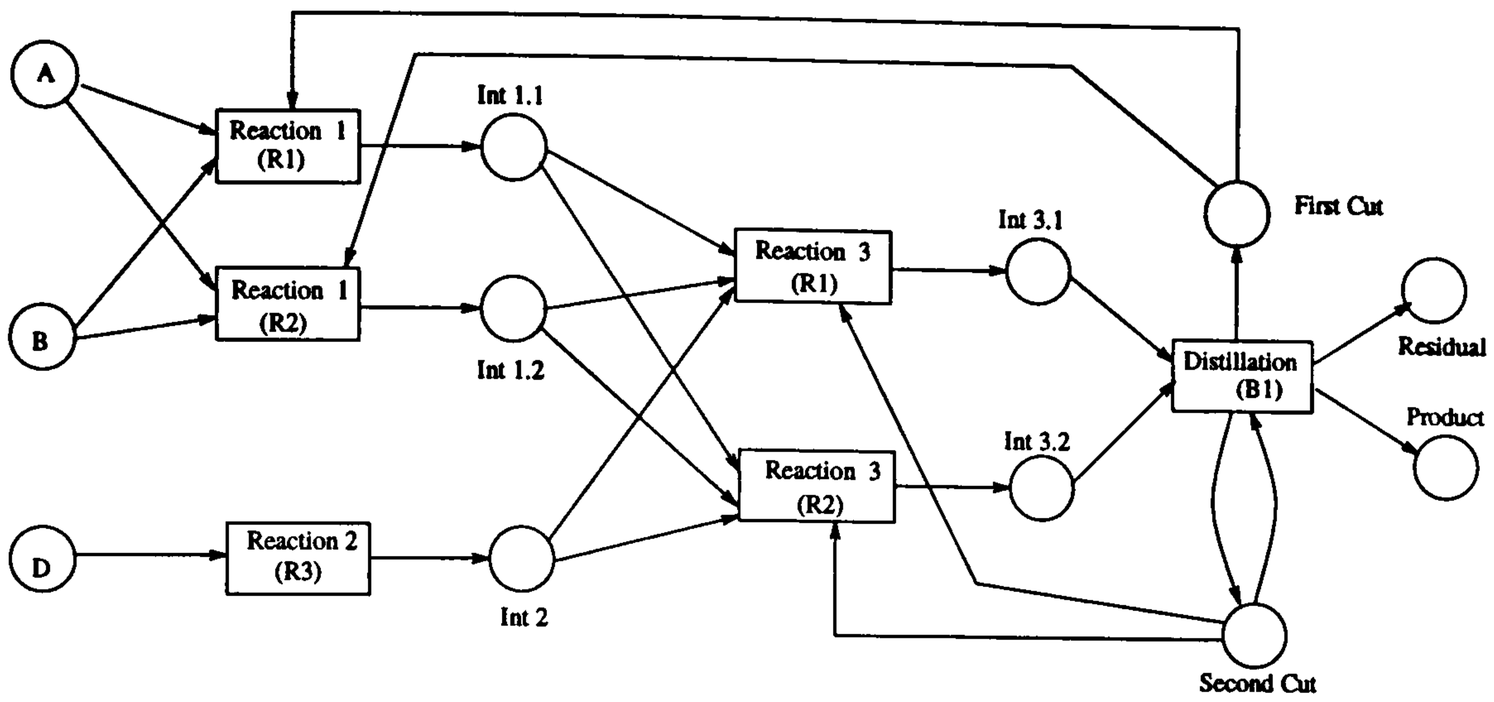

Figure 9.4: Modified State-Task Network

9.4.1. STN Modification

The first step in optimising this process is to modify the STN in figure 9.2 to take account of the fact that tasks Reaction 1 and Reaction 3 may be operated in different ways depending on whether they are carried out in R1 or R2, and consequently they may produce different materials. This modification is carried out in the manner presented in section 9.2 (*cf.* figure 9.1(c)) and results in the modified STN shown in figure 9.4. It can be seen that Reaction 1 has been split into two separate tasks, representing Reaction 1 performed in R1 or R2 respectively. The intermediate $Int1$ produced from each of these new tasks will generally be of different quality, and is therefore represented by two separate states $Int1.1$ and $Int1.2$ in figure 9.4. A similar splitting is applied to task Reaction 3.

We also note that all possible state-task interactions are allowed in the STN of 9.4. For instance, each of the two tasks created by splitting Reaction 3 is allowed to receive input from *both* states representing different qualities of $Int1.1$ and $Int1.2$.

9.4.2. Results and Discussion

The modelling of this process is performed as discussed in section 7.3.4. The overall model of the process involves a total of 815 differential and algebraic equations describing the task operation. The number of decision variables manipulated by the optimisation is 195 with 115 constraints

of which 101 are equalities. The solution of the optimisation problem using the SRQPD code (Chen and Macchietto, 1989) required 128 quadratic programming (QP) subproblems and 215 line-search evaluations of the objective function and constraints[1]. The total computation time was approximately 17 *hr* on a SUN SPARC 10/51.

The total net revenue of the process is approximately 61 $£/hr$ producing 1906 mol/hr of the desired product. This is achieved by consuming 960, 2510 and 3040 mol/hr of feedstocks A, B and D respectively. Material states $Int1.1$, $FirstCut$ and $SecondCut$ are not allowed to accumulate, with only negligible quantities of $Int2$, $Int3.1$ and $Int3.2$ accumulating. A detailed economic breakdown of the solution obtained is provided in Table 9.2.

The resulting solution indicates that reactor vessel R1 should perform both Reaction 1 and Reaction 3 throughout the time horizon whereas reactor vessel R2 is dedicated to Reaction 3. The recipe is summarised in the annotated State-Task Network of figure 9.5; task Reaction 1(R2) is not shown as it is not actually performed. Equipment item R1 spends 37 % and 63% of the production horizon performing Reaction 1(R1) and Reaction 3(R1) respectively.

Reaction 1(R1) consumes 7.73 and 11.46 $kmol/batch$ of A and B respectively and operates for 3.01 *hr*. The variation of cooling water, reactant B addition policy and the resulting temperature as shown in figure 9.6(a). Reaction 2(R3) consumes 30.00 $kmol/batch$ of D and operates for 8.00 *hr*. The variation of steam flowrate and the resulting temperature profile are given in figure 9.6(b).

Reaction 3(R1) consumes 14.34 and 13.76 $kmol/batch$ of $Int1.1$ and $Int2$ respectively. The variation of cooling water and the resulting temperature profile are given in figure 9.7(a). Reaction 3(R2) consumes 16.17 and 15.65 $kmol/batch$ of $Int1.1$ and $Int2$, as well as 2.58 $kmol/batch$ of $SecondCut$. The variation of cooling water and the resulting temperature profile are given in figure 9.7(b).

It is interesting to note that Reaction 3(R1) and Reaction 3(R2) both operate for 7.99 *hr* but with different cooling water policies and amounts of input states consumed. In particular, the distillation off-cut, $SecondCut$, is recycled back to Reactor 3($R2$) only.

The distillation task consumes 5.97 and 11.71 $kmol/batch$ of $Int3.1$ and $Int3.2$ and operates for 3.0 *hr*, producing 3.71, 0.97, 7.13 and 5.89 *kmol* of $FirstCut$, $SecondCut$, $Residual$ and

[1]The optimisation and integration tolerances were set to 10^{-2} and 10^{-5} respectively.

Material	Net Production Rate ($kmol/hr$)	Revenue (£/hr)
A	-0.956	-1.43
B	-2.512	-5.02
D	-3.042	-6.08
$Int1.1$	0.000	0.00
$Int2$	0.000	0.00
$Int3.1$	0.000	0.00
$Int3.2$	0.000	0.00
$FirstCut$	0.000	0.00
$SecondCut$	0.000	0.00
$Residual$	2.374	-2.37
$Product$	1.962	78.47
Total Production Revenue		**63.57**
Utility	Mean Consumption Rate ($tonne/hr$)	Cost (£/hr)
Cooling Water	12.92	0.06
Steam	0.41	2.38
Total Utility Cost		2.44
TOTAL NET REVENUE (£/hr)		**54.34**

Table 9.2: Economic breakdown of optimal solution

Product respectively. The optimal variation of the normalised reflux ratio in the distillation column and composition in the distillate tanks are shown in figure 9.8(a), and the reboiler composition trajectories in figure 9.8(b). The vapour flow to the total condenser is set at its maximum value of 12 $kmol/hr$ throughout the operation.

9.5. Conclusions

This chapter has aimed to relax some of the assumptions regarding the utilisation of plant equipment employed by our original formulation. In particular, it has considered the cases in which:

(a) an item of equipment may be used for more than one task;

(b) a task may be performed in more than one item of equipment.

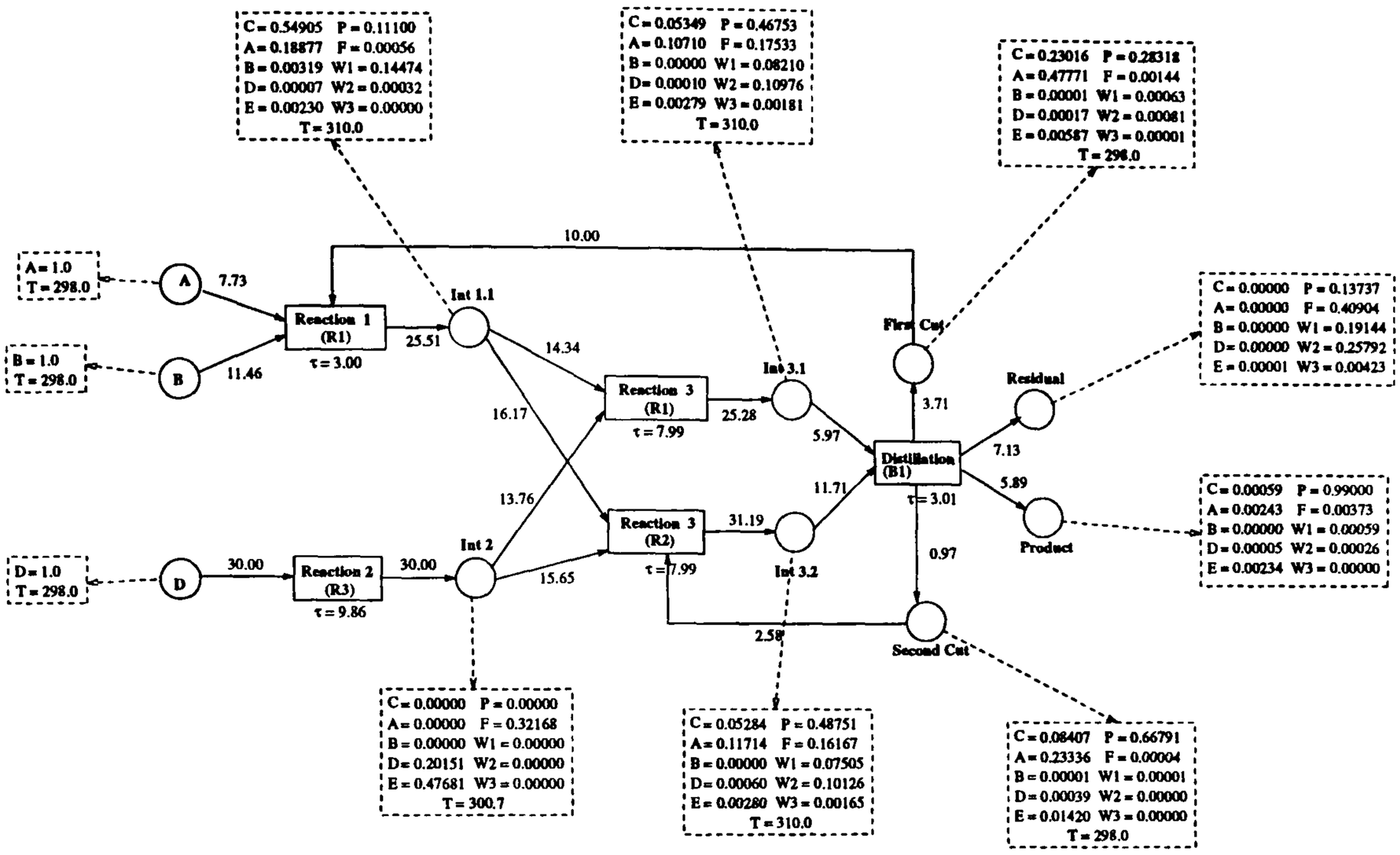

Figure 9.5: Optimal Process Recipe

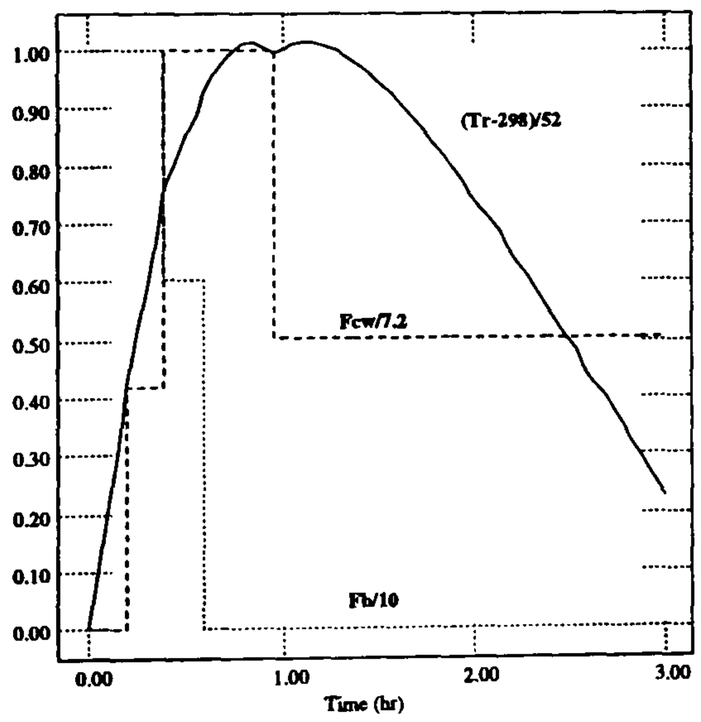

(a) Reaction 1(R1): Temperature (K), Cooling Water Flowrate ($tonne/hr$) and Reactant B Addition Rate ($kmol/hr$)

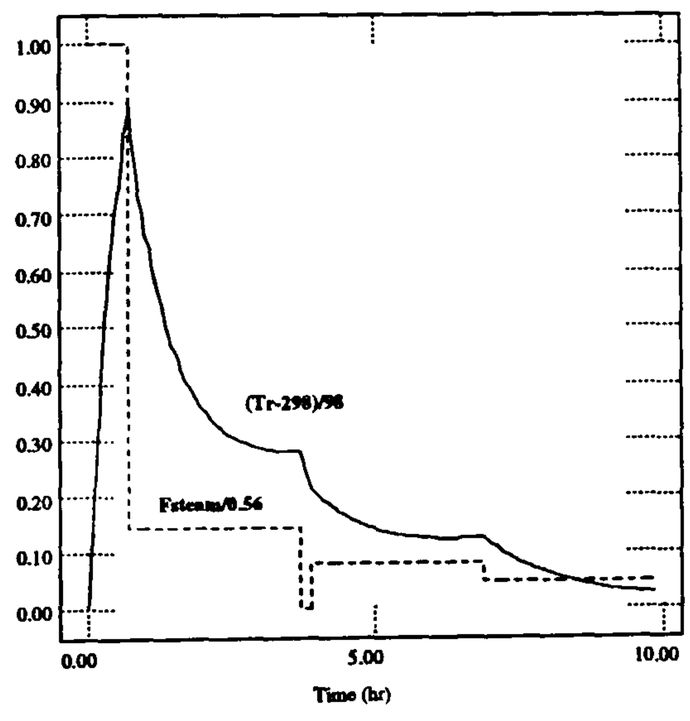

(b) Reaction 2: Temperature (K) and Steam Flowrate($tonne/hr$)

Figure 9.6: Reaction 1(R1) and Reaction 2: Optimal Operating Profiles

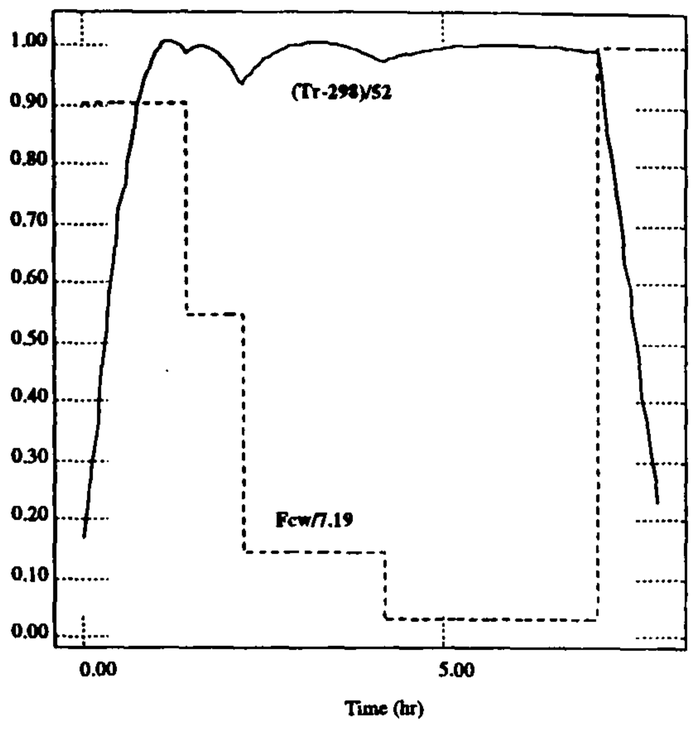

(a) Reaction 3(R1): Temperature (K) and Cooling Water Flowrate ($tonne/hr$)

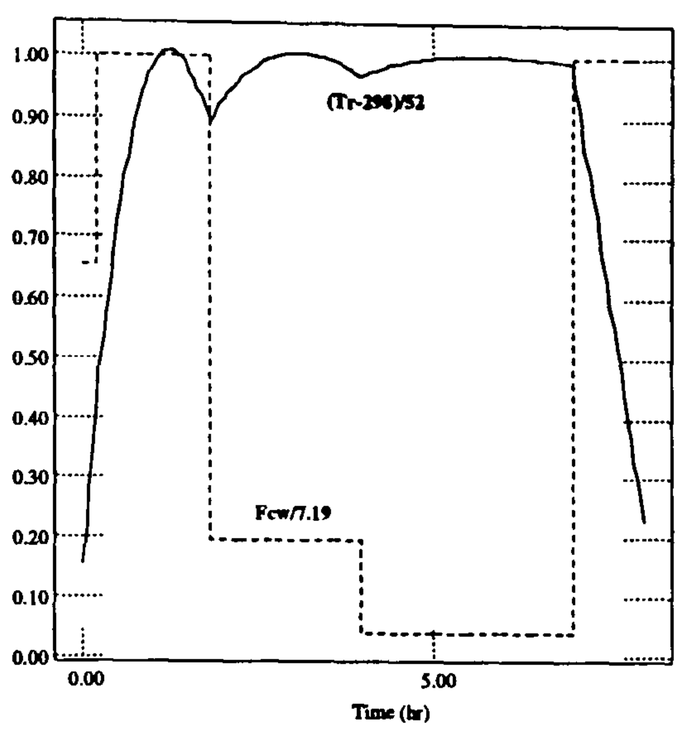

(b) Reaction 3(R2): Temperature (K) and Cooling Water Flowrate ($tonne/hr$)

Figure 9.7: Reaction 3(R1) and Reaction 3(R2): Optimal Operating Profiles

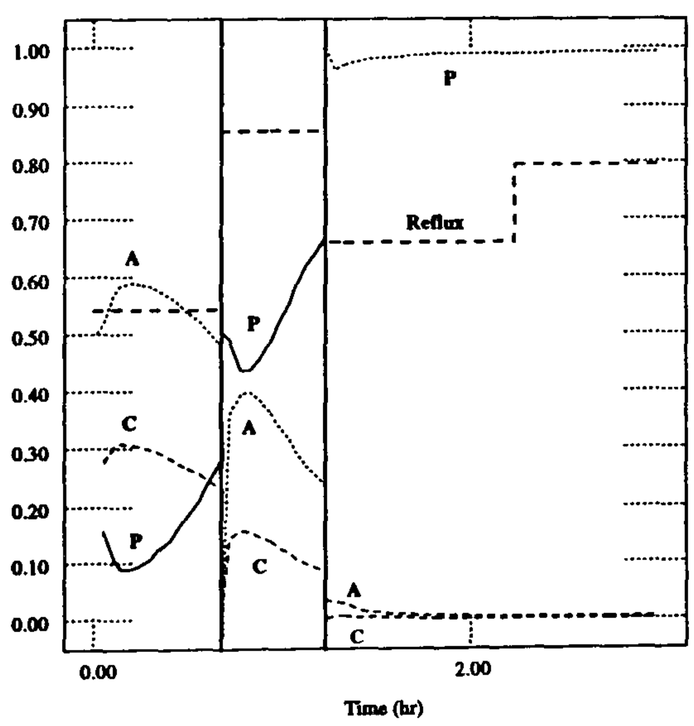

(a) Reflux Ratio Variation and Composition in Distillate Tanks

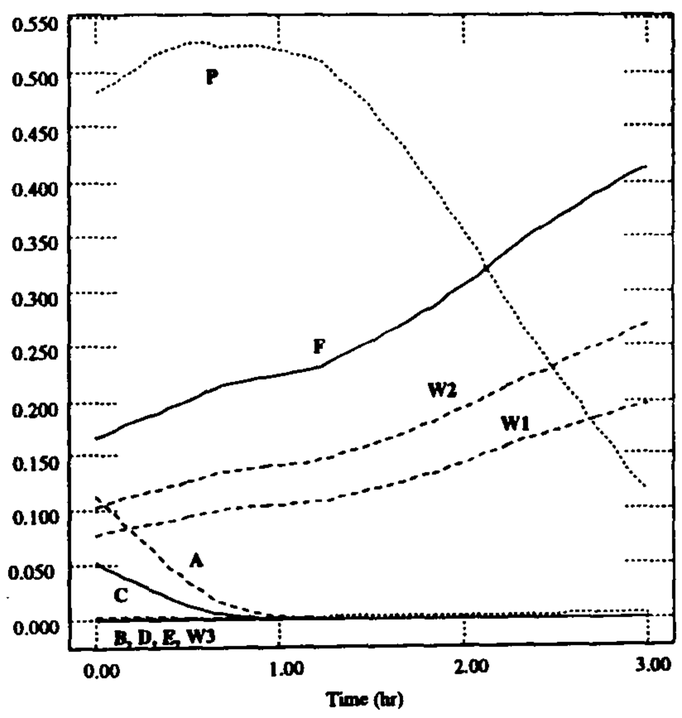

(b) Reboiler Composition

Figure 9.8: Distillation: Optimal Operating Profiles

In general, the more flexible use of equipment in the above manner leads to complex scheduling considerations. In order to alleviate this problem, we have assumed stability and unlimited availability of storage for all states of material in the process. With these assumptions, the mathematical formulation of the problem becomes relatively straightforward, the only significant complication being the need for modifying the process STN to allow for the fact that the same task may be carried out differently in different items of equipment. An example illustrating this procedure was presented in section 9.4.

Another situation that arises often in practice is when each equipment item is dedicated to a single task, but several *identical* items can be used for the same task. In this case, the assumption of stability of all states of material is unnecessary, and the process may be assumed to comprise a number of zero-wait trains as discussed in section 4.1. Only some minor modifications of the formulation presented in Chapter 4 are required. If m_i denotes the number of identical equipment items dedicated to task i, then the cycle time of the zero-wait train n is given by:

$$\tau_n^{cycle} \geq \frac{\tau_i}{m_i}, \qquad \forall n, i \in \mathcal{P}_n \tag{9.5}$$

assuming that the items are operating in an out-of-phase mode.

Constraint (9.5) replaces constraint (4.3) in the original formulation. The capital cost term in the objective function (4.11) must also be modified to take account of the multiple items of equipment:

$$max \qquad -\lambda \sum_i m_i C_i(\nu_i) - \sum_u C_u \sum_n \frac{1}{\tau_n^{cycle}} \sum_{i \in \mathcal{P}_n} U_{ui}(\tau_i) + \sum_s C_s R_s \tag{9.6}$$

Chapter 10

Conclusions and Directions for Future Work

10.1. Summary of the Work Presented in this Thesis

This thesis has considered the integrated design of general batch processes using detailed dynamic models to describe the behaviour of individual batch operations. It has argued that the use of accurate models is an essential requirement for the determination of designs that are both feasible and optimal.

A key aspect of the problem considered is the determination of the process recipe itself. It was demonstrated that the State-Task Network process representation, originally introduced for the development of general plant scheduling formulations, also provides a natural framework for the complete characterisation of process recipes.

The integrated design problem as described here starts with a given State-Task Network structure. This allows a variety of processes (*e.g.* multistep processes, processes with recycles, *etc.*) to be represented, as well as permitting the description of recipe superstructures. The introduction of the concept of "states" of material and their mathematical characterisation removes all direct interactions between tasks and greatly simplifies the formulation of the design problem for processes of arbitrary complexity.

A mathematical formulation was presented for the problem of batch process design. The formulation seeks to determine optimal values for both the design (*e.g.* equipment capacities)

and the operational characteristics (*e.g.* control variable profiles) of each task in the process so as to optimise an economic objective criterion. A variety of constraints may be imposed on task operation; these include both constraints that must hold at all times during the task operation (*e.g.* temperature upper bounds) and constraints that need to be enforced at a finite number of points (*e.g.* end-product purities). The formulation presented takes only limited account of plant scheduling considerations, being applicable to processes with unlimited intermediate storage and/or zero-wait storage policies.

The above formulation results in an infinite dimensional multistage dynamic optimisation problem. An algorithm based on the control parameterisation approach has been proposed to reduce this to a finite dimensional nonlinear programming (NLP) problem that can be solved using standard NLP algorithms and codes. The calculation of the values and gradients of the objective function and the constraints in this optimisation problem is carried out by integrating the DAE systems describing the tasks, and the associated sensitivity equations. These integrations are by far the most time-consuming part of the computation, and using task models of increasing detail and complexity results in a consequential increase in computational time. However, this increase in detail does not otherwise change the nature or size of the optimisation problem being solved.

10.2. Applicability of the Work Presented in this Thesis

A number of examples have been presented showing that it is both desirable and feasible to consider the optimal design of batch processes within a dynamic optimisation framework. The examples considered include processes involving both single and multiple processing steps, multiple recycles of material, plant operation subject to limited utility availability and multipurpose equipment items. Detailed dynamic models have been used for the various types of task occurring in these examples. These include tray-by-tray models for batch distillation columns, and models for single phase and two-phase batch reactors.

The use of dynamic optimisation for the optimal design and operation of batch unit operations is now well established. Much of this work can be viewed as a special case of the work presented in this thesis where the "process" being considered is described by a simple STN comprising a single task. However, the real interest is in applying our methodology to new types of batch processes. In this context, it is worth emphasising that our approach is entirely general with respect to the

types of unit operation that may be included in the design. The only requirement in this respect is the availability of appropriate models for these unit operations.

In recent years, great importance has been attached to the development of environmentally benign processes with special emphasis on continuous process operations. A traditional way of reducing waste effluents in such processes is by an end-of-pipe treatment. However, it often the case that changing the operation of a process might be a more profitable waste reduction option. Our batch process design methodology should offer a natural platform for waste effluent reduction in batch processes. The use of detailed dynamic models for this type of application is particularly important as very often the concentrations of toxic or otherwise undesirable components in effluent streams need to be reduced down to a few parts per million. In such situations, model inaccuracies may result in designs that fail to comply with environmental regulations.

10.3. Some Possible Directions for Future Work

As has been demonstrated by the examples presented in this thesis, the computational cost of solving integrated batch process design problems can be quite substantial. Most of this cost is associated with the computation of individual task trajectories and their sensitivities, as shown in figure 5.1. It is interesting to note, in this context, that these computations are completely independent for the various tasks under consideration, and can therefore be carried out in parallel. This implies that, provided a sufficient number of processors is available, the time required for evaluating the performance of *all* tasks in a given process will not exceed the time required for evaluating the *single most complex* task. Some preliminary experiments along these lines have, in fact, been carried out during the course of this work and have yielded some promising results. However, further work is required to produce and test a more robust implementation of these ideas.

A variety of direct extensions to our work would increase its applicability to integrated batch process design problems. One particularly useful extension would be the inclusion of integer decisions within the optimisation problem. This would permit a number of new types of problem to be considered including, for instance:

- the determination of discrete equipment parameters such as the number of trays in batch distillation columns;

- the use of STN "superstructures" (*cf.* figure 3.2) for the determination of the optimal recipe structure;
- the determination of the optimal number of equipment items of each type (*cf.* section 9.3);
- the consideration of "off-the-shelf" equipment items that are available only in certain discrete sizes.

From the mathematical point of view, the necessary extensions to the solution algorithm presented in Chapter 5 are relatively simple, at least at the conceptual level. In particular, the NLP problem being solved at the outer level of our decomposition algorithm would be replaced by a mixed integer nonlinear programming problem (MINLP). On the other hand, the evaluation of the task performance (*cf.* figure 5.1) will remain completely unaffected by this extension as the discrete decisions will have fixed values during this part of the computation. However, the computational details of this algorithm are likely to require a more detailed analysis.

A second possible extension of our methodology is with respect to the level of detail with which plant scheduling considerations are taken into account. In cases for which a new plant is to be constructed to implement the new process being designed, it could perhaps be argued that the existing methodology is already sufficient as it covers the two important cases of unstable intermediates (leading to the zero-wait operating policy) and stable ones (for which unlimited storage capacity is assumed to be available). However, this is certainly not the case for cases in which the new process is to be implemented in an existing plant with finite storage resources.

Finally, an important assumption underpinning all our work is the deterministic nature of all data used. Clearly, this will not be justified in many cases in which data, such as the composition of raw materials or the various thermophysical or kinetic parameters, are subject to (often considerable) uncertainty. Possible mechanisms for handling the latter in the context of optimal operating policies for single batch unit operations have recently been reviewed by Terwiesch *et al.* (1994). However, this remains very much an unsolved problem, especially when integrated batch processes of the type considered here are concerned.

References

B.S. Ahmad and P.I. Barton. Solvent recovery targeting for pollution prevention in pharmaceutical and specialty chemical manufacturing. In *Pollution prevention via process and product modifications*, volume 90, pages 59–73, 1995.

J.M. Albet, J.-M. Le Lann, X. Joulia, and B. Koehret. Rigorous simulation of multicomponent multisequence batch reactive distillation. In L. Puigjaner and A. Espuña, editors, *Computer-oriented Process Engineering*, pages 75–80, 1991.

R.J. Allgor, M.D. Barrera, P.I. Barton, and L.B. Evans. Optimal batch process development. In *Proceedings of PSE '94, Seoul*, pages 153–158, 1994.

T. Bhatia amd L.T. Biegler. Dynamic optimization in the planning and scheduling of multi-product batch plants. *Ind. Eng. Chem. Res*, 35:2234–2246, 1996.

A.P.F.D. Barbosa-Póvoa. *Detailed Design and Retrofit of Multi-purpose Batch Chemical Plants.* PhD thesis, University of London, 1994.

M.D. Barrera. *Optimal Design and Operation of Batch Processes.* PhD thesis, Massachusetts Institute of Technology, Cambridge, Massachusetts, 1990.

P.I. Barton and C.C. Pantelides. Modeling of combined discrete/continuous processes. *AIChE Journal*, 40:966–979, 1994.

P.I. Barton. *The Modelling and Simulation of Combined Discrete and Continuous Processes.* PhD thesis, University of London, 1992.

D.B. Birewar and I.E. Grossmann. Incorporating scheduling in the optimal design of multi-product batch plants. *Comput. chem. Engng.*, 13:141–161, 1989.

J.R. Bosley and T.F. Edgar. Appropriate modeling assumptions for batch distillation optimization and control. In *Proceedings of PSE '94, Seoul*, pages 477–482, 1994.

M. Caracotsios and W. E. Stewart. Sensitivity analysis of initial value problems with mixed ODEs and algebraic equations. *Comput. chem. Engng.*, 9:359–365, 1985.

C.L. Chen and S. Macchietto. SRQPD — Successive Reduced Quadratic Programming. Technical report, Centre for Process Systems Engineering, Imperial College, 1989.

C.L. Chen. *A Class of Successive Quadratic Programming Methods for Flowsheet Optimisation.* PhD thesis, University of London, 1988.

J.E Cuthrell and L.T. Biegler. On the optimization of differential-algebraic process systems. *AIChE Journal*, 33:1257–1270, 1987.

T.E. Daubert and R.P. Danner. Data compilation tables of properties of pure compounds. AIChE-DIPPR, 1985.

U.M. Diwekar and K.P. Madhavan. Batch-dist: A comprehensive package for simulation, design, optimization and optimal control of multicomponent batch distillation columns. *Comput. chem. Engng.*, 15:833–842, 1991.

U.M. Diwekar, K.P. Madhavan, and R.E. Swaney. Optimization of multicomponent batch distillation columns. *Ind. Eng. Chem. Res.*, 28:1011–1017, 1989.

U.M. Diwekar. Unified approach to solving optimal design-control problems in batch distillation. *AIChE Journal*, 38:1551–1563, 1992.

U.M. Diwekar. How simple can it be? - a look at the models for batch distillation. *Comput. chem. Engng.*, 18S:S451–S457, 1994.

J.M. Douglas. *Conceptual Design of Chemical Processes.* McGraw-Hill, 3rd edition, 1988.

A. M. Dunker. The decoupled direct method for calculating sensitivity coefficients in chemical kinetics. *Journal of Chemical Physics*, 81:2385–2393, 1984.

C. W. Gear. Simultaneous numerical solution of differential-algebraic equations. *IEEE Transactions on Circuit Theory*, CT-18:89–95, 1971.

T. Gundersen. Numerical aspects of the implementation of cubic equation of state in flash calculation routines. *Comput. chem. Engng.*, 6:245–255, 1982.

S. Hasebe and I. Hashimoto. Present status of batch process systems engineering in Japan. *NATO Advanced Study Institute on Batch Processing Systems Engineering, Antalya, Turkey*, 1992.

O.A. Iribarren, M.F. Malone, and H.E. Salomone. A heuristic approach for the design of hybrid batch-continuous processes. *Trans. IChemE*, 72:295–306, May 1994.

O.A. Iribarren. *Batch Chemical Processes Design.* PhD thesis, University of Massachusetts, Amherst, Massachusetts, 1985.

R.B. Jarvis and C.C. Pantelides. DASOLV — a differential-algebraic equation solver. Technical report, Centre for Process Systems Engineering, Imperial College, 1992.

E. Kondili, C.C. Pantelides, and R.W.H. Sargent. A general algorithm for short-term scheduling of batch operations. I-MILP formulation. *Comput. chem. Engng.*, 17:211–227, 1993.

M.A. Lázaro, A. Espuña, and L. Puigjaner. Comprehensive approach to production planning in multipurpose batch plants. *Comput. chem. Engng.*, 13:1031, 1989.

A.A. Linninger, S.A. Ali, E. Stephanopoulos, C. Han, and G. Stephanopoulos. Synthesis and assessment of batch processes for polution prevention. In *Polution prevention via process and product modifications*, volume 90, pages 46–57, 1995.

A.A. Linninger, S.A. Ali, and G. Stephanopoulos. Knowledge-based validation and waste management of batch pharmaceutical process designs. *Comput. chem. Engng.*, S20:S1431–S1436, 1996.

J.S. Logsdon and L.T. Biegler. Accurate determination of optimal reflux policies for the maximum distillate problem in batch distillation. *Ind. Eng. Chem. Res.*, 32:692–700, 1993.

J.S. Logsdon, U.M. Diwekar, and L.T.Biegler. On the simultaneous optimal-design and operation of batch distillation-columns. *Ind. Eng. Chem. Res.*, 28:1628–1639, 1989.

W. L. Luyben. Multicomponent batch distillation. 1. Ternary systems with slop recycle. *Ind. Eng. Chem. Res.*, 27:642–647, 1988.

A. Modi, J.P. Aumond, M. Mavrovouniotis, and G. Stephanopoulos. Rapid plant-wide screening of solvents for batch processes. *Comput. chem. Engng.*, S20:S375–S380, 1996.

J.M. Montagna, O.A. Iribarren, and F.C. Galiano. The design of multiproduct batch plants with process performance models. *Trans IChemE*, 72:783–791, November 1994.

K.R. Morison and R.W.H. Sargent. Optimisation of multistage processes described by differential-algebraic equations. *Lecture Notes in Mathematics, 1230: 86-102, Springer Verlag, Berlin*, 1986.

I.M. Mujtaba and S. Macchietto. Optimal operation of multicomponent batch distillation-multiperiod formulation and solution. *Comput. chem. Engng.*, 17:1191, 1993.

I.M. Mujtaba and S. Macchietto. Optimal design of multicomponent batch distillation columns - single and multiple separation duties. In *Proceedings of PSE '94, Seoul*, pages 179–184, 1994.

I.M. Mujtaba. *Optimal Operational Policies in Batch Distillation.* PhD thesis, University of London, 1989.

M. Nad and L. Spiegel. Simulation of batch distillation by computer and comparison with experiments. In *Proceedings CEF '87, Taormina, Italy*, pages 737–742, 1987.

M. Oh and C.C. Pantelides. A modelling and simulation language for combined lumped and distributed parameter processes. In *Proceedings of PSE '94, Seoul*, pages 37–44, 1994.

M. Oh. *Modelling and Simulation of Combined Lumped and Distributed Processes.* PhD thesis, University of London, 1995.

C. C. Pantelides and H. I. Britt. Multipurpose process modelling environments. In L. T. Biegler and M. F. Doherty, editors, *Proceedings of Foundations of Computer-Aided Design '94*, pages 128–141, Snowmass, Colorado, 1994. CACHE Publications.

L.G. Papageorgiou, M.S. Charalambides, N. Shah, and C.C. Pantelides. Optimal operation of thermally coupled processes. In *Proceedings of Escape 4, Dublin, Ireland*, pages 71–78, 1994.

L.G. Papageorgiou. *Optimal Scheduling of Multipurpose Batch/Semi-Continuous Plants.* PhD thesis, University of London, 1994.

R. Parakrama. Improving batch chemical processes. *The Chem. Engr.*, pages 24–25, 1985.

R.C. Reid, J.M. Prausnitz, and B.E. Poling. *The properties of gases and liquids.* R.R. Donnelley and Sons Company, 4th edition, 1987.

G.V. Reklaitis. Progress and issues in computer aided batch process design. In *Third Intl. Conf. on Foundations of Computer-Aided Process Design, Snowmass, Colorado*, pages 241–276, 1989.

G.V. Reklaitis. Overview of scheduling and planning of batch process operations. *NATO Advanced Study Institute on Batch Processing Systems Engineering, Antalya, Turkey*, 1992.

J.G. Renfro, A.M. Morshedi, and O.A. Asbjornsen. Simultaneous optimization and solution of systems described by differential/algebraic equations. *Comput. chem. Engng.*, 11:503–517, 1987.

D.W.T. Rippin. Simulation of single and multiproduct batch chemical plants for optimal design and operation. *Comput. chem. Engng.*, 7:137–156, 1983.

H.E. Salomone and O.A. Iribarren. Posynomial modelling of batch plants: A procedure to include process decision variables. *Comput. chem. Engng.*, 3:213–231, 1992.

H.E. Salomone, J.M. Montagna, and O.A. Iribarren. Dynamic simulations in the design of batch processes. *Comput. chem. Engng.*, 18(3):191–204, 1994.

R.W.H. Sargent and G.R. Sullivan. The development of an efficient optimal control package. In *Proceedings 8th IFIP conference on Optimisation Technology*, 1977. London, U.K.

N. Shah. *Efficient Scheduling, Planning and Design of Multipurpose Batch Plants.* PhD thesis, University of London, 1992.

J.M. Smith and H.C. Van Ness. *Introduction to Chemical Engineering Thermodynamics.* McGraw-Hill, 4th edition, 1987.

G. Soave. Equilibrium constants from a modified Redlich-Kwong equation of state. *Chem. Eng. Sci.*, 27:1197–1203, 1989.

S. Sundaram and L.B. Evans. Shortcut procedure for simulating batch distillation operations. *Ind. Eng. Chem. Res.*, 32:511–518, 1993.

S. Sundaram and L.B. Evans. Synthesis of separations by batch distillation. *Ind. Eng. Chem. Res.*, 32:500–510, 1993.

P. Terwiesch, M. Agarwal, and D.W.T. Rippin. Batch unit optimization with imperfect modeling: a survey. *Journal of Process Control*, 4:238–258, 1994.

B. Tricoire and M.F. Malone. Design of multiproduct batch processes for polymer production. In *Paper presented at the AIChE Annual Meeting, Miami, FL. Paper No. 134e.*, 1992.

B. Tricoire. *Design and Scheduling of Multiproduct Batch Plants with Application to Polymer Production.* PhD thesis, University of Massachusetts, Amherst, Massachusetts, 1992.

V.S. Vassiliadis, C.C. Pantelides, and R.W.H. Sargent. Optimization of discrete charge reactors. *Comput. chem. Engng.*, S18:S415–S420, 1993.

V.S. Vassiliadis, R.W.H. Sargent, and C.C. Pantelides. Solution of a class of multistage dynamic optimization problems. II.Problems with path constraints. *Ind. Eng. Chem. Res.*, 33:2123–2133, 1994.

V.S. Vassiliadis, R.W.H. Sargent, and C.C. Pantelides. Solution of a class of multistage dynamic optimization problems. I.Problems without path constraints. *Ind. Eng. Chem. Res.*, 33:2111–2122, 1994.

S. Watson, X. Joulia, S. Macchietto, J.-M. Le Lann, G. Vayrette, and J.J. Letourneau. Azeotropic batch distillation - new problems and some solutions. *Comput. chem. Engng.*, S19:S589–S596, 1995.

N.C. Yeh and G.V. Reklaitis. Synthesis and sizing of batch/semi-continuous processes: Single product plant. *Comput. chem. Engng.*, 11:639, 1987.

Appendix A

Mathematical Models for Batch Unit Operations

This appendix describes the mathematical models of the processing tasks utilised in the examples presented in this thesis. In section A.1 we consider the mathematical model for the transient behaviour of a multiphase reaction system. In section A.2 we consider the operation of a liquid phase reaction system. Finally, section A.3 considers the mathematical model for multicomponent batch distillation with multiple distillate cuts.

A.1. Two Phase Batch Reactor

This section provides the mathematical model for the transient behaviour of a multicomponent reactor, considering both liquid and vapour phases.

The reactor setup under consideration is shown in figure A.1. The raw materials can be added as an initial charge as well as semi-continuously thoughout the reactor operation. Any non-condensible by-products generated by the reaction scheme taking place in the reactor (see section 7.2) are allowed to escape. To avoid losing any reactants and desirable products, a partial condenser is utilised to condense these valuable materials and recycle them back to the reactor. For the purpose of the example presented in Chapter 7 of this thesis, we aggregate the two cooling loads on the reactor, (total condenser and cooling jacket) resulting in the approximated reactor setup shown in figure A.2. In developing the appropriate mathematical model, we have assumed

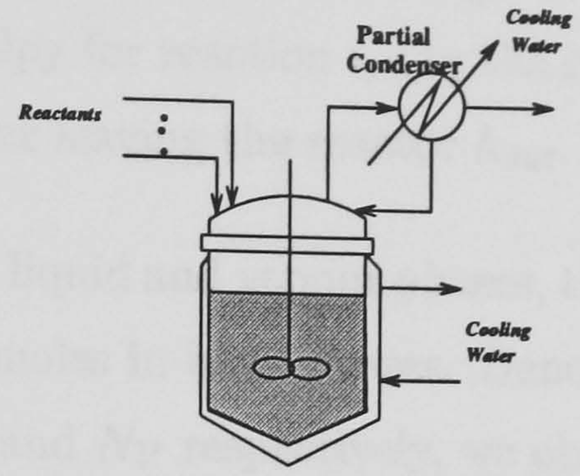

Figure A.1: Two Phase Batch Reactor

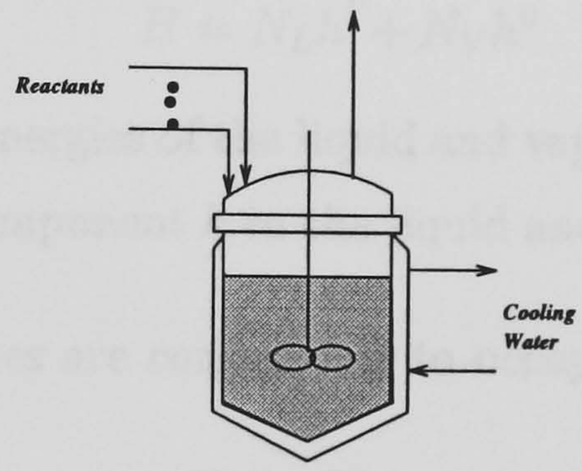

Figure A.2: Approximate Two Phase Batch Reactor

that the reactions take place in the liquid phase only. We consider a general set of reactions i, with the stoichiometric coefficients of component k in reaction i being denoted by ν_{ik}. We also assume ideal gas behaviour for the vapour phase and well-mixed liquid hold-up.

A material balance for component k over the entire unit yields:

$$\frac{dN_k}{dt} = \sum_s x_{ks} F_s^{in} + V_L \sum_i \nu_{ik} r_i - y_{k,out} F_{out} \qquad \forall \quad k \tag{A.1}$$

where N_k denotes the total molar hold-up of component k, V_L the volume of the liquid phase and r_i the reaction rate of reaction i. x_{ks} and F_s^{in} respectively denote the molar composition and amount of the feed streams. Also $y_{k,out}$ and F_{out} are the corresponding quantities in the vapour leaving the reactor.

The energy balance over the entire unit is:

$$\frac{dH}{dt} = \sum_s F_{in,s} h_{in,s} + V_L \sum_i r_i (-\Delta H_{Ri}) - Q_R - F_{out} h_{out} \tag{A.2}$$

where H is the total energy hold-up in the system, $h_{in,s}$ is the specific enthalpy of input material state s, ΔH_{Ri} the reaction enthalpy for reaction i, Q_R the rate of heat removal/addition and h_{out} the specific enthalpy of the vapour leaving the reactor h_{out}.

As the system contains both liquid and vapour phases, the total number of moles in the system is determined by the number of moles in both phases. Denoting the total number of moles in the liquid and vapour phases by N_L and N_V respectively, we obtain:

$$N_k = N_L x_k + N_V y_k \tag{A.3}$$

and

$$H = N_L h^l + N_V h^v \tag{A.4}$$

where h^l and h^v are the specific energies of the liquid and vapour phases respectively. Also, x_k and y_k denote the mole fraction of component k in the liquid and vapour phases respectively.

The liquid and vapour phases are constrained to occupy the available volume V within the unit. This leads to:

$$\frac{N_L}{\rho^l} + \frac{N_V}{\rho^v} = V \tag{A.5}$$

where ρ^l and ρ^v denote the density of the liquid and vapour phases respectively.

The liquid and vapour mole fractions are normalised:

$$\sum_k x_k = \sum_k y_k = 1 \tag{A.6}$$

and also obey thermodynamic equilibrium relations of the form:

$$y_k = K_k x_k \quad \forall \quad k \tag{A.7}$$

where K_k denotes the thermodynamic equilibrium constant of component k.

The flow of vapour leaving the reactor (F_{out}) is assumed to be pressure driven:

$$F_{out} = K_v (P - P^{atm})^{0.5} \tag{A.8}$$

where K_v, P and P^{atm} denote the valve constant, reactor pressure and atmospheric pressure respectively.

We note that the intensive properties $y_{k,out}$ and h_{out} of the vapour stream leaving the reactor are not necessarily identical to tha properties y_k and h^v inside the reactor. Instead, they are determined by the operation of the condenser. For instance, the vapour stream may be assumed to contain only a single component (*e.g.* an incondensible gas).

The above reactor model takes into account only the continuous addition of the feed streams. The discrete charge of a number of reactants at the start of the reactor operation is determined by the following initial conditions:

$$N_k(0) = \sum_s x_{ks} B_{in,s} \quad \forall \quad k \tag{A.9}$$

$$H(0) = \sum_s B_{in,s} h_{in,s} \tag{A.10}$$

where $B_{in,s}$ denotes the initial amount of input state s charged to the reactor.

A.2. Liquid Phase Batch Reactor

For many reaction schemes, the low volatility of the various reactants and products allows the utilisation of a liquid phase batch reactor. The mathematical model describing the transient behaviour of a multicomponent liquid phase reactor with both discrete and continuous reactant addition is described below.

Consider the batch reactor shown in figure A.3, with the set of feeds added as discrete charges at the start or continuously throughout the operation of the reactor denoted as B_s^{in} and F_s^{in} respectively. The mole fraction of component k in feed stream s is denoted as x_{ks}^{in}. Also, the specific enthalpy of feed stream s is denoted as h_s^{in}.

We utilise both material and energy balances to chartacterise the transient behaviour of batch reactor operation, assuming a well-stirred reaction mixture. A material balance on component k yields:

$$\frac{dN_k}{dt} = \sum_s x_{ks}^{in} F_s^{in} + V \sum_i \nu_{ik} r_i \quad \forall \quad k \tag{A.11}$$

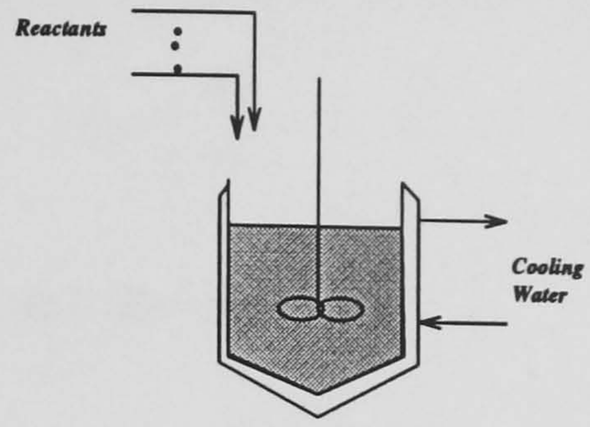

Figure A.3: Liquid Phase Batch Reactor

where N_k is the molar hold-up of component k, V is the volume of the reaction mixture, r_i is the reaction rate of reaction i and ν_{ik} is the stoichiometric coefficient of component k in reaction i.

The total molar hold-up (N) in the reactor is given by:

$$N = \sum_k N_k \tag{A.12}$$

For our examples, the reaction rate expression is a function of molar concentration (C_k) of the form:

$$r_i = k_i \prod_k C_k^{\beta_{ki}} \quad \forall \quad i \tag{A.13}$$

with the reaction rate constant (k_i) in the Arrhenius form:

$$k_i = A_i e^{\frac{-E_i}{RT}} \quad \forall \quad i \tag{A.14}$$

where β_{ki} denotes the order of the reaction i with respect to component k, A_i the frequency factor, E_i the activation energy, R the universal gas constant and T the temperature of the reaction mixture.

The molar concentration of component k is given by:

$$C_k = \frac{N_k}{V} \quad \forall \quad k \tag{A.15}$$

with the total volume of the reaction mixture given by:

$$V = \frac{N}{\rho^l} \tag{A.16}$$

where ρ^l denotes the density of the reactor contents.

The mole fraction of component k is denoted as x_k and is given by:

$$x_k = \frac{N_k}{N} \quad \forall \quad k \tag{A.17}$$

An energy balance on the entire unit yields:

$$\frac{dH}{dt} = \sum_s F_s^{in} h_s^{in} + V \sum_i r_i(-\Delta H_{Ri}) + Q_R \tag{A.18}$$

where H and ΔH_{Ri} denote the total enthalpy and reaction enthalpy for reaction i respectively.

The total enthalpy of the system is given by:

$$H = Nh^l \tag{A.19}$$

where h^l is the specific enthalpy of the reactor contents.

The above reactor model takes into account only the continuous addition of the feed streams. The discrete charge of a number of reactants at the start of the reactor operation is determined by the following initial conditions:

$$N_k(0) = \sum_s x_{ks}^{in} B_s^{in} \quad \forall \quad k \tag{A.20}$$

$$H(0) = \sum_s B_s^{in} h_s^{in} \tag{A.21}$$

A.3. Multicomponent Batch Distillation

We consider the case of multicomponent batch distillation producing multiple distillate cuts as shown in figure A.4. Our mathematical model for the description of the transient behaviour of a multicomponent batch distillation is based on a number of assumptions:

- No reaction,
- Negligible vapour hold-up,
- Adiabatic tray operation,

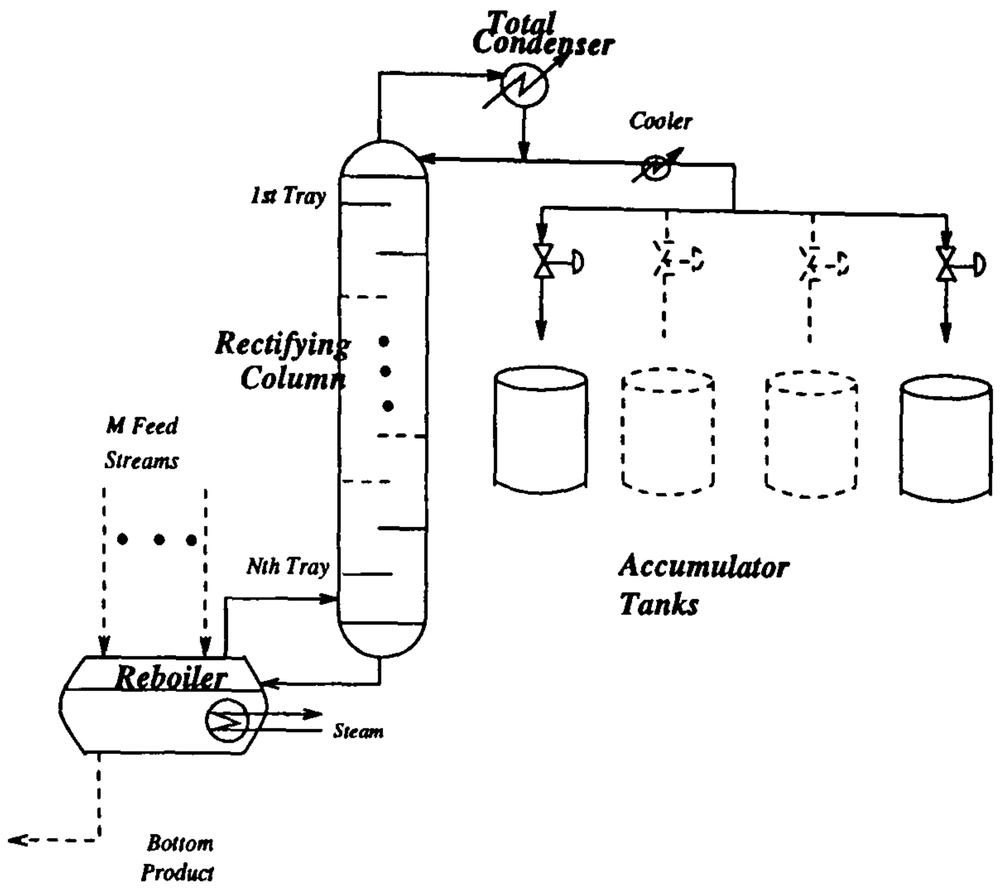

Figure A.4: Batch Distillation Column

- Perfect mixing,
- Constant plate and condenser hold-ups,
- Negligible column hydraulics,
- Fast energy dynamics.

Accumulator Tanks

Consider the case of a distillation column producing Z distillate cuts. Control valves direct the distillate flow to the appropriate accumulator tank. Numerically, the control variable ν_z is set to 1 when the corresponding valve is open, and 0 if the valve is closed.

An overall material balance over the zth accumulator tank yields:

$$\frac{dM_z}{dt} = \nu_z L_d \quad \forall \quad z \tag{A.22}$$

with the variation in mole fraction given by:

$$M_z \frac{dx_{zk}}{dt} = \nu_z L_d (x_{ck} - x_{zk}) \quad \forall \quad k, z \tag{A.23}$$

where M_z, L_d, x_{zk} and x_{ck} denote the molar hold-up in the zth accumulator tank, the molar distillate flow, the mole fraction in the distillate tank and mole fraction in the condenser tank (of component k) respectively.

Total Condenser

Since we have assumed a constant condenser hold-up, an overall balance yields:

$$V_1 = L_c + L_d \tag{A.24}$$

with the mole fraction variation given by:

$$M_c \frac{dx_{ck}}{dt} = V_1 y_{1k} - x_{ck}(L_d + L_c) \quad \forall \quad k \tag{A.25}$$

where M_c, V_1, L_c and y_{1k} denote the condenser hold-up, the vapour flow leaving the first tray, the amount refluxed and composition of the vapour leaving the first tray respectively.

The amount refluxed back to the top tray is related to the vapour flow to the condenser through:

$$L_c = rV_1 \tag{A.26}$$

where r is the normalised reflux ratio.

The energy Q_c required to condense the vapour to the condenser is given by:

$$Q_c = V_1(h_1^v - h_c^l) \tag{A.27}$$

where h_1^v and h_c^l denote the specific molar enthalpy of the vapour leaving the top tray and condenser liquid hold-up respectively.

Assuming that the liquid in the total condenser is at its bubble point, we have:

$$\sum_k K_{ck} x_{ck} = 1 \tag{A.28}$$

where K_{ck} denotes the equilibrium constant of component k.

Trays

An overall material balance over the nth tray for constant tray hold-up yields:

$$L_{n-1} + V_{n+1} = L_n + V_n \quad \forall \quad n \tag{A.29}$$

where L_{n-1}, V_{n+1}, denote the vapour flow from the top tray and the vapour flow from the bottom tray respectively. The liquid and vapour leaving the nth tray are denoted as L_n and V_n respectively.

The variation in composition in the nth tray is given by:

$$M_n \frac{dx_{nk}}{dt} = L_{n-1}x_{n-1,k} - L_n x_{nk} + V_{n+1}y_{n+1,k} - V_n y_{nk} \quad \forall \quad n,k \tag{A.30}$$

where M_n is the molar hold-up in the nth tray, x_{nk} and y_{nk} the mole fraction of the liquid and vapour phases of the nth tray, whereas $x_{n-1,k}$ and $y_{n+1,k}$ denote the mole fraction of the liquid from the top tray and vapour from the bottom tray respectively.

For adiabatic tray operation and assuming fast energy dynamics, the energy balance is of the form:

$$L_{n-1}h^l_{n-1} - L_n h^l_n + V_{n+1}h^v_{n+1} - V_n h^v_n = 0 \quad \forall \quad n \tag{A.31}$$

where variable h denotes specific enthalpy, with its superscript indicating the phase and its subscript indicating the tray number.

The liquid mole fraction is normalised:

$$\sum_k y_{nk} = 1 \quad \forall \quad n \tag{A.32}$$

with the vapour phase composition obeying the thermodynamic equilibrium relations of the form:

$$y_{nk} = K_{nk}x_{nk} \quad \forall \quad n,k \tag{A.33}$$

where K_{ck} denotes the equilibrium constant of component k.

Reboiler

A material balance for component k over the entire reboiler yields:

$$\frac{dM_{rk}}{dt} = L_N x_{Nk} - V_r y_{rk} \quad \forall \quad k \tag{A.34}$$

where M_{rk} denotes the amount of component k, L_N the liquid flow from the Nth tray, x_{Nk} the mole fraction of the liquid from the Nth tray, and V_r and y_{rk} the molar flowrate and mole fraction of the vapour leaving the reboiler respectively.

Assuming fast energy dynamics, the overall energy balance is of the form:

$$L_N(h_N^l - h_r^l) + V_r(h_r^l - h_r^v) + Q_r = 0 \tag{A.35}$$

The liquid mole fraction is normalised:

$$\sum_k y_{rk} = 1 \tag{A.36}$$

with the vapour phase composition obeying the thermodynamic equilibrium relations of the form:

$$y_{rk} = K_{rk} x_{rk} \quad \forall \quad k \tag{A.37}$$

A.4. Thermophysical Property Relations

A number of models have been utilised in the examples presented in this thesis for the prediction of thermophysical properties such as density, enthalpy and vapour pressure.

A.4.1. Density

The liquid and vapour densities of pure components are functions of temperature and pressure:

$$\rho_k^o = \rho_k\,(T, P) \quad \forall \quad k \tag{A.38}$$

In the case of liquid densities, it is possible to ignore the pressure and temperature effects and assume constant liquid densities and an ideal mixing rule for the density ρ^l of the liquid mixture:

$$\frac{1}{\rho^l} = \sum_k \frac{x_k}{\rho_k^o} \tag{A.39}$$

For gases that exhibit ideal gas behaviour, the molar density ρ^v of the mixture can be determined through the ideal gas law:

$$\rho^v = \frac{P}{RT} \quad \forall \quad k \tag{A.40}$$

A.4.2. Enthalpy

The specific enthalpy of pure component k in the vapour phase is assumed to be a function of temperature only:

$$h_k^v = h_k^v(T) \quad \forall \quad k \tag{A.41}$$

with the specific enthalpy in the liquid phase given by:

$$h_k^l = h_k^v - \Delta H_k^{vb} \quad \forall \quad k \tag{A.42}$$

where ΔH_k^{vb} is the specific enthalpy of vapourisation of component k.

The vapour phase specific enthalpy is frequently determined by integrating correlations for the isobaric specific heat capacity from a reference temperature T_{ref} up to the required temperature T:

$$h_k^v = \int_{T_{ref}}^{T} \left(a + bT + cT^2 + cT^3\right) dT \quad \forall \quad k \tag{A.43}$$

The specific enthalpy of a mixture is a function of composition. For the purposes of this work, we adopted ideal mixing rules for the specific enthalpy of a mixture:

$$h^l = \sum_k x_k h_k^l \tag{A.44}$$

$$h^v = \sum_k y_k h_k^v \tag{A.45}$$

Chen's method (Reid *et al.*, 1987) is adopted for the calculation of the specific enthalpy of vaporisation (ΔH_{vb} in $kJ/kmol$):

$$\Delta H_{vb} = RT_cT_{br}\frac{3.978T_{br} - 3.958 + 1.555\ln P_c}{1.07 - T_{br}} \tag{A.46}$$

where T_{br}, T_c, P_c and R denote the reduced boiling temperature, critical pressure, critical temperature and universal gas constant respectively.

The reduced boiling temperature is given by:

$$T_{br} = \frac{T_b}{T_c} \tag{A.47}$$

where T_b denotes the boiling point at atmospheric pressure.

A.4.3. Vapour-liquid Equilibrium

In a multicomponent multiphase system, the thermodynamic equilibrium relation between the vapour and liquid phases (for component k) is of the form:

$$y_k = K_k x_k \quad \forall \quad k \tag{A.48}$$

The proportionality constant (K_k), in its general form, is a function of temperature, pressure and liquid and vapour composition:

$$K_k = K\left(P, T, x_k, y_k\right) \quad \forall \quad k \tag{A.49}$$

Phase Equilibrium for Ideal Mixtures

Assuming ideal behaviour in the liquid and vapour phases, it is possible to ignore the effect of composition on the equilibrium constant as there is no interaction between the various components. Therefore, equation (A.49) simplifies to:

$$K_k = \frac{P_{vap,k}(T)}{P} \quad \forall \quad k \tag{A.50}$$

where $P_{vap,k}$ is the vapour pressure of pure component k and P is the pressure of the system under consideration.

The calculation of the vapour pressure of a pure component at a particular temperature is based on correlations which are derived from experiments and are readily available in the literature. In the context of this work, we have utilised three different correlations (see Appendix B):

$$\ln P_{vap,k} = -\frac{a}{T} + b \tag{A.51}$$

$$\ln P_{vap,k} = a - \frac{b}{T+c} \tag{A.52}$$

$$\ln P_{vap,k} = a + \frac{b}{T} + cT + d\ln T + eT^f \tag{A.53}$$

Phase Equilibrium for Non-ideal Mixtures

The equilibrium constant K for component i in a non-ideal mixture (Smith and Van Ness, 1987) of NC components is generally given by:

$$K_i = \frac{\phi_i^l}{\phi_i^l} \quad \forall \quad i = 1,..,NC \tag{A.54}$$

where ϕ_i^l and ϕ_i^v are the fugacity coefficients of component i in the liquid and vapour phase respectively.

In the context of some of the examples presented in Chapter 6, we have considered the calculation of vapour-liquid equilibria utilising the Soave-Redlich-Kwong equation of state. Using the cubic equation of state and simple mixing rules, it is possible to derive an analytical expression for the fugacity coefficient of each component in the liquid or vapour phase s (Reid *et al.*, 1987):

$$\begin{aligned} log(\phi_i^s) &= \left(\frac{b_i}{b_s^m}(Z_s - 1)\right) - ln(Z_s - B_s^*) \\ &+ \frac{A_s^*}{B_s^*}\left(\frac{b_i}{b_s^m} - 2\left(\frac{a_i}{a_s^m}\right)^{0.5}\right) ln\left(\frac{Z_s + B_s^*}{Z_s}\right) \quad \forall \quad i = 1,..,NC \end{aligned} \tag{A.55}$$

where Z_s is the compressibility factor of phase s. Given the critical temperature T_{ci} and pressure P_{ci}, and acentric factor ω_i of each component i, the parameters a_i, b_i, b_s^m,a_s^m, A_s^*, B_s^* as a function of composition z_i[1] are given by:

$$A_s^* = \frac{a_s^m P_t}{{R_g}^2 T^2} \quad \forall \quad s \tag{A.56}$$

where R_g is the universal gas constant

[1] z_i can be either liquid or vapour composition

$$B_s^* = \frac{b_s^m P_t}{R_g T} \quad \forall \quad s \tag{A.57}$$

$$a_s^m = \sum_i \sum_j z_i z_j (a_i a_j)^{0.5} \quad \forall \quad s \tag{A.58}$$

$$b_s^m = \sum_i z_i b_i \quad \forall \quad s \tag{A.59}$$

$$a_i = \frac{0.42748 {R_g}^2 {T_{ci}}^2}{P_{ci}} \left(1 + f_{wi}\left(1 - \left(\frac{T}{T_{ci}}\right)^{0.5}\right)\right)^2 \quad \forall \quad i = 1, .., NC \tag{A.60}$$

$$f_{wi} = 0.48 + 1.574\omega_i - 0.176{\omega_i}^2 \quad \forall \quad i = 1, .., NC \tag{A.61}$$

$$b_i = \frac{0.0866 R_g T_{ci}}{P_{ci}} \quad \forall \quad i = 1, .., NC \tag{A.62}$$

where T_{ci}, P_{ci}, and ω_i are pure component critical temperature, critical pressure and acentric factor respectively.

Equation (A.55) depends on the compressibility factor of both the liquid and vapour phases, calculated from the cubic equation of state (Soave, 1989) written in the form:

$${Z_s}^3 - {Z_s}^2 + (A_s^* - B_s^* - B_s^{*2}) Z_s - A^* B^* = 0 \quad \forall \quad s \tag{A.63}$$

Unfortunately, the solution of the cubic equation of state sometimes results in calculation failures with the equilibrium constant collapsing ($K_i \rightarrow 1.0$), in particular for a bad initial guess at high pressures and when the wrong root is selected (Gundersen, 1982). To overcome these deficiencies, Gundersen (1982) proposed an algorithm that calculates the correct root of the equation based on the values of Q_s and R_s, and the residual of equation (A.63) at $Z_s = \frac{1}{3}$. Assuming that only low pressure vapour-liquid equilibria calculations are required, selecting the largest root for the vapour phase and the smallest one for the liquid phase would suffice.

Appendix B

Input Data for Batch Process Design Problems

A number of examples have been presented in this thesis to demonstrate the various aspects of the proposed methodology for batch process design. The values of the various reaction kinetic parameters and thermophysical property coefficients utilised are presented in this Appendix.

B.1. Multicomponent Batch Distillation

The vapour-liquid equilibrium calculations are based on the Soave-Redlich-Kwong (SRK) model (see section A.4.2) and the heat of vaporisation is estimated through Chen's method (*cf.* equation A.46). The pure component critical parameter data (Daubert and Danner, 1985) utilised are given in Table (B.1). The values of the coefficients (Daubert and Danner, 1985) for the calculation of the specific enthalpy in J/mol (*cf.* equation A.43) are given in Table B.1.

The normal boiling temperatures (T_b) of cyclohexane, n-heptane and toluene are 353.5, 371.6 and 383.8 K respectively.

Compound	T_c K	P_c bar	ω
Cyclohexane	553.5	40.7	0.273
n-Heptane	540.3	27.4	0.263
Toluene	591.8	41.0	0.263

Table B.1: Multicomponent Batch Distillation: Critical Parameter Data

Coefficient	*Cyclohexane*	$n-Heptane$	*Toluene*
a	-3.7810E+1	-5.1466E+0	-2.4350E+1
b	5.5390E-1	6.7620E-1	5.1250E-1
c	-1.9530E-4	-3.6510E-4	-2.7650E-4
d	-1.5340E-8	7.6580E-8	4.9110E-8

Table B.2: Multicomponent Batch Distillation: Specific Enthalpy Data

B.2. Reaction-Distillation Process I

Reaction Kinetics

$$main \quad reaction \quad rate = k_1 C_A C_B \quad (kmol/hr.m^3) \tag{B.1}$$

$$side \quad reaction \quad rate = k_2 C_B C_C \quad (kmol/hr.m^3) \tag{B.2}$$

where C_A, C_B, C_C and C_D are the molar concentrations $(kmol/m^3)$ of components A, B, C and D respectively.

The kinetic rate constants $(m^3/hr.kmol)$ are of the Arrhenius form:

$$k_1 = 100.0e^{\frac{-17000}{RT}} \tag{B.3}$$

$$k_2 = 120.0e^{\frac{-20000}{RT}} \tag{B.4}$$

where T is the reaction temperature (K) and R the universal gas constant (8.314 $kJ/kmol.K$). The enthalpies of reaction for the main and side reactions are -60000.0 and -50000.0 $kJ/kmol$ respectively.

Cooling Jacket

The cooling jacket in the reactor vessel has a surface area of 30 m^2. An overall heat transfer coefficient of 5088.16 $kW/m^2.hr$ is assumed for the heat transfer between the reaction mixture and the cooling water. The inlet temperature of the cooling water is 288 K with a constant heat capacity of 4200.0 $kJ/tonne.K$.

Enthalpy and Density

The liquid and vapour specific enthalpy (h_k^l and h_k^v, in $kJ/kmol$) of pure components are calculated through equations (A.43) and (A.42) utilising coefficient a only (*i.e.* assuming constant specific heat capacity). The values of the coefficients a ($kJ/kmol/K$) and enthalpy of vapourisation ($kJ/kmol$) utilised are given in Table B.3. A reference temperature of 298 K is adopted.

Coefficient	A	B	C	D
a	172.3	200.0	160.0	155.0
ΔH_{vap}	31000.0	26000.0	28000.0	34000.0

Table B.3: Reaction-Distillation Process I: Enthalpy Data

The molar densities of pure components A, B, C and D in the liquid phase are 11.0, 16.0, 10.4 and 10.0 $kmol/m^3$ respectively.

Vapour Pressure

Equation (A.51) is utilised to calculated the vapour pressure (in bar) at a given temperature (in K). The values of the coefficients used are given in Table B.2.

Coefficient	A	B	C	D
a	4142.7500	3474.5600	3741.8800	4543.7100
b	11.7158	9.9404	9.9915	11.2599

Table B.4: Reaction-Distillation Process I: Vapour Pressure Data

B.3. Reaction-Distillation Process II

Reaction I Kinetics

The following reaction scheme is utilised in Reaction I:

$$\begin{aligned} R_1 + R_2 &\rightarrow I_1 & \Delta H_R &= -23.0 kcal/mol \\ R_1 + I_1 &\rightarrow A & \Delta H_R &= -15.0 kcal/mol \\ I_1 &\rightarrow C + G & \Delta H_R &= -5.0 kcal/mol \\ I_1 + C &\rightleftharpoons I_2 \\ CAT &\rightarrow CAT^* \end{aligned}$$

with the associated reaction rates:

$$\begin{aligned} rate \quad rxn1 &= k_1 C_{R_1} C_{R_2} \frac{C_{CAT}}{k_7 + C_{CAT}} \\ rate \quad rxn2 &= k_2 C_{R_1} C_{I_1} \\ rate \quad rxn3 &= k_3 C_{I_1} \\ rate \quad rxn4(fwd) &= k_4 C_{I_1} C_C \\ rate \quad rxn4(bwd) &= k_5 C_{I_2} \\ rate \quad rxn5 &= k_6 C_{CAT} \end{aligned}$$

where all concentrations are in mol/m^3 and the rates in $mol/m^3.hr$.

The rate constants are of the Arrhenius form, with the frequency factors and activation energies given in Table B.5.

Reaction II Kinetics

A single reaction takes place in Reaction II:

$$C + 2R_3 \rightarrow E \quad reaction \quad rate = kC_{R_3} C_C \quad (mol/dm^3.hr)$$

where the reaction rate constant k at the operating temperature of 348 K is 1.0 $dm^3/mol.hr$.

	Frequency Factor	Activation Energy
k_1	2.7E+11	18700.0
k_2	3.63E+6	10900.0
k_3	4.4E+14	24700.0
k_4	1.29E+5	7700.0
k_5	2.64E+13	21800.0
k_6	5.0E-1	0.0
k_7	7.0E-4	0.0

Table B.5: Reaction-Distillation Process II: Reaction Data

Reaction III Kinetics

The reaction taking place in Reaction III is:

$$R_4 + 2E \rightarrow D + 2R_3 \quad reaction \quad rate = kC_E^2$$

where the temperature (T in K) dependence of the rate constant k is given by:

$$k = 1.7910^{12} \times e^{\frac{19900}{1.987T}} \tag{B.5}$$

Cooling Jacket

The cooling jacket in the reactor vessel has a surface area of 7.2 m^2. An overall heat transfer coefficient of 5088.16 $kW/m^2.hr$ is assumed for the heat transfer between the reaction mixture and the cooling water. The inlet temperature of the cooling water is 293 K with a constant specific heat capacity of 4200.0 $J/kg.K$.

Enthalpy and Specific Volume

The ideal gas specific enthalpy ($J/kmol.K$) is given by equation (A.43) at a reference temperature of 298.3 K. Table B.6 provides the values of the relevant coefficients.

Vapour Pressure

Equation (A.53) is utilised to calculated vapour pressure (Pa) from temperature T (K). The values of the associated coefficients are given in Table B.3.

	$R1$	$R2$	$R3$	$R4$	I_1	I_2
Coefficient			Specific Heat Capacity $(J/kmol.K)$			
a	-29644.0	-1105.3	21152.0	33738.0	-657.0	-6784.0
b	783.51	314.64	70.924	-7.0176	961.38	1941.7
c	-0.57862	-0.20319	0.02587	0.027296	-0.5602	-1.1714
d	0.17853E-03	0.53214E-04	0.16647E-04	0.28516E-04	0.12E-03	0.26E-03
			Enthalpy of Vapourisation $(\times 10^8 \quad J/kmol)$			
	0.39984	0.29694	0.35278	0.40683	0.40288	0.60603
			Specific Volume (dm^3/mol)			
	0.07614	0.13578	0.0435	0.01964	0.13591	0.43351
			Mean Molecular Weight			
	58.08	134.33	32.042	18.015	176.33	366.72

	A	C	D	E	S
Coefficient			Specific Heat Capacity $(J/kmol.K)$		
a	-20884.0	-0.13542E+06	-24284	1143.0	-24355.0
b	1400.3	1522.7	2095.6	1113.1	512.46
c	-0.9224	-1.4824	-1.3704	0.6722	0.27654
d	0.24E-03	0.62E-03	0.34E-03	0.15E-03	0.49111E-04
			Enthalpy of Vapourisation $(\times 10^8 \quad J/kmol)$		
	0.62857	0.28323	0.6608	0.45471	0.333201
			Specific Volume (dm^3/mol)		
	0.19257	0.13159	0.64668	0.17095	0.11833
			Mean Molecular Weight		
	250.48	158.24	398.79	222.43	383.80

Table B.6: Reaction-Distillation Process II: Enthalpy and Specific Volume Data

Coefficient	$R1$	$R2$	$R3$	$R4$	I_1	I_2
a	58.959	100.41	58.71	65.154	115.72	127.31
b	-5591.9	-8482.7	-6364.7	-6842.9	-9833.5	-16097.0
c	0.0	0.43966E-02	-0.23901E-02	0.27835E-02	0.0	0.0
d	-5.3538	-11.435	4.7344	-6.1364	-13.169	-13.991
e	0.16714E-16	0.13959E-16	0.20888E-16	0.33117E-17	0.43E-16	0.31E-17
f	6.0	6.0	6.0	6.0	6.0	6.0

Coefficient	A	C	D	E	S
a	156.62	61.623	106.49	128.43	71.77
b	-17059.0	-5620.8	-16630.0	-11654.0	-6413.3
c	0.0	0.0	0.0	0.0	0.41663E-02
d	-18.041	-5.7449	-11.021	-14.768	-7.5054
e	0.93E-17	0.21E-16	0.71E-18	0.29E-16	0.542E-17
f	6.0	6.0	6.0	6.0	6.0

Table B.7: Reaction-Distillation Process II: Vapour Pressure Data

B.4. A Process with Zero-Wait Trains

Reaction Kinetics

The kinetic rate constants (k) utilised are of the Arrhenius form:

$$k = Ae^{\frac{-E_a}{RT}} \tag{B.6}$$

where T is the reaction temperature (K), R the universal gas constant (8.314 $kJ/kmol.K$), A the Arrhenius constant and E_a the activation energy.

The rate expressions and the associate reaction rate constants utilised are provided in Table B.8, with C_A, C_B, C_C, C_D, C_E and C_P as the concentrations ($kmol/m^3$) of components A, B, C, D, E and P respectively.

The pure component molar densities are 11.0, 16.0, 10.4, 10.0, 11.0, 16.0, 10.4, 10.0, 11.0 and

16.0 $kmol/m^3$ for compounds C, A, B, D, E, P, F, W_1, W_2 and W_3 respectively.

Task	*ReactionRate* $(m^3/hr.kmol)$	*Arrhenius Constant*	*Activation Energy* (kJ/K)	*Reaction Enthalpy* $(kJ/kmol)$
*Reaction*1	$k_1C_AC_B$	300.0	19000.0	-60000.0
	$k_2C_BC_C$	100.0	18500.0	-50000.0
*Reaction*2	k_3C_D	190.0	19000.0	+50000.0
	k_4C_E	150.0	20000.0	+45000.0
*Reaction*2	$k_5C_CC_E$	200.0	17000.0	-70000.0
	$k_6C_DC_P$	120.0	19000.0	-60000.0
*Reaction*2	$k_7C_BC_P$	110.0	19100.0	-35000.0

Table B.8: A Process with Zero-Wait Trains: Reaction Data

Thermophysical Data

The ideal gas heat capacity and vapour pressure are calculated through equations (A.43) and (A.52). The required data for each component are given in Table B.9 for the specific heat capacity $(kJ/kg.K)$ and Table B.10 for the vapour pressure (bar).

The enthalpies of vapourisation utilised in the calculation of the specific enthalpy of pure liquids are 34102.11, 33430.74, 33741.43, 42593.49, 44091.48, 49587.02, 62460.09, 44560.38, 44473.40 and 42727.56 $kJ/kmol$ for components C, A, B, D, E, P, F, W_1, W_2 and W_3 respectively.

The specific heat capacity of the cooling water is assumed to be 4200 $J/kg.K$.

B.5. Integrated Batch Process Design Subject to Limited Utility Availability

Reaction 1 Kinetics

$$main \quad reaction \quad rate = k_1C_AC_B \quad (kmol/hr.m^3) \tag{B.7}$$

$$side \quad reaction \quad rate = k_2C_C \quad (kmol/hr.m^3) \tag{B.8}$$

where C_A, C_B and C_C are the concentrations $(kmol/m^3)$ of components A, B and C respectively.

The kinetic rate constants are of the Arrhenius form:

Coefficient	C	A	B	D	E
a	16.810	39.790	39.790	3.869	5.669
b	0.9900	0.4928	0.4928	0.5045	0.3689
c	-11.382E-4	-3.558E-4	-3.558E-4	-2.639E-4	-2.865E-4
d	-5.732E-9	1.004E-9	1.004E-9	5.120E-8	9.877E-8

Coefficient	P	F	W_1	W_2	W_3
a	26.900	13.390	-6.544	-6.880	-7.118
b	0.4610	0.5033	1.0980	0.8499	1.1910
c	-2.710E-4	-2.931E-4	-6.155E-4	-6.506E-4	-6.674E-4
d	5.970E-8	6.619E-8	1.341E-7	1.981E-7	1.451E-7

Table B.9: A Process with Zero-Wait Trains: Specific Heat Capacity Data

Coefficient	C	A	B	D	E
a	9.4688	9.42	9.4	9.2000	9.0000
b	2974.94	3000.00	3060.10	3300.00	3390.00
c	-58.15	-58.00	-57.70	-55.00	-40.00

Coefficient	P	F	W_1	W_2	W_3
a	9.4405	11.0104	11.0104	11.0104	11.0104
b	3621.57	4392.15	4442.15	4492.15	4542.15
c	-64.19	-86.55	-86.55	-86.55	-86.55

Table B.10: A Process with Zero-wait Trains: Vapour Pressure Data

$$k_1 = 350.0e^{\frac{-20000}{RT}} \tag{B.9}$$

$$k_2 = 50.0e^{\frac{-20000}{RT}} \tag{B.10}$$

where T is the reaction temperature (K) and R the universal gas constant (8.314 $kJ/kmol.K$). The enthalpy of reaction for the main and side reactions are -60000.0 and -50000.0 $kJ/kmol$ respectively.

Reaction 2 Kinetics

$$reaction \quad rate = k_1 C_C C_E \quad (kmol/hr.m^3) \tag{B.11}$$

where C_C and C_E are the concentrations of components C and E respectively.

The kinetic rate constants are of the Arrhenius form:

$$k_1 = 100.0e^{\frac{-17000}{R_g T}} \tag{B.12}$$

$$k_2 = 50.0e^{\frac{-20000}{R_g T}} \tag{B.13}$$

where T is the reaction temperature (K) and R_g the universal gas constant (8.314 $kJ/kmol/K$).

Cooling Jacket

The cooling jacket in the reactor vessel has a surface area of 50 m^2. An overall heat transfer coefficient of 5088.16 $kW/m^2.hr$ is assumed for the heat transfer between the reaction mixture and the cooling water. The inlet temperature of the cooling water is 288 K with a constant heat capacity of 4200.0 $kJ/ton.K$.

Enthalpy and Density

The liquid and vapour specific enthalpy (h_{liq} and h_{vap}, in $kJ/kmol$) of pure components are calculated through equation (A.43) utilising coefficient a only (*i.e.* assuming constant specific heat capacity). The values of coefficients a ($kJ/kmol.K$) and enthalpies of vapourisation ($kJ/kmol$) utilised are given in Table B.5. A reference temperature of 296 K is adopted.

The density of components is assumed to be 11.0 $kmol/m^3$ for all components.

Coefficient	A	B	C	D	E	F
a	172.3	172.3	200.0	155.0	200.0	160.0
ΔH_{vap}	31000.0	31000.0	26000.0	34000.0	26000.0	28000.0

Table B.11: Integrated Batch Process Design Subject to Limited Utility Availability: Enthalpy Data

Vapour Pressure

Equation (A.51) is utilised to calculated the vapour pressure (in bar) at a given temperature (in K). The values of the coefficients utilised are given in Table B.5.

Coefficient	A	B	C	D	E	F
a	4142.7500	4142.7500	3474.5600	4543.7100	3474.56	3741.88
b	12.7158	12.7158	9.9404	11.2599	9.9404	9.9915

Table B.12: Integrated Batch Process Design Subject to Limited Utility Availability: Vapour Pressure Data